

**Molecular design of nanoparticle-based delivery vehicles  
for pneumonic plague**

by

**Bret Daniel Ulery**

A dissertation submitted to the graduate faculty  
in partial fulfillment of the requirements for the degree of  
DOCTOR OF PHILOSOPHY

Major: Chemical Engineering

Program of Study Committee:  
Balaji Narasimhan, Major Professor  
Michael J. Wannemuehler  
Aaron R. Clapp  
Eric W. Cochran  
Bryan H. Bellaire

Iowa State University

Ames, Iowa

2010

Copyright© Bret Daniel Ulery, 2010. All rights reserved.

# Table of Contents

Acknowledgements .....	V
CHAPTER 1 Introduction .....	1
1.1 Introduction .....	1
1.2 References .....	7
CHAPTER 2 Literature Review .....	11
2.1 Summary .....	11
2.2 Vaccine Delivery Systems .....	12
2.2.1 Introduction.....	12
2.2.2 Immune Response to a Foreign Substance .....	12
2.2.2.1 Innate Immune Response .....	13
2.2.2.2 Adaptive Immune Response .....	16
2.2.3 Vaccines.....	19
2.2.3.1 Whole Cell Vaccines .....	19
2.2.3.2 Subunit Vaccines .....	21
2.3 Degradable Polymers as Vaccine Adjuvants .....	22
2.3.1 Introduction.....	22
2.3.2 Polymers .....	24
2.3.2.1 Polyesters .....	27
2.3.2.2 Acid-Catalyzed Polymers .....	33
2.3.2.3 Polyanhydrides.....	36
2.3.2.5 Other Polymers .....	40
2.3.3 Polymeric Adjuvants .....	43
2.3.3.1 <i>In vivo</i> Efficacy .....	44
2.3.3.2 Polymer Interactions with APCs .....	50
2.4 <i>Yersinia Pestis</i> .....	53
2.4.1 Introduction & History .....	53
2.4.2 Bacterial Function within Host .....	54
2.4.2.1 Mammals .....	54
2.4.2.2 Flea .....	55
2.4.2.3 Human .....	56
2.4.3 Quorum Sensing in <i>Y. Pestis</i> .....	58
2.4.4 Bioterrorism Potential .....	59
2.4.5 Vaccines against <i>Y. Pestis</i> .....	60
2.5 Conclusions .....	61
2.6 References .....	63
CHAPTER 3 Research Objectives.....	97

CHAPTER 4 Polymer Chemistry Influences Monocytic Uptake of Polyanhydride Nanoparticles .....	99
4.1 Abstract .....	100
4.2 Introduction .....	101
4.3 Materials and Methods .....	104
4.3.1 Materials .....	104
4.3.2 Polyanhydride Synthesis and Characterization .....	104
4.3.3 Nanoparticle Fabrication and Characterization .....	104
4.3.4 Culture of THP-1 Human Monocytes and Co-Incubation with Nanoparticles .....	105
4.3.5 Fluorescence Microscopy Techniques .....	106
4.3.6 E $\alpha$ -RFP Antigen Preparation and Cellular Internalization by Monocytes .....	107
4.4 Results and Discussion .....	108
4.4.1 Nanoparticle Characterization .....	108
4.4.2 Cellular Interactions of Nanoparticles with Human Monocytes .....	110
4.4.2.1 Internalization .....	111
4.4.2.2 Intracellular localization .....	115
4.4.2.3 Antigen Internalization .....	118
4.5 Conclusions .....	121
4.6 Acknowledgements .....	122
4.7 References .....	123
 CHAPTER 5 Combining Population and Individual Analyses to Probe Immune Cell Interactions with Polyanhydride Nanoparticles .....	128
5.1 Abstract .....	129
5.2 Introduction .....	130
5.3 Materials and Methods .....	133
5.3.1 Materials .....	133
5.3.2 Polymer Synthesis, Nanoparticle Fabrication, and Characterization .....	134
5.3.3 Culture and Stimulation of C57BL/6 DCs .....	135
5.3.4 Cell Surface Markers .....	137
5.3.5 Cytokine Production .....	137
5.3.6 Intracellular Trafficking .....	138
5.4 Results .....	139
5.4.1 Nanoparticle Characterization .....	139
5.4.2 Cell Population-Based Analysis .....	141
5.4.3 Individual Cell-Based Analysis .....	146
5.5 Discussion .....	152
5.6 Conclusions .....	156
5.7 References .....	157

CHAPTER 6 Design of a Protective Single-dose Intranasal Nanoparticle-based Vaccine Platform for Respiratory Infectious Diseases .....	163
6.1 Abstract .....	164
6.2 Introduction .....	166
6.3 Materials and Methods .....	168
6.3.1 Materials.....	168
6.3.2 Polymer Synthesis and Characterization.....	168
6.3.3 Nanoparticle Design .....	169
6.3.4 Animal Vaccinations .....	171
6.3.5 F1-V Specific Enzyme-Linked Immunosorbent Assay (ELISA) .....	172
6.3.6 <i>Y. pestis</i> Challenge, Bacterial Burden, and Histopathology.....	173
6.3.7 Statistical Analysis.....	175
6.4 Results.....	175
6.4.1 Nanoparticle Characterization .....	175
6.4.2 Protection Against Live <i>Y. pestis</i> Challenge.....	178
6.4.3 Characterization of Antibody Response .....	185
6.5 Discussion .....	188
6.6 Conclusions .....	190
6.7 Acknowledgements.....	191
6.8 References .....	192
CHAPTER 7 Conclusions & Future Research .....	196
7.1 Conclusions .....	196
7.2 Future Work.....	197
7.2.1 <i>Yersinia pestis</i> Vaccine Optimization .....	198
7.2.2 Nanoparticle Vaccine Optimization.....	200
7.2.3 Novel Polymer & Particle Design.....	205
7.2.4 Novel Intracellular Quantification Tools .....	213
7.2.5. Acknowledgments.....	216
7.3 References .....	218

## Acknowledgements

In completing my Ph.D. at Iowa State University, there are so many people to acknowledge that have gotten me to where I am today. I would like to first thank everyone who has taken the opportunity to be a part of my life and who have pushed and inspired me to achieve my goals. Without their help I wouldn't be the person I am today. Space is limited so I will do my best to give credit where it is due.

First, and most importantly, I have to thank my wife, Eva. No one has been more supportive in helping me get through the rigors of my studies and research than her. She has tolerated my long hours, frustrated moods and high stress levels better than I could have ever asked for. She did all of this while earning her D.V.M. and being always willing to give me a back rub after a hard day. She is my inspiration and my best friend and there is no way I could have earned my Ph.D. without her by my side.

I would also like to thank my family for their never ending support. My parents, Dave and Darlene, have been pushing me to achieve my potential since they helped get me placed in the Talented and Gifted program in elementary school. From trips to Chicago museums to allowing me to graduate high school a year early, they have always been supportive of my dreams and happiness. They never complained when I needed to vent about my research and always have had words of encouragement to keep me going. They have been the best parents a son could ask for. My brother Chad has been a great friend who I have

always looked up to. He may not always understand the details of my work, but few people understand and appreciate my sense of humor like he does. For my extended family who gets as excited as I do when I discuss my research with them, I thank them for giving me the extra edge to finish.

Sincere gratitude goes to my major Professor Balaji Narasimhan for all his support, guidance and teaching. His passion for research has definitely rubbed off on me over the past four years. The work he has done is sending waves through the biomedical research community and I look forward to seeing presentations and papers in the future from the Narasimhan group. It has been an honor to work for him and I have truly been lucky to have had a mentor, and a friend, who cares as much about his students as he does.

I thank my program of study committee members, Professors Michael Wanneumuehler, Aaron Clapp, Eric Cochran, and Bryan Bellaire. I have had the unique opportunity to collaborate with each one of them directly and they all have positively impacted my ability to conduct research and have expanded my knowledge base. A second thanks is required for Michael Wannemuehler as he has acted as almost a second advisor during my graduate career. His knowledge and input has forced me to become a better scientist and to more critically evaluate my research.

One person who has had a profound impact on my career path is Professor Allan Guymon of the University of Iowa. After my junior year of undergrad, I knew I wanted to go to graduate school, but was unsure what

program would best fit my research goals. Planning to apply to programs in pharmacology and medicinal chemistry, Dr. Guymon convinced me I could go into chemical engineering and still be a researcher in the biomedical sciences. He gave me an undergraduate researcher position in his laboratory under Dr. Jason Clapper working on degradable polymeric retinal shunts and I have been hooked by biomaterials research ever since. Without his help, I don't believe I would have found research I love nearly as much as what I do now. In addition, his honesty and compassion makes him a unique advisor I am lucky to have been mentored by.

No graduate student works on an island and there have been so many researchers I have worked with that have helped me complete my work at Iowa State. Latrisha Petersen, Brenda Carrillo, Yashdeep Phanse, Devender Kumar, Dr. Jenny Wilson-Welder and Dr. Amanda Ramer-Tait have provided a network of outstanding co-workers whose assistance was critical to my graduation. Thanks also go to the assistance I received from Dr. Maria Torres, Dr. Ross Behling, Chelsea Sackett, Kathleen Ross, Ana Chavez-Santascoy, Lucas Huntimer, Senja Lopac and Avanti Sarkar. I have had the joy to advise the undergraduate researchers Bryce Williams, Andrew Glowacki, Ashley Yeager, Elise Schiltz, Kevin Pustulka, Kristina Staley and Anh Nguyen. Also, I would like to thank Dr. Jen O'Donnell for the enlightening research conversations we have had during my time at Iowa State. Thank you to Dr. Dennis Metzger for serving as a wonderful collaborator on the plague vaccine research.

Not to be forgotten, I owe a great deal of thanks to all the educators along the way who helped keep me on my path towards science and my Ph.D. Special thanks are in order to the teachers John Thorne, Dr. Charles Baker, Jim Stankevitz, Carrie Koch, Vicki Hollister and Mary Johnson for continually pushing me to be my best. In addition the teaching and advisement of Dr. Ge Wang, Dr. Geb Thomas, Dr. John Wiencek, Dr. Robert Deschenes and Dr. Alec Scranton had a profound impact on my undergraduate education. It was the work of these people that have convinced me teaching is a rewarding pursuit I hope to join them in with a career in academia.

I also acknowledge the financial support from the US Department of Defense – Office of Naval Research and the Aileen S. Andrew Foundation.

# CHAPTER 1

## Introduction

### 1.1 Introduction

The events of September 11<sup>th</sup>, 2001 and the anthrax attacks that followed over the subsequent months brought to the attention of all Americans the deadly mix of terrorism and advancements in microbiological techniques. In fact, it was proposed that a lone assailant working with as little as \$2,500 worth of laboratory equipment could produce the high-quality anthrax that was mailed to Senators Tom Daschle and Patrick Leahy and multiple news organizations.<sup>1</sup> While the Department of Defense has looked into better streamlining the design and storage of biodefense-based vaccines since 1998,<sup>2</sup> it was the events of 2001 coupled with the signing of the Project Bioshield Act in 2004 and the ten-fold increase in federal government biodefense-based spending from 2001 to 2008<sup>3</sup> that has pushed the research field forward. Unfortunately, even with these positive developments, a 2007 survey revealed that a mere few hundred biodefense-related prophylactic and therapeutic products are being developed with only thirteen being in Phase 3 clinical trials at the time.<sup>4</sup> In addition, biodefense vaccines that have been FDA-approved or are nearing approval have showed severe limitations. For example, the only anthrax vaccine licensed by the FDA, BioThrax<sup>®</sup>, requires a series of five doses administered at 0 and 4 weeks

and 6, 12 and 18 months to convey protection.<sup>5</sup> Only after completing the 18 month vaccine regimen is an individual considered fully protected and even then it is recommended that a yearly booster dose be administered to insure long-lasting protection. Designing targeted, sustained-delivery vehicles for these newly developed vaccines could go a long way in creating efficacious vaccine systems.

The polymeric drug delivery research field has shown great promise since its inception in the late 1960's.<sup>6</sup> Almost immediately, the importance of hydrolytically degradable materials that break down into non-toxic excretal or bioresorbable products in drug delivery became apparent.<sup>7</sup> Controlled release of a variety of therapeutic and prophylactic treatments has been achieved over the years. These polymeric devices have been shown to deliver everything from cancer chemotherapeutics<sup>8</sup> and oral insulin<sup>9</sup> to DNA-based<sup>10</sup> and protein-based<sup>11</sup> vaccines. The material properties of these carriers that make them excellent candidates for drug delivery include: enhanced potency, minimal toxicity, targeted delivery and controllable payload release. As illustrated in Fig. 1.1, controlled polymeric drug delivery has the potential to reduce the quantity and frequency of doses while maintaining appropriate systemic or local drug concentrations better than conventional delivery techniques.

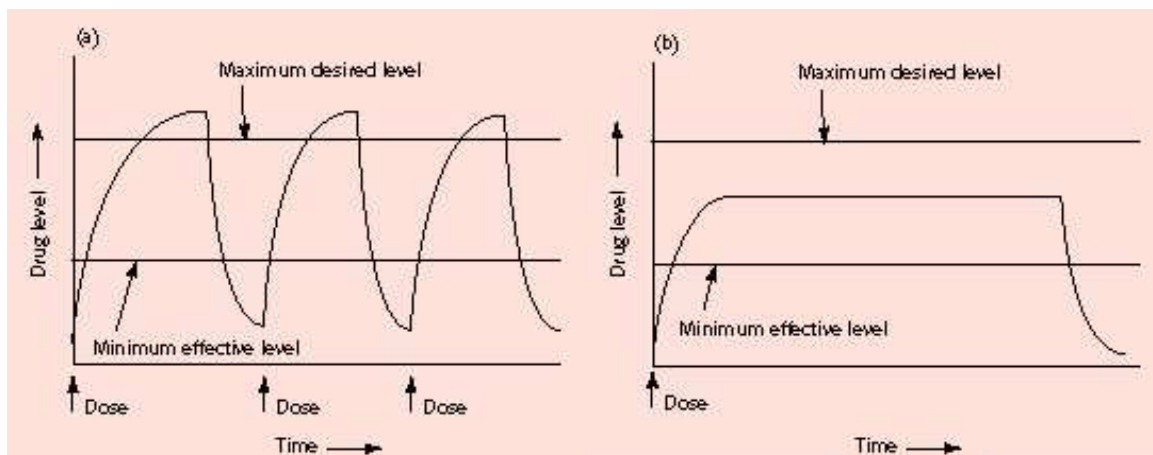


**Figure 1.1.** Conventional (left) versus controlled (right) drug delivery. (Reprinted from Ref. 12.)

While a wide array of polymers has been investigated for vaccine delivery applications, most research has focused on polyesters and polyanhydrides. Research has shown that both families of degradable polymers break down into biocompatible and bioresorbable products<sup>13,14</sup>, stabilize encapsulated antigens<sup>15,16</sup>, produce an adjuvant effect<sup>17,18</sup> and maintain controlled release of their payload.<sup>19,20</sup> Although both show potential, there are some key difference between polyanhydrides and polyesters. Polyanhydride devices degrade layer-by-layer leading to surface erosion where as polyesters allow high levels of water infiltration facilitating bulk erosion.<sup>21</sup> The mechanism of erosion strongly affects the release of encapsulated material. Surface erosion allows for encapsulated payload to be released in concert with polymer degradation<sup>22</sup>, whereas bulk erosion can lead to cargo release significantly ahead of carrier degradation.<sup>23</sup> Also, polyanhydride degradation is highly tunable due to flexibility in choosing polymer chemistry.<sup>24</sup> Polyesters possess limited potential to vary release profiles

by chemistry modulation.<sup>25</sup> The freedom in choosing therapeutic-appropriate payload discharge allows for better tailored vaccine delivery vehicles.

In order for a vaccine to be efficacious, it is imperative that the immune response be primed to the delivered antigen. In order for effective priming to be accomplished, antigen must be supplied to antigen presenting cells (APCs). If these APCs are properly activated and present the correct antigenic epitopes, an adaptive immune response can be mounted that will build long-term immunological memory.<sup>26</sup> Vaccine-induced memory is crucial to allowing the host to fight and survive bacterial and viral infections that cause high morbidity or devastating disease in non-vaccinated individuals. Nowhere is the need for improved vaccines strategies more crucial than in the biodefense field. A particularly severe bioterrorism weapon is *Yersinia pestis*, the causative agent of plague. Not only is it responsible for three worldwide pandemics, but in the wrong hands, it could be used to devastate countries and kill millions of people. While whole cell-killed<sup>27</sup> and attenuated-live vaccines<sup>28,29</sup> have been studied for a long time, the development of recombinant protein based vaccines has had its successes<sup>30</sup> and failures<sup>31</sup>. Proteins with enhanced expression during the quorum sensing process may lead to the identification of novel vaccine immunogens. Quorum sensing, a complex biological gene expression control system, is utilized by many bacteria like *Y. pestis* to activate virulence mechanisms once certain bacteria-friendly conditions are met.<sup>32</sup> While this is designed to protect bacterial populations from immune clearance, it could be

exploited to develop vaccine strategies for immune response focusing to bacteria near virulence.

In addition, as the field has transitioned from the use of whole cell lysates to recombinant proteins, the use of adjuvants, which are non-specific immune boosting substances, as part of the vaccine regimen is nearly ubiquitous.<sup>33</sup> By choosing delivery vehicles that also function as adjuvants, a dose-sparing, single-dose vaccine can be designed.

The overall objective of this research was to design novel polyanhydride nanoparticle-based vaccine delivery vehicles, which can function both as immunomodulatory biomaterials and long-term payload delivery systems. To accomplish this goal, two copolymers composed of three anhydride monomers were investigated. These copolymers are poly((1,6-bis(*p*-carboxyphenoxy)hexane)-co-(sebacic acid)) (CPH:SA) and poly((1,8-bis(*p*-carboxyphenoxy)-3,6-dioxaoctane))-co-(1,6-bis(*p*-carboxyphenoxy)hexane)) (CPTEG:CPH) (Fig. 1.2).

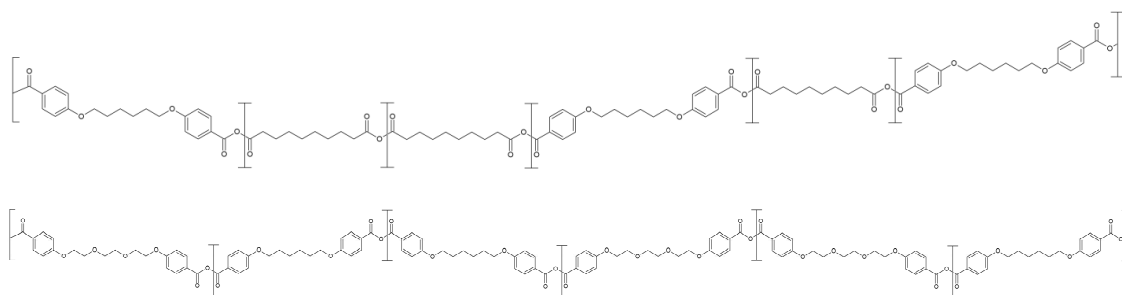


**Figure 1.2.** Chemical structures of random CPH:SA (top) and CPTEG:CPH (bottom) copolymers.

The interaction between nanoparticles and monocytes and the role polymer chemistry plays in mediating uptake of particles and soluble material is detailed in Chapter 4. An expansion of this analysis was undertaken in Chapter 5, where bone-marrow derived dendritic cells were investigated for how they processed nanoparticles and what effect this had on cellular activation. As biodefense is vitally important to our homeland security, the potential of nanoparticles as vaccine delivery vehicles that protect against pneumonic plague was investigated in Chapter 6. Lastly, knowledge gained from these experiments will be utilized to optimize nanoparticle-based vaccines against an array of diseases as well as develop novel nanoparticle-based platforms to address the limitations of current systems (Chapter 7).

## 1.2 References

1. Garvey, M. & Lichtblau, E. Loner Likely Sent Anthrax, FBI Says. *Los Angeles Times*. 10 Nov 2001, Print Edition A-1.
2. Department of Defense. Report on Biological Warfare Defense Vaccine Research & Development Programs. (July 2001). Retrieved on 26 February 2009 from <http://www.defenselink.mil/pubs/ReportonBiologicalWarfareDefenseVaccineRDPrgras-July2001.pdf>.
3. Franco, C. & Deitch, S. Billions for Biodefense: Federal Agency Biodefense Funding, FY2007 – FY2008. *Biosecurity and Biodefense: Biodefense Strategy, Practice, and Science*. **5**(2): 117 – 132 (2007).
4. Trull, M., du Laney, T.V. & Dibner, M.D. Turning biodefense dollars into products. *Nature Biotechnology*. **25**(2): 179 – 184 (2007).
5. Food and Drug Administration. BioThrax® (Anthrax Vaccine Adsorbed) Highlights of Prescribing Information. Emergent BioSolutions. Retrieved on 26 February 2009 from <http://www.fda.gov/Cber/label/biothraxLB.pdf>.
6. Majkus, V., Horakova, Z., Vymola, F. & Stol, M. Employment of hydron polymer antibiotic vehicle in otolaryngology. *Journal of Biomedical Materials Research*. **3**(3): 443 – 454 (1969).
7. Beasley, M. L. & Collins, R. L. Water-Degradable Polymers for Controlled Release of Herbicides and Other Agents. *Science*. **169**(3947): 769 – 770 (1970).
8. Brannon-Peppas, L. & Blanchette, J. O. Nanoparticle and targeted systems for cancer therapy. *Advanced Drug Delivery Reviews*. **56**(11): 1649 – 1659 (2004).
9. Babu, V. R., Patel, P., Mundargi, R. C., Rangaswamy, V. & Aminabhavi, T. M. Developments in polymeric devices for oral insulin delivery. *Expert Opinion on Drug Delivery*. **5**(4): 403 – 415 (2008).
10. Jilek, S., Merkle, H. P. & Walter E. DNA-loaded biodegradable microparticles as vaccine delivery systems and their interaction with dendritic cells. *Advanced Drug Delivery Reviews*. **57**(3): 377 – 390 (2005).

11. Bramwell, V. W., Eyles, J. E. & Alpar, H. O. Particulate delivery systems for biodefense subunit vaccines. *Advanced Drug Delivery Reviews*. **57**(9): 1247 – 1265 (2005).
12. Brannon-Peppas, L. Polymers in Controlled Drug Delivery. *Medical Plastics and Biomaterials*. **4**(6): 34 – 45 (1997).
13. Wise, D.L., Fellman, T.D., Sanderson, J.E. & Wentworth, R.L. Lactic/glycolic acid polymers. *Drug Carriers in Biology and Medicine*. G. Gregoriadis, Ed. Academic Press, New York, 237 – 270 (1979).
14. Leong, K.W., D'Amore, P.D., Marletta, M. & Langer, R. Bioerodible polyanhydrides as drug-carrier matrices. II. Biocompatibility and chemical reactivity. *Journal of Biomedical Materials Research*. **20**(1): 51 – 64 (1986).
15. Jiang, W. & Schwendeman S.P. Stabilization of Tetanus Toxoid Encapsulated in PLGA Microspheres. *Molecular Pharmaceutics*. **5**(5): 808 – 817 (2008).
16. Tabata, Y., Gutta, S. & Langer, R. Controlled delivery systems for proteins using polyanhydride microspheres. *Pharmaceutical Research*. **10**(4): 487 – 496 (1993).
17. Hampl, J., Dittrich, M., Franz, J., Reschova, S. & Stephanek, J. Adjuvant activity of linear aliphatic polyester and branched aliphatic oligoester microspheres. *International Journal of Pharmaceutics*. **144**(1): 107 – 114 (1996).
18. Kipper, M.J., Wilson, J.H., Wannamuehler, M.J. & Narasimhan, B. Single dose vaccine based on biodegradable polyanhydride microspheres can modulate immune response mechanism. *Journal of Biomedical Materials Research Part A*. **76A**(4): 798 – 810 (2006).
19. Zou, J., Shi, W., Wang, J. & Bo, J. Encapsulation and controlled release of a hydrophobic drug using an novel nanoparticle-formed hyperbranched polyester. *Macromolecular Bioscience*. **5**(7): 662 – 668 (2005).
20. Shen, E., Kipper, M.J., Dziadul, B., Mee-Kyung, L. & Narasimhan, B. Mechanistic relationships between polymer microstructure and drug release kinetics in bioerodible polyanhydrides. *Journal of Controlled Release*. **82**(1): 115 – 125 (2002).

21. von Burkersroda, F., Schedl, L. & Gopferich, A. Why degradable polymers undergo surface erosion or bulk erosion. *Biomaterials*. **23**(21): 4221 – 4231 (2002).
22. Gopferich, A. Bioerodible implants with programmable drug release. *Journal of Controlled Release*. **44**(2-3): 271 – 281 (1997).
23. Bittner, B., Witt, C., Mader, K. & Kissel, T. Degradation and protein release properties of microspheres prepared from biodegradable poly(lactide-co-glycolide) and ABA triblock copolymers: influence of buffer media on polymer erosion and bovine serum albumin release. *Journal of Controlled Release*. **60**(2-3): 297 – 309 (1999).
24. Determan, A.S., Trewyn, B.G., Lin, V.S.-Y., Nilsen-Hamilton, M. & Narasimhan B. Encapsulation, stabilization, and release of BSA-FITC from polyanhydride microspheres. *Journal of Controlled Release*. **100**(1): 97 – 109 (2004).
25. Wang, Y., Challa, P., Epstein, D.L. & Yuan, F. Controlled release of ethancrylic acid from poly(lactide-co-glycolide) films for glaucoma treatment. *Biomaterials*. **25**(18): 4279 – 4285 (2004).
26. Janeway, C.A., Travers, P., Walport, M. & Sclomchik, M.J., editors. Immunobiology the immune system in health and disease. 6<sup>th</sup> edition. New York, NY: Garland Publishing. (2005).
27. Haffkine, W.M. Remarks on the plague prophylactic fluid. *British Medical Journal*. **1**(1902): 1461 – 1462 (1897).
28. Strong, R.P. Protective inoculation against plague. *Journal of Medical Research*. **18**(2): 325 – 346 (1908).
29. Girard, G. Immunity in plague. Acquisitions supplied by 30 years of work on the 'Pasteurella pestis Ev' (Girard and Robic) strain. *Biology and Medicine (Paris)*. **52**: 631 – 731 (1963).
30. Leary, S.E., Griffin, K.F., Garmony, H.S., Williamson, E.D. & Titball, R.W. Expression of an F1/V fusion protein in attenuated Salmonella typhimurium and protection of mice against plague. *Microbiological Pathology*. **23**(3): 167 – 179 (1997).

31. Pitt, M.L. Non-human primates as a model for pneumonic plague. Public Workshop on Animal Models and Correlates of Protection for Plague Vaccines. Retrieved on 9 March 2009 from <http://www.fda.gov/cber/minutes/plague101304t.pdf>.
32. Miller, M.B. & Bassler, B.L. Quorum sensing in bacteria. *Annual Reviews Microbiology*. **55**: 165 – 199 (2001).
33. Guy, B. The perfect mix: Recent progress in adjuvant research. *Nature Reviews Microbiology*. **5**(7): 505 – 517 (2007).

# CHAPTER 2

## Literature Review

### 2.1 Summary

Particle-based drug carriers can be composed of a number of different polymers or biologically-derived materials. Due to their biocompatible, bioresorbable and non-toxic properties, degradable polymers are excellent candidates for therapeutic and prophylactic medicinal strategies. In addition, these biomaterials can be tailored to meet treatment requirements, including controlled release rate and targeted delivery. Section 2.2 outlines the manner in which vaccines initiate an immune response and convey immunity. The capacity for polymeric carriers to function as vaccine delivery systems will be discussed in Section 2.3. Different polymer families and tailoring initiated immune responses will be explored. Section 2.4 overviews an especially insidious bacterial species, *Yersinia pestis*. The causative agent of plague will be explored from historical and treatment perspectives.

## **2.2 Vaccine Delivery Systems**

### **2.2.1 Introduction**

Over the past 200 years, the advancement of vaccines is one of humankind's greatest achievements. Since Edward Jenner gave cowpox pus to people, conveying cross reactive protection against small pox, there has been worldwide eradication of small pox and elimination of polio from the developed world as well as near eradication of other deadly diseases like diphtheria.<sup>1,2</sup> Despite advances, there still exist grand challenges in the design of efficacious vaccination strategies. One sobering fact is that the World Health Organization (WHO) estimates that 1 in 7 global childhood deaths (1.4 million in 2002) is caused by diseases we have vaccines for.<sup>3</sup> In developing countries this mortality rate is even higher. Development of vaccine adjuvant and delivery systems could lead to single dose vaccines. The use of polymeric vaccine carriers that function as adjuvants may be one the best options to solving this global issue. In order to develop complex, multi-disciplinary research-based solutions, one must understand how the immune response functions, how vaccines stimulate that response to convey protection and the currently available polymeric delivery systems.

### **2.2.2 Immune Response to a Foreign Substance**

In order to fabricate novel vaccines strategies, an overview of how the immune system functions is essential. The immune response is composed of a complex network of heavily regulated cell processes and interactions that are

interrelated. This network is composed of two linked systems called the innate and adaptive immune systems.<sup>4</sup>

#### 2.2.2.1 Innate Immune Response

The innate immune system is involved in surveillance and detection of foreign invaders. Common components of this response are phagocytic cells, Natural Killer (NK) cells,  $\gamma\delta$  T cells, anti-microbial peptides and the complement system.<sup>5</sup> First detailed by Drs. Charles Janeway and Ruslan Medzhitov, the innate immune system uses a relatively small set of systems to identify foreign bodies. The bacterial associated components identified by innate immunity are called pathogen-associated molecular patterns (PAMPs).<sup>6</sup> PAMPs are relatively conserved across bacteria and are recognized by pattern recognition receptors (PRRs) on phagocytic cells. Multiple PRRs exist, including mannose and scavenger receptors, but receptors of particular importance are the Toll-like receptors (TLRs). TLRs allow for a critical phagocytic and antigen presenting cell (APC), the dendritic cell (DC), to recognize a group of common microbial ligands (e.g., unmethylated bacterial DNA (CpG) and lipopolysaccharide (LPS)).<sup>5</sup> Stimulation of TLRs causes a cascade down a signaling pathway ultimately leading to the activation of transcription factors necessary to cause cell maturation, migration and antigen presentation.<sup>7</sup> DCs are found in all body tissues and are the primary cell type that initiates and regulates the adaptive immune response.<sup>8</sup> There are three ways by which DCs can acquire antigen to present to the adaptive immune response. This can be accomplished by

phagocytosis (i.e., internalization of solid particles into vesicles) of bacteria, particles, or cellular debris; macropinocytosis, “cellular drinking”, of soluble material; and triggered endocytic uptake through mannose, complement or Fc receptor activation. Upon activation by antigen internalization and co-stimulation through TLRs or cytokines, which are chemical communication signals, DCs mature and are able to migrate to the draining lymph node. Maturation causes DCs to lose their phagocytic capability and drastically increase the surface expression of migratory molecules like CCR7 and DC-SIGN and stimulation molecules like CD40, CD80, CD86 and MHC I/II. Peptide fragments (8 to 17 amino acids in length), called epitopes, of processed antigen are transported to major histocompatibility complexes I (MHC I) or II (MHC II) to allow for T cell recognition and activation.<sup>7,9</sup> Antigens processed by internalization through phagocytosis go through the exogenous pathway in which phagosomes merge with lysosomes to create a proteolytic environment used to degrade antigens. Peptides generated from this method are able to be effectively loaded into MHC II and presented on the cell surface. Antigens found within the cytosol of the cell are degraded by proteasomes and chaperon proteins (TAPs) transport these peptides into the endoplasmic reticulum (ER) where they can be loaded into MHC I and trafficked to the cell surface for presentation. This is referred to as the endogenous pathway. Fig. 2.1 shows the two methods of antigen processing.

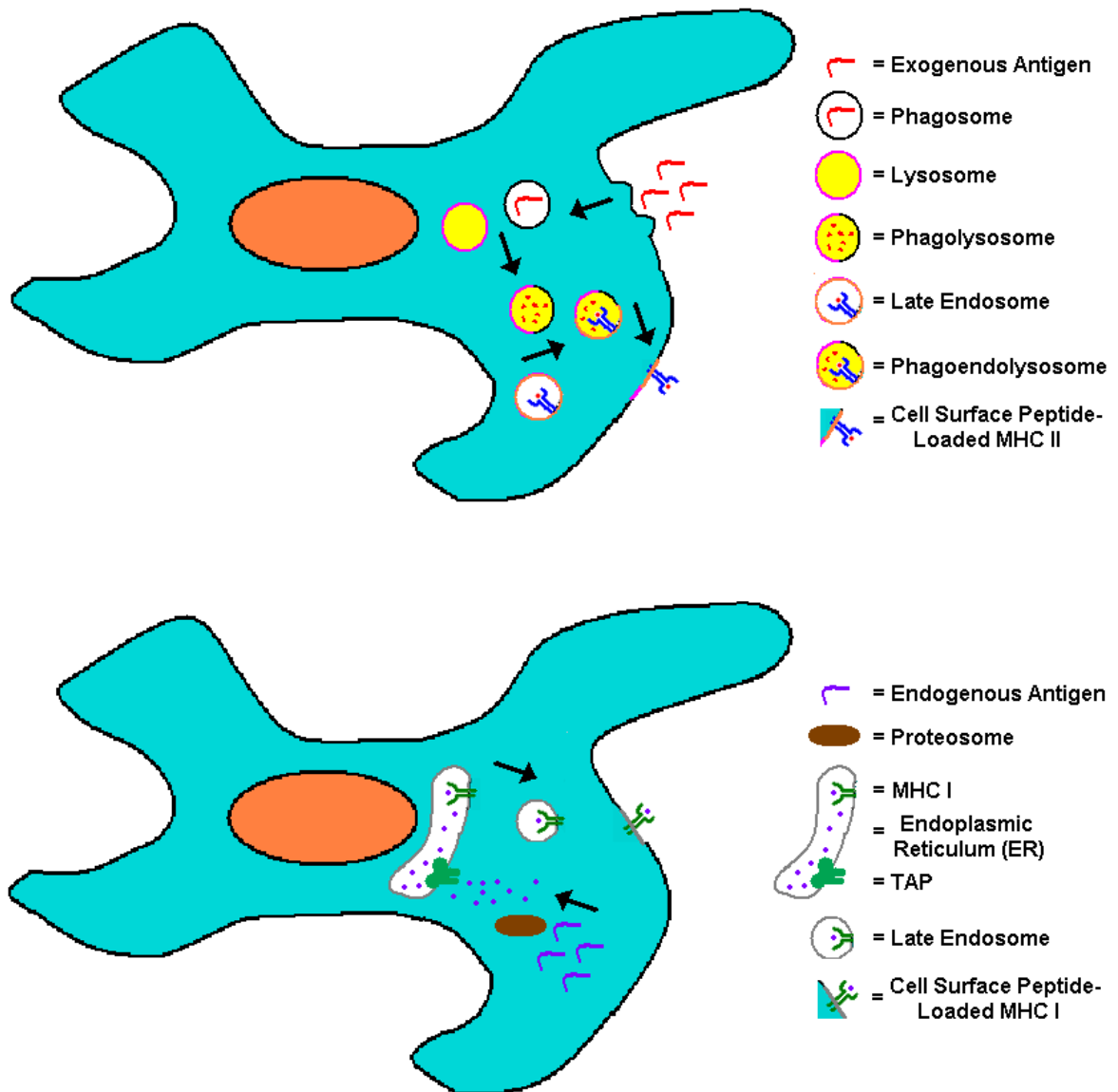


**Figure 2.1.** Exogenous (top) and endogenous (bottom) antigen presentation pathways. External antigen is trafficked by vesicles to mediate degradation, loading of MHC II and presentation on the cell surface. Internal antigen (e.g. viral or intracellular bacteria) is degraded, trafficked to the ER, loaded into MHC I and presented on the cell surface.

After DCs have successfully migrated to the draining lymph node and presented antigen, they are able to interact with T cells and bridge innate and adaptive immune responses.

#### 2.2.2.2 Adaptive Immune Response

The adaptive immune response is traditionally considered to have two branches: cell-mediated immunity (CMI) and humoral immunity. There are two other arms that play a role in the overall immune response, the Th17 response and the T regulatory response. The distinction of which response is dominant depends on a multitude of factors initialized by the DC to CD4<sup>+</sup> T helper cell interaction. CD4<sup>+</sup> T cells are classified as Th1, Th2, Th17 or Treg.<sup>10-12</sup> A Th1 immune response is characterized by the production of IFN- $\gamma$  and TNF- $\beta$  cytokines and IgG2a/c antibodies and normally associated with activated macrophages and delayed-type hypersensitivity of CMI.<sup>278</sup> A Th2 immune response is characterized by the production of IL-4, IL-5, IL-10 and IL-13 and the secretion of IgG1 and IgE antibodies.<sup>13</sup> Th1-type immune responses are generally directed at intracellular pathogen like viruses and intracellular bacteria (e.g., *Brucella abortus*) whereas Th2-type immune responses are generally directed at extracellular bacteria in which antibodies can be used to neutralize toxins and bacterial adhesion.<sup>14</sup> Th17 responses are considered inflammatory, but their role in vaccinology is unknown.<sup>10</sup> This response is marked by a production of IL-17 and has been thought to be protective during acute inflammation, but is also associated with chronic inflammatory disease.

It should be noted that these responses often act in concert to clear infection. There often does seem to be one dominant response and if effective follows the intracellular (Th1) versus extracellular (Th2) argument. DCs assist in CD4<sup>+</sup> T cell differentiation by the secretion of some of the cytokines mentioned above in addition to the presentation of antigen. Activated DCs produce TNF- $\alpha$ , IL-1 $\beta$ , IL-6, IL-8, IL-12 and IL-10. The cytokine profile secreted directly affects the delineation of CD4<sup>+</sup> T cells. Also, co-stimulation (CD40, CD80 and CD86) is important. If antigen presentation occurs, but co-stimulatory markers are absent, then the DCs can induce ineffective T cell activation like anergy (tolerance).<sup>15</sup> Fig. 2.2 provides an overview of the interaction between DCs and CD4<sup>+</sup> T cells.

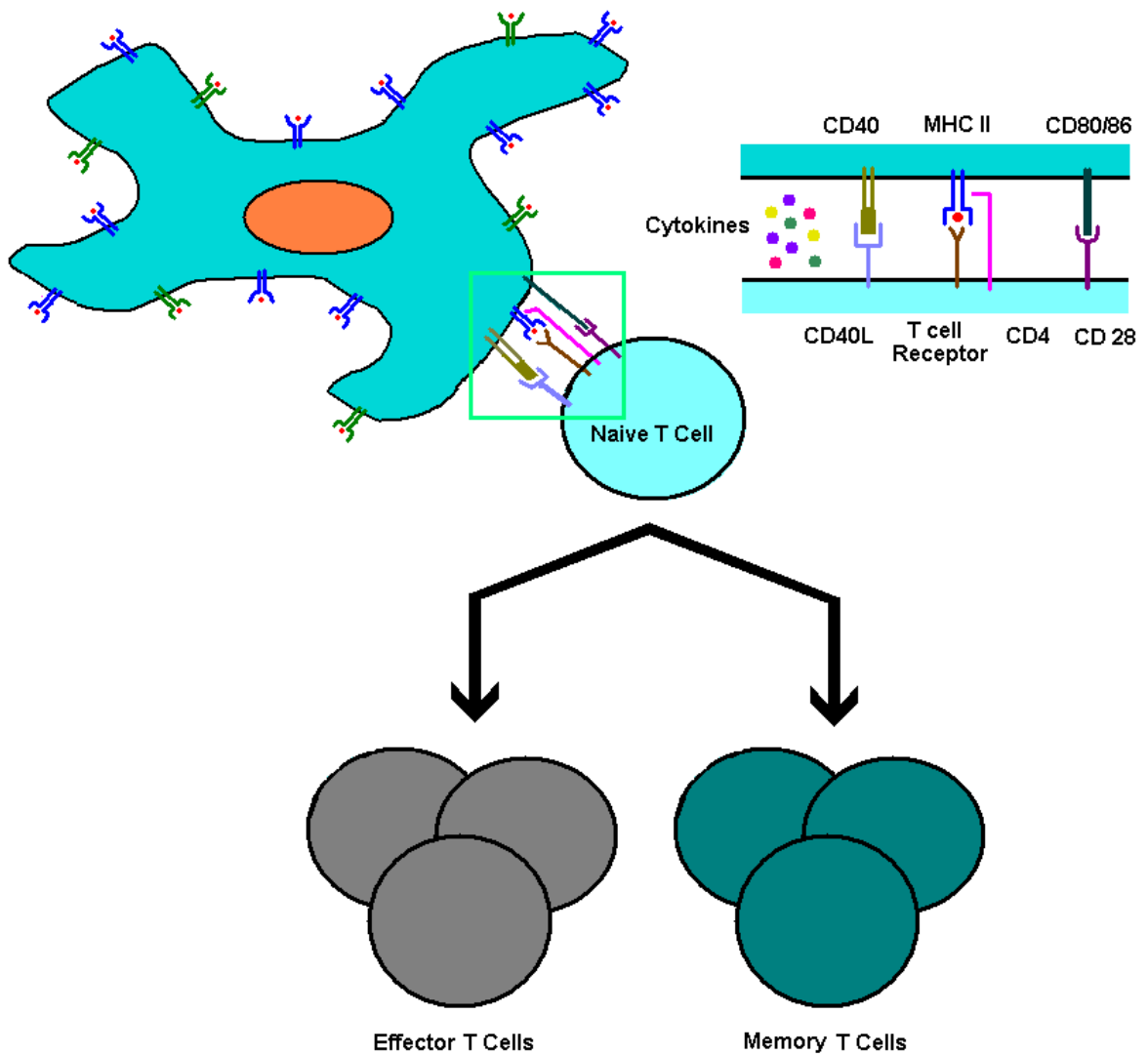


**Figure 2.2.** Multiple signals from DCs influence the differentiation of naïve T cells. The MHC to T cell receptor, co-stimulation and cytokine signaling all direct this response. DC cytokine secretion of IL-12 indicates a push towards Th1 and IL-4 results in Th2. In response, Th1 cells produce IFN- $\gamma$  and Th2 cells produce IL-4, IL-5 and IL-10.

### 2.2.3 Vaccines

Vaccines function best when they mimic the immune response that would be generated if the disease had been contracted. In order to achieve this goal, some portion of the disease causing agent is given, often with a non-specific immune boosting substance called an adjuvant. Typical vaccine regimens employ an initial dose followed by two to three booster doses. The multiple doses allow for high immunogen quantities to be exposed to the immune system at different times. The first dose initiates the response of DCs and naïve immune cells (primary response) with the following doses activating memory immune cells characterized by a more robust and speedier response (secondary response).<sup>7</sup> Most vaccines induce protection through neutralizing antibodies instead of CMI induction.<sup>16</sup> Vaccines can be classified into two categories, whole cell and subunit.

#### 2.2.3.1 Whole Cell Vaccines

Outside of natural infections, vaccines possessing modified organisms induce the most potent and long lasting immune response in the host. The two types of whole cell vaccines used are live attenuated and whole killed.

Live attenuated vaccination requires the fewest number of doses, can confer lifelong immunity, and requires no adjuvants.<sup>17</sup> Since these vaccines are composed of living organisms they are able to replicate and cause a mild, limited infection with the natural release of microbial compounds that synergistically induce the host response almost identically to natural infection. With live

vaccination, attenuation is required. This is often accomplished by repetitive passage (at least 10 times) in an animal host or *in vitro* to isolate naturally occurring attenuated genetic mutants. Recent advancements in microbiology now allow for known induction of mutations through genetic recombineering easing the attenuation process and making it much safer since specific virulence attributes can be knocked out at the genetic level.<sup>18</sup> Sometimes cross reactivity of two similar microorganisms that produce similar or identical epitopes can be used in vaccination. Edward Jenner's original small pox vaccine contained cow pox puss that had enough similarity to small pox that it conveyed protection while only giving the host a mild infection.<sup>19</sup> While live attenuated vaccines have many beneficial properties, there are a number of issues with their use. When working with a live organism, there is a possibility for it to persist in the host, revert back to a pathogenic strain or induce disease in immunocompromised individuals. If persistence occurs then there is a high likelihood that the disease can spread and infect non-vaccinated people. In addition, live vaccines have serious potential to cause side-effects ranging from injection site inflammation to systemic disease. Finally, many diagnostic tests cannot identify differences between persistent avirulent microorganisms given by vaccination and naturally occurring infections.<sup>20</sup> These factors limit the potential of live attenuated vaccines.

Another vaccination strategy is to use whole-killed vaccines. Microorganisms are treated with chemicals or heat to kill them while preserving

their cellular integrity. Whole-killed vaccines can be potent inducers of humoral immunity because most of the virulence factors and important epitopes are still present.<sup>17</sup> These vaccines cannot replicate so there is no risk of persistent infection, reversion to virulence, or spread of disease. Also, whole killed vaccines are more stable and usually very cost effective. However, killed vaccines often require multiple doses and rarely induce strong CMI responses. Adverse side effects are common ranging from severe pain to redness and swelling due to the presence of microbial stimulants like LPS and other TLR ligands.<sup>21,22</sup> When using either type of whole cell vaccine, the significant consequences can outweigh the benefits.

#### 2.2.3.2 Subunit Vaccines

Subunit vaccines contain only a portion of the organism being vaccinated against. The most common subunit vaccines are composed of toxoids, which are inactive bacterial toxins. Two common vaccines are formaldehyde-inactivated diphtheria and tetanus toxoids. Other subunit vaccines are protein- and carbohydrate-based. Currently, vaccines against influenza virus (hemagglutinin-binding protein) and meningitis (polysaccharide capsule) are used.<sup>23,24</sup> A final group of subunit vaccines is centered on the delivery of pathogenic DNA. DNA coding for a target epitope is delivered using a viral vector or DNA-containing particulates to DCs.<sup>23,25</sup> Host cells express the foreign epitope and it is able to be presented in the context of both MHC I and II allowing for both humoral and cellular immunity.<sup>7</sup> While DNA vaccines have yet to be FDA approved, there are

many currently in phase I, II and III human trials.<sup>26</sup> Subunit vaccines have several advantages over whole cell vaccines. By using specific, protective epitopes in subunit vaccines, nearly all side effects are eliminated since the microbial components that trigger strong innate responses are no longer delivered to the host. This allows for subunit vaccines to be considered extremely safe and new technologies have made them inexpensive to produce. The decrease in non-specific response has its downside. These immunogens tend to be very weakly immunogenic and require multiple doses to convey protection.<sup>27</sup> In order to enhance subunit vaccines, the delivery of adjuvants (e.g., monophosphoryl lipid A – MPLA) is necessary. While subunit vaccines can induce high antibody titers, they rarely induce protective T cell responses. In order to overcome these issues, the development of specialized adjuvants is necessary.

## **2.3 Degradable Polymers as Vaccine Adjuvants**

### **2.3.1 Introduction**

Adjuvants are immunoenhancing materials that typically have three major functions: 1) allow for slow release of the antigen; 2) facilitate antigen targeting to antigen presenting cells (APCs) and promote phagocytosis; 3) modulate and enhance the immune response.<sup>28-30</sup> It is also possible that adjuvants provide a danger signal to the immune system that mimics infection and enhances the immune response to the vaccine.<sup>31</sup>

Slow antigen release can be accomplished by entrapping antigen in a poorly eroding substance which can act as a depot for vaccine delivery. The use

of alum, a combination of aluminum phosphate and aluminum hydroxide, is the most commonly used adjuvant in human medicine. Alum makes a gel-like matrix that allows for a delayed release of antigen. Recently, oil adjuvants like MF59 (squaline oil emulsion with muramyl tripeptide) have been shown to have beneficial adjuvant behavior with satisfactory safety making them potential candidates for human use.<sup>32,33</sup> Small particles composed of stabilized lipids, phospholipids, or proteins (e.g. virosomes and liposomes) allow for gradual release by incorporating antigens into their backbones. Another approach is to use degradable polymer microparticles ( $>1 \mu\text{m}$ ) or nanoparticles ( $<1 \mu\text{m}$ ) with encapsulated antigen to provide sustained release. Thus, many different vehicles can be used to provide antigen depots.

Enhancement of the immune response by targeted delivery to or activation of APCs is another role of adjuvants. This can be accomplished by properties of the antigen, facets of the carrier, inclusion of immunostimulatory molecules or some combination thereof. Many toxins (e.g. pertussis and cholera toxins) actually have high binding selectivity that facilitate their uptake by APCs.<sup>31,34</sup> While these make great vaccines, their overwhelming stimulation of an anti-toxin immune response may overshadow the response to the antigen of interest making them less than ideal adjuvants.<sup>31</sup> Other bacterially-derived immunostimulants like LPS (a surface carbohydrate from gram-negative bacteria) have been shown to activate NF- $\kappa$ B by CD14 and TLR4 causing the overwhelming production of pro-inflammatory cytokines.<sup>32,35</sup> The response is so

strong in humans that LPS cannot be used in human vaccine preparations leaving few options for adjuvants that can safely enhance APC responses.

Immune modulation is influenced by a number of characteristics of the adjuvant/antigen delivery system.<sup>36,37</sup> These include, but are not limited to, delivery route, antigen dose, duration of antigen delivery, number of immunizations, co-stimulatory molecule inclusion, and delivery system. The compilation of these effects results in the overall immune bias (Th1, Th2 or a balance) of the vaccine. The clear role of the vaccinologist is to exploit these factors to induce an immune response that will best mimic disease and therefore convey protection. Currently, the FDA approved adjuvants, alum and MF59, have shown limited ability to induce a Th1 type immune response that may be helpful in preventing some diseases.<sup>32,38</sup> In addition, oil-based liposomal adjuvants that do produce a Th1 dominant response induce severe side-effects including inflammation, tissue reactivity, and even granuloma formation.<sup>39</sup> With these limitations, a vaccine delivery system that provides sustained payload delivery, facilitates APC activation, and possesses tunable immunomodulatory properties would be highly desirable. Degradable polymers hold the potential to meet all of these needs.

### **2.3.2 Polymers**

In order to overcome many of the limitations in vaccine design, polymeric materials have been studied. Polymers are materials that contain a large number of repeating units called monomers. The chemical structure of monomers and

their linkers as well as the number of monomers covalently linked together dictate mechanical, thermal, and processability parameters of the material. Polymers like DNA, proteins and polysaccharides have always been present in nature. Over the past 100 years, synthetically derived polymers have given rise to a wide range of materials from plastic beverage containers to automotive bodies. The development of polymers for use in biomedical applications has had an overwhelming effect on the improvement of medical care. From maintaining product sterility to disposable syringes, polymers have changed the face of medicine. In addition to medical products, polymers have more recently been used as part of the therapeutic solution. In the 1960's, Edward Schmitt and Rocco Polistina recognized the potential for degradable polymer fibers as surgical sutures and biomedical implants.<sup>40-42</sup> Since then polymeric biomaterials have been incorporated into a wide range of therapies from the delivery of chemotherapeutics to tissue engineering scaffolds. For application in vaccine delivery, the capacity for polymeric materials to be biocompatible and excretal is desirable. Degradable polymers best fit these requirements.

Degradable polymers possess a chemical bond in their structure that can be cleaved. This bond is hydrolytically labile in which the presence of water breaks the bond adding a hydrogen atom to one product and an hydroxyl group to the other product as seen in Fig. 2.3.

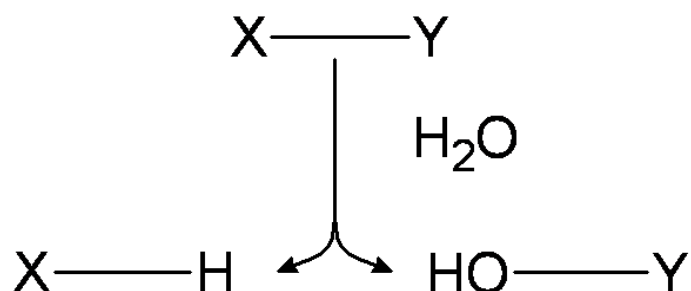


**Figure 2.3.** The hydrolytically sensitive bond X-Y is cleaved by a water molecule yielding the products of X-H and HO-Y.

Since each degradable polymer contains a large number of these bonds, the polymer is able to maintain many impressive physical properties (mechanical strength, processibility, etc.) while having degradation products that are excretable or bioresorbable. Polymers are classified by their chemistry with each family possessing unique characteristics. Figure 2.4 overviews the five degradable polymeric families (polyesters, acid-catalyzed polymers, polyanhydrides, polyethers, and other polymers) that will be discussed in this review.

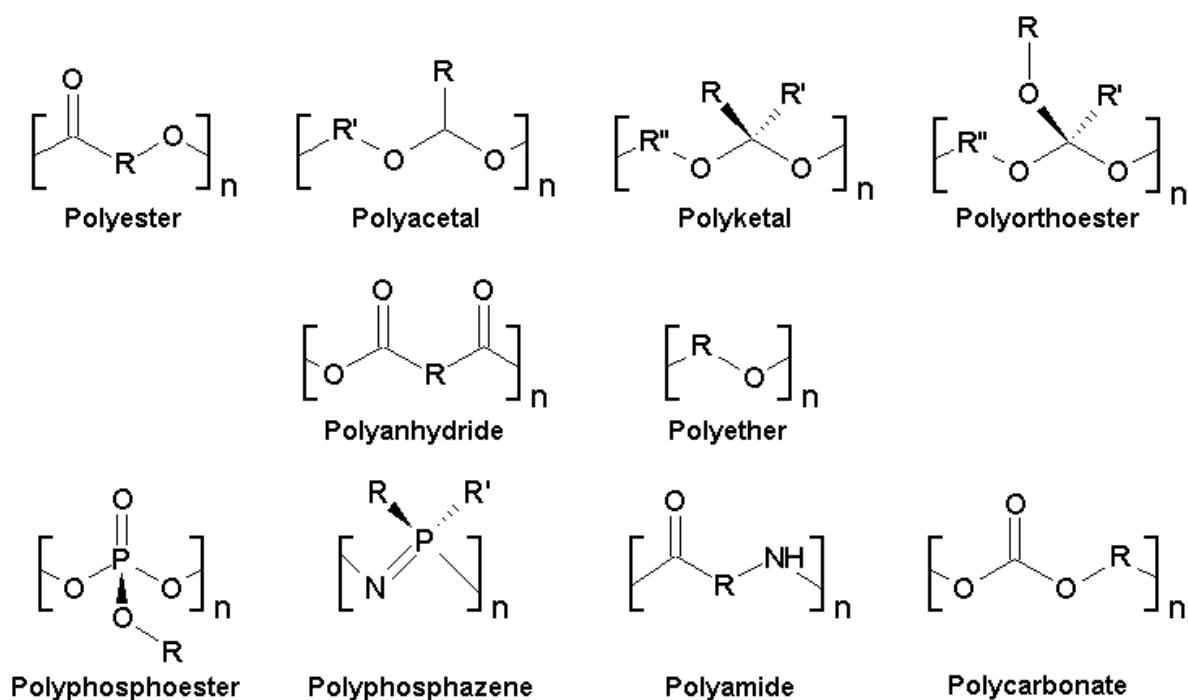


**Figure 2.4.** Chemical structures of typical degradable polymers used in vaccine delivery.

### 2.3.2.1 Polyesters

Biomedical applications of polyesters have been known for over 40 years. Polyesters are commercially available and FDA-approved for human use making them potentially useful biomaterials. One of their greatest properties is their low cytotoxicity which is attributable to the fact that they degrade into cellular metabolites that are easily uptaken and processed by cells.<sup>43,44</sup> Degradable polyesters that have potential for vaccine delivery applications include poly(lactic acid) (PLA), poly(lactic-co-glycolic acid) (PLGA), poly(3-hydroxybutyric acid) (P3HB), poly(4-hydroxybutyric acid) (P4HB) and poly( $\epsilon$ -caprolactone) (PCL) (Fig. 2.5).

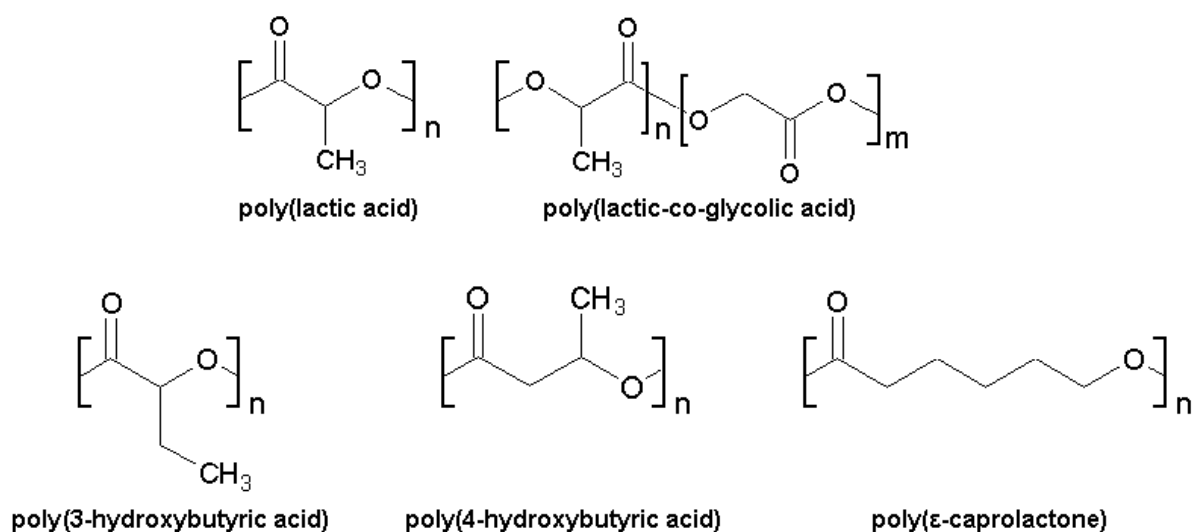


**Figure 2.5.** Chemical structures for degradable polyesters.

Extensive research has been published on PLA<sup>45-51</sup> and PLGA<sup>48-58</sup> systems in drug delivery. They have been used for the delivery of everything from chemotherapeutics to vaccines. Poly(glycolic acid) (PGA) by itself has limited vaccine delivery capabilities because it is so hydrophilic it releases payload too rapidly and it is difficult to process by typical polymer solvents. Instead PGA has mostly been used in degradable sutures.<sup>59-63</sup> P3HB and P4HB have been studied for their drug delivery potential,<sup>64-68</sup> but so far their rapid release<sup>69,70</sup> (almost all payload released within 24 hours), very slow polymer degradation<sup>71,72</sup> (*in vitro* and *in vivo* polymer weight loss between 5% and 15% at 6 months) and extensive initiation of inflammatory responses<sup>73,74</sup> have made them poor candidates for vaccine applications. PCL has been studied more extensively than PHB<sup>75-87</sup> and is FDA-approved for drug delivery and sutures. However, PCL has

been shown to undergo extremely slow degradation<sup>75,76,83-85</sup> (*in vitro* and *in vivo* polymer weight loss of between 14 and 20% around 1 year), release payload with high burst (40 – 70%) followed by very slow remaining extended release, and possess agent-dependent loading efficiency<sup>77-80,82,86,87</sup> (14 – 70%) making it questionable for vaccine delivery applications.

For polyesters, as well as other degradable polymers, the erosion mechanism of the material is of significant importance. *von Burkersroda et al.*<sup>88</sup> provide an overview of the kinetics that dictate whether a degradable polymer will undergo surface, bulk, or a combined erosion profiled. Essentially the erosion mechanism depends on the magnitude of water diffusion into the device compared to the rate at which the material undergoes dissolution. For degradable polymers, dissolution is heavily dependent on polymeric bond hydration. Fig. 2.6 illustrates the differences in these mechanisms.

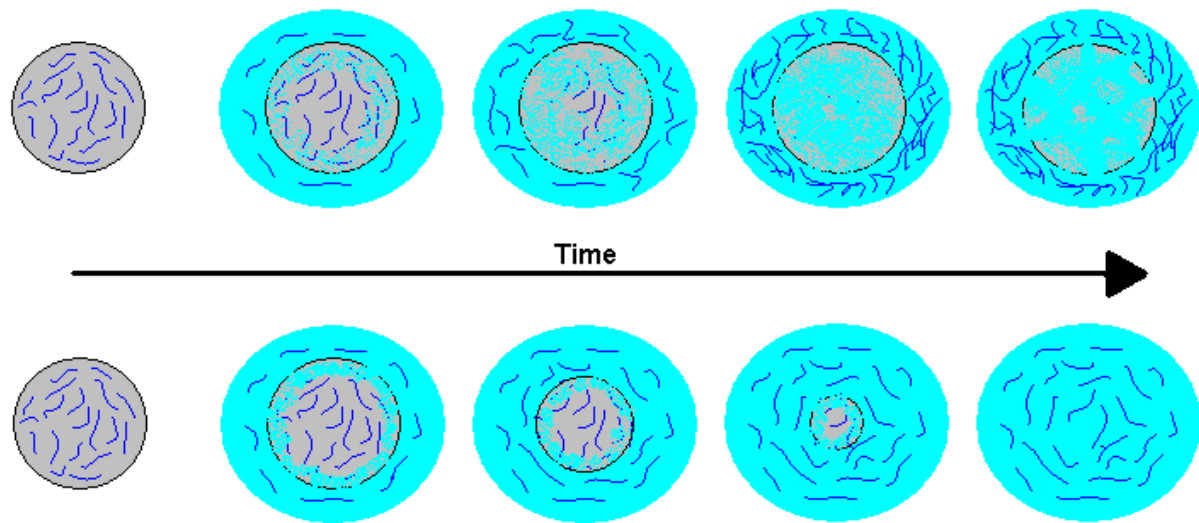


**Figure 2.6.** Schematic comparing bulk and surface erosion. In bulk erosion (top), water penetrates the device quickly allowing for the dissolution of encapsulated material almost exclusively by diffusion. In surface erosion (bottom), water cannot penetrate the device and must force dissolution at the surface to degrade the material layer-by-layer.

Bulk erosion is characterized by a diffusion dependent release of payload since water will reach the encapsulated material much more quickly than the degradation and erosion of the polymeric device. In addition, once water infiltration has occurred, all hydrolytically labile bonds can be attacked simultaneously throughout the material. These types of materials tend to fissure and break into smaller subunits before completing degradation. In contrast, when water diffuses slowly compared to the rate of erosion, the material is said to be surface eroding. These devices require the degradation of the surface polymer and dissolution of the resulting monomer to allow for encapsulated payload release.

Within bulk erosion there exist two erosion profiles, fast degrading and slow degrading. The differences are highlighted in Fig. 2.7.

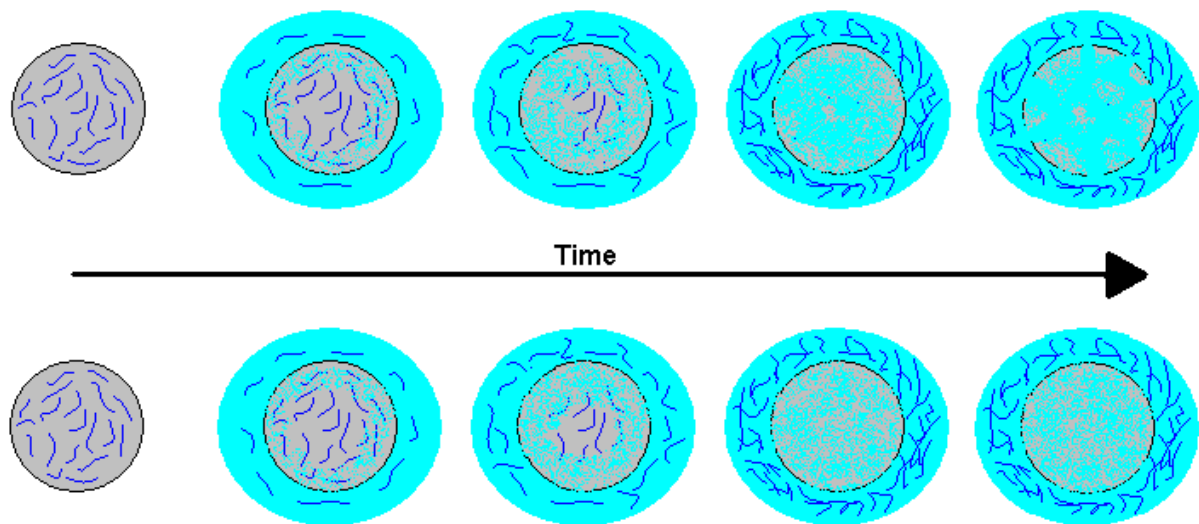


**Figure 2.7.** Schematic comparing bulk eroding systems possessing fast and slow polymeric degradation. In fast degrading systems (top), while payload release is still a function of diffusion, the material degrades and breaks apart rather quickly after release. In slow degrading systems (bottom), even though water has diffused through the bulk and released encapsulated materials, the device's degradation is very slow.

When degradation is quick, the device can be broken apart and digested or excreted by the body. This is desirable since payload has already been released and the function of the delivery device has finished. When degradation is slow, the device is able to persist. In most applications this behavior is unwanted since it can lead to inflammation or even a granulomatous response in which the biomaterial is coated in immune cells.<sup>89</sup>

All polyesters undergo bulk erosion due to the stability of ester bonds, but the degradation of these bonds is dependent on the chemistry of the backbone between bonds. For PGA, the single carbon chain allows for the polymer to be very hydrophilic. Even though PLA has only a two carbon chain backbone, its degradation is significantly slower. For PGA, PLA and PLGA, the degradation is quick enough for the polymer to be considered a fast degrading, bulk eroding material. In the cases of P3HB, P4HB and PCL, the polyester device can persist for years with little degradation. In nearly all examples of biomaterial use, this is an undesirable property and one of the major reasons these polymers have yielded little potential as vaccine delivery vehicles.

Even with the extensive use of polyesters in drug delivery applications, there still exist significant shortcomings with their use. The biggest issues are the limited flexibility in tuning payload release, the formation of low pH microenvironments, and the constant moisture exposure of payload. Since PLA and PLGA are the only suitable polyester vaccine delivery options as of now, there is a significant lack of control in payload release. While the lactic acid component of PLGA can be easily modulated between 50% and 100%, the release profiles of encapsulated material do not significantly change.<sup>90-92</sup> Coating the surface of devices<sup>90,93</sup> has been used to overcome this issue, but changing surface chemistry could drastically modulate function and interaction with the host and host cells.

Another issue with polyesters is that when they degrade, their monomers (lactic acid and glycolic acid) significantly decrease the pH of their environment to as low as 1.5.<sup>94,95</sup> Many drugs can be significantly affected by low pH, especially recombinant protein and subunit based vaccines (e.g., tetanus toxoid and diphtheria toxoid).<sup>44,96,97</sup> Also, the bulk erosion of polyesters allows for significant residence time with water for encapsulated materials. These factors combine to allow for sensitive amino acids like aspartic acid to hydrolyze very quickly<sup>98</sup> and proteins like insulin and uterocalin to aggregate, hydrolyze, and change conformation.<sup>99-101</sup> In order to neutralize monomer acidity, the incorporation of bases ( $\text{Mg}(\text{OH})_2$  and  $\text{MgCO}_3$ ) into PLGA has been proposed.<sup>102,103</sup> While the acidity was reduced, the requirement of multiple compounds (stabilizers, anti-acids, etc.) in addition to desired payload could modulate release profiles and decrease encapsulation efficiency. While polyesters have been extensively used in drug and vaccine delivery, they possess significant limitations that must be accounted for in order to improve their function.

#### 2.3.2.2 Acid-Catalyzed Polymers

The need for surface degrading polymers for drug delivery led Dr. Joseph Heller to the discovery of acid-catalyzed polymers.<sup>104-109</sup> Acid-catalyzed polymers used in drug delivery have focused on the potential of polyacetals, polyketals and polyorthoesters (Fig. 2.8).

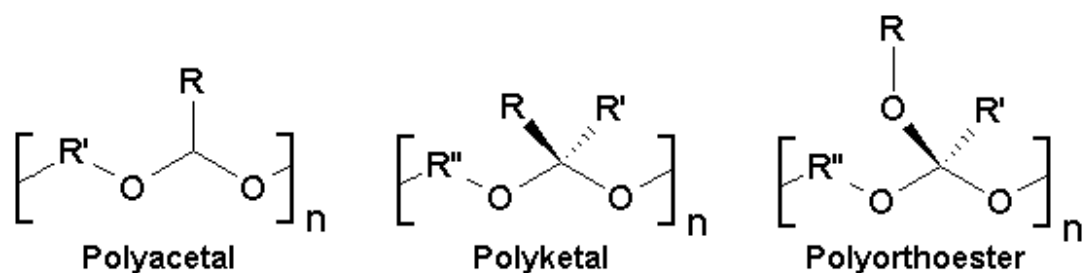


**Figure 2.8.** Chemical structures for acid-catalyzed polymers.

Non-degradable polyacetals have been used biomedically as fracture stabilizers and prosthetic materials (Delrin<sup>®</sup>) for over 30 years.<sup>110-114</sup> Lately, the use of acid-catalyzed degradable polyacetals for drug delivery has been more extensively investigated.<sup>115-120</sup> The approaches for therapeutic delivery being explored with polyacetals are polymer conjugation<sup>115-117</sup>, thermoresponsive gels<sup>118</sup> and microparticles.<sup>119,120</sup> In each study, drug was released much more significantly when pH was lowered from normal body pH (7.4) to between 5 and 5.5. When conjugated poly(ethylene glycol) (PEG) is incorporated into the polyacetal backbone, the polymer is hydrophilic and persists without cellular uptake leading to longer, sustained chemotherapeutic delivery.<sup>115</sup> In addition, polyacetal microparticles were able to be extensively uptake by macrophages when the correct backbone chemistry is chosen.<sup>120</sup> These early experiments provide evidence that polyacetals could be used to selectively deliver payload.

Similar to polyacetals, drug delivery with polyketals is an emerging field of research.<sup>121-125</sup> Approaches for drug delivery have used nanoparticles and microparticles (200 nm to 5  $\mu$ m). The design of these particles has been for the

delivery of antigens and therapeutics to macrophages as vaccines<sup>125</sup> or in the treatment of acute respiratory diseases<sup>124</sup>, respectively. While early results are promising, more research is necessary to determine the capabilities of these materials.

While polyorthoesters<sup>126,127</sup> have been studied for much longer than polyacetals and polyketals, research in drug delivery did not intensify until polymer synthesis techniques improved in the early 1990's. Drug delivery with polyorthoesters now includes cancer chemotherapeutics<sup>128-130</sup>, periodontal therapies<sup>131,132</sup>, anti-inflammatory drugs<sup>133</sup>, intraocular delivery<sup>134,135</sup>, anesthetics<sup>136</sup>, proteins<sup>137</sup> and DNA delivery.<sup>138</sup> The two most commonly used polyorthoester-based devices are implants and microparticles. Currently, release from these polymers, even in normal body pH conditions is not long enough for vaccine applications, but new polyorthoesters are being synthesized, like poly(ortho ester amides)<sup>139</sup>, which may lead to the development of more gradual payload-releasing polymers.

While less attention has been given to acid-catalyzed polymers than other families of polymers, their properties provide unique opportunities for their application in vaccine delivery. Antigen presenting cells (APCs) break down material internalized by endocytosis with the assistance of lysosomal fusion.<sup>140</sup> The lysosome possesses a number of tools used to degrade and process material including radical oxygen and nitrogen intermediates, enzymes and proton pumps. The proton pumps are of particular interest since they are able to

drastically reduce vesicle pH from 7.4 to between 5 and 5.5.<sup>140</sup> Acid-catalyzed polymers can utilize this behavior to improve vaccine delivery. By maintaining polymer structure in normal physiological pH and rapidly degrading in lysosomal pH, acid-catalyzed polymer vaccine delivery vehicles can direct their payload release within APCs. In addition, the degradation products of this family of polymers have been shown to not induce microenvironment pH changes and are very biocompatible.<sup>120</sup> As the field of acid-catalyzed polymers matures, vaccine delivery applications may be further developed.

### 2.3.2.3 Polyanhydrides

Since initial research showed polyanhydrides to possess good biocompatibility and drug delivery potential, significant research has been conducted with these materials.<sup>141-155</sup> The general chemical structure for a polyanhydride is shown in Fig. 2.9.

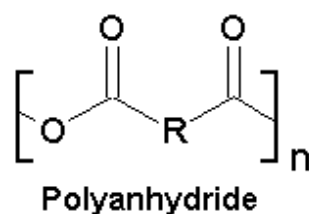


**Figure 2.9.** Chemical structure of a polyanhydride.

Research in polyanhydride drug delivery spans treatments for glaucoma<sup>156,157</sup>, Alzheimer's disease<sup>158,159</sup>, cartilage repair<sup>160</sup>, brain cancer<sup>161,162</sup>, osteomyelitis<sup>163,164</sup>, seizure suppression<sup>165</sup> and prolonged delivery of

anesthetic<sup>166</sup>, chemotherapeutics<sup>167,168</sup>, insulin<sup>169</sup>, analgesic<sup>170</sup>, antibiotic<sup>171</sup> and proteins.<sup>172</sup> The reason polyanhydrides are able to be used in the delivery of such a large number of therapeutics for a variety of diseases is due to their unique material properties not possessed by most other polymeric families. *von Burkersroda et al.*<sup>88</sup> state that the half-life of anhydride degradation is two orders of magnitude greater than polyketals and polyorthoesters, five orders of magnitude greater than polyacetals and six orders of magnitude greater than polyesters. This indicates that anhydrides are very susceptible to hydrolytic degradation. By tuning the degree of hydrophobicity of the backbone chemistry, polyanhydride devices can be modulated from fast degrading (10 days) to very slow degrading (over 1 year). With most backbone chemistries (aliphatic or aromatic hydrocarbons), the devices act as surface degrading materials. The incorporation of hydrophilic groups (e.g., ethylene glycol) shifts the degradation towards a combination of bulk and surface erosion. In addition, the monomers released from polyanhydride degradation are not nearly as acidic (4.2 – 7.5) as those in polyester degradation (1.5 – 3.6).<sup>152,173</sup> The milder pH microenvironment combined with surface erosion preventing hydrolytic aggregation make polyanhydrides promising materials for recombinant protein and subunit vaccine delivery.

### 2.3.2.4 Polyethers

Synthetically derived and naturally-inspired polyethers have been used in polymeric drug delivery for nearly 30 years.<sup>174-176</sup> The most commonly used polyethers for drug delivery are shown in Fig. 2.10.

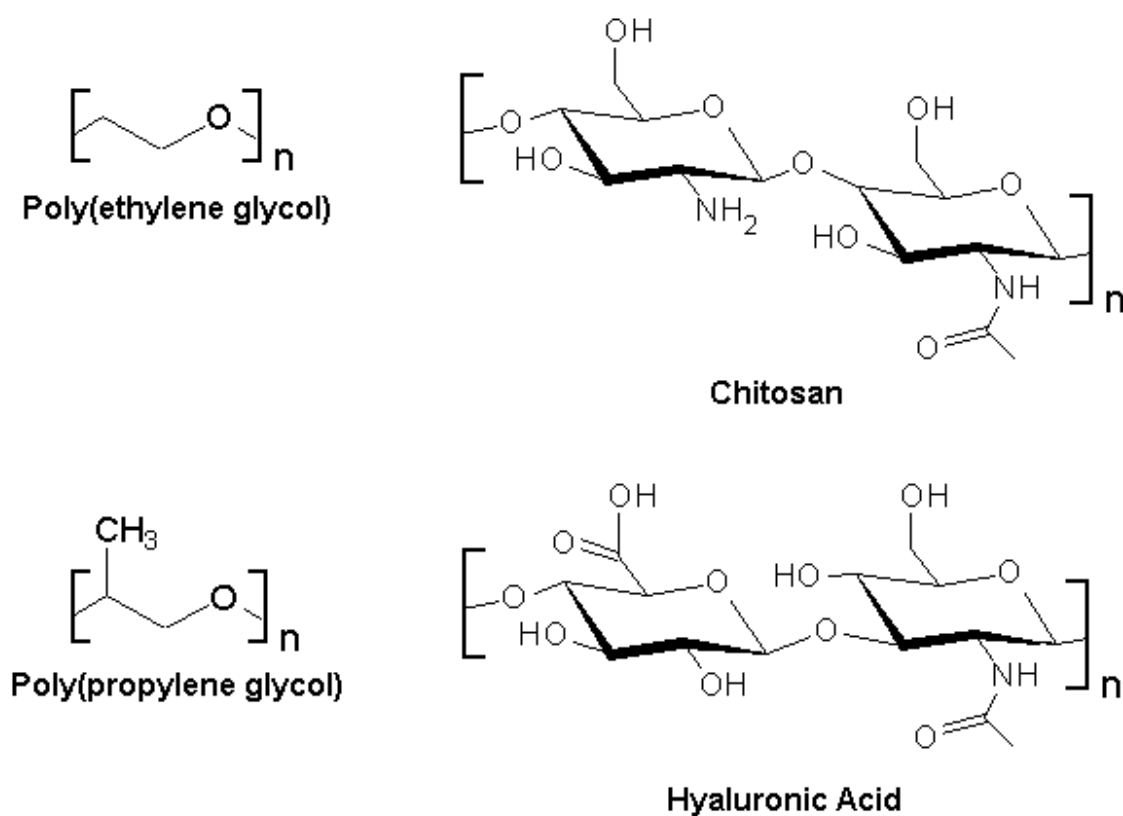


**Figure 2.10.** Chemical structures of polyethers.

Poly(ethylene glycol) (PEG) and poly(propylene glycol) (PPG) have been used in numerous biomaterials from triblock Pluronic ( $[\text{PEG}]_n-[\text{PPG}]_m-[\text{PEG}]_n$ ) to being used in concordance with many of the previously described polymer groups.

Pluronic is of particular importance since the hydrophobic PPG and hydrophilic PEG form very small micelle particles (~ 10 to 100 nm in diameter)<sup>177</sup> by self assembly in water. This amphiphilic material allows for high payload loading (20 to 30 wt%)<sup>178</sup> of hydrophobic drugs into the core while possessing a hydrophilic shell making the particles easy to administer. Also, amphiphilicity allows for the particle to interact with biological membranes and hydrophobic surfaces. Other polymeric groups have benefited from the research of PEG. Drug devices fabricated out of polyesters, polyanhydrides and acid-catalyzed polymers coated with PEG have been shown to possess a "stealth" effect in which the hydrophilic PEG opposes interactions with the host, especially phagocytosis and cellular adhesion.<sup>179-181</sup> PEG has also been incorporated into the backbone of these polymers to facilitate desired characteristics like amphiphilicity in polyanhydrides<sup>182,183</sup>, acid catalyzed polymers<sup>118,119,184</sup> and PCL.<sup>185,186</sup>

Naturally derived polymers like chitosan and hyaluronic acid have shown promise as drug delivery vehicles as well.<sup>187-190</sup> These polymers are used in a similar fashion as the synthetic polyethers. In drug delivery they have been used as hydrogels<sup>187,188</sup>, microparticles<sup>190</sup>, as stealth or Trojan coatings<sup>189</sup> or polymerized with other polymers of interest.

Polyethers do not readily undergo hydrolytic degradation since the ether bond is very stable in water. Instead, polyethers can be either degraded by enzymes or through oxidation or can be dissociated from the device and excreted. While there are specific enzymes for chitosan (papain) and hyaluronic

acid (hyaluronidase), polyether degradation has only been extensively reported in bacterial cultures.<sup>191,192</sup> The use of high molecular weight PEG is of most concern since slow *in vivo* degradation could lead to significant accumulation. It appears that the use of polyesters in combination with other biomaterials or in low molecular weight forms may be safest.

### 2.3.2.5 Other Polymers

While the four groups introduced so far make up the majority of polymers used in degradable drug delivery, there are others polymers currently being studied. Some of the most promising are presented in Fig. 2.11.

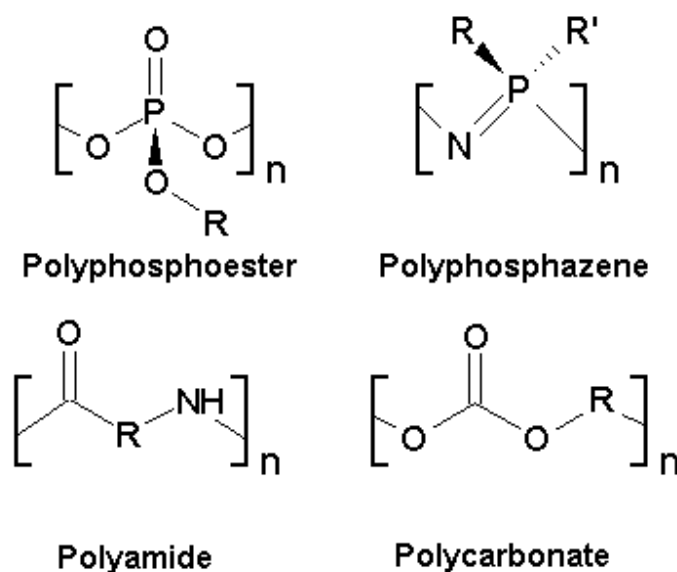


**Figure 2.11.** Chemical structures of other degradable polymers of interest.

Originally used as flame retardant materials, polyphosphoesters, also called polyphosphates, have emerged as potential drug delivery vehicles over the past

two decades.<sup>174,193-196</sup> While these polymers are being investigated for delivery of a number of different therapeutics, most research has focused on the delivery of cancer and gene therapies due to the nucleic acid backbone mimicry of the polymer. Hydrophobic polyphosphoesters have been used to deliver taxol in a manner significantly better than polyester or soluble taxol alone.<sup>196</sup> Hydrophilic polyphosphoesters show tremendous promise in the non-viral delivery of DNA.<sup>197,198</sup> Direct gene delivery by phosphoesters is promising since these new polymers are biocompatible and degradable unlike traditional cationic polymers.<sup>199</sup>

Another phosphate-based degradable polymer, polyphosphazene, has been studied for over 20 years and was originally adapted for use in drug delivery by Drs. Cato Laurencin and Robert Langer in 1987.<sup>200</sup> Polyphosphazenes are unique in that they have near universal flexibility for side-group substitution. Unlike other polymerization processes, the backbone is nearly impossible to disrupt by active groups in the side chains and side group substitution is performed after polymerization has been completed.<sup>201</sup> Provided the correct side groups are chosen, the phosphonitrogen bond is hydrolytically unstable. These polymers could be used for the delivery of diuretics<sup>202</sup>, vaccines<sup>203-205</sup>, analgesics,<sup>206,207</sup> insulin,<sup>208</sup> chemotherapeutics<sup>209</sup> and DNA.<sup>210</sup>

While polyamides have been used as suture fibers (nylon)<sup>211</sup> and as membranes to resist microfloral and enzymatic damage for some time<sup>212,213</sup>, only recently has the research focused on drug delivery applications.<sup>214-220</sup> The

applications of these polymers range from delivery across the blood-brain barrier,<sup>214</sup> delivery of DNA,<sup>219</sup> and intracellular endolysosomal disruption.<sup>216</sup> Unfortunately, the amide bond is even more hydrolytically stable than the ester bond and is 10 fold more stable than an anhydride bond.<sup>88</sup> Amides can be catalyzed by strong acids or some enzymes, but the enzymes identified so far are all bacterial in origin.<sup>221</sup> Limited hydrolysis and unknown enzymatic degradation have kept polyamides from being further investigated as drug delivery vehicles.

Polycarbonates were originally developed for biomedical use by Drs. Joachim Kohn and Robert Langer in 1986.<sup>222</sup> While poly(iminocarbonates) initially showed great promise as vaccine adjuvants and delivery vehicles<sup>222</sup>, the carbonate bond was easier to synthesize for their novel tyrosine-derived polymers.<sup>223</sup> Polycarbonate research has shown that they are resistant to acid degradation<sup>224</sup>, have backbone-independent release over long periods of time<sup>223</sup> and do not result in a high pH microenvironment.<sup>225</sup> They have been used to deliver analgesics<sup>226</sup> and chemotherapeutics.<sup>227</sup> While early research is promising, being unable to tailor polymer properties to generate desired release profiles limits the potential for these materials.

In addition to the degradable polymers reviewed above, other novel chemistries are being developed. One of the current trends has been the development of combination polymers. Examples of these are poly(ester amides), poly(ortho ester amides), poly(anhydride esters) and poly(ether ester

amides). These materials are often fabricated in block or alternating structures. The thrust behind designing these new polymers is to take advantage of the best material properties of each family.

### **2.3.3 Polymeric Adjuvants**

Degradable polymers have been studied specifically as adjuvants and vaccine delivery vehicles for about 15 years.<sup>54</sup> Some promising results continue to make these attractive materials for the development of single dose vaccines.<sup>228,229</sup> The ability to stabilize and sustain release of immunogens over an extended period of time has been a hallmark of polymeric vaccine delivery systems. In addition, other adjuvants (e.g. MPLA and CpG DNA) may be encapsulated within polymer particles to synergistically enhance the immune response and create pathogen mimicking particles.<sup>230</sup> Polymer chemistry has been shown to induce immunomodulatory behavior in the host which could greatly expand the capabilities of these devices.<sup>231</sup> Maintenance of vaccine efficacy by polymer-based systems was independent of delivery route (oral, intranasal and parenteral), which is another benefit of these materials.<sup>232</sup>

Controlled release of antigen is provided by one of two profiles, pulsatile or continuous. Pulsatile release is characterized by short burst of payload release, whereas continuous release is achieved when payload is released slowly and constantly over time. When APCs take up releasing particles, antigen can be delivered intracellularly to facilitate the initiation of the immune response. Uptake would seem to be helpful for continuous systems, but disadvantageous

for pulsatile delivery. For pulsatile systems, the particles should be a depot that can hold off secondary release until a later time. Continuous release has the advantage of being able to continually prime the immune response whereas pulsatile release could cause the induction of high antibody levels mimicking traditional multi-dose vaccination schedules.

The two most widely studied polymer classes for vaccine delivery are polyesters<sup>43,53,54,96,97,102,232-236</sup> and polyanhydrides.<sup>141,237-247</sup> Other polymers have also been evaluated and some have shown success<sup>119,137,203-205,222,248-252</sup>. Since drug delivery by nanoparticles is a newly emerging area of research, most published work is on microparticles.

#### 2.3.3.1 *In vivo* Efficacy

Polyester microparticles have been the most widely studied polymer delivery vehicles. They have been proven effective as vaccine strategies by the induction of protective immunity *in vivo*.<sup>54,232-236</sup> Antigen-loaded microparticles have been shown to create a depot for antigen delivery and enhanced particle uptake by APCs.<sup>234</sup> Specifically, PLGA uptake by both macrophages after intraperitoneal injection and dendritic cells after intradermal route has been published.<sup>253</sup> Gupta et al. have shown that blank PLGA microparticles can enhance cytokines and cause cell proliferation when they are exposed to either macrophages or DCs *in vitro*.<sup>44</sup> Furthermore, PLGA microparticles have been shown to enhance antigen presentation via MHC I leading to increased cytotoxic T cell activation.<sup>254-256</sup> In these studies, many experiments were conducted *in*

*vitro* and included MPLA or multiple doses. Hence, the results convolute the argument of the polymer microparticles by itself. PLGA microparticle-based vaccines have been successful in inducing immune response to antigens for *Yersinia pestis*, HIV, *Bordetella pertussis*, measles virus, diphtheria toxin, ricin toxoid, and others.<sup>44,257,258</sup> Vaccine delivery routes include intradermal, intravaginal, intranasal, oral and parenteral. Vaccinated animals in some studies showed responses over a year after single immunization.<sup>44,258</sup> Many groups have published work on single-dose vaccines based on PLGA microparticles.<sup>259-262</sup> There is no consensus opinion on whether all of this evidence proves PLGA-based vaccines are more efficacious than alum. Some studies show higher antibody titers<sup>255</sup> whereas other studies show similar or lower titers.<sup>259</sup> In addition to titer data, there seems to be incongruent literature about what type of immune response PLGA microparticles elicit. These uncertainties may be as attributable to antigenic dose, encapsulation method, immunization route and particle size.<sup>256,263</sup> An example of these effects was demonstrated when intraperitoneal delivery induced a Th1 response while intramuscular delivery induced a Th2 response.<sup>256</sup> Despite all of their promise, no PLGA-based vaccines have been FDA approved.

Polyanhydrides offer many unique advantages over polyesters including surface erosion, protein stabilization, and chemistry-dependent degradation. They have been approved by the FDA for use as biomedical devices and have been shown to be able to be processed into payload-encapsulated

microparticles<sup>126</sup> and nanoparticles<sup>152,264</sup> with relative ease. Kipper et al. were able to show unique tetanus toxoid (TT) immunization potential with polyanhydride microparticles.<sup>231</sup> Microparticles were loaded with small quantities of TT and delivered to mice. These experiments showed that antigenicity was maintained and that the microparticles acted as superb adjuvants to the toxoid vaccine. The most interesting finding was that the particles induced immunomodulatory behavior *in vivo*. Antibody titers (IgG1 & IgG2a) were compared by enzyme-linked immunosorbent assay (ELISA) to determine the balance of the (Th2 – antibody-mediated v Th1 – cell-mediated) response generated by the vaccine. As expected, TT alone gave a Th2 dominant response. When TT was delivered solubly as well as encapsulated within 20:80 CPH:SA or 50:50 CPH:SA microparticles, a balanced Th1/Th2 response was initiated. This is the first time polyanhydride-based immunomodulatory behavior has been shown in vaccination. Recent research has shown that 50:50 CPTEG:CPH nanoparticles delivered in a single-dose intranasally were able to induce long-lived, high affinity IgG1 antibody that was able to maintain long-term protection against plague through 23 weeks post-vaccination.<sup>265</sup> With strong immune responses generated by polyanhydrides of different size and chemistry with different vaccine candidates, polyanhydrides can be utilized as a vaccine delivery platform against a wide array of infectious diseases.

There have been limited efforts focused on polyanhydride-based vaccine delivery. Some groups have looked at the use of vaccine delivery with conjugate

chemistry systems that contain an anhydride bond and a secondary degradable bond. One attempt was the design of poly(anhydride-co-imide) with the adjuvant L-tyrosine (trimellitylimido-L-tyrosine) copolymerized with CPH:SA.<sup>239,243</sup> While vaccine release from these polymers was shown to be carried out in a controlled manner and polymer implants inserted into mice were well tolerated, publications about this material ceased 10 years ago. More recent literature by Pfeiffer et al. shows the design of poly(ester-anhydride):poly( $\beta$ -amino ester) microparticles and nanoparticles to deliver DNA to macrophages.<sup>244</sup> While the work does not explicitly state that the novel material will be used for DNA vaccines, other research conducted by this group gives evidence that this is probably the intended use.

Few studies have been conducted to compare polyesters to polyanhydrides as vaccine delivery vehicles, but some give insight into the potential of polyanhydrides. Mathiowitz et al. showed that microparticles and nanoparticles composed of poly(fumaric-co-sebacic acid) (FA:SA) had strong adhesive interactions with gastrointestinal mucosal surfaces in rats.<sup>266</sup> PLA showed minimal association and uptake. Facilitating mucosal adhesion is crucial to delivering antigen for mucosal immunization. Unsurprisingly, they showed that DNA and anticoagulant delivery by FA:SA was much better than that from PLA alone. In a different study, methylvinylether / maleic anhydride polymer [p(PVM/MA)] nanoparticles were shown to effectively deliver *Salmonella enteritidis* extract yielded a 80% survival among mice. While p(PVM/MA) is non-

degradable, it still possesses an anhydride group. In another study, these particles were able to provide non-specific protection against *S. enteridis* whereas poly( $\epsilon$ -caprolactone) could not. Thus, the anhydride chemistry was able to mediate an interaction the polyester could not.

Two other polymers (chitosan and polyphosphazenes) have also shown significant promise as degradable vaccine delivery vehicles. Chitosan, a synthetic cationic polysaccharide, has been shown to be easy to formulate into antigen-loaded microparticles.<sup>267</sup> The immune bias for chitosan microparticle vaccines seems to be more dependent on the route of delivery than the nature of the adjuvant itself.<sup>268,269</sup> Intranasal delivery of N-trimethyl chitosan chloride (TMC) loaded with diphtheria toxoid enhanced the immune response over a conventional alum-based vaccine.<sup>267</sup> This was probably a result of nasal mucosa penetration by chitosan due to its mucoadhesive properties.<sup>270,271</sup> Additional studies have shown that molecular weight and quaternization of the trimethyl group greatly influence the magnitude of the immune response.<sup>272</sup>

Polyphosphazenes have also shown promise as an adjuvant. In 1997, Payne et al. of the Virus Research Institute showed poly[di(carboxylatophenoxy)phosphazene] (PCPP) was a very potent adjuvant for influenza.<sup>204</sup> In this experiment they used soluble polymer, so it functioned only as an adjuvant and not as a delivery vehicle as well. The adjuvanticity was so robust that after a single immunization, mice maintained high antibody titers for at least 6 months. It would take 3 separate doses of adjuvants like MP59 and

MPLA to reach the antibody titers found in this study. The group showed that even aged mice (22 months old) could achieve a robust antibody response to influenza virus adjuvanted with PCPP. In addition, they were able to show its adjuvanticity potential with other immunogens for the diseases hepatitis B and herpes. In 2007, Muwiri et al. published work recently studying PCPP as well as a new polymer, poly[di(sodium carboxylatoethylphenoxy)phosphazene] (PCEP).<sup>205</sup> Chemical structures of these two polymers are shown in Fig. 2.12.

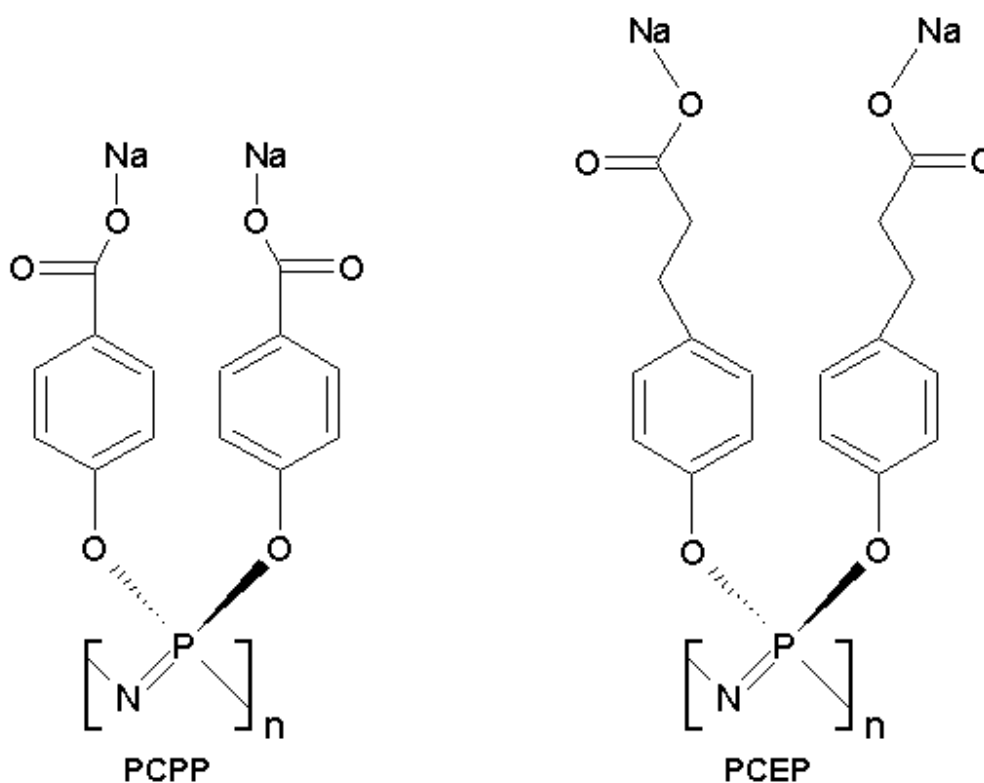


**Figure 2.12.** Chemical structures of PCPP and PCEP polymers.

Their work demonstrates that both polyphosphazines are excellent adjuvants for BSA and X:31 H3:N2 influenza antigen. BSA-specific antibody titers were greatly

increased for both adjuvants and X:31-specific antibody titers were very high for just PCEP when compared to both the antigen alone and the antigen with alum. In addition, the number of IFN- cytokine secreting cells were much greater for X:31 with PCEP than with any of the other groups. This complements the higher IgG2a titers seen compared to any of the other groups. All mice had high numbers of IL-4 cytokine secreting cells. This data shows the potential to use soluble phosphazene polymers as adjuvants over traditionally accepted ones.

### 2.3.3.2 Polymer Interactions with APCs

While degradable polymers have been shown to function as strong adjuvants *in vivo*, little is known about the mechanisms these materials exploit to initiate a robust immune response. Recent research has studied the interaction of polymers with APCs to better understand this behavior. Cell population-based analysis has been used to investigate the overall effect of particles on a group of cells. In research with APCs, this includes utilizing flow cytometric evaluation of fluorescently-tagged monoclonal antibody detection of cell surface marker expression and enzyme-linked immunosorbent assay or multiplex conjugated-bead assay detection of APC secreted cytokines. These techniques have been used to probe the interactions between APCs and particles composed of polyesters<sup>229,273-277</sup> and polyanhydrides.<sup>279-283</sup>

Research conducted by Audran et al. was the first to show PLGA microparticles could enhance antigen delivery to APCs, dendritic cells (DCs) and macrophages, *in vitro*.<sup>229</sup> Further studies conducted by Samuel and

colleagues<sup>273,274</sup> showed that PLGA nanoparticles were able to be internalized by dendritic cells (DCs) and enhance cell surface marker expression (MHC II and CD86). When particles were loaded with MUC1 mucin peptide, a cancer antigen, DCs were able to activate naïve T cells and cause their proliferation. Most recent work by Babensee and colleagues<sup>275-277</sup> verified the results observed by Samuel but also showed that PLGA particles were able to induce production of the pro-inflammatory cytokines TNF- $\alpha$  and IL-6. Sharp et al. showed that PLGA particles may be causing DC activation by specific uptake through the NALP3 inflammasome causing the production of the strong pro-inflammatory cytokine, IL-1 $\beta$ .<sup>278</sup> While a very interesting mechanistic finding, this result was only seen when DCs were co-stimulated with PLGA particles and LPS.

Research conducted by Narasimhan and colleagues has shown a direct correlation between polyanhydride chemistry and DC activation.<sup>279-283</sup> Petersen et al. showed that as nanoparticle hydrophobicity increased, DC cell surface marker expression (MHC II, CD40, CD86 and CD209) decreased, but cytokine secretion (IL-6 and IL-12p40) increased.<sup>279,280</sup> This result was supported by Torres et al. for polyanhydride microparticles.<sup>281</sup> Ulery et al. have shown that nanoparticles composed of a copolymer of very hydrophobic and amphiphilic monomers can induce both enhanced DC cell surface marker expression and cytokine secretion.<sup>282</sup> Carrillo et al. further enhanced DC activation by chemically modifying the nanoparticle surface with carbohydrates that facilitate uptake through pathogen recognition receptors.<sup>283</sup>

Another technique, individual cell-based analysis, has been used to probe how particles traffic within cells. Fluorescent microscopy of individual cells probed with fluorescently-tagged monoclonal antibodies detecting intracellular processes is used to determine particle internalization and intracellular fate. This technique has been utilized to probe trafficking of degradable polymer particles in many cell types<sup>284-286</sup>, but only recently has been used to investigate particle behavior in APCs.<sup>264,281,287</sup> Shen et al. shows that antigen loaded PLGA nanoparticles are able to escape the endosomal pathway and deliver payload to the cytosol for extended periods of time.<sup>287</sup> PLGA stimulated DCs were able to induce antigen-specific T cell IL-2 production at a 1000-fold lower antigen dose than soluble antigen alone showing promise for DC mediated immune activation with these particles. Ulery et al. has shown polyanhydride chemistry dictates intracellular nanoparticle behavior in both macrophages<sup>264</sup> and DCs.<sup>281</sup> It was shown that hydrophobic nanoparticles get internalized, trafficked by the endosomal pathway and degraded over 48 hours. In contrast, nanoparticles composed of a copolymer of hydrophobic and amphiphilic monomers were actually able to mediate their own aggregation inside lysosomal compartments. This behavior is very similar to bacterial replication giving these particles a “pathogen-like” effect that may explain their ability to enhance cell surface marker expression and cytokine secretion unlike any other chemistry. Coupling of these two types of analyses (population and individual cell) may lead to further understanding of how degradable polymers initiate immune responses.

## **2.4 *Yersinia Pestis***

### **2.4.1 Introduction & History**

*Yersinia pestis*, the causative agent of plague, is a gram-negative, non-motile bacterium which has caused three pandemics, a number of endemics and is believed to have killed between 50 to 200 million people.<sup>288</sup> The first plague, the Justinian plague, began in Egypt in 541 A.D. and quickly spread throughout Mediterranean Europe and the Middle East over the next 3 years. For the next 100 years, epidemics cycled every 8 to 12 years causing untold damage that eventually spread to the entire known world.<sup>289</sup> After a 700 year lapse of nearly any disease outbreak, the Black Death (2<sup>nd</sup> Plague Pandemic) wreaked havoc, especially on Europe from 1347 to 1351 A.D. During that time an estimated 30 to 40% of Europe's population perished (17 to 28 million people).<sup>290</sup> While epidemics quelled after the 1480's, outbreaks were still prevalent until the 17<sup>th</sup> century. The most recent event, the third pandemic, is believed to have started in the 1850's in China following war in the Yunnan Province.<sup>291</sup> By 1900, plague had spread throughout the world including the United States. Endemics continued to occur into the 1950's, but the spread of disease and its mortality were lowered due to better public health measures and antibiotics, respectively. It was during the Hong Kong epidemic of 1894 that Alexandre Yersin and Shibasaburo Kitasato independently announced the identification of the cause of the pandemic, *Yersinia pestis*.<sup>292</sup> Yersin was able to use antiserum developed from the isolated organism to cure a plague patient in 1896.<sup>293</sup> During the

Manchurian outbreak, L-T. Wu was able to identify the difference between the bubonic and pneumonic form of the disease. This led to the use of aerosol protective measures that significantly decreased transmission. Also, this outbreak led to L-T. Wu, R.P. Strong, and others recording the most detailed epidemiological and pathological human data on pneumonic plague we have today.<sup>294,295</sup> Since this last outbreak, significant research has been conducted to define post-exposure antibiotic protocols and to design *Y. pestis* vaccines. While antibiotics can prevent mortality and allow for the host to clear infection, they must be administered within 24 hours of exposure or their effectiveness is severely diminished.<sup>292</sup> Often antibiotics (e.g., ciprofloxacin) are administered to anyone who may have been exposed to prevent the onset of disease. In order to better fight this disease, development of new therapeutic and prophylactic strategies is necessary.

#### **2.4.2 Bacterial Function within Host**

In order to develop new strategies, the transmission route of *Y. pestis* needs to be understood. Hosts tend to be one of three types, mammal, flea, or human.

##### **2.4.2.1 Mammals**

The natural reservoirs of *Y. pestis* are rodents and other animals, whereas humans are only accidental hosts. Since plague can infect such a wide variety of mammals, response is host-specific. Many carnivores from domestic dogs and

ferrets to coyotes and skunks are highly resistant to plague. Ingestion of plague infected rodents usually leads to limited to mild disease that is normally survived and cleared.<sup>296</sup> On the other hand, domestic cats and some rodents appear to be responsive to plague.<sup>297</sup> Like most infections the response by a population is very heterogeneous. While many cats and rodents die, some will have moderate natural resistance due to weakened bacteria or previous exposure. The persistence of bacteria within these hosts makes them a reservoir of bacteria that can be transmitted among the population and externally to other species. Particularly good enzoonotic hosts include some rats and gerbils<sup>298</sup> and in the United States, mice and voles.<sup>299</sup> Transfer occurs between rodents through contact and to other species by fleas.

#### 2.4.2.2 Flea

The flea is the most common transfer vehicle of plague from animal to animal and animal to human. Two days after fleas uptake bacteria from an infected host through a blood meal, bacteria replicate and create cohesive brown masses that extend through the stomach, the proventriculus, helps break up blood for digestion, and the esophagus. Between 3 and 9 days the clotting coats the entire proventriculus making it nearly impossible for the flea to gain sustenance.<sup>300</sup> The flea attempts to digest blood, but instead the blood mixes with the bacteria and gets delivered back into the host. The flea is unable to feed and eventually dies, but not without first delivering *Y. pestis* to a new host.

### 2.4.2.3 Human

In humans, there are two common mechanisms for bacterial uptake. The first is that a flea regurgitates infected blood during an attempted feed. This route, when bacteria is originally contracted from a rodent, is called sylvatic plague.<sup>298</sup> It is by far the most common method by which humans contract plague. The number of human plague cases by this method greatly increases when rodent populations go through widespread epizootics.<sup>301</sup> It is theorized that this occurs because fleas typically get their meals from rodents, but are forced to change species during epizootic incidences. Often they change over to feeding on humans and deliver *Y. pestis*. The other route is by person to person transfer often in the form of respirator droplets.

When *Y. pestis* enters the human host, it is able to cause any of three types of clinical disease: bubonic, systemic or pneumonic. If bacteria are delivered by flea transfer, then bubonic plague is the most likely disease to progress. Bacteria travel to the lymph node where they take up residence between 2 and 6 days after initial exposure. The lag time for this response is thought to be caused by the bacteria adjusting from the flea in which temperature was ambient-dependent to a host with a much higher body temperature. Patients usually experience fever, headaches, the chills and the development of very tender lymph nodes (buboes). Symptoms can also include nausea and vomiting.<sup>302</sup> These buboes become necrotic with rapidly growing populations of

bacteria. Finally, bacteremia or secondary septicemia ends up causing death in about 50% of patients who get bubonic plague.

In primary septicemic plague, the bubo is not formed and sepsis occurs within just a few days. Mortality rate is about 50% or greater because undifferentiated sepsis treatment is not effective against *Y. pestis*. The disease looks clinically similar to septicemias caused by other gram-negative bacteria. Onset of primary septicemia is very quick (1 to 2 days) and can be deadly.

A rare third disease can occur which is called primary pneumonic plague. In this case, bacteria are able to move to the lung and take up residence. In one study, about 12% of patients developed pneumonic plague from bubonic or septicemic plague.<sup>303</sup> Rapid onset of flu-like symptoms occurs with a persistent cough followed by the production of very bloody sputum. The incubation period for pneumonic plague is only 1 to 3 days. This form of the disease is nearly 100% deadly and allows for the aerosol transfer of bacteria infected droplets from person to person. Once transferred from lungs to lung, death occurs even more rapidly since the bacteria have adjusted to the human lungs as sites of proliferation and response. Most cases of pneumonic plague over the last 80 years<sup>304</sup> have been determined to be transmitted as aerosols by house cats and not by human to human transmission.<sup>303</sup>

In any disease type, it has been shown that *Y. pestis* is able to accumulate with limited interaction with neutrophils and apoptosis of macrophages.<sup>305</sup> The inability for the host to facilitate a robust immune response and the speed with

which plague become virulent indicates the need for research into efficacious vaccine systems.

### 2.4.3 Quorum Sensing in *Y. Pestis*

Quorum sensing (QS) is the use of population density dependent chemical switches to regulate gene activation and deactivation. It was first described in *Vibrio fischeri* where if the concentration of cells is high enough the bacteria activate the production of a fluorescent protein.<sup>306</sup> A cartoon depicting *V. fischeri* and its QS system is shown in Fig. 2.13.

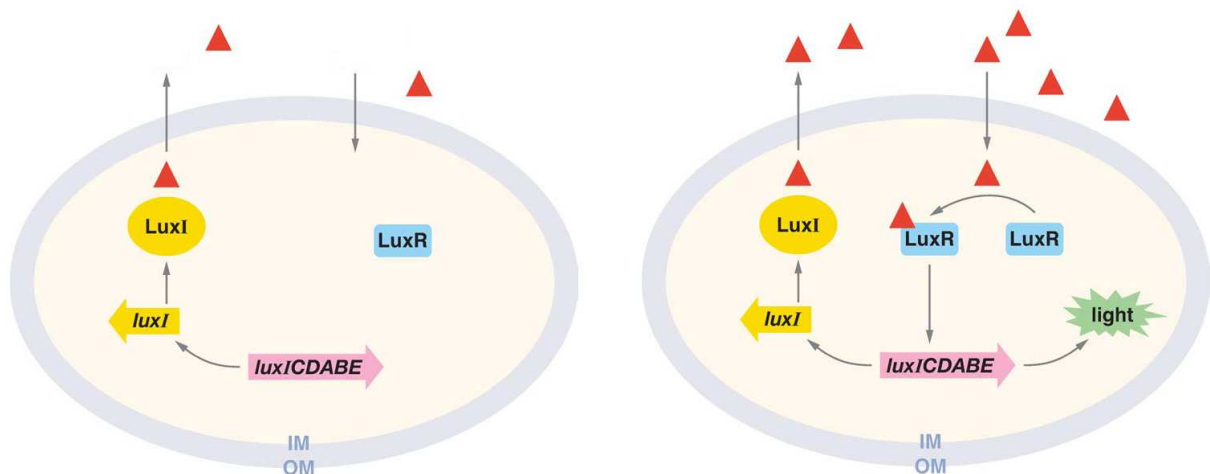


**Figure 2.13.** LuxIR network for *V. fischeri*. LuxI produces a QS agent synthase. This synthase produces small molecular weight signals that can freely diffuse in and out of cells. When the concentration of cells is not very high (left) there is not very much free signal. In comparison, if the concentration of cells is high (right) then a significant amount of signal permeates the cells. When this happens, LuxR binds the signal and becomes an active promoter for the luciferase operon. Upon activation luciferase is produced in high quantities and the cell fluoresces. It is worth noting that promotion of the luciferase operon also produces more LuxI causing a positive feedback loop. Reprinted and modified from Ref. 306.

While *V. fischeri* uses QS for bioluminescence there are many bacteria that exploit this technique to allow for density dependent virulence. *Staphylococcus aureus*, *Staphylococcus pseudintermedius*, *Salmonella typhimurium* and *Pseudomonas aeruginosa* all utilize QS systems to regulate their virulence.<sup>307</sup> *Y. pestis* utilizes three QS systems with two being of the LuxIR subtype (Fig. 2.20) and the other being LuxS (AI-2 peptide) together for biofilm formation and potentially for virulence applications.<sup>308-311</sup> While the complete function of these QS systems has yet to be elucidated, their use in biofilm formation provides evidence that the bacteria are using them to promote their survival in the host. By identification of proteins that are up- or down-regulated during QS, new vaccine candidates could be identified and explored for their ability to induce protection.

#### **2.4.4 Bioterrorism Potential**

While the need for therapy and prophylaxis for naturally occurring *Y. pestis* infections is important, it is the bacteria's potential as a bioterrorism agent that has truly driven the research towards improved pre- and post-exposure treatments. The ability for plague, especially in the pneumonic form, to disseminate quickly, kill within a matter of days, and be released in large population centers makes *Y. pestis* one of the greatest bioterrorism threats faced. For this reason, the United States Department of Defense and Centers for Disease Control and Prevention have categorized plague as a Category A pathogen.<sup>312</sup> The ability for plague to be genetically altered to overcome vaccination is an additional fear. The F1 antigen is considered a potent

immunogen that vaccinates hosts against the capsular protein of *Y. pestis*.<sup>313</sup> Sadly, the same tools that allowed for the isolation of good subunit vaccines like F1 can be used to engineer weapons-grade bacteria that can overcome these vaccines. In 1995, Drozdov et al. showed that a simple mutagenesis could remove the capsule of *Y. pestis* and maintain virulence.<sup>314</sup> Additional mutations like this could prove disastrous for defense against this bioterror agent. Another issue is the development of antibiotic resistant strains of plague. Luckily, the limited exposure of humans to *Y. pestis* since the inception of antibiotics has kept nearly all naturally occurring infections very susceptible to traditional antibiotic treatment protocols. In 1996, two cases of significantly antibiotic resistant strains in Madagascar caused a major scare. The potentially more dangerous aspect is that due to the high sequence homology of the *Y. pestis* resistance plasmid to one found in Typhi, many experts wondered if this new strain was created by natural or synthetic means.<sup>315</sup> Also, it has become known since the collapse of the Soviet Union that they were actively trying to weaponize plague.<sup>316</sup> In order to combat the issue of bioterrorism, robust and efficacious vaccination strategies must be developed.

#### **2.4.5 Vaccines against *Y. Pestis***

The first plague vaccine developed consisted of a heat-killed broth of densely grown, virulent *Y. pestis*.<sup>317</sup> This formulation probably conveyed great immunity to bubonic plague, but it was known to cause serious adverse side-effects including a fever of 102 °F. Further testing showed that this early vaccine

was not protective of mice to the pneumonic form of plague.<sup>318</sup> A formalin-killed vaccine was developed by Meyer and colleagues in the mid 1950's<sup>319</sup> and was used by the United States military during the Vietnam War, but has since been withdrawn when it was shown to have no protection against pneumonic plague.<sup>320</sup> Since these early vaccines, the development of subunit vaccines has been the main focus for the field. The two most commonly research recombinant proteins are caf1 (F1) and LcrV (V).<sup>321</sup> Most recently a fusion protein (rF1-V) of the two has been evaluated as a plague antigen.<sup>322,323</sup> While original mouse studies looked very promising, rF1-V failed to convey protection to African green monkeys even though protection was shown in cynomolgus macaques.<sup>324</sup> The absence of a plague vaccine in the United States has made this research field all the more important to protect American citizens and military personnel against bioterror attacks.

## **2.5 Conclusions**

While a number of different degradable polymers could be used in vaccine delivery, polyanhydrides exhibit properties like surface erosion, chemical flexibility, and protein stabilization that make them excellent candidates as adjuvants. The advancement in laboratory techniques now enables the fabrication and delivery of nanoparticles. Nanoparticles may be used as mucosal vaccine delivery systems due to their favorable characteristics of size and surface charge. Novel delivery systems have become more important as vaccine research has transitioned from the use of whole killed and live attenuated to

subunit vaccines. The reduction in side effects and allergy has been coupled with decrease immune response. Polyanhydride particle-based systems that can function both as adjuvants and slow-release delivery devices show great promise. Once these materials are designed, they can be evaluated with known or novel immunogens for their ability to convey protection against a number of different diseases including those with bioterrorism implications.

## 2.6 References

1. Roberts, M. Polio not eradicated 50 years on. BBC News. (2005). Retrieved on 28 March 2009 from <http://news.bbc.co.uk/2/hi/health/4433507.stm>.
2. Atkinson, W., Hamborsky, J., McIntyre, L. & Wolfe, S. Diphtheria in epidemiology and prevention of vaccine-preventable disease. *Washington D.C. Public Health Foundation*. 59 – 70 (2007).
3. Vaccine Preventable Diseases. World Health Organization. (2002). Retrieved on 28 Mar 2009 from [http://www.who.int/immunization\\_monitoring/diseases/en](http://www.who.int/immunization_monitoring/diseases/en).
4. Ehlers, S. Commentary: Adaptive immunity in the absence of innate immune responses? The un-Tolled truth of the silent invaders. *European Journal of Immunology*. **34**(7): 1783 – 1788 (2004).
5. Harlan, D.M., Karp, C.L., Matzinger, P., Munn, D.H., Ransohoff, R.M. & Metzger, D.W. Immunological concerns with bioengineering approaches. *Annals of New York Academy of Sciences*. **961**: 323 – 330 (2002).
6. Medzhitov, R. & Janeway, C. Innate immune recognition: mechanisms and pathways. *Immunological Reviews*. **173**(1): 89 – 97 (2000).
7. Janeway, C.A., Travers, P., Walport, M. & Sclomchik, M.J., editors. Immunobiology the immune system in health and disease. 6<sup>th</sup> edition. New York, NY: Garland Publishing. (2005).
8. Iwasaki, A. Mucosal dendritic cells. *Annual Review of Immunology*. **25**: 381 – 418 (2007).
9. Santana, M.A. & Rosenstein, Y. What it takes to become an effector T cell: The process, the cells involved and the mechanisms. *Journal of Cell Physiology*. **195**(3): 392 – 401 (2003).
10. Annunziato, F., Cosmi, L., Santarasci, V., Maggi, L., Liotta, F., Mazzinghi, B., Parente, E., Fili, L., Ferri, S., Frosali, F., Giudici, F., Romagnani, P., Parronchi, P., Tonelli, F., Maggi, E. & Romagnani, S. Phenotypic and functional features of human Th17 cells. *Journal of Experimental Medicine*. **204**(8): 1849 – 1861 (2007).

11. Villadangos, J.A. & Schnorrer, P. Intrinsic and cooperative antigen-presenting functions of dendritic-cell subsets in vivo. *Nature Reviews Immunology*. **7**(7): 543 – 555 (2007).
12. Rogers, P.R. & Croft, M. CD28, Ox-40, LFA-1, and CD4 modulation of Th1/Th2 differentiation is directly dependent on the dose of antigen. *Journal of Immunology*. **164**(6): 2955 – 2963 (2000).
13. McNeela, E.A. & Mills, K.H. Manipulating the immune system: Humoral versus cell-mediated immunity. *Advanced Drug Delivery Reviews*. **51**(1-3): 43 – 54 (2001).
14. Brewer, J.M. & Pollock, K.G.J. Adjuvant-induced Th2 and Th1 dominated immune responses. In: Kaufmann, S.H.E., editor. Novel vaccination strategies, 1<sup>st</sup> edition. Weinheim: WILEY-VCH Verlag GmbH & Co. KGaA. 147 – 163 (2004).
15. Heath, W.R., Belz, G.T., Behrens, G.M., Smith, C.M., Forehan, S.P., Parish, I.A., Davey, G.M., Wilson, N.S., Carbone, F.R. & Villadangos, J.A. Cross-presentation, dendritic cell subsets, and the generation of immunity to cellular antigens. *Immunological Reviews*. **199**: 9 -26 (2004).
16. Zinkernagel, R.M. Immunological memory and vaccines against acute cytopathic and noncytopathic infections. In: Broom, B.R & Lambert P-H., editors. The vaccine book, 1<sup>st</sup> edition. San Diego, CA: Academic Press, 169 – 182 (2003).
17. Ebensen, T., Link, C. & Guzman, C.A. Classical bacterial vaccines. In: Kaufman, S.H., editor. Novel vaccination strategies. Weinheim: Wiley-VCH, 221 – 242 (2004).
18. Dorner, F. & Barrett, P.N. Vaccine technology: Looking to the future. *Annals of Medicine*. **31**(1): 51 – 60 (1999).
19. Birmingham, M. & Stein, C. The burden of vaccine preventable diseases. In: Bloom, B.R. & Lambert, P-H., editors. The vaccine book, 1<sup>st</sup> edition. San Diego, CA: Academic Press, 169 – 182 (2003).
20. Breard, E., Sailleau, C., Coupier, H., Mure-Ravaud, K., Hammoumi, S., Gicquel, B., Hamblin, C., Dubourget, P. & Zientara, S. Comparison of genome segments 2, 7 and 10 of bluetongue viruses serotype 2 for differentiation between field isolates and vaccine strain. *Veterinary Research*. **34**(6): 777 – 789 (2003).

21. Sato, Y. & Sato, H. Development of acellular pertussis vaccines. *Biologicals*. **27**(2): 61 – 69 (1999).
22. Sidey, F.M, Furman, B.L. & Wardlaw, A.C. Effect of hyperreactivity to endotoxin on the toxicity of pertussis vaccine and pertussis toxin in mice. *Vaccine*. **7**(3): 237 – 241 (1989).
23. Plotkin, S.A. Disease states and vaccination: Selected cases – Introduction. In: Bloom, B.R. & Lambert, P-H. The vaccine book. 1<sup>st</sup> edition. San Diego, CA: Academic Press, 179 – 188 (2003).
24. Coenen, F., Tolboom, J.T.B.M. & Frijlink, H.W. Stability of influenza sub-unit vaccine: Does a couple of days outside the refrigerator matter? *Vaccine*. **24**(4): 525 – 531 (2006).
25. Wang, C., Ge, Q., Ting, D., Nguyen, D., Shen, H.R., Chen, J., Eisen, H.N., Heller, J., Langer, R. & Putnam, D. Molecularly engineering poly(ortho ester) microspheres for enhanced delivery of DNA vaccines. *Nature Materials*. **3**(3): 190 – 196 (2004).
26. Clinical Trials: US National Institutes of Health. Retrieved on 29 Mar 2009 from <http://clinicaltrials.gov/ct/action/GetStudy>.
27. Vogel, F.R. & Powell, M.F. A compendium of vaccine adjuvants and excipients. In: Powell, M.F. & Newman, M.J., editors. Vaccine design – The subunit and adjuvant approach, 1<sup>st</sup> edition. New York: Plenum Press, 141 – 227 (1995).
28. Cox, E., Verdonck, F., Vanrompay, D. & Goddeeris, B. Adjuvants modulating mucosal immune responses or directing systems responses towards the mucosa. *Veterinary Research*. **37**(3): 511 – 539 (2006).
29. Lutsiak, M.E., Kwon, G.S. & Samuel, J. Biodegradable nanoparticle delivery of Th2-biased peptides for induction of Th1 immune responses. *Journal of Pharmaceutics and Pharmacology*. **58**(6): 739 – 747 (2006).
30. Petrovsky, N. & Aguilar, J.C. Vaccine adjuvants: current state and future trends. *Immunology and Cell Biology*. **82**(5): 488 – 496 (2004).
31. Janeway, C.A., Travers, P., Walport, M. & Sclomchik, M.J., editors. Immunobiology the immune system in health and disease. 6<sup>th</sup> edition. New York, NY: Garland Publishing. (2005).

32. Singh, M. & O'Hagan, D.T. Recent advances in veterinary vaccine adjuvants. *International Journal of Parasitology*. **33**(5-6): 469 – 478 (2003).
33. Ott, G., Barchfeld, G.L., Chernoff, D., Radhakrishnan, R., van Hoogevest, P. & Van Nest, G. Design and evaluation of a safe and potent adjuvant for human vaccines. In: Powell, M.F. & Newman, M.J., editors. *Vaccine design – The subunit and adjuvant approach*, 1<sup>st</sup> edition. New York: Plenum, 277 – 294 (1995).
34. McNeela, E.A. & Mills, K.H. Manipulating the immune system: Humoral versus cell-mediated immunity. *Advanced Drug Delivery Reviews*. **51**(1-3): 43 – 54 (2001).
35. Foster, N. & Hirst, B.H. Exploiting receptor biology for oral vaccination with biodegradable particulates. *Advanced Drug Delivery Reviews*. **57**(3): 431 – 450 (2005).
36. Newman, K.D., Samuel, J. & Kwon, G. Ovalbumin peptide encapsulated in Poly(D,L-lactic-co-glycolic acid) microspheres is capable of inducing a T helper type 1 immune response. *Journal of Controlled Release*. **54**(1): 49 – 59 (1998).
37. Hunter, R.L. Overview of vaccine adjuvants: present and future. *Vaccine*. **20**(Suppl 3): S7 – S12 (2002).
38. O'Hagan, D.T., Wack, A. & Podda, A. MF59 is a safe and potent vaccine adjuvant for flu vaccines in humans: What did we learn during its development? *Clinical Pharmacology & Therapeutics*. **82**(6): 740 – 744 (2007).
39. Straw, B.E., Shin, S., Callihan, D. & Petersen, M. Antibody production and tissue irritation in swine vaccinated with *Actinobacillus* bacterins containing various adjuvants. *Journal of the American Veterinary Medical Association*. **196**(4): 600 – 604 (1990).
40. Schmitt, E.E. & Polistina, R.A. Cylindrical prosthetic devices of polyglycolic acid. United States Patent No. 3,297,033. (1963).
41. Schmitt, E.E. & Polistina, R.A. Polyglycolic acid prosthetic devices. United States Patent No. 3,463,158. (1967).
42. Schmitt, E.E. & Polistina, R.A. Surgical dressings of absorbable polymers. United States Patent No. 3,875,937 (1973).

43. Gunatillake, P.A. & Adhikari, R. Biodegradable synthetic polymers for tissue engineering. *European Cells and Materials*. **5**: 1 – 16 (2003).
44. Gupta, R.K., Singh, M. & O'Hagan, D.T. Poly(lactide-co-glycolide) microparticles for the development of single-dose controlled-release vaccines. *Advanced Drug Delivery Reviews*. **32**(3): 225 – 246 (1998).
45. Yeung, E. & Chaw, C.S. Cyclosporin-loaded poly(lactide) microparticles: effect of TPGS. *Journal of Microencapsulation*. **26**(1): 9 – 17 (2009).
46. Maretschek, S., Greiner, A. & Kissel, T. Electrospun biodegradable nanofiber nonwovens for controlled release of proteins. *Journal of Controlled Release*. **127**(2): 180 – 187 (2008).
47. Bunger, C.M., Grabow, N., Sternberg, K., Kroger, C., Ketner, L., Schmitz, K.P., Kreutzer, H.J., Ince, H., Nienaber, C.A., Klar, E. & Schareck, W. Sirolimus-eluting biodegradable poly-L-lactide stent for peripheral vascular application: a preliminary study in porcine carotid arteries. *Journal of Surgical Research*. **139**(1): 77 – 82 (2007).
48. Bain, D.F., Munday, D.L. & Smith, A. Modulation of rifampicin release from spray-dried microspheres using combinations of poly(DL-lactide). *Journal of Microencapsulation*. **16**(3): 369 – 385 (1999).
49. Ozalp, Y., Ozdemir, N. & Hasirci, V. Vancomycin release from poly(D,L-lactide) and poly(lactide-co-glycolide) disks. *Journal of Microencapsulation*. **19**(1): 83 – 94 (2002).
50. Lu, J., Jackson, J.K., Gleave, M.E. & Burt, H.M. The preparation and characterization of anti-VEGFR2 conjugated, paclitaxel-loaded PLLA or PLGA microspheres for the systemic targeting of human prostate tumors. *Cancer Chemotherapy and Pharmacology*. **61**(6): 997 – 1005 (2008).
51. Ataman-Onal, Y., Munier, S., Ganee, A., Terrat, C., Durand, P.Y., Battail, N., Martinon, F., Le Grand, R., Charles, M.H., Delair, T. & Verrier, B. Surfactant-free anionic PLA nanoparticles coated with HIV-1 p24 protein induced enhanced cellular and humoral responses in various animal models. *Journal of Controlled Release*. **112**(2): 175 – 185 (2006).
52. Liu, S-J., Kau, Y-C., Liaw, C-W. & Peng, Y-J. In vitro elution of vancomycin/amikacin/steroid from solvent-free biodegradable sclera plugs. *International Journal of Pharmaceutics*. **370**(1-2): 75 – 80 (2009).

53. Chong, C.S., Cao, M., Wong, W.W., Fischer, K.P., Addison, W.R., Kwon, G.S., Tyrrell, D.L. & Samuel, J. Enhancement of T-helper type 1 immune responses against hepatitis B virus core antigen by PLGA nanoparticle vaccine delivery. *Journal of Controlled Release*. **102**(1): 85 – 99 (2005).
54. Alonso, M.J., Gupta, R.K., Min, C., Siber, G.R. & Langer, R. Biodegradable microspheres as controlled-release tetanus toxoid delivery systems. *Vaccine*. **12**(4): 299 – 306 (1994).
55. Feng, S-S., Mei, L., Anitha, P., Gan, C.W. & Zhou, W. Poly(lactide)-vitamin E derivative/montmorillonite nanoparticle formulations for the oral delivery of Docetaxel. *Biomaterials*. **30**(19): 3297 – 3306 (2009).
56. Wang, D., Robinson, D.R., Kwon, G.S. & Samuel, J. Encapsulation of plasmid DNA in biodegradable poly(D,L-lactic-co-glycolic acid) microspheres as a novel approach for immunogene delivery. *Journal of Controlled Release*. **57**(1): 9 – 18 (1999).
57. Goforth, R., Salem, A.K., Zhu, X., Miles, S., Zhang, X.Q., Lee, J.H. & Sandler, A.D. Immune stimulatory antigen loaded particles combined with depletion of regulatory T-cells induce potent tumor specific immunity in a mouse model of melanoma. *Cancer Immunology and Immunotherapy*. **58**(4): 517 – 530 (2009).
58. Lu, H.H., Kofron, M.D., El-Amin, S.F., Attawia, M.A. & Laurencin, C.T. In vitro bone formation using muscle-derived cells: a new paradigm for bone tissue engineering using polymer-bone morphogenetic protein matrices. *Biochemical and Biophysics Research Community*. **305**(4): 882 – 889 (2003).
59. Cocke, W.M. Dexon - a new suture material: its use in plastic surgery. *Southern Medical Journal*. **65**(5), 629 – 630 (1972).
60. MacKinnon, A.E. & Brown, S. Skin Closure with polyglycolic acid (Dexon). *Postgraduate Medical Journal*. **54**(632): 384 – 385 (1978).
61. Lee, S., Fung, Y.C., Mastuda, M., Xue, H., Schneider, D. & Han, K. The development of mechanical strength of surgically anastomosed arteries sutured with Dexon. *Journal of Biomechanics*. **18**(2): 81 – 89 (1985).
62. Howard, C.B., McKibbin, B. & Ralis, Z.A. The use of Dexon as a replacement for the calcaneal tendon in sheep. *Journal of Bone and Joint Surgery*. **67**(2): 313 – 316 (1985).

63. Berry, M.F., Rosato, E.F. & Williams, N.N. Dexon mesh splenorrhaphy for intraoperative splenic injuries. *The American Surgeon*. **69**(2): 176 – 180 (2003).
64. Pouton, C.W. & Akhtar, S. Biosynthetic polyhydroxyalkanoates and their potential in drug delivery. *Advanced Drug Delivery Review*. **18**(2): 133 – 162 (1996).
65. Piddubnyak, V., Kurock, P., Matuszowicz, A., Glowala, M., Fiszler-Kierkowska, A., Jedlinski, Z., Juzwa, M. & Krawczyk, Z. Oligo-3-hydroxybutyrates as potential carriers for drug delivery. *Biomaterials*. **25**(22): 5271 – 5279 (2004).
66. Li, J., Li, X., Ni, X., Wang, X., Li, H., Leong, K.W. Self-assembled supramolecular hydrogels formed by biodegradable PEO-PHB-PEO triblock copolymers and alpha-cyclodextrin for controlled drug delivery. *Biomaterials*. **27**(22): 4132 – 4140 (2006).
67. Chen, C., Yu, C.H., Cheng, Y.C., Yu, P.H.F. & Cheung, M.K. Biodegradable nanoparticles of amphiphilic triblock copolymers based on poly(3-hydroxybutyrate) and poly(ethylene glycol) as drug carriers. **27**(27): 4804 – 4814 (2006).
68. Shishatskaya, E.I., Voinova, O.N., Goreva, A.V., Mogilnaya, O.A. & Volova, T.G. Biocompatibility of polyhydroxybutyrate microspheres: in vitro and in vivo evaluation. *Journal of Materials Science: Materials in Medicine*. **19**(6): 2493 – 2502 (2008).
69. Kassab, A.C., Xu, K., Denkbaz, E.B., Dou, Y., Zhao, S. & Piskin, E. Rifampicin carrying polyhydroxybutyrate micropatible spheres as potential chemoembolization agent. *Journal of Biomaterials Science Polymer Edition*. **8**(12): 947 – 961 (1997).
70. Sendil, D., Gursel, I., Wise, D.L. & Hasirci, V. Antibiotic release from biodegradable PHBV microparticles. *Journal of Controlled Release*. **59**(2): 207 – 217 (1999).
71. Gogolewski, S., Jovanovic, M., Perren, S.M., Dillon, J.G. & Hughes, M.K. Tissue response and *in vivo* degradation of selected polyhydroxyacids: Polylactides (PLA), poly(3-hydroxybutyrate) (PHB), and poly(3-hydroxybutyrate-co-3-hydroxyvalerate) (PHB/VA). *Journal of Biomedical Materials Research*. **27**(9): 1135 – 1148 (1993).

72. Qu, X-H., Wu, Q., Zhang, K-Y. & Chen, G.Q. In vivo studies of poly(3-hydroxybutyrate-co-3-hydroxyhexanoate) based polymers: Biodegradation and tissue reactions. *Biomaterials*. **27**(19): 3540 – 3548 (2006).
73. Unverdorben, M., Spielberger, A., Schywalsky, M., Labahn, D., Hartwig, S., Schneider, M., Lootz, D., Behrend, D., Schmitz, K., Degenhardt, R., Schaldach, M. & Vallbracht, C. A polyhydroxybutyrate biodegradable stent: preliminary experience in the rabbit. *Cardiovascular and Interventional Radiology*. **25**(2): 127 – 132 (2002).
74. Giavaresi, G., Tschon, M., Daly, J.H., Liggat, J.J., Sutherland, D.S., Agheli, H., Fini, M., Torricelli, P. & Giardino, R. In vitro and in vivo response to nanotopographically-modified surfaces of poly(3-hydroxybutyrate-co-3-hydroxyvalerate) and polycaprolactone. *Journal of Biomaterials Science Polymer Edition*. **17**(12): 1405 – 1423 (2006).
75. Pitt, C.G., Gratzl, M.M., Jeffcoat, A.R., Zweidinger, R. & Schindler, A. Sustained drug delivery systems II: Factors affecting release rates from poly(epsilon-caprolactone) and related biodegradable polyesters. *Journal of Pharmaceutical Science*. **68**(12): 1534 – 1538 (1979).
76. Pitt, C.G., Gratzl, M.M., Kimmer, G.L., Surles, J. & Schindler, A. Aliphatic polyesters II. The degradation of poly(DL-lactide), poly(epsilon-caprolactone), and their copolymers in vivo. *Biomaterials*. **2**(4): 215 – 220 (1981).
77. Bodmeier, R. & Chen, H. Preparation and characterization of microspheres containing the anti-inflammatory agents, indomethacin, ibuprofen, and ketoprofen. *Journal of Controlled Release*. **10**(2): 167 – 175 (1989).
78. Dordunoo, S.K., Jackson, J.K., Arsenault, L.A., Oktaba, A.M., Hunter, W.L. & Burt, H.M. Taxol encapsulation in poly(epsilon-caprolactone) microspheres. *Cancer Chemotherapy and Pharmacology*. **36**(4): 279 – 282 (1995).
79. Jameela, S.R., Suma, N. & Jayakrishana, A. Protein release from poly(epsilon-caprolactone) microspheres prepared by melt encapsulation and solvent evaporation techniques: a comparative study. *Journal of Biomaterials Science Polymer Edition*. **8**(6): 457 – 466 (1997).

80. Ferranti, Y., Maochais, H., Chabenat, C., Orecchioni, A.M. & Lafont, O. Primidone-loaded poly ( $\epsilon$ -caprolactone) nanocapsules: incorporation efficiency and in vitro release profile. *International Journal of Pharmaceutics*. **193**(1): 107 – 111 (1999).
81. Chen, D., Chen, H., Bei, J. & Wang, S. Morphology and biodegradation of microspheres of polyester-polyether block copolymer based on polycaprolactone/poly lactide/poly(ethylene oxide). *Polymer International*. **49**(3): 269 – 276 (2000).
82. Bhavsar, M.D. & Amiji, M.M. Development of novel biodegradable polymeric nanoparticles-in-microsphere formulation for local plasmid DNA delivery in the gastrointestinal tract. *AAPS PharmSciTech*. **9**(1): 288 – 294 (2008).
83. Woodward, S.C., Brewer, P.S., Moatamed, F., Schindler, A. & Pitt, C.G. The intracellular degradation of poly(epsilon-caprolactone). *Journal of Biomedical Materials Research*. **19**(4): 437 – 444 (1985).
84. Cha, Y. & Pitt, C.G. The biodegradability of polyester blends. *Biomaterials*. **11**(2): 108 – 112 (1990).
85. Chapanian, R., Tse, M.Y., Pang, S.C. & Amsden, B.G. Long term in vivo degradation and tissue response to photo-cross-linked elastomers prepared from star-shaped prepolymers of poly(-caprolactone-co-D,L-lactide). *Journal of Biomedical Materials Research Part A*. **92**(3): 830 – 842 (2010).
86. Silva-Cunha, A., Fialho, S., Naud, M-C. & Behar-Cohen, F. Poly- $\epsilon$ -caprolactone intravitreal devices: In vivo study. *Investigative Ophthalmology & Visual Science*. **50**(5): 2312 – 2318 (2009).
87. Jiao, Y.Y., Ubrich, N., Marchand-Arvier, M., Vigneron, C., Hoffman, M. & Maincent, P. Preparation and in vitro evaluation of heparin-loaded polymeric nanoparticles. *Drug Delivery*. **8**(3): 135 – 141 (2001).
88. von Burkersroda, F., Schedl, L. & Gopferich, A. Why degradable polymers undergo surface erosion or bulk erosion. *Biomaterials*. **23**(21): 4221 – 4231 (2002).
89. Griffiths, M.M., Langone, J.J. & Lightfoote, M.M. Biomaterials and Granulomas. *METHODS: A companion to methods in Enzymology*. **9**(2): 295 – 304 (1996).

90. Wang, Y., Challa, P, Epstein, D.L. & Yuan, F. Controlled release of ethacrynic acid from poly(lactide-co-glycolide) films for glaucoma treatment. *Biomaterials*. **25**(18): 4279 – 4285 (2004).
91. Zhang, Z., Lee, S.H., Gan, C.W. & Feng, S-S. In vitro and in vivo investigation on PLA-TPGS nanoparticles for controlled and sustained small molecule chemotherapy. *Pharmaceutical Research*. **25**(8): 1925 – 1935.
92. Budhian, A., Siegel, S.J. & Winey, K.I. Controlling the in vitro release profiles for a system of haloperidol-loaded PLGA nanoparticles. *International Journal of Pharmaceutics*. **346**(1-2): 151 – 159 (2008).
93. Li, J., Yuan, X., He, F. & Mak, A.F. Hybrid coating of hydroxapatite and collagen with poly(D,L-lactic-co-glycolic acid) scaffold. *Journal of Biomedical Materials Research B: Applied Biomaterials*. **86B**(2): 381 – 388 (2008).
94. Fu, K., Pack, D.W., Klibanov, A.M. & Langer, R. Visual evidence of acidic environment within degrading poly(lactic-co-glycolic acid) (PLGA) microspheres. *Pharmaceutical Research*. **17**(1): 100 – 106 (2000).
95. Ding, A.G. & Schwendeman, S.P. Acidic microclimate pH distribution in PLGA microspheres monitored by confocal laser scanning microscopy. *Pharmaceutical Research*. **25**(9): 2041 – 2052 (2008).
96. Jiang, W. & Schwendeman, S.P. Stabilization of a model formalinized protein antigen encapsulated in poly(lactide-co-glycolide)-based microspheres. *Journal of Pharmaceutical Science*. **90**(10): 1558 – 1569 (2001).
97. Xing, D.K., Crane, D.T., Bolgiano, B., Corbel, M.J., Jones, C. & Sesardic, D. Physicochemical and immunological studies on the stability of free and microsphere-encapsulated tetanus toxoid in vitro. *Vaccine*. **14**(13): 1205 – 1213 (1996).
98. Schwendeman, S.P., Costantino, H.R., Gupta, R.K. & Langer, R. in *Controlled Drug Delivery: Challenge and Strategies* (ed. Park, K.) 229 – 267 (ACS, Washington, D.C., 1997)
99. Costantino, H.R., Langer, R. & Klibanov, A.M. Moisture-induced aggregation of lyophilized insulin. *Pharmaceutical Research*. **11**(1): 21 – 29 (1994).

100. Flower, D., North, A. & Attwood, T. Mouse oncogene protein 24p3 is a member of the lipocalin family. *Biochemical and Biophysics Research Community*. **180**(1): 69 – 74 (1991).
101. Playford, R., Belo, A., Poulson, R., Fitzgerald, A.J., Harris, K., Pawluczyk, I., Ryon, J., Darby, T., Nilsen-Hamilton, M., Ghosh, S. & Marchbank, T. Effects of mouse and human lipocalin homologues 24p3/lcn2 and neutrophil gelatinase-associated lipocalin on gastrointestinal mucosal integrity and repair. *Gastroenterology*. **131**(3): 809 – 817 (2006).
102. Cui, C., Stevens, V.C. & Schwendeman, S.P. Injectable polymer microspheres enhance immunogenicity of a contraceptive peptide vaccine. *Vaccine*. **25**(3): 500 – 509 (2007).
103. Jiang, W. & Schwendeman, S.P. Stabilization of tetanus toxoid encapsulated in PLGA microspheres. *Molecular Pharmaceutics*. **5**(5): 808 – 817 (2008).
104. Choi, N. & Heller, J. Drug delivery devices manufactured from poly(orthoesters) and poly(orthocarbonates). United States Patent No. 4,093,709. (1975).
105. Choi, N. & Heller, J. Erodible agent releasing device comprising poly(orthoesters) and poly(orthocarbonates). United State Patent No. 4,138,344. (1977).
106. Choi, N. & Heller, J. Structured orthoester and orthocarbonate drug delivery devices. United States Patent No. 4,131,648. (1978).
107. Choi, N. & Heller, J. Novel orthoester polymers and orthocarbonate polymers. United States Patent No. 4,180,646. (1978).
108. Heller, J. Controlled release of biologically active compounds from bioerodible polymers. *Biomaterials*. **1**(1): 51 – 57 (1980).
109. Heller, J., Penhale, W.H. & Helwing, R.F. Preparation of poly(ortho esters) by the reaction of diketene acetals and polyols. *Journal of Polymer Science: Polymer Letters Edition*. **18**(9): 619 – 624 (1980).
110. Brown, S.A. & Mayor, M.B. The biocompatibility of materials for internal fixation of fractures. *Journal of Biomedical Materials Research*. **12**(1): 67 – 82 (1978).

111. Molster, A.O., Gjerdet, N.R., Langeland, N., Levken, J. & Alho, A. Controlled bedding instability in the healing of diaphyseal osteotomies in the rat femur. *Journal of Orthopaedic Research*. **5**(1): 29 – 35 (1987).
112. Mathiesen, E.B., Lindgren, J.U., Reinholt, F.P. & Sudmann, E. Tissue reactions to wear products from polyacetal(Delrin) and UHMW polyethylene in top hip replacement. *Journal of Biomedical Materials Research*. **21**(4): 459 – 466 (1987).
113. McKellop, H.A., Rostlund, T. & Bradley, G. Evaluation of wear in an all-polymer total knee replacement. Part 1: laboratory testing of polyethylene on polyacetal bearing surfaces. *Clinical Materials*. **14**(2): 117 – 126 (1993).
114. McKellop, H.A., Milligan, H.L. & Rostlund, T. Long-term biostability of polyacetal (Delrin) implants. *The Journal of Heart Valve Disease*. **5** (Suppl 2): S238 – S242 (1996).
115. Tomilson, R., Heller, J., Brocchini, S. & Duncan, R. Polyacetal-doxorubicin conjugates designed for pH dependent degradation. *Bioconjugate Chemistry*. **14**(6): 1096 – 1106 (2003).
116. Vicent, M.J., Tomilson, R., Brocchini, S. & Duncan, R. Polyacetal-diethylstilboestrol: a polymeric drug designed for pH-triggered activation. *Journal for Drug Targeting*. **12**(8): 491 – 501 (2004).
117. Yurkovetskiy, A.V., Hiller, A., Syed, S., Yin, M., Lu, X.M., Fischman, A.J. & Papisov, M.I. Synthesis of a macromolecular camptothecin conjugate with dual phase drug release. *Molecular Pharmaceutics*. **1**(5): 375 – 382 (2004).
118. Schacht, E., Toncheva, V., Vandertaelen, K. & Heller, J. Polyacetal and poly(ortho ester)-poly(ethylene glycol) graft copolymer thermogels: preparation, hydrolysis and FITC-BSA release studies. *Journal of Controlled Release*. **116**(2): 219 – 225 (2006).
119. Khaja, S.D., Lee, S. & Murthy, N. Acid-degradable protein delivery vehicles based on metathesis chemistry. *Biomacromolecules*. **8**(5): 1391 – 1395 (2007).
120. Paramonov, S.E., Bachelder, E.M., Beaudette, T.T., Standley, S.M., Lee, C.C., Dashe, J. & Frechet, J.M. Fully acid-degradable biocompatible polyacetal microparticles for drug delivery. *Bioconjugate Chemistry*. **19**(4): 911 – 919 (2008).

121. Heffernan, M.J. & Murthy, N. Polyketal nanoparticles: a new pH-sensitive biodegradable drug delivery vehicle. *Bioconjugate Chemistry*. **16**(6): 1340 – 1342 (2005).
122. Lee, S., Yang, S.C., Heffernan, M.J., Taylor, W.R. & Murthy, N. Polyketal microparticles: a new delivery vehicle for superoxide dismutase. *Bioconjugate Chemistry*. **18**(1): 4 -7 (2007).
123. Yang, S.C., Bhide, M., Crispe, I.N., Taylor, W.R. & Murthy, N. Polyketal copolymers: a new acid-sensitive delivery vehicle for treating acute inflammatory diseases. *Bioconjugate Chemistry*. **19**(6): 1164 – 1169 (2008).
124. Gongora, M.C., Lob, H.E., Landmesser, U., Guzik, T.J., Martin, W.D., Ozumi, K., Wall, S.M., Wilson, D.S., Murthy, N., Gravanis, M., Fukai, T. & Harrison, D.G. Loss of extracellular superoxide dismutase leads to acute lung damage in the presence of ambient air: a potential mechanism underlying adult respiratory distress syndrome. **173**(4): 915 – 926 (2008).
125. Heffernan, M.J., Kasturi, S.P., Yang, S.C., Pulendran, B. & Murthy, N. The stimulation of CD8+ T cells by dendritic cells pulsed with polyketal microparticles containing ion-paired protein antigen and poly(inosinic acid)-poly(cytidylic acid). *Biomaterials*. **30**(5): 910 – 918 (2009).
126. Shih, C., Higuchi, T. & Himmelstein, K.J. Drug delivery from catalysed erodible polymeric matrices of poly(ortho ester)s. *Biomaterials*. **5**(4): 237 – 240 (1984).
127. Heller, J. Controlled drug release from poly(ortho esters). *Annals of the New York Academy of Sciences*. **446**: 51 – 66 (1985).
128. Bernatchez, S.F., Merkli, A., Minh, T.L., Tabatabay, C., Anderson, J.M. & Gurny, R. Biocompatibility of a new semisolid bioerodible poly(ortho ester) intended for the ocular delivery of 5-fluorouracil. *Journal of Biomedical Materials Research*. **28**(9): 1037 – 1046 (1994).
129. Merkli, A., Heller, J., Tabatabay, C. & Gurny, R. Purity and stability assessment of a semi-solid poly(ortho ester) used in drug delivery systems. *Biomaterials*. **17**(9): 897 – 902 (1996).
130. Sintzel, M.B., Heller, J., Ng, S.Y., Tabatabay, C., Schwach-Abdellaoui, K. & Gurny, R. In vitro drug release from self-catalyzed poly(ortho ester): case study of 5-fluorouracil. *Journal of Controlled Release*. **55**(2-3): 213 – 218 (1998).

131. Roskos, K.V., Fritzing, B.K., Rao, S.S., Armitage, G.C. & Heller, J. Development of a drug delivery system for the treatment of periodontal disease based on bioerodible poly(ortho esters). *Biomaterials*. **16**(4): 313 – 317 (1995).
132. Heller, J., Barr, J., Ng, S.Y., Shen, H.R., Schwach-Abdellaoui, K., Gurny, R., Viven-Castioni, N., Loup, P.J., Baehni, P. & Mombelli, A. Development and applications of injectable poly(ortho esters) for pain control and periodontal treatment. *Biomaterials*. **23**(22): 4397 – 4404 (2002).
133. Solheim, E., Pinholt, E.M., Andersen, R., Bang, G. & Sudmann, E. Local delivery of indomethacin by a polyorthoester inhibits reossification of experimental bone defects. *Journal of Biomedical Materials Research*. **29**(9): 1141 – 1146 (1995).
134. Sintzel, M.B., Heller, J., Ng, S.Y., Taylor, M.S., Tabatabay, C. & Gurny, R. Synthesis and characterization of self-catalyzed poly(ortho ester). *Biomaterials*. **19**(7-9): 791 – 800 (1998).
135. Einmahl, S., Behar-Cohen, F., Tabatabay, C., Savoldelli, M., D'Hermies, F., Chauvand, D., Heller, J. & Gurny, R. A viscous bioerodible poly(ortho ester) as a new biomaterial for intraocular application. *Journal of Biomedical Materials Research*. **50**(4): 566 – 573 (2000).
136. Deng, J.S., Li, L., Tian, Y., Ginsburg, E., Widman, M. & Myers, A. In vitro characterization of polyorthoester microparticles containing bupivacaine. *Pharmaceutical Development and Technology*. **8**(1): 31 – 38 (2003).
137. Shi, M., Yang, Y.Y., Chaw, C.S., Goh, S.H., Moochhala, S.M., Ng, S. & Heller, J. Double walled POE/PLGA microspheres: encapsulation of water-soluble and water-insoluble proteins and their release properties. *Journal of Controlled Release*. **89**(2): 167 – 177 (2003).
138. Nguyen, D.N., Raghavan, S.S., Tashima, L.M., Lin, E.C., Fredette, S.J., Langer, R.S. & Wang, C. Enhancement of poly(orthoester) microspheres for DNA vaccine delivery by blending with poly(ethylenimine). *Biomaterials*. **29**(18): 2783 – 2793 (2008).
139. Tang, R., Palumbo, R.N., Ji, W. & Wang, C. Poly(ortho ester amides): Acid-labile temperature-responsive copolymers for potential biomedical applications. *Biomacromolecules*. **10**(4): 722 – 727 (2009).

140. Gatti, E. & Pierre, P. Understanding the cell biology of antigen presentation: the dendritic cell contribution. *Current Opinion in Cell Biology*. **15**(4): 468 – 473 (2003).
141. Rosen, H.B., Chang, J., Wnek, G.E., Lindhardt, R.J. & Langer, R. Bioerodible polyanhydrides for controlled drug delivery. *Biomaterials*. **4**(2): 131 – 133 (1983).
142. Bindschaedler, C., Leong, K., Mathiowitz, E. & Langer, R. Polyanhydride microsphere formulation by solvent extraction. *Journal of Pharmaceutical Science*. **77**(8): 696 – 698 (1988).
143. Tabata, Y. & Langer, R. Polyanhydride microspheres that display near-constant release of water-soluble drug compounds. *Pharmaceutical Research*. **10**(3): 391 – 399 (1993).
144. Tabata, Y., Domb, A. & Langer, R. Injectable polyanhydride granules provide controlled release of water-soluble drugs with a reduced initial burst. *Journal of Pharmaceutical Science*. **83**(1): 5 – 11 (1994).
145. Shieh, L., Tamada, J., Chen, I., Pang, J., Domb, A. & Langer, R. Erosion of a new family of biodegradable polyanhydrides. *Journal of Biomedical Materials Research*. **28**(12): 1465 – 1475 (1994).
146. Gopferich, A. Erosion of composite polymer matrices. *Biomaterials*. **18**(5): 397 – 403 (1997).
147. Gao, J., Niklason, L., Zhao, X.M. & Langer, R. Surface modification of polyanhydride microspheres. *Journal of Pharmaceutical Research*. **87**(2): 246 – 248 (1998).
148. Leach, K.J. & Mathiowitz, E. Degradation of double-walled polymer microspheres of PLLA and P(CPP:SA)20:80. I. In vitro degradation. *Biomaterials*. **19**(21): 1973 – 1980 (1998).
149. Burkoth, A.K., Burdick, J. & Anseth, K.S. Surface and bulk modifications to photocrosslinked polyanhydrides to control degradation behavior. *Journal of Biomedical Materials Research*. **51**(3): 352 – 359 (2000).
150. Berklund, C., Kipper, M.J., Narasimhan, B., Kim, K.K. & Pack D.W. Microsphere size, precipitation kinetics and drug distribution control drug release from biodegradable polyanhydride microspheres. *Journal of Controlled Release*. **94**(1): 129 – 141 (2004).

151. Allard, L., Cheynet, V., Oriol, G., Gervasi, G., Imbert-Laurenceau, E., Mandrand, B., Delair, T. & Mallet, F. Antigenicity of recombinant proteins after regioselective immobilization onto polyanhydride-based copolymers. *Bioconjugate Chemistry*. **15**(3): 458 – 466 (2004).
152. Pfeifer, B.A., Burdick, J.A. & Langer, R. Formulation and surface modification of poly(ester-anhydride) micro- and nanospheres. *Biomaterials*. **26**(2): 117 – 124 (2005).
153. Torres, M.P., Vogel, B.M., Narasimhan, B. & Mallapragada, S.K. Synthesis and characterization of novel polyanhydrides with tailored erosion mechanisms. *Journal of Biomedical Materials Research Part A*. **76**(1): 102 – 110 (2006).
154. Shelke, N.B. & Aminabhavi, T.M. Synthesis and characterization of novel poly(sebacic anhydride-co-Pluronic F68/F127) biopolymeric microspheres for the controlled release of nifedipine. *International Journal of Pharmaceutics*. **345**(1-2): 51 – 58 (2007).
155. Jain, J.P., Modi, S. & Kumar, N. Hydroxy fatty acid based polyanhydride as drug delivery system: synthesis, characterization, in vitro degradation, drug release, and biocompatibility. *Journal of Biomedical Materials Research Part A*. **84**(3): 740 – 752 (2008).
156. Lee, D.A., Keong, K.W., Panek, W.C., Eng, C.T. & Glasglow, B.J. The use of bioerodible polymers and 5-fluorouracil in glaucoma filtration surgery. *Investigative Ophthalmology & Visual Science*. **29**(11): 1692 – 1697 (1988).
157. Jampel, H.D., Thibault, D., Leong, K.W., Uppal, P. & Quigley, H.A. Glaucoma filtration surgery in nonhuman primates using taxol and etoposide in polyanhydride carriers. *Investigative Ophthalmology & Visual Science*. **34**(11): 3076 – 3083 (1993).
158. Wu, M.P., Tamada, J.A., Brem, H. & Langer, R. In vivo versus in vitro degradation of controlled release polymers for intracranial surgical therapy. *Journal of Biomedical Materials Research*. **28**(3): 387 – 395 (1994).
159. Howard, M.A. 3<sup>rd</sup>, Gross, A., Grady, M.S., Langer, R.S., Mathiowitz, E., Winn, H.R. & Mayberg, M.R. Intracerebral drug delivery in rats with lesion-induced memory deficits. *Journal of Neurosurgery*. **71**(1): 105 – 112 (1989).

160. Lucas, P.A., Laurencin, C., Syftestad, G.T., Domb, A., Goldberg, V.M., Caplan, A.I. & Langer, R. Ectopic induction of cartilage and bone by water-soluble proteins from bovine bone using a polyanhydride delivery device. *Journal of Biomedical Materials Research Part A*. **24**(7): 901 – 911 (1990).
161. Brem, H., Kader, A., Epstein, J.I., Tamargo, R.J., Domb, A., Langer, R. & Leong, K.W. Biocompatibility of a biodegradable, controlled-release polymer in the rabbit brain. *Selective Cancer Chemotherapeutics*. **5**(2): 55 – 65 (1989).
162. Jampel, H.D., Kopa, P., Leong, K. & Quigley, H.A. In vitro release of hydrophobic drugs from polyanhydride disks. *Ophthalmic Surgery*. **22**(1): 676 – 680 (1991).
163. Laurencin, C.T., Gerhart, T., Witschger, P., Satcher, R., Domb, A., Rosenberg, A.E., Hanff, P. & Edsberg, L., Hayes, W. & Langer, R. Bioerodible polyanhydrides for antibiotic drug delivery: in vivo osteomyelitis treatment in a rat model system. *Journal of Orthopaedic Research*. **11**(2): 256 – 262 (1993).
164. Nelson, C.L., Hickmon, S.G. & Skinner, R.A. Treatment of experimental osteomyelitis by surgical debridement and the implantation of bioerodible, polyanhydride-gentamicin beads. *Journal of Orthopaedic Research*. **15**(2): 249 – 255 (1997).
165. Kubek, M.J., Liang, D., Byrd, K.E. & Domb, A.J. Prolonged seizure suppression by a single implantable polymer-TRH microdisk preparation. *Brain Research*. **809**(2): 189 – 197 (1998).
166. Masters, D.B., Berde, C.B., Dutta, S., Turek, T. & Langer, R. Sustained local anesthetic release from bioerodible polymer matrices: a potential method for prolonged regional anesthesia. *Pharmaceutical Research*. **10**(10): 1527 – 1537 (1993).
167. Park, E.S., Maniar, M. & Shah, J.C. Biodegradable polyanhydride devices of cefazolin sodium, bupivacaine, and taxol for local drug delivery: preparation, and kinetics and mechanism of in vitro release. *Journal of Controlled Release*. **52**(1-2): 179 – 189 (1998).
168. Storm, P.B., Moriarity, J.L., Tyler, B., Burger, P.C., Brem, H. & Weingart, J. Polymer delivery of camptothecin against 9L gliosarcoma: release, distribution, and efficacy. *Journal of Neurooncology*. **56**(3): 209 – 217 (2002).

169. Carino, G.P., Jacobs, J.S. & Mathiowitz, E. Nanosphere based oral insulin delivery. *Journal of Controlled Release*. **65**(1-2): 261 – 269 (2000).
170. Erdmann, L. & Uhrich, K.E. Synthesis and degradation characteristics of salicylic acid-derived poly(anhydride-esters). *Biomaterials*. **21**(19): 1941 – 1946 (2000).
171. Deng, J.S., Meisters, M., Li, L., Setesak, J., Claycomb, L., Tian, Y., Stephens, D. & Widman, M. The development of an injection-molding process for a polyanhydride implant containing gentamicin sulfate. *PDA Journal of Pharmaceutical Science and Technology*. **56**(2): 65 – 77 (2002).
172. Weiner, A.A., Bock, E.A., Gipson, M.E. & Shastri, V.P. Photocrosslinked anhydride systems for long-term protein release. *Biomaterials*. **29**(15): 2400 – 2407 (2008).
173. Determan, A.S., Wilson, J.H., Kipper, M.J., Wannemuehler, M.J. & Narasimhan, B. Protein stability in the presence of polymer degradation products: consequences for controlled release formulations. **27**(17): 3312 – 3320 (2006).
174. Donbrow, M. & Samoelov, Y. Controlled release of tripeleminamine and other drugs dispersed in ethyl cellulose PEG films [proceedings]. *Journal of Pharmacy and Pharmacology*. **28**(Suppl): 23P (1976).
175. Meyskens, F.L., Jr., Graham, V., Chvapil, M., Dorr, R.T., Alberts, D.S. & Surwit, E.A. A phase I trial of beta-all-trans-retinoic acid delivered via a collagen sponge and a cervical cap for mild or moderate intraepithelial cervical neoplasia. *Journal of the National Cancer Institute*. **71**(5): 921 – 925 (1983).
176. Kawashima, Y., Handa, T., Kasai, A., Takenaka, H., Lin, S.Y. & Ando, Y. Novel method for the preparation of controlled-release theophylline granules coated with a polyelectrolyte complex of sodium polyphosphate-chitosan. *Journal of Pharmaceutical Science*. **74**(3): 264 – 268 (1985).
177. Kabanov, A.V., Nazarova, I.R., Astafieva, I.V., Batrakova, E.V., Alakhov, V.Y., Yaroslavov, A.A. & Kabanov, V.A. Micelle formation and solubilization of fluorescent probes in poly(oxyethylene-b-oxypropylene-b-oxyethylene) solutions. *Macromolecules*. **28**(7): 2303 – 2314 (1995).

178. Kozlov, M., Melik-Nubarov, N., Bartrakova, E. & Kabanov, A. Relationship between pluronic block copolymer structure, critical micellization concentration and partitioning coefficients of low molecular mass solution. *Macromolecules*. **33**(9): 3305 – 3313 (2000).
179. Romberg, B., Hennick, W.E. & Storm, G. Sheddable coatings for long-circulating nanoparticles. *Pharmaceutical Research*. **25**(1): 55 – 71 (2007).
180. Lacasse, F.X., Filion, M.C., Phillips, N.C., Escher, E., McMullen, J.N. & Hildgen, P. Influence of surface properties at biodegradable microsphere surfaces: effects on plasma protein adsorption and phagocytosis. *Pharmaceutical Research*. **15**(2): 312 – 317 (1998).
181. Zhang, X., He, H., Yen, C., Ho, W. & Lee, L.J. A biodegradable, immunoprotective, dual nanoporous capsule for cell-based therapies. *Biomaterials*. **29**(31): 4253 – 4259 (2008).
182. Shelke, N.B. & Aminabhavi, T.M. Synthesis and characterization of novel poly(sebacic anhydride-co-Pluronic F68/F127) biopolymeric microspheres for the controlled release of nifedipine. *International Journal of Pharmaceutics*. **345**(1-2): 51 – 58 (2007).
183. Hou, S., McCauley, L.K. & Ma, P.X. Synthesis and erosion properties of PEG-containing polyanhydrides. *Molecular Bioscience*. **7**(5): 620 – 628 (2007).
184. Yang, Y.Y., Wan, J.P., Chung, T.S., Pallathadka, P.K., Ng, S. & Heller, J. POE-PEG-POE triblock copolymeric microspheres containing protein. I. Preparation and characterization. *Journal of Controlled Release*. **75**(1-2): 115 – 128 (2001).
185. Huynh, D.P., Nguyen, M.K., Pi, B.S., Kim, M.S., Chae, S.Y., Lee, K.C., Kim, B.S., Kim, S.W. & Lee, D.S. Functionalized injectable hydrogels for controlled insulin delivery. *Biomaterials*. **29**(16): 2527 – 2534 (2008).
186. Huang, M.J., Gou, M.L., Qian, Z.Y., Dai, M., Li, X.Y., Cao, M., Wang, K., Zhao, J., Yang, J.L., Lu, Y., Tu, M.J. & Wei, Y.Q. One-step preparation of poly(epsilon-caprolactone)-poly(ethylene glycol)-poly(epsilon-caprolactone) nanoparticles for plasmid DNA delivery. *Journal of Biomedical Materials Research Part A*. **86**(4): 979 – 986 (2008).
187. Ta, H.T., Dass, C.R. & Dunstan, D.E. Injectable chitosan hydrogels for localized cancer therapy. *Journal of Controlled Release*. **126**(3): 205 – 216 (2008).

188. Shamji, M.F., Hwang, P., Bullock, R.W., Adams, S.B., Nettles, D.L. & Setton, L.A. Release and activity of anti-TNF $\alpha$  therapeutics from injectable chitosan preparations for local drug delivery. *Journal of Biomedical Materials Research Part B: Applied Biomaterials*. **90**(1): 319 – 326 (2009).
189. Zhang, X., Sharma, K.K., Boeglin, M., Ogier, J., Mainard, D., Voegel, J.C., Mely, Y. & Benkirane-Jessel, N. Transfection ability and intracellular DNA pathway of nanostructured gene-delivery systems. *Nano Letters*. **8**(8): 2432 – 2436 (2008).
190. Gomez-Gaete, C., Fattal, E., Silva, L., Besnard, M. & Tsapis, N. Dexamethasone acetate encapsulation into Trojan particles. *Journal of Controlled Release*. **128**(1): 41 – 49 (2008).
191. Ohta, T., Tani, A., Kimbara, K. & Kawai, F. A novel nicotinoprotein aldehyde dehydrogenase involved in polyethylene glycol degradation. *Applied Microbiology and Biotechnology*. **68**(5): 639 – 646 (2005).
192. Frings, J., Schramm, E. & Schink, B. Enzymes involved in anaerobic polyethylene glycol degradation by pelobacter venetianus and bacteriodes strain PG1. *Applied Environmental Microbiology*. **58**(7): 2164 – 2167 (1992).
193. Dion, A., Langman, M., Hall, G. & Filiaggi, M. Vancomycin release behavior from amorphous calcium polyphosphate matrices intended for osteomyelitis treatment. *Biomaterials*. **26**(35): 7276 – 7285 (2005).
194. Vinogradov, S.V., Zeman, A.D., Batrakova, E.V. & Kabanov, A.V. Polyplex nanogel formulations for drug delivery of cytotoxic nucleoside analogs. *Journal of Controlled Release*. **107**(1): 143 – 157 (2005).
195. Ditto, A.J., Shah, P.N., Lopina, S.T. & Yun, Y.H. Nanospheres formulated from L-tyrosine polyphosphate as a potential intracellular delivery device. *International Journal of Pharmaceutics*. **368**(1-2): 199 – 206 (2009).
196. Harper, E., Dang, W., Lapidus, R.G. & Garver Jr., R.I. Enhanced efficacy of a novel controlled release paclitaxel formulation (PACLIMER delivery system) for local-regional therapy of lung cancer tumor nodules in mice. *Clinical Cancer Research*. **5**(12): 4242 – 4248 (1999).
197. Kabanov, A.V. Taking polycation gene delivery systems from in vitro to in vivo. *Pharmaceutical Science and Technology*. **2**(9): 365 – 372 (1999).

198. Pouton, C.W. & Seymour, L.W. Key issues in non-viral gene delivery. *Advanced Drug Delivery Reviews*. **46**(1-3): 187 – 203 (2001).
199. De Smedt, S.C., Demeester, J. & Hennink, W.E. Cationic polymer based gene delivery systems. *Pharmaceutical Research*. **17**(2): 113 – 126 (2000).
200. Laurencin, C.T., Koh, H.J., Neenan, T.X., Allcock, H.R. & Langer, R. Controlled release using a new bioerodible polyphosphazene matrix system. *Journal of Biomedical Materials Research*. **21**(10): 1231 – 1246 (1987).
201. Lakshmi, S., Katti, D.S. & Laurencin, C.T. Biodegradable polyphosphazenes for drug delivery applications. *Advanced Drug Delivery Reviews*. **55**(4): 467 – 482 (2003).
202. Allcock, H.R., Pucher, S.R. & Scopelianos, A.G. Poly[(amino acid ester)phosphazenes] as substrates for the controlled release of small molecules. *Biomaterials*. **15**(8): 563 – 569 (1994).
203. Payne, L.G., Jenkins, S.A., Andrianov, A. & Roberts, B.E. Water-soluble phosphazene polymers for parenteral and mucosal vaccine delivery. *Pharmaceutical Biotechnology*. **6**: 473 – 493 (1995).
204. Payne, L.G., Jenkins, S.A., Woods, A.L., Grund, E.M., Geribo, W.E., Loebelenz, J.R., Andrianov, A.K. & Roberts, B.E. Poly[di(carboxylatophenoxy)phosphazene] (PCPP) is a potent immunoadjuvant for an influenza vaccine. *Vaccine*. **16**(1): 92 – 98 (1998).
205. Muwiri, G., Benjamin, P., Soita, H., Townsend, H., Yost, R., Roberts, B., Andrianov, A.K. & Babiuk, L.A. Poly[di(sodium carboxylatoethylphenoxy)phosphazene] (PCEP) is a potent enhancer of mixed Th1/Th2 immune responses in mice immunized with influenza virus antigens. *Vaccine*. **25**(7): 1204 – 1213 (2007).
206. Veronese, F.M., Marsilio, F., Caliceti, P., De Filippis, P., Giunchedi, P. & Lora, S. Polyorganophosphazene microspheres for drug release: polymer synthesis, microspheres preparation, in vitro and in vivo naproxen release. *Journal for Controlled Release*. **52**(3), 227 – 237 (1998).

207. Zhang, J.X., Li, X.J., Qiu, L.Y., Li, X.H., Yan, M.Q., Yi, J. & Zhu, K.J. Indomethacin-loaded polymeric nanocarriers based on amphiphilic polyphosphazenes with poly (N-isopropylacrylamide) and ethyl tryptophan as side groups: Preparation, in vitro and in vivo evaluation. **116**(3): 322 – 329 (2006).
208. Caliceti, P., Veronese, F.M. & Lora, S. Polyphosphazene microspheres for insulin delivery. *International Journal of Pharmaceutics*. **211**(1-2): 57 – 65 (2000).
209. Kim, J.K., Toti, U.S., Song, R. & Sohn, Y.S. A macromolecular prodrug of doxorubicin conjugate to a biodegradable cyclotriphosphazene bearing a tetrapeptide. *Bioorganic & Medicinal Chemistry Letters*. **15**(15): 3576 – 3579 (2005).
210. Yang, Y., Xu, Z., Chen, S., Gao, Y., Gu, W., Chen, L., Pei, Y. & Li, Y. Histidylated cationic polyorganophosphazene/DNA self-assembled nanoparticles for gene delivery. *International Journal of Pharmaceutics*. **353**(1-2): 277 – 282 (2008).
211. Berens, C., Breakey, A.S. & Carter, G.Z. Braided white nylon sutures for muscle operations, sclera resections, evisceration, and plastic surgery. *American Journal of Ophthalmology*. **42**(4 Part 1): 611 – 618 (1956).
212. Wood, D.A. & Whateley, T.L. A study of enzyme and protein microencapsulation – some factors affecting the low apparent enzymic activity yields. *Journal of Pharmacy and Pharmacology*. **34**(9): 552 – 557 (1982).
213. O'Neill, I. Reactive microcapsules for detection of carcinogen sources in the gut. *Journal of Microencapsulation*. **10**(3): 283 – 308 (1993).
214. Pardridge, W.M., Boado, R.J. & Kang, Y.S. Vector-mediated delivery of a polyamide (“peptide”) nucleic acid analogue through the blood-brain barrier in vivo. *Proceedings of the National Academy of Sciences of the United States of America*. **92**(12): 5592 – 5596 (1995).
215. Asayama, S., Maruyama, A., Cho, C-S. & Akaike, T. Design of comb-type polyamide copolymers for a novel pH-sensitive DNA carrier. *Bioconjugate Chemistry*. **8**(6): 833 – 838 (1997).

216. Richardson, S.C.W., Patrick, N.G., Man, Y.K.S., Ferruti, P. & Duncan, R. Poly(amidoamine)s as potential nonviral vectors: Ability to form interpolyelectrolyte complexes and to mediate transfection in vitro. *Biomacromolecules*. **2**(3): 1023 – 1028 (2001).
217. Patrick, N.G., Richardson, S.C.W., Casolaro, M., Ferruti, P. & Duncan, R. Poly(amidoamine)-mediated intracytoplasmic delivery of ricin A-chain and gelonin. *Journal of Controlled Release*. **77**(3): 225 – 232 (2001).
218. Vandamme, T.F. & Brobeck, L. Poly(amidoamine) dendrimers as ophthalmic vehicles for ocular delivery of pilocarpine nitrate and tropicamide. *Journal of Controlled Release*. **102**(1): 23 – 38 (2005).
219. Khandare, J., Kolhe, P., Pillai, O., Kannan, S., Lieh-Lai, M. & Kannan, R.M. Synthesis, cellular transport, and activity of polyamidoamine dendrimer-methylprednisolone conjugates. *Bioconjugate Chemistry*. **16**(2): 330 – 337 (2005).
220. Romberg, B., Metselaar, J.M., Baranyi, L., Snel, C.J., Bungler, R., Hennink, W.E., Szebeni, J. & Storm, G. Poly(amino acid)s: promising enzymatically degradable stealth coatings for liposomes. *International Journal of Pharmaceutics*. **331**(2): 186 – 189 (2007).
221. Heumann, S., Eberl, A., Fischer-Colbrie, G., Pobeheim, H., Kaufmann, F., Ribitsch, D., Cavaco-Paulo, A. & Guebitz, G.M. Surface hydrolysis of polyamide with a new polyamidase from *Beauveria brongniartii*. *Biocatalysis and Biotransformation*. **26**(5): 371 – 377 (2008).
222. Kohn, J. & Langer, R. Poly(iminocarbonates) as potential biomaterials. *Biomaterials*. **7**(3): 176 – 182 (1986).
223. Bourke, S.L. & Kohn, J. Polymers derived from the amino acid L-tyrosine: polycarbonates, polyarylates and copolymers with poly(ethylene glycol). *Advanced Drug Delivery Reviews*. **55**(4): 447 – 466 (2003).
224. Thanoo, B.C., Sunny, M.C. & Jayakrishnan, A. Oral sustained-release drug delivery systems using polycarbonate microspheres capable of floating on the gastric fluid. *Journal of Pharmacy and Pharmacology*. **45**(1): 21 – 24 (1993).
225. Tangpasuthadol, V., Pendharkar, S.M., Peterson, R.C. & Kohn, J. Hydrolytic degradation of tyrosine-derived polycarbonates, a class of new biomaterials. Part II: 3-yr study of polymeric devices. *Biomaterials*. **21**(23): 2379 – 2387 (2000).

226. Joseph, N.J., Lakshmi, S. & Jayakrishnan, A. A floating-type oral dosage form for piroxicam based on hollow polycarbonate microspheres: in vitro and in vivo evaluation in rabbits. *Journal of Controlled Release*. **79**(1-3): 71 – 79 (2002).
227. Liu, J., Zeng, F. & Allen, C. Influence of serum protein on polycarbonate-based copolymer micelles as a delivery system for a hydrophobic anti-cancer agent. *Journal of Controlled Release*. **103**(2): 481 – 497 (2005).
228. Cleland, J.L. Single-administration vaccines: controlled-release technology to mimic repeated immunization. *Trends in Biotechnology*. **17**(1): 25 – 29 (1999).
229. Audran, R., Peter, K., Dannull, J., Men, Y., Scandella, E., Groettrup, M., Gander, B. & Corradin, G. Encapsulation of peptides in biodegradable microspheres prolongs their MHC class-I presentation by dendritic cells and macrophages in vitro. *Vaccine*. **21**(11-12): 1250 – 1255 (2003).
230. Diwan, M., Elamanchili, P., Cao, M. & Samuel, J. Dose sparing of CpG oligodeoxynucleotide vaccine adjuvants by nanoparticle delivery. *Current Drug Delivery*. **1**(4): 405 – 412 (2004).
231. Kipper, M.J., Wilson, J.H., Wannemuehler, M.J. & Narasimhan, B. Single dose vaccine based on biodegradable polyanhydride microspheres can modulate immune response mechanism. *Journal of Biomedical Materials Research Part A*. **76A**(4): 798 – 810 (2006).
232. Johansen, P., Corradin, G., Merkle, H.P. & Gander, B. Release of tetanus toxoid from adjuvants and PLGA microspheres: How experimental set-up and surface adsorption fool the pattern. *Journal of Controlled Release*. **56**(1-3): 209 – 217 (1998).
233. Hamdy, S., Elamanchili, P., Alshamsan, A., Molavi, O., Satou, T. & Samuel, J. Enhanced antigen-specific primary CD4+ and CD8+ responses by codelivery of ovalbumin and toll-like receptor ligand monophosphoryl lipid A in poly(D,L-lactic-co-glycolic) nanoparticles. *Journal of Biomedical Materials Research Part A*. **81**(3): 652 – 662 (2007).
234. O'Brien, C.N. & Guidry, A.J. Formulation of poly(DL-lactide-co-glycolide) microspheres and their ingestion by bovine leukocytes. *Journal of Dairy Science*. **79**(11): 1954 – 1959 (1996).

235. Jiang, W., Gupta, R.K., Deshpande, M.C. & Schwendeman, S.P. Biodegradable poly(lactic-co-glycolic acid) microparticles for injectable delivery of vaccine antigens. *Advanced Drug Delivery Reviews*. **57**(3): 391 – 410 (2005).
236. Gupta, R.K., Chang, A.C. & Siber, G.R. Biodegradable polymer microspheres as vaccine adjuvants and delivery systems. *Developments in Biological Standardization*. **92**: 63 – 78 (1998).
237. Mathiowitz, E., Ron, E., Mathiowitz, G., Amato, C. & Langer, R. Morphological characterization. 1. Crystallinity of polyanhydride copolymers. *Macromolecules*. **23**(13): 3212 – 3218 (1990).
238. Leong, K.W., D'Amore, P.D., Marletta, M. & Langer, R. Bioerodible polyanhydrides as drug-carrier matrices. II. Biocompatibility and chemical reactivity. *Journal of Biomedical Materials Research*. **20**(1): 51 – 64 (1986).
239. Hanes, J., Chiba, M. & Langer, R. Degradation of porous poly(anhydride-co-imide) microspheres and implications for controlled macromolecule delivery. *Biomaterials* **19**(1-3): 163-172 (1998).
240. Domb, A.J., Amselem, S., Shah, J. & Maniar, M. Polyanhydrides: synthesis and characterization. *Advances in Polymer Science*. **107**: 94 – 141 (1993).
241. Shen, E., Kipper, M.J., Dziadul, B., Lim, M-K. & Narasimhan, B. Mechanistic relationships between polymer microstructure and drug release kinetics in bioerodible polyanhydrides. *Journal of Controlled Release*. **82**(1): 115 – 125 (2002).
242. Tamada, J. & Langer, R. The development of polyanhydrides for drug delivery applications. *Journal of Biomaterials Science Polymer Edition*. **3**(4): 315 – 353 (1992).
243. Chiba, M., Hanes, J. & Langer, R. Controlled protein delivery from biodegradable tyrosine-containing poly(anhydride-co-imide) microspheres. *Biomaterials*: **18**(13), 893 – 901 (1997).
244. Pfeifer, B.A., Burdick, J.A., Little, S.R. & Langer, R. Poly(ester-anhydride):poly( $\beta$ -amino ester) micro- and nanospheres: DNA encapsulation and cellular transfection. *International Journal of Pharmaceutics*. **304**(1-2): 210 – 219 (2005).

245. Leong, K.W., Kost, J., Mathiowitz, E. & Langer, R. Polyanhydrides for controlled release of bioactive agents. *Biomaterials* **7**(5): 364 – 371 (1986).
246. Seidel, J.O., Uhrich, K.E., Laurencin, C.T. & Langer, R. Erosion of poly(anhydride-co-imides): A preliminary mechanistic study. *Journal of Applied Polymer Science*. **62**(8): 1277 – 1283 (1996).
247. Fu, J., Fiegel, J., Krauland, E. & Hanes, J. New polymeric carriers for controlled drug delivery following inhalation or injection. *Biomaterials*. **23**(22): 4425 – 4433 (2002).
248. Baudner, B.C., Giuliani, M.M., Verhoef, J.C., Rappuoli, R., Junginger, H.E. & Giudice, G.D. The concomitant use of the LTK63 mucosal adjuvant and chitosan-based delivery system enhances the immunogenicity and efficacy of intranasally administered vaccines. *Vaccine*. **21**(25-26): 3837 – 3844 (2003).
249. Illum, L., Farraj, N.F. & Davis, S.S. Chitosan as a novel nasal delivery system or peptide drugs. *Pharmaceutical Research*. **11**(8): 1186 – 1189 (1994).
250. Alpar, H.O., Somavapu, S., Atuh, K.N. & Bramwell, V.W. Biodegradable microadhesive particulates for nasal and pulmonary antigen and DNA delivery. *Advanced Drug Delivery Reviews*. **57**(3): 411 – 430 (2005).
251. Boonyo, W., Junginger, H.E., Waranuch, N., Polnok, A. & Pitaksuteepong, T. Chitosan and trimethyl chitosan chloride (TMC) as adjuvants for inducing immune responses to ovalbumin in mice following nasal administration. *Journal of Controlled Release*. **121**(3): 168 – 175 (2007).
252. Greenland, J.R. & Letvin, N.L. Chemical adjuvants for plasmid DNA vaccines. *Vaccine*. **25**(19): 3731 – 3741 (2007).
253. Newman, K.D., Elamanchili, P., Kwaon, G.S. & Samuel, J. Uptake of poly(D,L-lactic-co-glycolic acid) microspheres by antigen-presenting cells in vivo. *Journal of Biomedical Materials Research*. **60**(3): 480 – 486 (2002).
254. Audran, R., Peter, K., Dannull, J., Men, Y., Scandella, E., Goettrup, M., Gander, B. & Corradin, G. Encapsulation of peptides in biodegradable microspheres prolongs their MHC class-I presentation by dendritic cells and macrophages in vitro. *Vaccine*. **21**(11-12): 1250 – 1255 (2003).

255. Evans, J.T., Ward, J.R., Kern, J. & Johnson, M.E. A single vaccination with protein-microspheres elicits a strong CD8 T-cell-mediated immune response against Mycobacterium tuberculosis antigen Mtb8.4. *Vaccine*. **22**(15-16): 1964 – 1972 (2004).
256. Conway, M.A., Madrigal-Estevas, L., McClean, S., Brayden, D.J. & Mills, K.H. Protection against Bordetella pertussis infection following parenteral or oral immunization with antigens entrapped in biodegradable particles: effect of formulation and route of immunization on induction of Th1 and Th2 cells. *Vaccine*. **19**(15-16): 1940 – 1950 (2001).
257. McNeela, E.A. & Mills, K.H. Manipulating the immune system: Humoral versus cell-mediated immunity. *Advanced Drug Delivery Reviews*. **51**(1-3): 43 – 54 (2001).
258. Gupta, R.K., Alroy, J., Alonso, M.J., Langer, R. & Siber, G.R. Chronic local tissue reactions, long-term immunogenicity and immunological priming of mice and guinea pigs to tetanus toxoid encapsulated in biodegradable polymer microspheres composed of poly lactide-co-glycolide polymers. *Vaccine*. **15**(16): 1716 – 1723 (1997).
259. Walker, K.B., Xing, D.K., Sesardic, D. & Corbel, M.J. Modulation of the immune response to tetanus toxoid by polylactide-polyglycolide microspheres. *Developments in Biological Standardization*. **92**: 259 – 267 (1998).
260. Men, Y., Thomasin, C., Merkle, H.P., Gander, B. & Corradin, G. A single administration of tetanus toxoid in biodegradable microspheres elicits T cell and antibody responses similar or superior to those obtained with aluminum hydroxide. *Vaccine*. **13**(7): 683 – 689 (1995).
261. Raghuvanshi, R.S., Katare, Y.K., Lalwani, K., Ali, M.M., Singh, O. & Panda, A.K. Improved immune response from biodegradable polymer particles entrapping tetanus toxoid by use of different immunization protocol and adjuvants. *International Journal of Pharmaceutics*. **245**(1-2): 109 – 121 (2002).
262. Peyre, M., Sesardic, D., Merkle, H.P., Gander, B. & Johansen, P. An experimental divalent vaccine based on biodegradable microspheres induces protective immunity against tetanus and diphtheria. *Journal of Pharmaceutical Science*. **92**(5): 957 – 966 (2003).

263. Gupta, R.K., Chang, A.C. & Siber, G.R. Biodegradable polymer microspheres as vaccine adjuvants and delivery systems. *Developments in Biological Standardization*. **92**: 63 – 78 (1998).
264. Ulery, B.D., Phanse, Y., Sinha, A., Wannemuehler, M.J., Narasimhan, B. & Bellaire, B.H. Polymer chemistry influences monocytic uptake of polyanhydride nanoparticles. *Pharmaceutical Research*. **26**(3): 683 – 690 (2009).
265. Ulery, B.D., Kumar, D., Ramer-Tait, A.E., Metzger, D.W., Wannemuehler, M.J. & Narasimhan, B. Design of a protective single-dose intranasal nanoparticle-based vaccine platform for respiratory infectious diseases. *PLoS One*, submitted for publication.
266. Mathiowitz, E., Jacob, J.S., Jong, Y.S., Carino, G.P., Chickering, D.E., Chaturvedi, P., Santos, C.A., Vijayaraghavan, K., Montgomery, S., Bassett, M. & Morrell C. Biologically erodible microspheres as potential oral drug delivery systems. *Nature*. **386**(6623): 410 – 414 (1997).
267. Amidi, M., Pellikaan, H.C., Hirschberg, H., de Boer, A.H., Crommelin, D.J., Hennink, W.E., Kersten, G. & Jiskoot, W. Diphtheria toxoid-containing microparticulate powder formulation for pulmonary vaccination: Preparation, characterization and evaluation in guinea pigs. *Vaccine*. **25**(37-38): 6818 – 6829 (2007).
268. Breard, E., Sailleau, C., Coupier, H., Mure-Ravaud, K., Hammoumi, S., Gicquel, B., Hamblin, C., Dubourget, P. & Zientara, S. Comparison of genome segments 2, 7 and 10 of bluetongue viruses serotype 2 for differentiation between field isolates and vaccine strain. *Veterinary Research*. **34**(6): 777 – 789 (2003).
269. Baudner, B.C., Giuliani, M.M., Verhoef, J.C., Rappuoli, R., Junginger, H.E. & Giudice, G.D. The concomitant use of the LTK63 mucosal adjuvant and chitosan-based delivery system enhances the immunogenicity and efficacy of intranasally administered vaccines. *Vaccine*. **21**(25-26): 3837 – 3844 (2003).
270. Illum, L., Farraj, N.F. & Davis, S.S. Chitosan as a novel nasal delivery system or peptide drugs. *Pharmaceutical Research*. **11**(8): 1186 – 1189 (1994).
271. Alpar, H.O., Somavapu, S., Atuh, K.N. & Bramwell, V.W. Biodegradable microadhesive particulates for nasal and pulmonary antigen and DNA delivery. *Advanced Drug Delivery Reviews*. **57**(3): 411 – 430 (2005).

272. Boonyo, W., Junginger, H.E., Waranuch, N., Polnok, A. & Pitaksuteepong, T. Chitosan and trimethyl chitosan chloride (TMC) as adjuvants for inducing immune responses to ovalbumin in mice following nasal administration. *Journal of Controlled Release*. **121**(3): 168 – 175 (2007).
273. Diwan, M., Elamanchili, P., Lane, H., Gainer, A. & Samuel J. Biodegradable nanoparticle mediated antigen delivery to human cord blood derived dendritic cells for induction of primary T cell responses. *Journal of Drug Targeting*. **11**(8-10): 495 – 507 (2003).
274. Elamanchili, P., Diwan, M., Cao, M. & Samuel, J. Characterization of poly(D,L-lactic-co-glycolic acid) based nanoparticulate system for enhanced delivery of antigens to dendritic cells. *Vaccine*. **22**(19): 2406 – 2412 (2004).
275. Yoshida, M. & Babensee, J.E. Poly(lactic-co-glycolic acid) enhances maturation of human monocyte-derived dendritic cells. *Journal of Biomedical Materials Research Part A*. **71A**(1): 45 – 52 (2004).
276. Yoshida, M. & Babensee, J.E. Differential effects of agarose and poly(lactic-co-glycolic acid) on dendritic cell maturation. *Journal of Biomedical Materials Research Part A*. **79A**(2): 393 – 408 (2006).
277. Yoshida, M., Mata, J. & Babensee, J.E. Effect of poly(lactic-co-glycolic acid) contact on maturation of murine bone marrow-derived dendritic cells. *Journal of Biomedical Materials Research Part A*. **80A**(1): 7 – 12 (2007).
278. Sharp, F.A., Ruane, D., Claass, B., Creagh, E., Harris, J., Malyala, P., Singh, M., O'Hagan, D.T., Petrilli, V., Tschopp, J., O'Neill, L.A. & Lavelle, E.C. Uptake of particulate vaccine adjuvants by dendritic cells activates the NALP3 inflammasome. *Proceedings of the National Academies of Science*. **106**(3): 870 – 875 (2009).
279. Petersen, L.K., Xue, L., Wannemuehler, M.J., Rajan, K. & Narasimhan, B. The simultaneous effect of polymer chemistry and device geometry on the in vitro activation of murine dendritic cells. *Biomaterials*. **30**(28): 5131 – 5142 (2009).
280. Petersen, L.K., Yeager, A., Ulery, B.D., Ramer-Tait, A.E., Wannemuehler, M.J. & Narasimhan, B. The role of polymer chemistry in the uptake of polyanhydride nanoparticles and the activation mechanisms of antigen presenting cells. *Biomaterials*, to be submitted.

281. Torres, M.P., Wilson-Welder, J.H., Ramer-Tait, A.E., Bellaire, B.H., Wannemuehler, M.J. & Narasimhan, B. In vitro activation of dendritic cells using polyanhydride microspheres: promising implications for vaccine design. *Biomaterials*, to be submitted.
282. Ulery, B.D., Petersen, L.K., Phanse, Y., Broderick, S., Ramer-Tait, A.E., Rajan, K., Wannemuehler, M.J., Bellaire, B.H. & Narasimhan, B. Combining population and individual analyses to probe immune cell interactions with polyanhydride nanoparticles. *Nature Materials*, to be submitted.
283. Carrillo-Conde, B., Madrigal, A., Bellair, B.H., Wannemuehler, M.J. & Narasimhan, B. Targeting dendritic cells with functionalized polyanhydride nanoparticles. *Biomaterials*, to be submitted.
284. Liu, J., Jiang, Z., Zhang, S. & Saltzman, W.M. Poly(omega-pentadecalactone-co-butylene-co-succinate) nanoparticles as biodegradable carriers for camptothecin delivery. *Biomaterials*. **30**(29): 5707 – 5719 (2009).
285. Ho, Y.P., Chen, H.H., Leong, K.W. & Wang, T.H. Evaluating the intracellular stability and unpacking of DNA nanocomplexes by quantum dots-FRET. *Journal of Controlled Release*. **116**(1): 83 – 89 (2006).
286. Cartiera, M.S., Johnson, K.M., Rajendran, V., Caplan, M.J. & Saltzman, W.M. The uptake and intracellular fate of PLGA nanoparticles in epithelial cells. *Biomaterials*. **30**(14): 2790 – 2798 (2009).
287. Shen, H., Ackerman, A.L., Cody, V., Giodini, A., Hinson, E.R., Cresswell, P., Edelson, R.L., Saltzman, W.M. & Hanlon, D.J. Enhanced and prolonged cross-presentation following endosomal escape of exogenous antigens encapsulated in biodegradable nanoparticles. *Immunology*. **117**(1): 78 – 88 (2006).
288. Perry, R.D. & Fetherston, J.D. *Yersinia pestis* – Etiologic Agent of Plague. *Clinical Microbiology Reviews*. **10**(1): 35 – 66 (1997).
289. Biraben, J-N. & Le Goff, J. The plague in the early middle ages. In: Foster, R. & Ranum, O., editors. *Biology of man in history*. Baltimore: The John Hopkins Press, 48 – 80 (1975).
290. Gottfried, R.S. *The black death. Natural and human disaster in medieval Europe*. New York, The Free Press, (1983).

291. Barnes, A.M. & Quan, T.J. Plague. In: Bartlett, J.G. & Blacklow, N.R., editors. *Infectious diseases*. Philadelphia: W.B. Saunders Co., 1285 – 1291 (1992).
292. Butler, T. *Plague and other Yersinia infections*. New York, Plenum Press, (1983).
293. Bendiner, E. Alexandre Yersin: pursuer of plague. *Hospital Practice*. **24**(3A), 121 – 124, 127 – 128, 131 – 132, 135, 138, 141 – 142 & 147 – 148 (1989).
294. Chernin, E. Richard Pearson Strong and the Manchurian epidemic of pneumonic plague, 1910 – 1911. *Journal of the History of Medicine and Allied Sciences*. **44**(3): 296 – 319 (1989).
295. Wu, L-T. *Plague Fighter: the autobiography of a modern Chinese physician*. Cambridge: W. Heffer & Sons Ltd., (1959).
296. Marchette, N.J., Lundgren, D.L., Nicholes, P.S., Bushman, J.B. & Vest, D. Studies on infectious diseases in wild animals in Utah. II. Susceptibility of wild mammals to experimental plague. *Zoonoses Research*. **1**: 225 – 250 (1962).
297. Gasper, P.W., Barnes, A.M., Quan, T.J., Benzinger, J.P., Carter, L.G., Beard, M.L. & Maupin, G.O. Plague (*Yersinia pestis*) in cats: description of experimentally induced disease. *Journal of Medical Entomology*. **30**(1): 20 – 26 (1993).
298. Christie, A.B. Plague: review of ecology. *Ecology of Disease*. **1**(2-3): 111 – 115 (1982).
299. Quan, S.F. & Kartman, L. Ecological studies of wild rodent plague in the San Francisco bay area of California. VIII. Susceptibility of wild rodents to experimental plague infections. *Zoonoses Research*. **1**: 121 – 144 (1962).
300. Cavanaugh, D.C. Specific effect of temperature upon transmission of the plague bacillus by the original rat flea, *Xenophyslla cheopis*. *American Journal of Topical Medicinal Hygenin*. **20**(2): 264 – 272 (1971).
301. Craven, R.B., Maupin, G.O., Beard, M.L., Quan, T.J. & Barnes, A.M. Reported cases of human plague infections in the united states 1970 – 1991. *Journal of Medical Entomology*. **30**(4): 758 – 761 (1993).

302. von Reyn, C.F., Weber, N.S., Tempest, B., Barnes, A.M., Poland, J.D., Boyce, J.M. & Zalma, V. Epidemiologic and clinical features of an outbreak of bubonic plague in New Mexico. *Journal of Infectious Disease*. **136**(4): 489 – 494 (1977).
303. Doll, J.M., Zeitz, P.S., Ettestad, P., Bucholtz, A.L., Davis, T. & Gage, K. Cat-transmitted fatal pneumonic plague in a person who traveled from Colorado to Arizona. *Journal of Tropical Medicine and Hygiene*. **51**(1): 109 – 114 (1994).
304. Meyer, K.F. Pneumonic plague. *Bacteriology Reviews*. **25**: 249 – 261 (1961).
305. Welch, T.J., Fricke, W.F., McDermott, P.F., White, D.G., Rosso, M.L., Rasko, D.A., Mammel, M.K., Eppinger, M., Rosovitz, M.J., Wagner, D., Rahalison, L., Leclerc, J.E., Hinshaw, J.M., Lindler, L.E., Cebula, T.A., Carniel, E. & Ravel, J. Multiple antimicrobial resistance in plague: an emerging health risk. *PLoS ONE*, **2**(3): e309 (2007).
306. Waters, C.M. & Bassler, B.L. Quorum sensing: cell-to-cell communication in bacteria. *Annual Review of Cell and Developmental Biology*. **21**: 319 – 346 (2005).
307. Boyen, F., Eeckhaut, V., Van Immerseel, F., Pasmans, F., Ducatelle, R. & Haesebrouck, F. Quorum sensing in veterinary pathogens: Mechanisms, clinical importance and future perspectives. *Veterinary Microbiology*. **135**(3-4): 187 – 195 (2009).
308. Jarrett, C.O., Deak, E., Isherwood, K.E., Oyston, P.C., Fischer, E.R., Whitney, A.R., Kobayashi, S.D., DeLeo, F.R. & Hinnebusch, B.J. Transmission of *Yersinia pestis* from an infectious biofilm in the flea vector. *The Journal of Infectious Diseases*. **190**(4): 783 – 792 (2004).
309. Kirwan, J.P., Gould, T.A., Schweizer, H.P., Bearden, S.W., Murphy, R.C. & Churchill, M.E. Quorum-sensing signal synthesis by the *Yersinia pestis* acyl-homoserine lactone synthase Yspl. *Journal of Bacteriology*. **188**(2): 784 – 788 (2006).
310. Atkinson, S., Sockett, R.E., Camara, M. & Williams, P. *Current Issues in Molecular Biology*. **8**(1): 1 – 10 (2006).
311. Perry, R.D. & Fetherston, J.D. Advances in experimental medicine and biology. The genus *Yersinia*: from genomics to function. New York: Springer, 178 – 191 (2007).

312. Department of Defense. Report on Biological Warfare Defense Vaccine Research & Development Programs. (July 2001). Retrieved on 26 Feb 2009 from <http://www.defenselink.mil/pubs/ReportonBiologicalWarfareDefenseVaccineRDPrgras-July2001.pdf>.
313. Smiley, S.T. Current challenges in the development of vaccines for pneumonic plague. *Expert Review of Vaccines*. **7**(2): 209 – 221 (2008).
314. Drozdov, I.G., Anisimov, A.P., Samoilova, S.V., Yezhov, I.N., Yeremin, S.A., Karlyshev, A.V., Krasilnikova, V.M. & Kravchenko V.I. Virulent non-capsulate *Yersinia pestis* variants constructed by insertion mutagenesis. *Journal of Medical Microbiology*. **42**(4): 264 – 268 (1995).
315. Lindler, L.E. *Yersinia pestis* as an emerged pathogen. In: Lindler, L.E., Lebeda, F.J. & Korch, G. Biological weaponse defense. New York: Humana Press, 481 – 505 (2005).
316. Zilinskas, R.A. The anti-plague system and the Soviet biological warfare program. *Critical Review in Microbiology*. **32**(1): 47 – 64 (2006).
317. Haffkine, W.M. Remarks on the plague prophylactic fluid. *British Medical Journal*. **1**(1902): 1461 – 1462 (1897).
318. Lien-Teh, W. A treatise on pneumonic plague. League of Nations Health Organization. Geneva, Switzerland, (1926).
319. Meyer, K.F. Effectiveness of live or killed plague vaccines in man. *Bulletin of the World Health Organization*. **42**(5): 653 – 666 (1970).
320. Norinder, U. & Osterberg, T. Theoretical calculation and prediction of drug transport processes using simple parametes and partial least squares projections to latent squares projections to latent structures (PLS) statistics. The use of electrotopical state indices. *Journal of Pharmaceutical Science*. **90**(8): 1076 – 1085.
321. Williamson, E.D., Eley, S.M., Stagg, A.J., et al. A sub-unit vaccine elicits IgG in serum, spleen cell cultures and bronchial washings and protects immunized animals against pneumonic plague. *Vaccine*. **15**(10): 1079 – 1084 (1997).

322. Williamson, E.D., Flick-Smith, H.C., Lebutt, C., Rowland, C.A., Jones, S.M., Waters, E.L., Gwyther, R.J., Miller, J., Packer, P.J. & Irving, M. Human immune response to a plague vaccine comprising recombinant F1 and V antigens. *Infectious Immunity*. **73**(6): 3598 – 3608 (2005).
323. Morris, S.R. Development of a recombinant vaccine against aerosolized plague. *Vaccine*. **25**(16): 3115 – 3117 (2007).
324. Pitt, M.L. Non-human primates as a model for pneumonic plague. Public Workshop on Animal Models and Correlates of Protection for Plague Vaccines. (2004). Retrieved on 9 March 2009 from <http://www.fda.gov/cber/minutes/plague101304t.pdf>.

## CHAPTER 3

### Research Objectives

The overall goal of this research is to design single-dose vaccines utilizing antigen-encapsulated polyanhydride nanoparticles that function as both excellent adjuvants and robust vaccine delivery vehicles. In order to achieve this goal, development of a nanoparticle fabrication technique was undertaken. Once this was accomplished, nanoparticles of varied polymer chemistry were evaluated *in vitro* and *ex vivo* for their ability to interact and stimulate antigen presenting cells. The knowledge gained from these experiments was used to rationally choose which polymer chemistries held the greatest potential as single-dose vaccine delivery vehicles. The polyanhydride nanoparticles with favorable characteristics were loaded with *Yersinia Pestis* antigens and evaluated *in vivo* in murine models for their capacity to induce a protective immune response.

The specific goals (SG) for this research are as follows:

**SG1:** Development of a technique to reproducibly fabricate polyanhydride nanoparticles.

**SG2:** Assessment of the effect of polymer chemistry on in vitro interactions between antigen presenting cells and polyanhydride nanoparticles.

**SG3:** In vivo evaluation of polyanhydride nanoparticles as single-dose vaccine delivery vehicles for the vaccine immunogen F1-V against *Y. pestis*.

## **CHAPTER 4**

# **Polymer Chemistry Influences Monocytic Uptake of Poly(anhydride Nanoparticles**

**Reprinted from a paper published in Pharmaceutical  
Research 26(3), 683 – 690, Copyright © 2009**

**Bret D. Ulery,<sup>1</sup> Yashdeep Phanse,<sup>2</sup> Avanti Sinha,<sup>2</sup>  
Michael J. Wannemuehler,<sup>2</sup> Balaji Narasimhan,<sup>1</sup> and  
Bryan H. Bellaire<sup>2</sup>**

**<sup>1</sup>Department of Chemical and Biological Engineering,  
Iowa State University, Ames, IA 50011, USA.**

**<sup>2</sup>Department of Veterinary Microbiology and  
Preventative Medicine, Iowa State University, Ames, IA  
50011, USA.**

#### 4.1 Abstract

Polyanhydride nanoparticles hold significant promise for use as vaccine delivery vehicles. In order to better understand the mechanism by which these materials initiate an immune response they were incubated with THP-1 human monocytic cells. Nanoparticles were prepared by an anti-solvent nanoprecipitation technique yielding particles with similar morphology and particle diameter (200 to 600 nm) regardless of polymer chemistry. Exposure of nanoparticles composed of poly(sebacic acid) (poly(SA)) and 20:80 poly(1,6-bis(p-carboxyphenoxy)hexane-co-sebacic acid) (CPH:SA) to THP-1 monocytes were readily internalized whereas 50:50 CPH:SA nanoparticles had more limited uptake. When soluble fluorescently-labeled protein antigen was added with nanoparticles, antigen uptake was enhanced and negatively correlated to the hydrophobicity of the polymer chemistry. These results demonstrate the importance of choosing polyanhydride chemistries that facilitate enhanced interactions with antigen presenting cells in order to initiate an efficacious immune response.

## 4.2 Introduction

Bioerodible polymers have been studied as sustainable drug delivery vehicles for over thirty years.<sup>1</sup> Polyesters and polyanhydrides are two families of polymers that are strong candidates for biomedical applications because of the biocompatibility and bioresorbability of their degradation products.<sup>2</sup> While polyesters, like poly(lactic-co-glycolic acid) (PLGA), have been approved by the FDA for many in vivo applications<sup>3</sup>, their suitability for use as vaccine delivery vehicles is affected by various factors that negatively impact the stability of encapsulated proteins. Research has shown that the bulk-erodible polyester-based delivery systems display rapid release profiles<sup>4,5</sup>, produce low pH microenvironments<sup>6-8</sup>, and can initiate moisture-induced protein aggregation.<sup>8-10</sup> In contrast, polyanhydrides are characterized by chemistry-dependent surface erosion and payload release<sup>11-13</sup>, moderate pH microenvironments<sup>8,14,15</sup>, and superior protein stabilization capabilities.<sup>10,16,17</sup> Polyanhydrides have been used to deliver plasmid DNA<sup>18</sup>, proteins<sup>9,13,17</sup>, small molecular weight drugs<sup>11,19,20</sup>, and vaccine immunogens.<sup>21,22</sup> Alterations of polyanhydride chemistry modulate degradation rates from weeks to years, which can be exploited to best fit therapeutic needs.<sup>9,11,16</sup> In addition, polyanhydride microspheres used as vaccine delivery vehicles exhibit a chemistry-dependent, immunomodulatory adjuvant effect.<sup>22</sup> Kipper et al. showed that encapsulating tetanus toxoid (TT) into polyanhydride microspheres or co-delivering free TT along with the microspheres enhanced antigen-specific immune responses.<sup>22</sup> Furthermore, the relative

increase of polymer hydrophobicity effectively modulated the immune response from a dominant  $T_H2$  (humoral) to a  $T_H0$  (balanced) response. Together, these results indicate that polyanhydride microspheres are promising vehicles for vaccine delivery.

The polyanhydride chemistries used in the present study were copolymers of sebacic anhydride (SA) and 1,6-bis-(*p*-carboxyphenoxy)hexane (CPH) anhydride with chemical structures as shown in Fig. 4.1. With aromatic rings, the CPH unit is more hydrophobic than the aliphatic SA unit. Copolymers containing higher compositions of CPH have been shown to degrade slower than copolymers containing higher compositions of SA.<sup>9</sup>

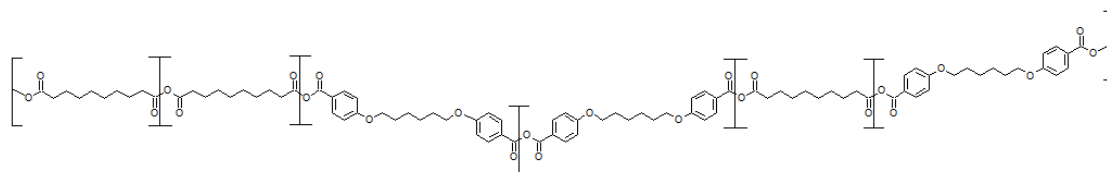


**Figure 4.1.** Chemical structure of a random CPH:SA copolymer.

In the last several decades, the in vivo applications utilizing polymer carriers have transitioned from the use of large, implanted pellets (~1 mm) to microspheres (~5-20  $\mu\text{m}$ ) and, more recently, to nanoparticles (~100-500 nm).<sup>1,11</sup> In comparison to implants, microspheres (or nanoparticles) do not require surgical insertion or removal<sup>22</sup>, can carry multiple drugs<sup>20,23</sup>, and are phagocytosed by antigen presenting cells (APCs).<sup>24</sup> Inhalation and intranasal delivery can be realized with particles that are small enough to pass through the finely porous networks of the nasal, tracheal, and pulmonary filtration

systems.<sup>25,26</sup> In addition, multiple studies have shown that polymeric nanoparticles gain ready access into sub-mucosal layers of the nasal-associated and gut-associated lymphoid tissues much more effectively than microparticles.<sup>27-29</sup> In comparison to microspheres, nanoparticles were more readily taken up by APCs.<sup>30</sup> Collectively, these characteristics underpin the functional diversity and enhanced capabilities of polyanhydride nanoparticles.

In order for polyanhydride nanoparticles to function as efficacious vaccine adjuvants, they must possess the ability to stimulate and to deliver antigen to APCs. In the present study, we chose to use confocal microscopy to monitor both intracellular and extracellular interactions between polyanhydride nanoparticles and APCs.<sup>31</sup> In addition, confocal microscopy allowed us to monitor the potential for polyanhydride nanoparticles to deliver antigen via the endocytic pathway by evaluating the co-localization of polyanhydride nanoparticles within specific sub-cellular compartments associated with antigen processing and presentation. Our data demonstrate that systematically varying the chemistry of polyanhydride nanoparticles (by varying the SA content in a CPH:SA copolymer) significantly affects nanoparticle uptake by human monocytic cells. In addition, we demonstrate that polymer chemistry significantly influences the uptake of a model antigen (E $\alpha$  tagged with red fluorescent protein (RFP), henceforth referred to as E $\alpha$ -RFP) by human monocytic cells.

## **4.3 Materials and Methods**

### **4.3.1 Materials**

Sebacic acid (99%), 4-hydroxybenzoic acid, 1-methyl-2-pyrrolidinone anhydrous (99.5%), 1,6-dibromohexane (98.5%) and fluorescein-isothiocyanate-dextran (FITC-dextran) were purchased from Sigma-Aldrich (Milwaukee, WI). All other chemicals were purchased from Fisher Scientific (Pittsburgh, PA) and used as received.

### **4.3.2 Polyanhydride Synthesis and Characterization**

Synthesis of SA and CPH pre-polymers and copolymers was performed as previously described.<sup>11,12,32</sup> The resulting polymers were characterized using <sup>1</sup>H nuclear magnetic resonance to verify polymer chemistry, gel permeation chromatography to analyze molecular weight, and differential scanning calorimetry to determine glass transition temperature and crystallinity. All properties evaluated showed that the synthesized polymers were within accepted ranges.<sup>11,12</sup>

### **4.3.3 Nanoparticle Fabrication and Characterization**

FITC-dextran loaded nanoparticles were fabricated by polyanhydride anti-solvent nanoencapsulation (PAN), similar to the method reported by Mathiowitz et al. for poly (fumaric acid-co-sebacic acid) polymers.<sup>33</sup> Polymer (145.5 mg) was dissolved in methylene chloride (5 mL) held at room temperature for poly(SA) and 20:80 CPH:SA and 0 °C for 50:50 CPH:SA. FITC-dextran (4.5 mg) was

homogenized at 30,000 rpm for 30 s to create a suspension. The polymer/fluorescein solution was rapidly poured into a bath of petroleum ether at an anti-solvent to solvent ratio of 80:1 held at room temperature for poly(SA) and 20:80 CPH:SA and -40 °C for 50:50 CPH:SA (due to the lower glass transition temperature for 50:50 CPH:SA<sup>12</sup>). Polymer solubility changes due to the presence of anti-solvent caused spontaneous particle formation. These particles were removed from the anti-solvent by filtration (by aspiration using a Buechner funnel and Whatman #2 filter paper) and then dried overnight under vacuum. The procedure yielded a fine powder with at least 70% recovery. The nanoparticle morphology was investigated using scanning electron microscopy (JEOL 840A, JEOL Ltd., Tokyo, Japan). Particle diameter was determined using quasi-elastic light scattering (Zetasizer Nano, Malvern Instruments Ltd., Worcester, United Kingdom).

#### **4.3.4 Culture of THP-1 Human Monocytes and Co-Incubation with Nanoparticles**

Tissue culture and subsequent derivation of adherent THP-1 monocytes was performed according to published reports<sup>34</sup> with some modification.<sup>35</sup> Briefly, suspension THP-1 cells were grown using RPMI 1640 growth medium supplemented with 10% newborn calf serum, 10 mM Glutamax, 25 mM HEPES, and 10 µg/ml penicillin-streptomycin antibiotics (complete RPMI). Adherent monocytes were derived from suspension cultures by stimulating cells with 5 nM phorbol-12-myristic-13-acetate (PMA) in 24 well tissue culture plates containing

10 mm glass coverslips inside each well at a final density of  $5 \times 10^5$  cells per well. Following 24 h PMA incubation, cultures were washed with PBS and incubated in fresh RPMI without PMA for 24 h before nanoparticles were added.

Polyanhydride nanoparticles (in the form of dry powder) of poly(SA), 20:80 CPH:SA, or 50:50 CPH:SA were weighed and added to PBS (pH 7.4) at a stock concentration of 10 mg/ml. The nanoparticles were briefly sonicated on ice for a total process time of 1 min alternating 10 sec pulse ON, 15 sec Pulse OFF. Nanoparticles (100  $\mu\text{g}$ ) were added to cell culture medium (0.5 ml/well), briefly mixed by pipetting before cultures were returned to the incubator (37  $^{\circ}\text{C}$ , 5 %  $\text{CO}_2$ ). In order to evaluate phagocytic processes, the nanoparticles were co-incubated with the THP-1 cells for 30 min. Cultures were washed and the cells were placed back in the incubator for 2 h prior to analysis. In order to evaluate endocytic processes, the nanoparticles were co-incubated with the THP-1 cells for 6 h. Cultures were washed and the cells were placed back in the incubator for 48 h prior to analysis.

#### **4.3.5 Fluorescence Microscopy Techniques**

To observe time-dependent interactions of individual monocytes with nanoparticles, cell monolayers incubated with nanoparticles at indicated times were fixed with 4% para-formaldehyde (PFA) for 10 min at room temperature, and then washed with PBS. Acidic vesicles and lipid rafts in cell monolayers were labeled by incubating cells for 20 minutes prior to fixation with either LysoTracker at 1/2000 dilution (DND-99) (acidic vesicles) or Alexa555 conjugated Cholera

Toxin  $\beta$ -subunit (CTx) at 1/150 dilution (lipid rafts) (Molecular Probes-Invitrogen, Carlsbad, CA). Intracellular structures were immunofluorescently stained by incubating fixed coverslips with primary and secondary antibodies in PBS containing albumin and 0.1% saponin (BSP).<sup>35</sup> Stained coverslips were washed and mounted on glass slides (Pro-Long w/ Dapi; Molecular Probes-Invitrogen). Epifluorescence and immunofluorescence microscopy was performed using either an Olympus IX-61 inverted microscope equipped with blue, green, and red filter sets with a cooled CCD camera or by an inverted Leica NTS laser scanning confocal microscopy (LSCM). The LSCM is equipped with ApoChromatic 63X oil and 100X oil objectives and UV, Argon, Krypton and HeNe laser lines equipped with three photomultiplier detection tubes. Optimal step size for Z-stack image data was determined empirically from pilot studies to be 0.3  $\mu\text{m}$  (data not shown). Co-localization analysis, relative nanoparticle uptake comparisons, and final images were prepared using Image J v1.36b image analysis software loaded with particle counting algorithms.<sup>36</sup>

#### **4.3.6 E $\alpha$ -RFP Antigen Preparation and Cellular Internalization by Monocytes**

The IPTG inducible E $\alpha$ -RFP expression construct was a kind gift from Dr. Marc Jenkins (Department of Microbiology, Center for Immunology, University of Minnesota Medical School)<sup>37</sup> and introduced into *Escherichia coli* DH5 $\alpha$  by heat shock followed by selecting 50 mg/ml ampicillin-resistant colonies. Broth cultures of transformed bacteria were induced by the addition of IPTG to overnight

cultures. Crude cell lysates prepared using the Novagen Bugbuster extraction reagent (Gibbstown, NJ) were passed through a Profinity IMAC Ni-charged resin (BioRad; Hercules, CA). Imidazole eluted E $\alpha$ -RFP protein was dialyzed overnight at 4°C and final preparations were shown to be free of detectable LPS contamination by the limulus ameobocyte lysate (LAL) assay (Cambrex; Walkersville,MD). Fluorescence signal intensity of internalized protein was detected using standard epi-fluorescence microscopy employing TRITC/rhodamine filter set with 510-560 nm excitation and 575-645 emission. Image black levels for the RFP protein were set using cells not incubated with RFP. Exposure times for RFP detection were kept constant throughout the experimental groups to facilitate accurate comparative analysis. Bar graphs of the relative pixel intensity of internalized RFP were calculated from RAW-RFP images using the ImageJ/plugin/histogram function. These bar graphs reveal the relative pixel intensity of the RFP protein detected in the presence and absence of nanoparticles.

## **4.4 Results and Discussion**

### **4.4.1 Nanoparticle Characterization**

Scanning electron photomicrographs of the FITC-dextran loaded nanoparticles of varying formulations are presented in Fig. 4.2. The photomicrographs show that the nanoparticles appear circular, and while there are some small variations, the nanoparticles appear to be relatively uniform in

size and shape. Light scattering size distribution data show nanoparticle diameters for all polymers fall between 200 and 800 nm.

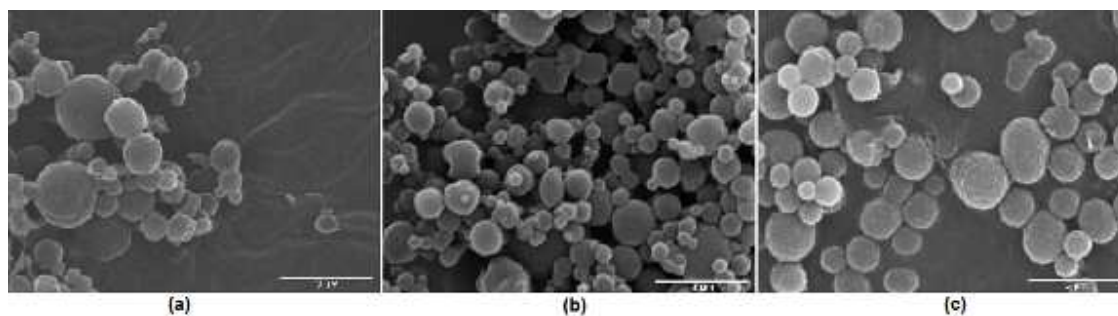


**Figure 4.2.** Scanning electron photomicrographs of (a) poly(SA) nanoparticles, (b) 20:80 CPH:SA nanoparticles and (c) 50:50 CPH:SA nanoparticles.

Every batch of nanoparticles was analyzed by light scattering and particle size was measured using duplicate samples. For each chemistry, the data from three different lots of nanoparticles were analyzed in this manner and the compiled data are shown in Table 4.1. The standard deviations were determined for the overall accumulated size distribution data for each polymer.

**Table 4.1.** Particle size data compiled from light scattering measurements (n=3). Data reported as mean  $\pm$  S.D.

Polymer	Average Particle Diameter (nm)
poly SA	283 $\pm$ 45
20:80 CPH:SA	348 $\pm$ 48
50:50 CPH:SA	397 $\pm$ 121

Analysis shows that there is no statistically significant difference in average particle size among the different polymer formulations ( $p = 0.13$ ). This data

demonstrates that polyanhydride nanoparticles fabricated by the PAN method can be reproducibly prepared with similar morphology and particle diameters regardless of copolymer chemistry. Having particles of similar size is important in limiting the variables that are introduced into *in vitro* and *in vivo* experiments, especially when evaluating a chemistry effect. While not statistically significant, there was a slight trend for a positive correlation between particle size and CPH content. The thermodynamic and kinetic balance between nucleation and growth dictates the resulting average particle size. The soluble material must nucleate particles and then more material can either precipitate on the surface of these already formed particles or new particles can be nucleated.<sup>38</sup> Copolymers with a higher SA content are less hydrophobic and more non-polar than those with a higher CPH content. When precipitating from a polar solvent into an aliphatic anti-solvent bath, copolymers with a higher SA content may more easily nucleate new particles. If nucleation is favored, it would cause more particles to be formed with a smaller average particle size.

#### **4.4.2 Cellular Interactions of Nanoparticles with Human Monocytes**

To determine whether or not polymer chemistry affects nanoparticle internalization and intracellular deposition within APCs, adherent human THP-1 monocytes were incubated separately with poly(SA), 20:80 CPH:SA, or 50:50 CPH:SA nanoparticles. LSCM was utilized to evaluate and compare the interactions of nanoparticles with cells and their eventual intracellular localization.

#### 4.4.2.1 Internalization

Nanoparticles introduced into cell culture medium did not form large aggregates and remained uniformly dispersed prior to settling at the bottom of the tissue culture well during co-incubation with the THP-1 cells. The nanoparticles were then rapidly internalized by THP-1 monocytes via cellular events consistent with phagocytosis (Fig. 4.3). Observations supporting this conclusion include: centrifugation-independent internalization, temperature-dependent internalization, and internalization in the absence of an overabundance of extracellular particles. Confocal photomicrographs in Fig. 4.3 depict monocytes that have internalized nanoparticles and values presented in Table II indicate the percentage of THP-1 cells per field of view that have cell associated nanoparticles at 2 or 48 h post internalization. Cells were imaged at 1000x total magnification and the average number of cells in each Field of View (FOV) was 25. FOVs were randomly selected and the numbers of THP-1 cells with FITC-loaded polyanhydride nanoparticles or without nanoparticles were recorded. The percentages and standard deviations of THP-1 cells positive for nanoparticles were calculated from values for  $\geq 5$  FOV images for each nanoparticle chemistry and time point (cells with FITC-nanoparticles/total # cells scored). The total cells scored positively for clear association with FITC nanoparticles were combined from data collected over 3 to 5 independent experiments.

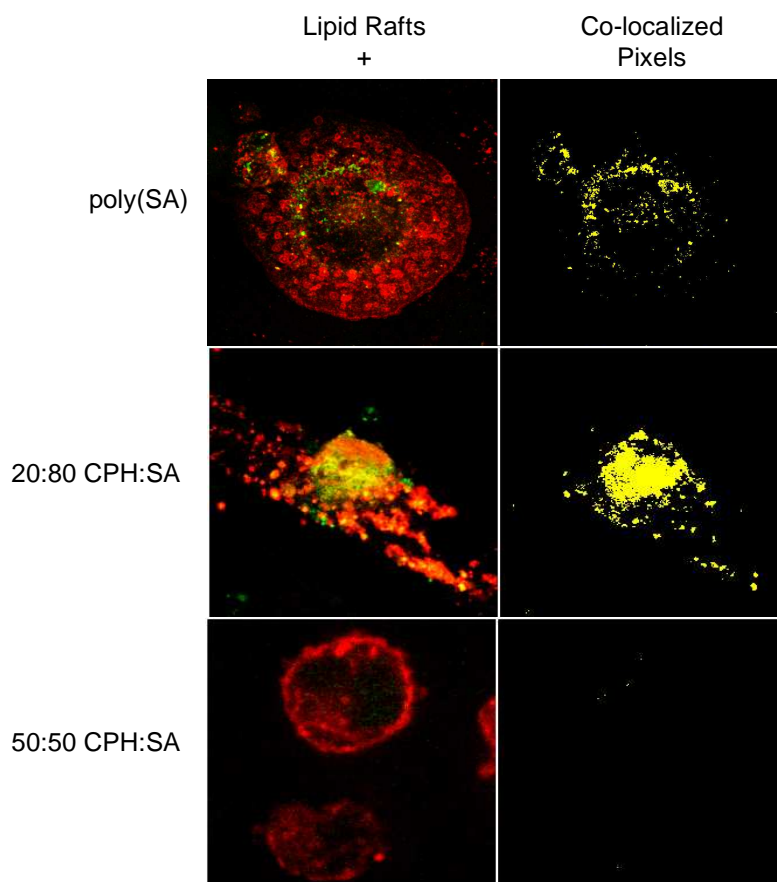


**Figure 4.3.** Confocal photomicrographs of FITC-labeled polyanhydride nanoparticles internalized by THP-1 cells. Adherent monocytes were incubated with nanoparticles for 30 min before cultures were washed and continued to incubate for an additional 2 h. Poly(SA) and 20:80 CPH:SA nanoparticles were internalized to a much greater extent than 50:50 CPH:SA nanoparticles. The majority of internalized poly(SA) and 20:80 CPH:SA were bound by cholesterol rich membranes as indicated by the high degree of co-localization (yellow). Representative images were captured by LSCM. Lipid rafts (red) were identified using Alexa 555 CTx (Molecular Probes). Scale bar = 5  $\mu$ m.

The data in Table II indicate that in the experiments designed to evaluate phagocytosis where the exposure to nanoparticles was 30 min, the least hydrophobic polymers (i.e., poly(SA)) were more rapidly internalized than the more hydrophobic (i.e., CPH-containing) polymers (Fig. 4.3). In contrast, the 48 h

co-localization experiments employ a longer exposure time of nanoparticles with cells lasting 6 h. In these experiments, where endocytosis plus the initial phagocytosis would contribute to total nanoparticle uptake, it was observed that ~96% of the THP-1 cells contained poly(SA) nanoparticles, while the uptake of 20:80 CPH:SA and 50:50 CPH:SA was ~91% and ~53%, respectively. These results indicate that the chemistry of the polyanhydride nanoparticles affects the uptake efficiency of these nanoparticles by monocytes. Unlike CPH-containing nanoparticles, poly(SA) nanoparticles were more efficiently internalized by phagocytic processes (30 min exposure to cells) and did not require the extended time (6 h) associated with endocytic processes. The more hydrophobic nanoparticles (i.e., CPH-rich) were not internalized by phagocytic pathways (~8%). However, with time, all the formulations were internalized; but, 50:50 CPH:SA nanoparticles were internalized to a lesser extent (~53%, Table 4.2). Overall, monocyte uptake of polyanhydride nanoparticles correlated with decreasing hydrophobicity (poly(SA) > 20:80 CPH:SA > 50:50 CPH:SA).

**Table 4.2.** Association of polyanhydride nanoparticles with THP-1 cells varies depending on polymer chemistry.

Polymer	Percent monocytes with internalized nanoparticles*	
	2 h (phagocytosis)	48 h (phagocytosis and endocytosis)
<b>Poly(SA)</b>	87.9% ± 17.1%	96.3% ± 11.7%
<b>20:80 CPH:SA</b>	27.1% ± 14.8%	91.2% ± 22.2%
<b>50:50 CPH:SA</b>	8.1% ± 10.6%	53.1% ± 28.3

\* Average percent nanoparticles positive monocytes calculated per 100x field of view image

The degree of hydrophobicity may indeed be an important factor influencing nanoparticle uptake. The hydrophobic nature of these particles may facilitate their interaction with hydrophobic lipid-rich micro-domains in the cell membrane, including lipid rafts. Lipid rafts contain many membrane-bound cofactors that comprise receptor complexes, such as receptors for complement, antibodies, and serum and extracellular matrix proteins.<sup>39-41</sup> In contrast with phagocytosis, increasing polymer hydrophobicity may facilitate closer nanoparticle-to-cell interactions and increase the probability of internalization through constitutive endocytic or macropinocytotic pathways. These hydrophobic interactions facilitate nanoparticle internalization by direct association with surface receptors or through direct interactions with the plasma membrane. Pattern recognition receptors (PRRs) are another key receptor type found in lipid rafts of APCs. PRRs recognize pathogen-associated molecular patterns (PAMPs), which are repetitive patterns of molecular structure found in both microorganisms and the mammalian host. Examples of PAMPs include lipopolysaccharide and flagellin from bacteria as well as hyaluronan and uric acid

from mammals. All of these PAMPs signal “danger” to the host, be it in the context of infection or cellular damage. Hydrophobic characteristics have been ascribed to many PAMPs and are thought to be partly responsible for their immunostimulatory properties.<sup>42</sup> In the context of the polyanhydride co-polymers, surface patterns of intervening hydrophobic moieties (e.g., CPH and SA, Fig. 1) may mimic PAMPs, facilitate interactions with PRRs present on the surface of APCs and subsequently enhance the ability of APCs to activate T cells.<sup>43,44</sup> Internalization and co-localization of antigen-loaded nanoparticles within the endocytic pathway may, in part, explain the adjuvanticity of polyanhydride nanoparticles.<sup>22</sup>

#### 4.4.2.2 Intracellular localization

In general, intracellular degradation and processing of exogenously presented antigen occurs when lysosomes fuse with late endosomes containing antigen. In contrast, endogenous antigen is processed within the cytosol by the proteasome.<sup>45</sup> As a result, antigen fate (i.e., MHC I vs MHC II presentation) is largely decided by intracellular location. Given the variable surface chemistry presented by the different polyanhydrides, we compared the intracellular distribution of nanoparticles 48 h after uptake. The majority of particles were found to be intact and located within membrane bound vesicles that were characterized as acidic and CTx<sup>+</sup> (Fig. 4.4). In these photomicrographs, the FITC-dextran containing nanoparticles appear green, the acidic vesicles are red (Lysotracker), and co-localized nanoparticles within acidic vesicles appear

yellow. The data indicates that all the polyanhydride chemistries studied resulted in localization of the nanoparticles into the acidic phagolysosomal compartments of the cells.

The majority of these particles were rapidly targeted to the endosomal pathway, and localized within vesicles exhibiting staining characteristics and morphology consistent with MHC class II loading compartments.<sup>46</sup> Interestingly, at 48 h, ~10 % of the poly(SA) and 20:80 CPH:SA nanoparticles did not appear to be located within acidic or lipid raft containing vesicles (Fig. 4.4). A lack of localization within either of these major intracellular compartments is consistent with nanoparticles that are free within the cellular cytosol. Release of antigen from nanoparticles located within the cellular cytosol would be processed and directed to the MHC class I presentation pathway.<sup>45</sup> However, the data presented in Fig. 4.3 and Fig. 4.4 would only suggest that small amounts of nanoparticles can reach the cytosol and that further experiments are warranted.

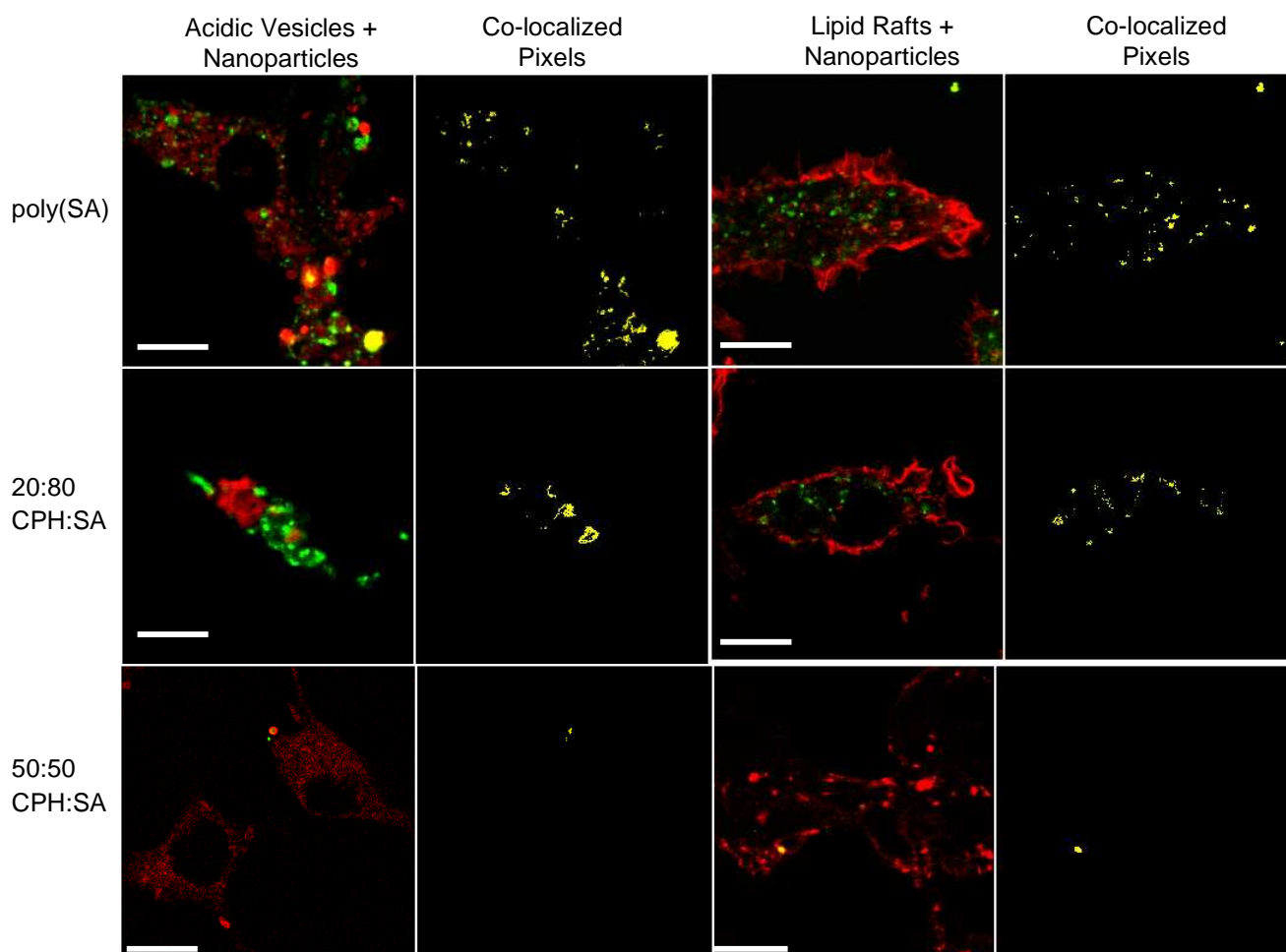


**Figure 4.4.** Confocal images of the intracellular localization of FITC-nanoparticles in THP-1 cells 48 h after uptake. Representative images were captured by LSCM and processed using ImageJ. The majority of internalized poly(SA) and 20:80 CPH:SA nanoparticles were bound by cholesterol rich membranes as indicated by the high degree of co-localization (yellow). Acidic vesicles (two left columns) were identified using the pH responsive LysoTracker dye (red) and cholesterol rich lipid rafts (two right columns) were visualized using Alexa 555 conjugated CTx (red, Molecular Probes). Note the general absence of FITC 50:50 CPH:SA nanoparticles compared to 20:80 CPH:SA and poly(SA). Scale bar = 5  $\mu$ m.

#### 4.4.2.3 Antigen Internalization

As previously discussed, polyanhydride nanoparticles serve as antigen delivery platforms to APCs. Nanoparticle-encapsulated immunogens would be released intracellularly following internalization and slow polymer degradation.<sup>8</sup> However, some nanoparticles may release antigen prior to uptake, providing a source of soluble antigen delivered to APCs via endocytosis. To evaluate the ability of nanoparticles to stimulate soluble antigen internalization by APCs, the THP-1 cells were co-incubated with blank nanoparticles (poly(SA), 20:80 CPH:SA, or 50:50 CPH:SA) and soluble E $\alpha$ -RFP<sup>37</sup>, fixed, and visualized by epifluorescence microscopy. Representative photomicrographs and bar graphs summarizing cell associated RFP data are provided in Fig. 4.5.

Comparisons among the three chemistries reveal that after 2 h of co-incubation, all three chemistries dramatically increased the amount of soluble antigen internalized by monocytes. A potential mechanism for the increase in uptake stimulated by the nanoparticles is that the protein itself is able to adsorb on the surface of nanoparticles that are then subsequently internalized by the APC. However, preliminary experiments failed to detect soluble RFP adsorbing onto FITC-labeled nanoparticles (data not shown) and culture conditions include ample amounts of serum proteins present in the 10% fetal bovine serum supplemented medium. Moreover, the dramatic increase in the uptake of soluble RFP was also detected for 50:50 CPH:SA even though these particles serve as poor targets for uptake themselves (Table 4.2, Fig. 4.3, and Fig. 4.4). This data

demonstrates that the chemistry of the polyanhydride nanoparticles influences the ability of APCs to internalize soluble antigen.

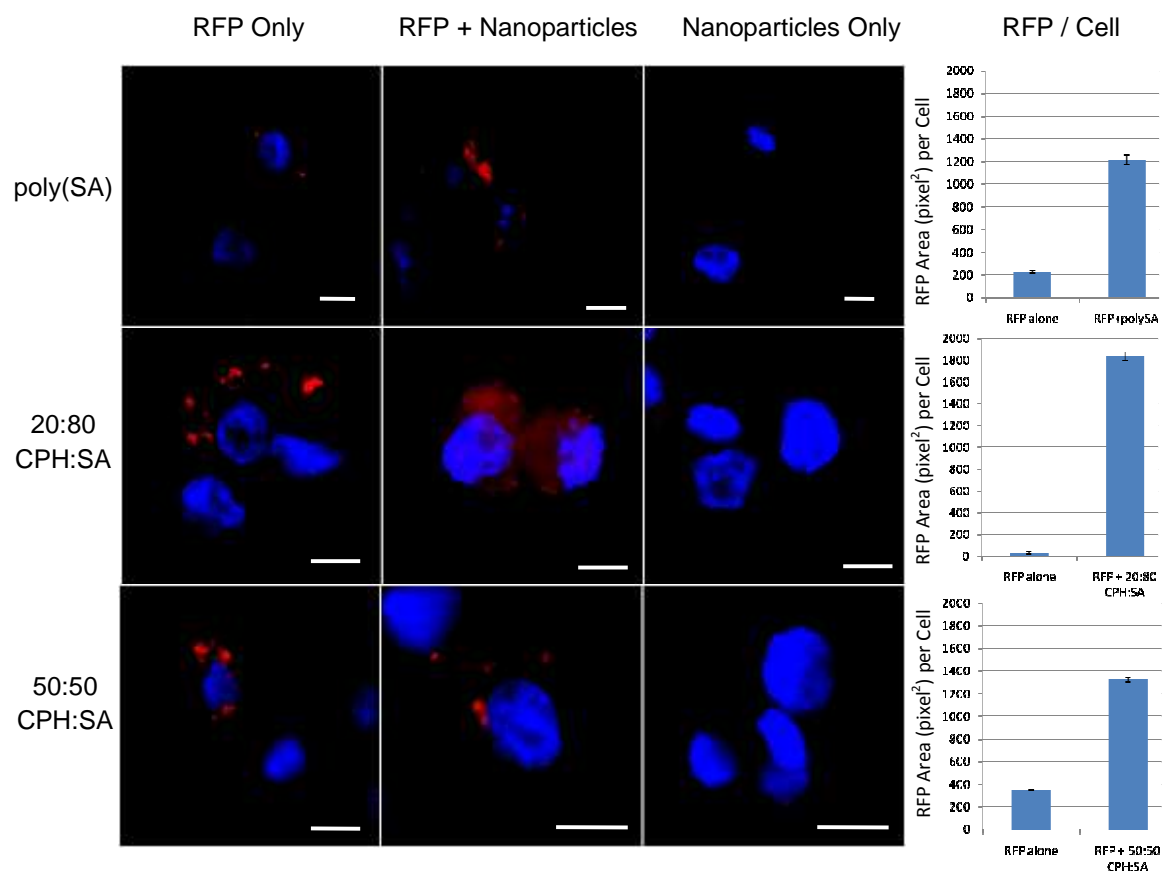


**Figure 4.5.** Enhanced uptake of soluble E $\alpha$ -RFP (red) antigen by monocytes (nuclei blue) after co-incubation with polyanhydride nanoparticles for 2 h. Data demonstrated that the poly(SA) nanoparticles enhanced antigen internalization more readily than did 20:80 CPH:SA followed by 50:50 CPH:SA. Representative epifluorescent images were captured and processed using identical exposure and ImageJ settings. Adjacent bar graphs summarize the average amount of RFP detected per cell. Pixel areas within each image correspond to relative intensity of RFP signal detected inside cells. Values from 3 randomly selected fields of view were used to calculate averages and standard deviation. Scale bar = 5  $\mu$ m.

#### **4.5 Conclusions**

The unique cellular interactions elicited by polyanhydride nanoparticles are a function of the particles' distinct physical and chemical properties that modulate the persistence and intracellular distribution of antigen. We observed that polyanhydride nanoparticles were internalized and distributed within human monocytes in a chemistry-dependent manner. We also found that chemistry influences the ability of nanoparticles to enhance monocytic uptake of soluble antigen. Together, this data highlights the importance of chemistry in designing polyanhydride nanoparticles as vaccine or drug delivery vehicles intended for specific applications and/or targeting desired intracellular locations.

#### **4.6 Acknowledgements**

B.N. and M.J.W. acknowledge financial support from the US Department of Defense – Office of Naval Research (ONR Award # N00014-06-1-1176) and the Grow Iowa Values Fund. B.H.B. acknowledges startup funds provided by Iowa State University-College of Veterinary Medicine and the Office of Biotechnology. B.D.U acknowledges financial support from the Aileen S. Andrew Foundation. The authors acknowledge useful discussions with Dr. Amanda Ramer-Tait and Jenny Wilson-Welder. B.N. dedicates this work to Nicholas A. Peppas on the wonderful occasion of his sixtieth birthday.

#### 4.7 References

1. Preis, I. & Langer, R.S. A single-step immunization by sustained antigen release. *Journal of Immunological Methods*. **28**(1-2), 193 – 197 (1979).
2. Wilson-Welder, J.H., et al., Vaccine adjuvants: Current challenges and future approaches. *Journal of Pharmaceutical Science*. **98**(4), 1278 – 1316 (2008).
3. Schwendeman, S.P. Recent advances in the stabilization of proteins encapsulated in injectable PLGA delivery systems. *Critical Reviews in Therapeutic Drug Carrier Systems*. **19**(1), 73 – 98 (2002).
4. Gopferich, A., Polymer Bulk Erosion. *Macromolecules*. **30**(9), 2598 – 2604 (1997).
5. Wang, Y., et al. Controlled release of ethacrynic acid from poly(lactide-co-glycolide) films for glaucoma treatment. *Biomaterials*. **25**(18), 4279 – 4285 (2004).
6. Fu, K., et al. Visual evidence of acidic environment within degrading poly(lactic-co-glycolic acid) (PLGA) microspheres. *Pharmaceutical Research*. **17**(1), 100 – 106 (2000).
7. Ding, A.G. & Schwendeman, S.P. Acidic microclimate pH distribution in PLGA microspheres monitored by confocal laser scanning microscopy. *Pharmaceutical Research*. **25**(9), 2041 – 2052 (2008).
8. Determan, A.S., et al. Protein stability in the presence of polymer degradation products: consequences for controlled release formulations. *Biomaterials*. **27**(17), 3312 – 3320 (2006).
9. Determan, A.S., et al. Encapsulation, stabilization, and release of BSA-FITC from polyanhydride microspheres. *Journal of Controlled Release*. **100**(1), 97 – 109 (2004).
10. Zhu, G., S.R. Mallery & Schwendeman, S.P. Stabilization of proteins encapsulated in injectable poly(lactic-co-glycolic acid). *Nature Biotechnology*. **18**(1), 52 – 57 (2000).
11. Kipper, M.J., et al. Design of an injectable system based on bioerodible polyanhydride microspheres for sustained drug delivery. *Biomaterials*. **23**(22), 4405 – 4412 (2002).

12. Shen, E., et al. Mechanistic relationships between polymer microstructure and drug release kinetics in bioerodible polyanhydrides. *Journal of Controlled Release*. **82**(1), 115 – 125 (2002).
13. Ron, E., et al., Controlled release of polypeptides from polyanhydrides. *Proceedings of the National Academy of Sciences of the United States of America*. **90**(9), 4176 – 4180 (1993).
14. Shieh, L., et al. Erosion of a new family of biodegradable polyanhydrides. *Journal of Biomedical Materials Research*. **28**(12), 1465 – 1475 (1994).
15. Jain, J.P., et al., Role of polyanhydrides as localized drug carriers. *Journal of Controlled Release*. **103**(3), 541 – 563 (2005).
16. Determan, A.S., et al. The role of microsphere fabrication methods on the stability and release kinetics of ovalbumin encapsulated in polyanhydride microspheres. *Journal of Microencapsulation*. **23**(8), 832 – 843 (2006).
17. Tabata, Y., Gutta, S. & Langer, R. Controlled delivery systems for proteins using polyanhydride microspheres. *Pharmaceutical Research*. **10**(4), 487 – 496 (1993).
18. Pfeifer, B.A., et al. Poly(ester-anhydride):poly(beta-amino ester) microspheres and nanoparticles: DNA encapsulation and cellular transfection. *International Journal of Pharmaceutics*. **304**(1-2), 210 – 219 (2005).
19. Shelke, N.B. and Aminabhavi, T.M. Synthesis and characterization of novel poly(sebacic anhydride-co-Pluronic F68/F127) biopolymeric microspheres for the controlled release of nifedipine. *International Journal of Pharmaceutics*. **345**(1-2), 51 – 58 (2007).
20. Hsu, W., et al. Local delivery of interleukin-2 and adriamycin is synergistic in the treatment of experimental malignant glioma. *Journal of Neurooncology*. **74**(2), 135 – 140 (2005).
21. Hanes, J., Chiba, M. & Langer, R. Degradation of porous poly(anhydride-co-imide) microspheres and implications for controlled macromolecule delivery. *Biomaterials*. **19**(1-3), 163 – 172 (1998).
22. Kipper, M.J., et al. Single dose vaccine based on biodegradable polyanhydride microspheres can modulate immune response mechanism. *Journal of Biomedical Materials Research Part A*. **76**(4), 798 – 810 (2006).

23. Berkland, C., et al. Microsphere size, precipitation kinetics and drug distribution control drug release from biodegradable polyanhydride microspheres. *Journal of Controlled Release*. **94**(1), 129 – 141 (2004).
24. Lacasse, F.X., et al. Influence of surface properties at biodegradable microsphere surfaces: effects on plasma protein adsorption and phagocytosis. *Pharmaceutical Research*. **15**(2), 312 – 317 (1998).
25. Schwab, J.A. & Zenkel, M. Filtration of particulates in the human nose. *Laryngoscope*, **108**(1), 120 – 124 (1998).
26. Jaques, P.A. & Kim, C.M. Measurement of total lung deposition of inhaled ultrafine particles in healthy men and women. *Inhalation Toxicology*. **12**(8), 715 – 731 (2000).
27. Desai, M.P., et al. Gastrointestinal uptake of biodegradable microparticles: effect of particle size. *Pharmaceutical Research*. **13**(12), 1838 – 1845 (1996).
28. Jung, T., et al. Tetanus toxoid loaded nanoparticles from sulfobutylated poly(vinyl alcohol)-graft-poly(lactide-co-glycolide): evaluation of antibody response after oral and nasal application in mice. *Pharmaceutical Research*. **18**(3), 352 – 360 (2001).
29. Illum, L. Nanoparticulate systems for nasal delivery of drugs: a real improvement over simple systems? *Journal of Pharmaceutical Science*. **96**(3), 473 – 483 (2007).
30. Desai, M.P., et al. The mechanism of uptake of biodegradable microparticles in Caco-2 cells is size dependent. *Pharmaceutical Research*. **14**(11), 1568 – 1573 (1997).
31. Fuller, J.E., et al. Intracellular delivery of core-shell fluorescent silica nanoparticles. *Biomaterials*. **29**(10), 1526 – 1532 (2008).
32. Conix, A. Poly[1,3-bis(p-carboxyphenoxy)propane anhydride]. *Macromolecular Synthesis*. **2**, 95 – 98 (1966).
33. Mathiowitz, E., et al. Biologically erodible microspheres as potential oral drug delivery systems. *Nature*. **386**(6623), 410 – 414 (1997).

34. Stokes, R.W. & Doxsee, D. The receptor-mediated uptake, survival, replication, and drug sensitivity of *Mycobacterium tuberculosis* within the macrophage-like cell line THP-1: a comparison with human monocyte-derived macrophages. *Cellular Immunology*. **197**(1), 1 – 9 (1999).
35. Bellaire, B.H., Roop, R.M. II, & Cardelli, J.A. Opsonized virulent *Brucella abortus* replicates within nonacidic, endoplasmic reticulum-negative, LAMP-1-positive phagosomes in human monocytes. *Infection and Immunity*. **73**(6), 3702 – 3713 (2005).
36. *ImageJ*. Image Processing and Analysis in Java. Retrieved on 3 August 2008 from <http://rsb.info.nih.gov/ij/>.
37. Itano, A.A., et al. Distinct dendritic cell populations sequentially present antigen to CD4 T cells and stimulate different aspects of cell-mediated immunity. *Immunity*. **19**(1), 47 – 57 (2003).
38. Mathiowitz, E., et al. Process for preparing microparticles through phase inversion phenomena. United States Patent No. 6,616,869 (2003).
39. Lajoie, P. & Nabi, I.R. Regulation of raft-dependent endocytosis. *Journal of Cellular and Molecular Medicine*. **11**(4), 644 – 53 (2007).
40. Gupta, N. & DeFranco, A.L. Visualizing lipid raft dynamics and early signaling events during antigen receptor-mediated B-lymphocyte activation. *Molecular Biology of the Cell*. **14**(2), 432 – 444 (2003).
41. Wolf, Z., et al. Monocyte cholesterol homeostasis correlates with the presence of detergent resistant membrane microdomains. *Cytometry Part A*. **71**(7), 486 – 494 (2007).
42. Seong, S.Y. & Matzinger, P. Hydrophobicity: an ancient damage-associated molecular pattern that initiates innate immune responses. *Nature Reviews Immunology*. **4**(6), 469 – 478 (2004).
43. Netea, M.G., et al. From the Th1/Th2 paradigm towards a Toll-like receptor/T-helper bias. *Antimicrobial Agents and Chemotherapy*. **49**(10), 3991 – 3996 (2005).
44. Elamanchili, P., et al. "Pathogen-mimicking" nanoparticles for vaccine delivery to dendritic cells. *Journal of Immunotherapy*. **30**(4), 378 – 395 (2007).

45. Goldberg, A.L., et al. The importance of the proteasome and subsequent proteolytic steps in the generation of antigenic peptides. *Molecular Immunology*. **39**(3-4), 147 – 164 (2002).
46. Hiltbold, E.M. & Roche, P.A. Trafficking of MHC class II molecules in the late secretory pathway. *Current Opinion in Immunology*. **14**(1), 30 – 35 (2002).

## CHAPTER 5

# Combining Population and Individual Analyses to Probe Immune Cell Interactions with Polyanhydride Nanoparticles

A paper to be submitted to *Nature Materials*, 2010.

Bret D. Ulery<sup>1,\*</sup>, Latrisha K. Petersen<sup>1,\*</sup>, Yashdeep Phanse<sup>2</sup>, Scott Broderick<sup>3</sup>, Amanda E. Ramer-Tait<sup>2</sup>, Krishna Rajan<sup>3</sup>, Michael J. Wannemuehler<sup>2</sup>, Bryan H. Bellaire<sup>2</sup>, and Balaji Narasimhan<sup>1</sup>

\* These authors contributed equally to this work.

<sup>1</sup> Department of Chemical and Biological Engineering, Iowa State University, Ames, Iowa 50011, USA

<sup>2</sup> Department of Veterinary Microbiology and Preventive Medicine, Iowa State University, Ames, Iowa 50011, USA

## 5.1 Abstract

Polyanhydrides, a class of hydrolytically degradable polymers, possess monomer chemistry flexibility allowing for their material properties and degradation to be tailored for use in biomedical applications in controlled payload release, tissue engineering and/or immune response activation. In the design of polyanhydride nanoparticle-based vaccine adjuvants and delivery vehicles, understanding the mechanism by which these materials initiate an immune response is critical. This study investigates the effect nanoparticle polymer chemistry has on the activation of murine bone marrow derived dendritic cells (DCs). To assess activation, cell surface marker expression, cytokine secretion and intracellular nanoparticle trafficking, were studied. Nanoparticle hydrophobicity determined DC response yielding cellular activation, shock or even death. These results suggest that polymer chemistry can be chosen to best tailor nanoparticles to initiate desired immune responses.

## 5.2 Introduction

Recent advancements in vaccine development have focused on the utilization of adjuvants (non-specific immune boosting substances) to increase effectiveness. Everything from viral<sup>1,2</sup> and bacterial vectors<sup>3,4</sup> to liposomes<sup>5,6</sup> and degradable polymers<sup>7-10</sup> have been investigated to design systems that function not only as adjuvants, but also as directed delivery vehicles. Research on degradable polymers holds significant promise since material properties can be tailored to allow for long-term<sup>8,10</sup> and directed antigen delivery<sup>7,8</sup>, immune activation<sup>9,10</sup>, and immune response modulation.<sup>10</sup>

While a number of degradable polymer families (polyesters<sup>7,9</sup>, polyethers<sup>11,12</sup>, and polyphosphazenes<sup>13,14</sup>) have been investigated for vaccine applications, polyanhydrides offer a unique set of features making them exceptional candidates. Polyanhydrides are FDA-approved, biocompatible, bioresorbable, surface-eroding polymers in which polymer degradation and subsequent payload release are directly correlated to polymer chemistry.<sup>15-18</sup> Copolymers based upon the combination of the monomers 1,6-bis-(*p*-carboxyphenoxy) hexane (CPH) and sebacic acid (SA) and copolymers based upon 1,8-bis-(*p*-carboxyphenoxy-3,6-dioxaoctane) (CPTEG) and CPH were studied in this work. Research has shown that these polyanhydride chemistries possess moderate pH microenvironments (upon degradation)<sup>19,20</sup>, protein stabilization capabilities<sup>10,15,16,21-23</sup>, and immune activation potential.<sup>10,22,24,25</sup> In order to utilize polyanhydrides as vaccine delivery vehicles, particle formation

offers the ability to protect encapsulated antigen from rapid immune clearance and mediate antigen delivery to cells of interest. Recent research has shown that antigen-loaded polyanhydride nanoparticles (<1  $\mu\text{m}$ ) delivered as a single-dose, intranasal formulation conveyed protection against lethal challenge with *Yersinia pestis*, the causative agent of plague, through 23 weeks post-vaccination.<sup>26</sup> While nanoparticles were able to convey long-term immunity, the underlying mechanism(s) for this action are still unclear.

The cells primarily responsible for the initiation of an immune response are a class of antigen presenting cells (APCs) called dendritic cells (DCs).<sup>27</sup> Once DCs are activated they increase their cell surface expression of major histocompatibility complexes (MHC) I and II to present processed antigen to T cells in lymphoid organs. Also, they express co-stimulatory molecules (CD40, CD80, and CD86) that assist in directing T cell activation.<sup>27</sup> Other markers, like CD209, are thought to play a role in T cell activation as well as assist in DC trafficking to the draining lymphoid tissue.<sup>28</sup> Activated DCs also secrete chemical signals called cytokines (IL-1 $\beta$ , IL-6, IL-10, IL-12, TNF- $\alpha$ , etc.) to help direct the nature of the immune response.<sup>27</sup> By better understanding the mechanism by which polymer particle adjuvants induce DC activation *in vitro*, rational design of vaccines can be accomplished before experiments are conducted in animal models and clinical trials in humans.

When evaluating interactions of polymer particles with cells, two types of analyses have been commonly utilized: cell population-based and individual cell-

based. In cell population-based analysis, the overall effect of particles on a group of cells is explored. In research with DCs, this includes utilizing flow cytometric evaluation of fluorescently-tagged monoclonal antibody detection of cell surface marker expression and enzyme-linked immunosorbent assay or multiplex conjugated-bead assay detection of DC secreted cytokines. These techniques have been used to probe the interactions between DCs and particles composed of polyesters<sup>29-33</sup>, polyethers<sup>34</sup>, polyethylenimides<sup>35,36</sup>, chitosan<sup>37,38</sup>, and polyanhydrides.<sup>22,25</sup> These studies have shown that polymer particles of certain chemistries have the capacity to activate DCs. In individual cell-based analysis, fluorescent microscopy of individual cells probed with fluorescently-tagged monoclonal antibodies detecting intracellular processes is used to determine particle internalization and intracellular fate. This technique has been utilized to probe trafficking of degradable polymer particles in lung cancer cells<sup>39</sup>, cervical cancer cells<sup>40</sup>, kidney cells<sup>41</sup>, epithelial cells<sup>42,43</sup>, and dendritic cells.<sup>44</sup> These studies have provided insights on how cells internalize and process degradable particles via the endocytic pathway.

Each type of analysis generates data that describes the effect of particles on cells, but only provides one side of the argument. While cell population-based analysis has shown the capacity for particles to initiate immune responses, the mechanisms that govern these reactions have yet to be detailed. In contrast, individual cell-based analysis has been used to follow intracellular particle trafficking, but these observations have yet to be linked to their effect on cells.

The primary focus of this study was to correlate intracellular polyanhydride nanoparticle behavior observed by fluorescent microscopy to DC activation as evaluated by cell surface marker expression and cytokine secretion. Linking these experiments will fulfill a critical gap in our understanding of how particles interact with immune cells at both the cellular and molecular levels, thereby enabling new insights on nanoparticle-based vaccine design.

## **5.3 Materials and Methods**

### **5.3.1 Materials**

Carboxylic diacid monomer synthesis required the use of 1,6-dibromohexane (98.5%), 4-hydroxybenzoic acid (96%), 1-methyl-2-pyrrolidinone anhydrous (99.5%), triethylene glycol (99%) purchased from Sigma Aldrich (St. Louis, MO); 4-*p*-fluorobenzonitrile (98%) purchased from Apollo Scientific (Stockport, Cheshire, England); and sodium hydroxide, sulfuric acid, acetonitrile, dimethyl formamide, toluene and potassium carbonate purchased from Fisher Scientific (Fairlawn, NJ). Polymerization and nanoparticle fabrication utilized acetic anhydride, chloroform, petroleum ether, ethyl ether, methylene chloride and hexanes from Fisher Scientific. DC culture medium included RPMI 1640, HEPES buffer, L-glutamate, penicillin-streptomycin, gentamycin acquired from Mediatech (Herndon, VA); heat inactivated fetal calf serum acquired from Valley Biomedical (Winchester, VA); and granulocyte macrophage colony stimulating factor (GM-CSF) acquired from PeproTech (Rocky Hill, NJ). Materials used in flow cytometry were: mouse serum; unlabeled CD36/16 Fc $\gamma$ R purchased from

Southern Biotech (Birmingham, AL);  $\beta$ -mercaptoethanol and unlabeled rat immunoglobulin (rat IgG) purchased from Sigma Aldrich; peridinin-chlorophyll proteins-Cy5.5 (PerCP/Cy5.5) conjugated anti-mouse MHC II (I-A/I-E) (clone M5/114.15.2) purchased from Biolegend (San Diego, CA); unlabeled hamster IgG, phycoerythrin (PE) conjugated anti-mouse MHC I (clone 34-1-2s), fluorescein isothiocyanate (FITC) conjugated anti-mouse CD86 (clone GL-1), allophycocyanin (APC) conjugated anti-mouse CD40 (clone 1C10), Alexa Fluor<sup>®</sup> 700 anti-mouse CD11c (clone N418), biotin conjugated anti-mouse CIRE (DC-SIGN or CD209) (clone 5H10), and allophycocyanin-Cy7 (APC-Cy7) conjugated streptavidin; and corresponding isotypes: PerCP-Cy5.5 conjugated rat IgG2b  $\kappa$  (clone RTK 4530), PE conjugated rat IgG2 K (clone eBM2a), FITC conjugated rat IgG1 K (clone eBR2a), APC conjugated rat IgG2a K (clone eBR2a), Alexa Fluor 700 conjugated Armenian hamster IgG (clone eBio299Arm), and biotin conjugated rat IgG2a (clone eBM2a). All of these reagents were purchased from e-Bioscience (San Diego, CA). *E. coli* lipopolysaccharide (LPS) was acquired from Sigma Aldrich. FluoSpheres<sup>®</sup> (0.2  $\mu\text{m}$  and 2  $\mu\text{m}$ ), FITC-loaded carboxylate-modified polystyrene particles (PS particles), were purchased from Invitrogen (Carlsbad, CA).

### 5.3.2 Polymer Synthesis, Nanoparticle Fabrication, and Characterization

Synthesis of CPTEG and CPH diacids, SA and CPH pre-polymers, and CPH:SA and CPTEG:CPH copolymers was performed as previously described.<sup>17,18,45</sup> The resulting polymers were characterized using <sup>1</sup>H nuclear

magnetic resonance spectroscopy to verify polymer chemistry and purity, gel permeation chromatography to analyze polymer molecular weight, and differential scanning calorimetry to determine polymer glass transition temperature and crystallinity. All properties evaluated showed that the synthesized polymers were within accepted ranges.<sup>17,18,45</sup>

Both FITC-dextran loaded and blank nanoparticles were fabricated by the polyanhydride anti-solvent nanoencapsulation (PAN) method modified from the protocol reported in Ulery et al.<sup>24</sup> Polymer was dissolved in methylene chloride at 0 °C at a concentration of 25 mg/mL. For loaded nanoparticles, FITC-dextran was sonicated for 15 s at a concentration of 1% of total batch weight to form a suspension. The polymer/polysaccharide solution was rapidly poured into a bath of pentane held at -20 °C at an anti-solvent to solvent ratio of 80:1. Penetration of anti-solvent into the polymer solution microenvironment caused spontaneous nanoparticle formation; the particles were subsequently filtered by Whatman No. 50 paper filters in a Buchner funnel. This procedure yielded a fine powder with at least 60% recovery. Nanoparticle morphology was investigated using scanning electron microscopy (SEM, JEOL 840A, JEOL Ltd., Tokyo, Japan). Quasi-elastic light scattering (QELS) was employed using a Zetasizer Nano (Malvern Instruments Ltd., Worcester, UK) to determine nanoparticle size.

### **5.3.3 Culture and Stimulation of C57BL/6 DCs**

DCs were harvested and grown as described previously.<sup>25</sup> C57BL/6 mice were euthanized, cells were extracted from bones and plated at approximately 5

million cells per T75 flask in GM-CSF DC media. They were fed on days 3 and 6 and plated into 24 well plates on day 8 at a density of approximately 2 million cells per well in 1 mL GM-CSF free DC media. Wells were split into those analyzed for nanoparticle-induced cell surface marker expression and cytokine secretion and those analyzed for intracellular trafficking of nanoparticles.

Stimulation groups for cell surface marker expression and cytokine secretion consisted of: 400 ng/mL LPS (positive control); no stimulation (NS) (negative control); and 250 µg/mL of blank nanoparticles composed of poly(SA), 50:50 CPH:SA, poly(CPH), 50:50 CPTEG:CPH, and poly(CPTEG). Treatments were applied to the DCs on day 9 and incubated for 48 h. On day 11, supernatants were collected for cytokine analysis and cells were stained for flow cytometry analysis.

Stimulation groups for intracellular trafficking of nanoparticles consisted of: polystyrene particles (PS particles), which were used as a control for particle internalization and 250 µg/mL of 1% FITC-dextran loaded nanoparticles composed of poly(SA), 50:50 CPH:SA, poly(CPH), 50:50 CPTEG:CPH, and poly(CPTEG). Treatment were applied to the DCs on day 9 and allowed to incubate for 30 min or 6 h. Cultures were washed with PBS and replenished with media to incubate for an additional 2 h or 42 h, respectively. Cells were then stained for intracellular trafficking markers as described below.

### 5.3.4 Cell Surface Markers

Expression of cell surface markers including MHC I, MHC II, CD40, CD86, CD209 and CD11c was assessed after 48 h incubation as described previously.<sup>25</sup> Adherent DCs were placed on ice and harvested by vigorous pipetting, then placed in polystyrene tubes (BD Falcon™, Franklin Lakes, NJ) and centrifuged at 4 °C at 250 rcf for 10 min. Cells were blocked with Fc blocking solution (PBS buffer with 0.1% anti-CD16/CD32, 0.1% unlabeled hamster IgG, 1% rat IgG, 1% mouse serum, 0.1% sodium azide, and 1% FBS) for 1 h. After blocking, the DCs were stained by monoclonal antibodies for the cell surface markers above and fixed with a stabilizing fixative (BD Bioscience, San Jose, CA). The samples were analyzed using a Becton-Dickinson FACSCanto flow cytometer (San Jose, CA) and FlowJo (TreeStar Inc, Ashland, OR). Cells were gated for single-cell populations and cell viability before cell surface marker expression analysis was conducted.

### 5.3.5 Cytokine Production

After incubation of the DCs with the stimulation treatments for 48 h, 200 µL of supernatants were collected from the cultures and assayed for the presence of IL-6, IL-10, IL-12p40, and TNF- $\alpha$  using the Luminex® Multiplex assay system (Austin, TX).

### 5.3.6 Intracellular Trafficking

To observe time-dependent intracellular trafficking of individual nanoparticles within DCs, cells were assessed similarly to previous work.<sup>24</sup> DCs were incubated for the indicated times, fixed with 4% paraformaldehyde (PFA) for 10 min at room temperature, and then washed with PBS. Polymerized actin was labeled by incubating DCs for 10 min after fixation with Alexa 568 conjugated phalloidin mushroom toxin (Molecular Probes-Invitrogen) at a 1:150 dilution. Lysosomes were immunofluorescently stained by incubating fixed coverslips with ID-4B anti-LAMP-1 (lysosomal-associated membrane protein 1) monoclonal antibody at a 1:50 dilution followed by Cy3-conjugated goat anti-mouse at a 1:150 dilution in PBS containing albumin and 0.1% saponin (BSP). Stained coverslips were washed with PBS and mounted on glass slides (Pro-Long w/ Dapi; Molecular Probes-Invitrogen). Epifluorescence and immunofluorescence microscopy were performed using either an using either an Olympus IX-71 inverted microscope with blue, green, and red filter sets with a cooled CCD camera or by an inverted Olympus Fluoview<sup>TM</sup> 1000 laser scanning confocal microscopy (LSCM). The LSCM is equipped with ApoChromatic x63 oil and x100 oil objectives and UV, Argon, Krypton and HeNe laser lines equipped with three photomultiplier detection tubes. Z-stack step size of 0.25  $\mu\text{m}$  was used. Intracellular trafficking analysis and final images were prepared using ImageJ v1.36b (NIH, Bethesda, MD) image analysis software loaded with particle counting algorithms.<sup>46</sup>

## 5.4 Results

### 5.4.1 Nanoparticle Characterization

Scanning electron photomicrographs of nanoparticles of varying chemistry are shown in Fig. 5.1a-e. The photomicrographs show that the nanoparticles appear spherical and relatively uniform in size and shape. Light scattering size distribution analysis (Fig. 5.1f) confirms that the diameters for nanoparticles of all chemistries fall between 100 nm and 1  $\mu$ m. Every batch of nanoparticles was analyzed in duplicate with a total of three distinct batches for each of the chemistries being evaluated. Mean particle diameters and corresponding standard errors are shown in the caption to Fig. 5.1. No statistically significant differences were found in the size and morphology of blank versus 1% FITC-dextran loaded nanoparticles (data not shown). Particle size followed a trend of smaller particles corresponding to increased oxygen content in the polymer backbone (i.e., higher CPTEG or CPH content). This observation may be explained by the nucleation and growth theory of precipitation<sup>47</sup>, wherein the increased oxygen content may make the polymer less soluble in the non-solvent (pentane) forcing increased nucleation sites leading to smaller particle size.

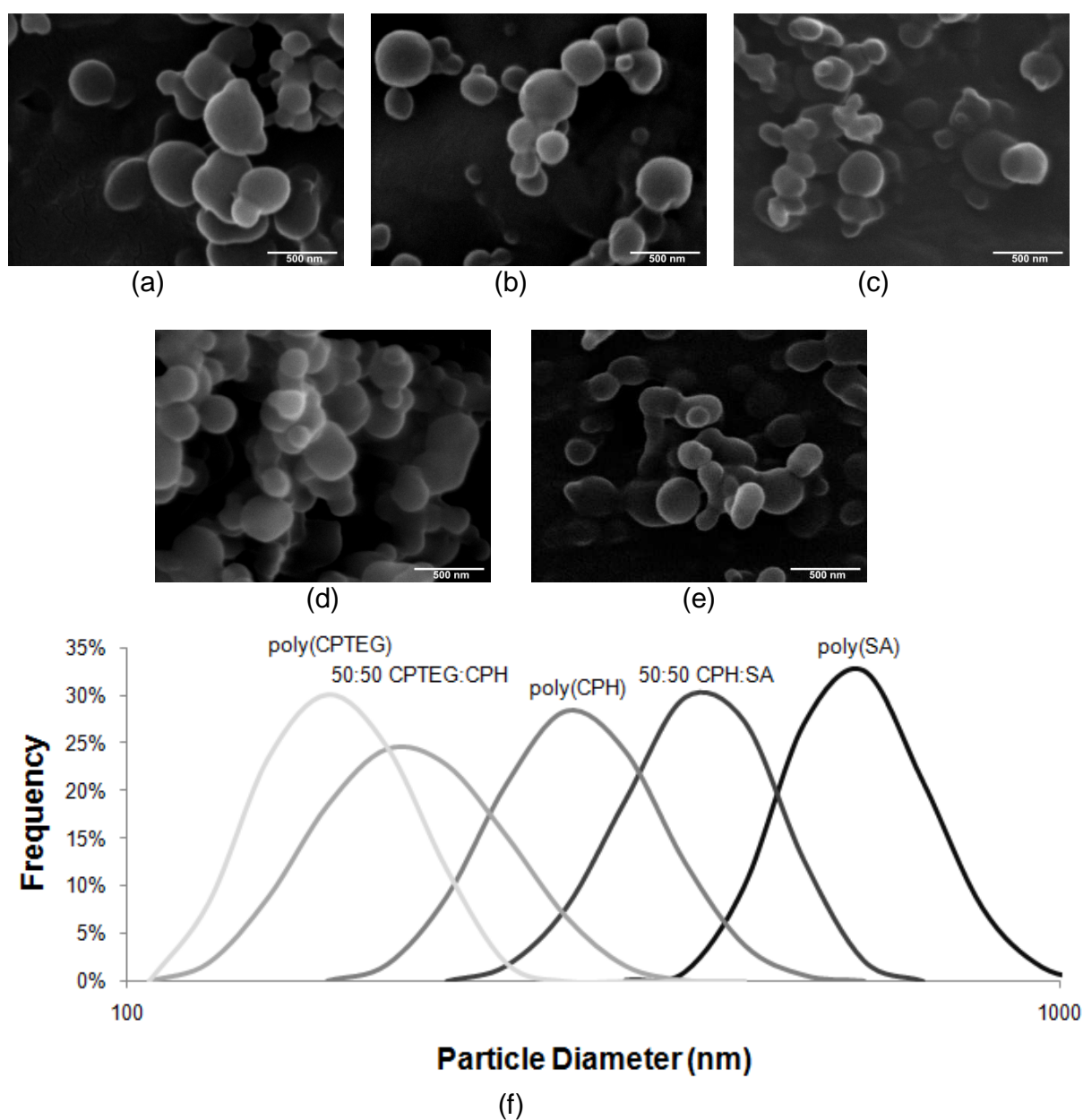


**Figure 5.1.** Representative SEM images of nanoparticles composed of (a) poly(SA), (b) 50:50 CPH:SA, (c), poly(CPH), (d) 50:50 CPTEG:CPH and (e) poly(CPTEG) with scale bars of 500 nm. (f) An overlap of particle size as determined by QELS averaged from three independent samples. Average particle diameters and standard errors are as follows: poly(SA) ( $616 \pm 62$ ), 50:50 CPH:SA ( $415 \pm 44$ ), poly(CPH) ( $310 \pm 36$ ), 50:50 CPH:SA ( $206 \pm 27$ ) and poly(CPTEG) ( $170 \pm 17$ ).

### 5.4.2 Cell Population-Based Analysis

Nanoparticles of varying chemistries and controls (negative: NS and positive: LPS) were co-incubated with bone-marrow derived DCs for 48 h and cell surface markers of interest (MHC I, MHC II, CD40, CD86, CD209, and CD11c) were stained by fluorescently tagged monoclonal antibodies and evaluated by flow cytometry. Side-scatter v forward-scatter plots (Fig. 5.2) show that increased nanoparticle hydrophobicity correlated to an overall population of less viable cells (shift of cells to a low forward-scatter profile).

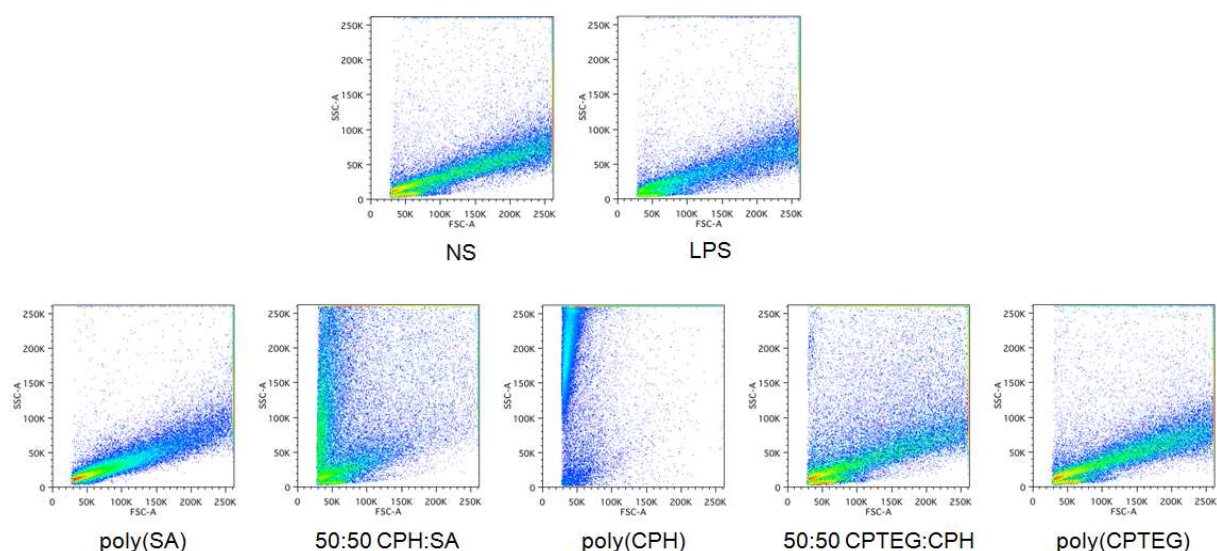


**Figure 5.2.** Side-Scatter (SSC-A) versus Forward-Scatter (FSC-A) plots for each treatment group. All graphs are representative images.

Analysis showed that only <3% of cells co-incubated with poly(CPH) nanoparticles (which was the most hydrophobic chemistry studied) were viable (data not shown), so further flow cytometry analysis was not conducted with this chemistry. Cells incubated with all other chemistries had cell population viability

>60% and this population was composed of >83% CD11c (DC specific marker) positive cells (data not shown). Supplemental Fig. 5.3 shows peak shifts for the markers of interest from isotype (non-specific binding) controls.

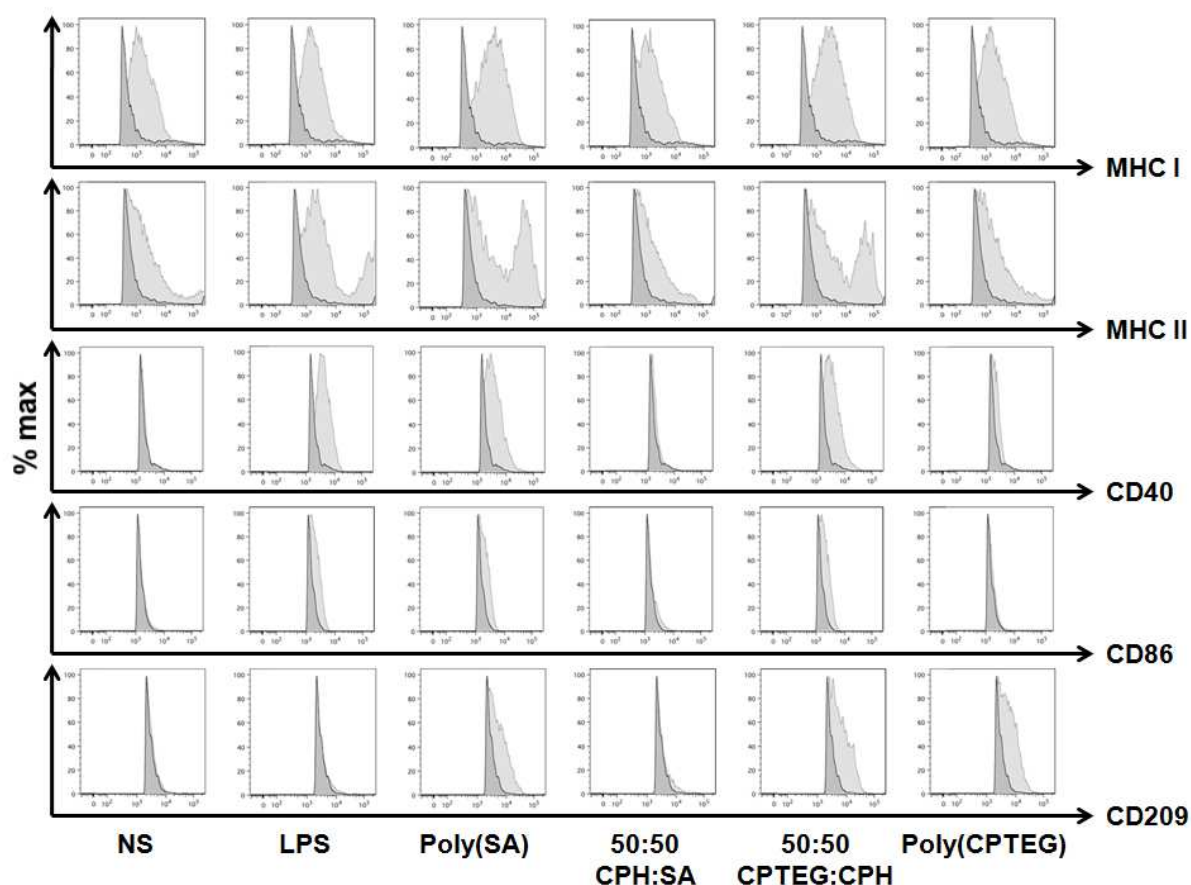


**Figure 5.3.** Cell surface marker expression (mean fluorescence intensity (MFI)) as represented with histograms of MHC I, MHC II, CD40, CD86 and CD209 after 48 h incubation of polyanhydride nanoparticles with DCs. All histograms are representative images and show the peak shift between the treatment group (light grey) from the isotype control (dark grey).

Mean fluorescence intensities (MFIs) for each marker for each stimulus were averaged and the data is compiled in Fig. 5.4. Surface expression of MHC I,

MHC II, CD40, and CD86 was enhanced for cells incubated with LPS or nanoparticles composed of poly(SA) or 50:50 CPTEG:CPH over the non-stimulated cells. Expression remained at background levels for cells stimulated with 50:50 CPH:SA or poly(CPTEG) nanoparticles. CD209 expression was dramatically increased due to the presence of poly(SA), 50:50 CPTEG:CPH, or poly(CPTEG) nanoparticles and remained near background in the presence of LPS or 50:50 CPH:SA nanoparticles. CD209 expression increased for cells exposed to less hydrophobic nanoparticles.

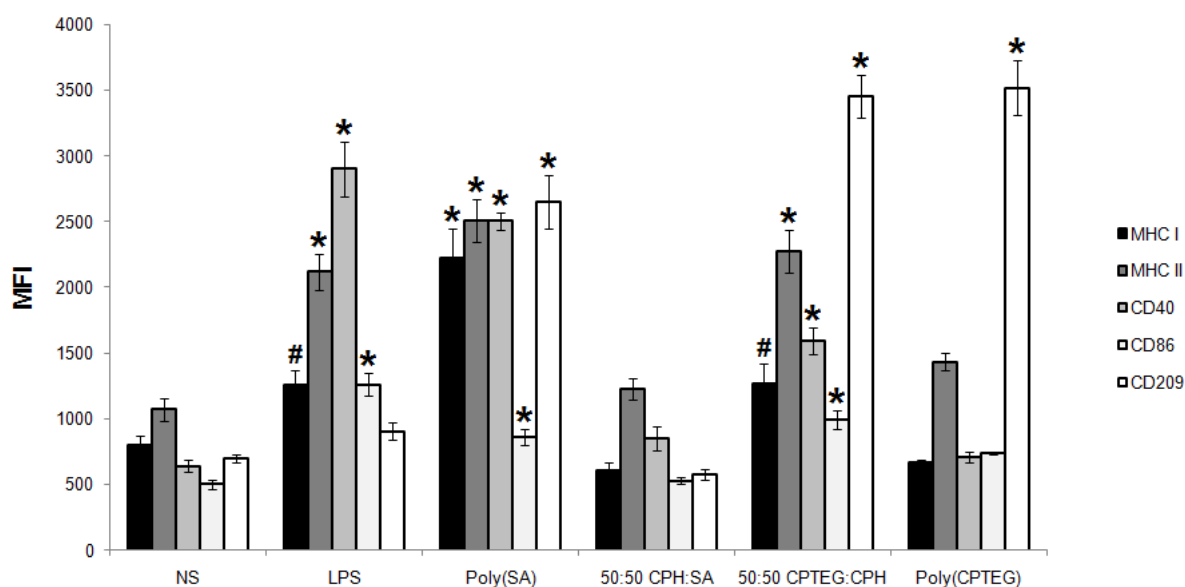


**Figure 5.4.** Analysis of MHC I, MHC II, CD40, CD86 and CD209 expression by C57BL/6 DCs. These histograms represent the complete set of results of MFI expression of cell surface markers for cells stimulated with NS, LPS and nanoparticles composed of poly(SA), 50:50 CPH:SA nanoparticles, 50:50 CPTEG:CPH, and poly(CPTEG). Data is representative of a minimum of 8 replicates per group. Error bars represent standard error. Average MFIs for NS (negative control) stimulated DCs are MHC I (799), MHC II (1069), CD40 (702), CD86 (503) and CD209 (702). # = p-value < 0.005 and \* = p-value < 0.001 (compared to NS).

Supernatants from these cell cultures were analyzed by a multiplex bead assay (LUMINEX<sup>®</sup>) for the presence of IL-6, IL-10, IL-12p40 and TNF- $\alpha$ . For all nanoparticle chemistries, no IL-10 production above background levels was detected (data not shown). Statistically significant quantities of IL-6, IL-12p40 and TNF- $\alpha$  were secreted from cells exposed to 50:50 CPH:SA or 50:50 CPTEG:CPH nanoparticles, but not cells exposed to poly(SA) or poly(CPTEG) nanoparticles (Fig. 5.5). The cytokine release caused by nanoparticles was considerably less than LPS induced levels as shown in the figure caption. This result follows the trend that more hydrophobic particles elicited increased cytokine levels.

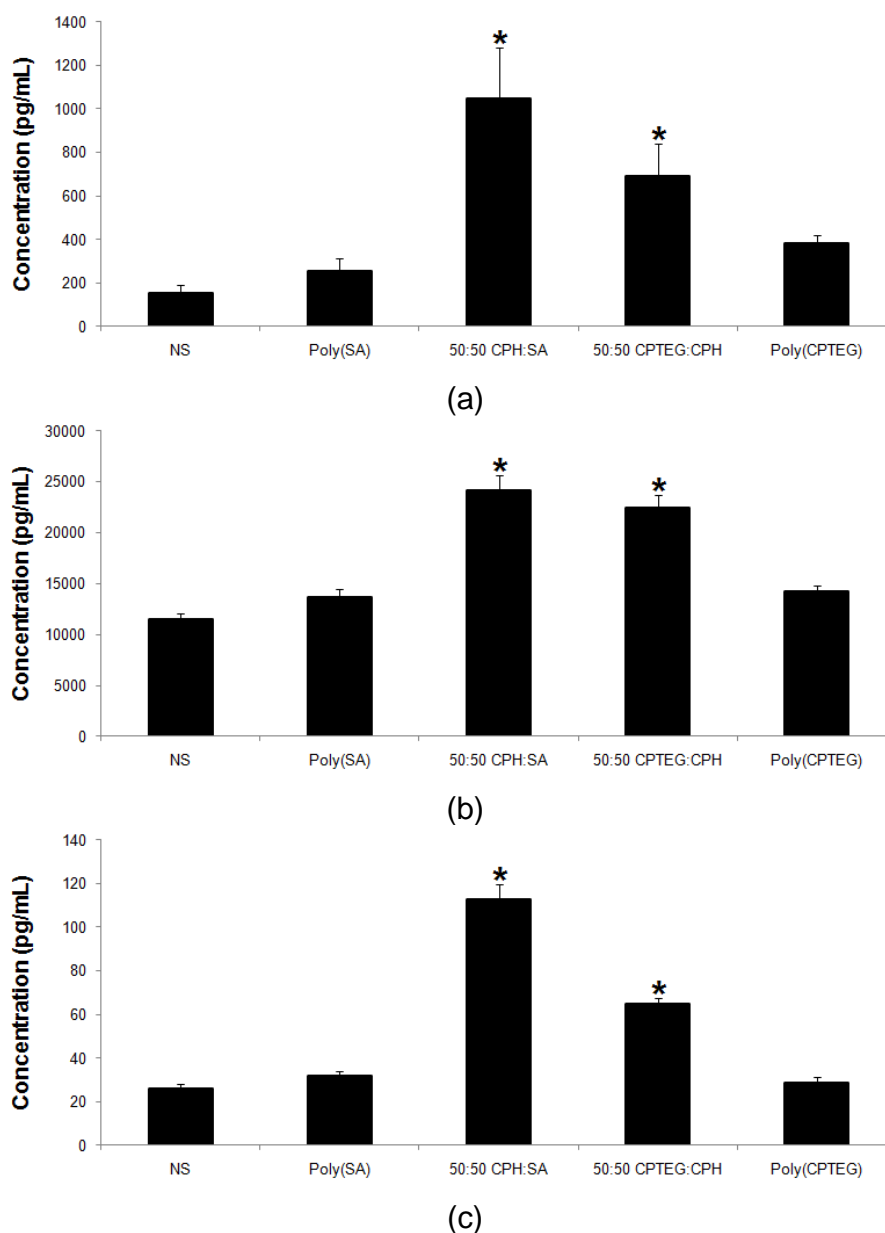


**Figure 5.5.** Analysis of (a) IL-6, (b) IL-12p40, and (c) TNF- $\alpha$  secretion by C57BL/6 DCs. These histograms represent the complete set of results of cytokine secretion by DCs stimulated with NS and nanoparticles composed of poly(SA), 50:50 CPH:SA, 50:50 CPTEG:CPH, and poly(CPTEG). Data is representative of a minimum of 8 replicates per stimulation group. Error bars represent standard error. Average cytokine concentrations in pg/ml secreted by LPS (positive control) and poly(CPH) stimulated DCs are IL-6 (>50,000 and 3,800), IL-12p40 (>50,000 and >50,000) and TNF- $\alpha$  (3,700 and 1,900). \* = p-value  $\leq$  0.002 (compared to NS).

### 5.4.3 Individual Cell-Based Analysis

Polyanhydride nanoparticles and PS particles (0.2 and 2  $\mu\text{m}$ ) were pulsed with DCs for 30 min and 6 h, washed and fixed and fluorescently stained at 2.5 h and 48 h post-exposure, respectively for polymerized actin and LAMP-1.

Polymerized actin staining was used to determine nanoparticle internalization by DCs and LAMP-1 staining was used to determine the presence of internalized nanoparticles in lysosomal vesicles. Confocal microscopy showed nearly all nanoparticles co-localized with polymerized actin (data not shown), which is utilized to traffic material within the cell. This result indicates that the nanoparticles were internalized by DCs.

The ability for nanoparticles to be processed by the exogenous pathway requires processing through lysosomal vesicle fusion.<sup>48</sup> To determine the nature of the internalization process, pulse times of 30 min and 6 h were chosen to allow for analysis of phagocytic events and a combination of phagocytic and endocytic events, respectively. Confocal photomicrographs of LAMP-1 staining at 2.5 h post-incubation (Fig. 5.6) showed little difference in overall cell morphology and nanoparticle appearance. Because it is difficult to distinguish between individual nanoparticles and aggregates of nanoparticles using confocal imaging and because polyanhydride nanoparticles are able to undergo deformation-induced particle aggregation to form blob-like clusters, the data are presented as “nanoparticle agglomerates.” The PS particles control showed significant internalization of the smaller 0.2  $\mu\text{m}$  particles, but few larger 2  $\mu\text{m}$  particles. This

is an expected result for the 30 min pulse time. Nearly all nanoparticle agglomerates regardless of chemistry were shown to be associated with LAMP-1 (yellow).

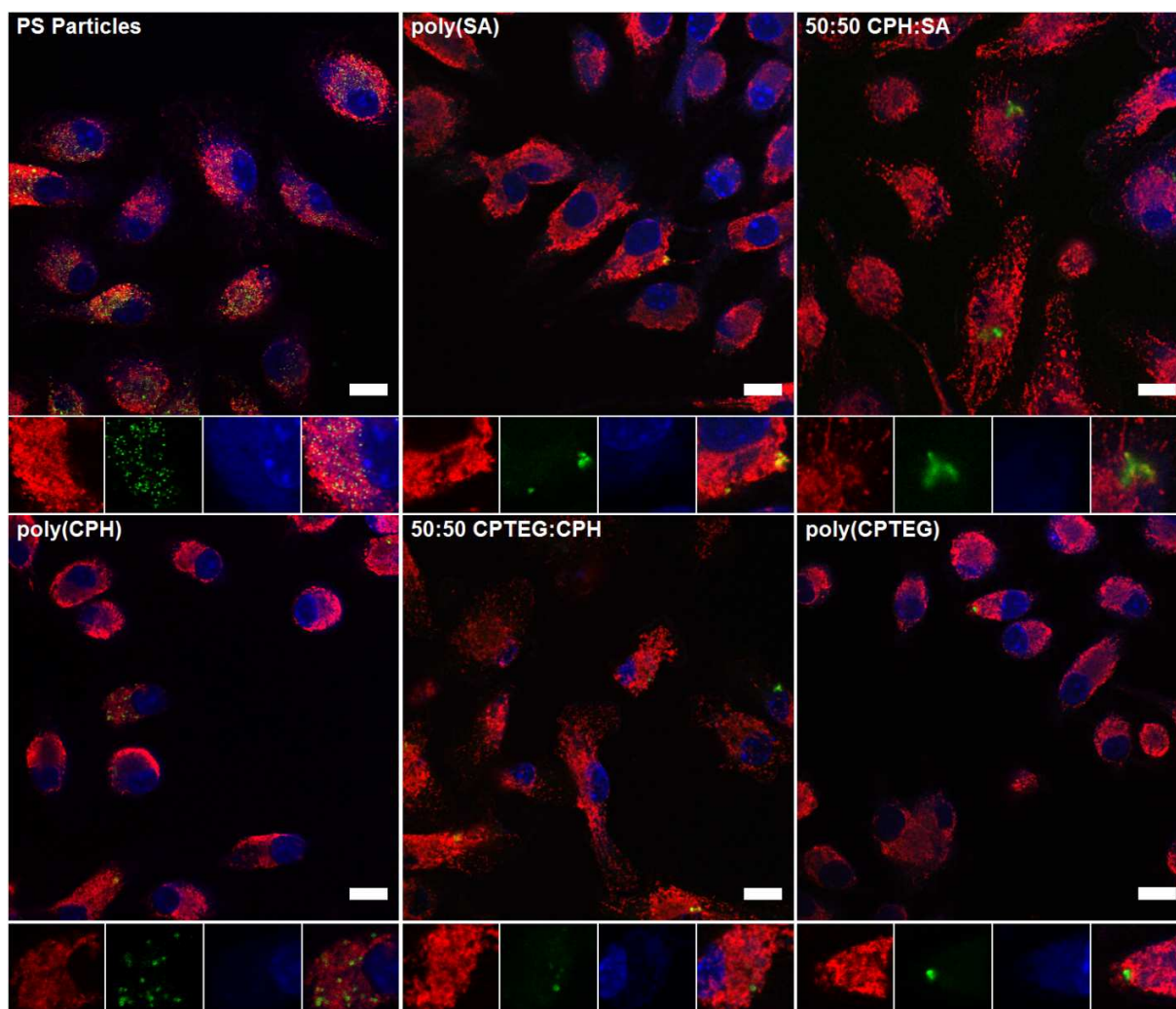


**Figure 5.6.** Confocal photomicrographs of FITC-encapsulated PS particles and polyanhydride nanoparticles (*green*) internalized by BMDC fixed and stained at 2.5 h. Lysosomes (*red*) were identified using an anti-LAMP-1 (ID-4B) antibody. No major differences in dendritic cell health and morphology were observed among the different particles chemistries which are reflected in the representative wide field images above. Higher magnification of a selected region of interest provides greater detail of the spatial relationship between particles and lysosomes. All chemistries were internalized with the majority of particles found inside LAMP-1+ vesicles as evidenced by overlap (*yellow*). Scale bar = 10  $\mu\text{m}$ .

In contrast, confocal photomicrographs of LAMP-1 staining at 48 h post-incubation (Fig. 5.7) showed significant differences in cell health and nanoparticle agglomerate morphology based on polymer chemistry. The PS particles control showed significant internalization of both small and large particles as anticipated. DCs exposed to nanoparticle agglomerates of the most hydrophobic chemistry (poly(CPH)) were in far lower concentrations than those incubated with other chemistries and the cells exposed to poly(CPH) showed significant rounding indicating poor health. DCs exposed to moderately hydrophobic nanoparticle agglomerates (50:50 CPH:SA and 50:50 CPTEG:CPH) had larger aggregates persisting inside the cell. These aggregates appear to be co-localized with LAMP-1 indicating their presence inside lysosomal vesicles. DCs exposed to the least hydrophobic nanoparticles (poly(SA) and poly(CPTEG)) show diffusive staining correlating to significant release of encapsulated payload. In addition, many of the least hydrophobic aggregates appear to be unassociated with lysosomes indicating they may have escaped to the cytosol. An interesting observation for 50:50 CPTEG:CPH nanoparticle agglomerates is that they appear to be both persisting inside lysosomes forming very large aggregates and releasing their payload payload in these vesicles (bright yellow).

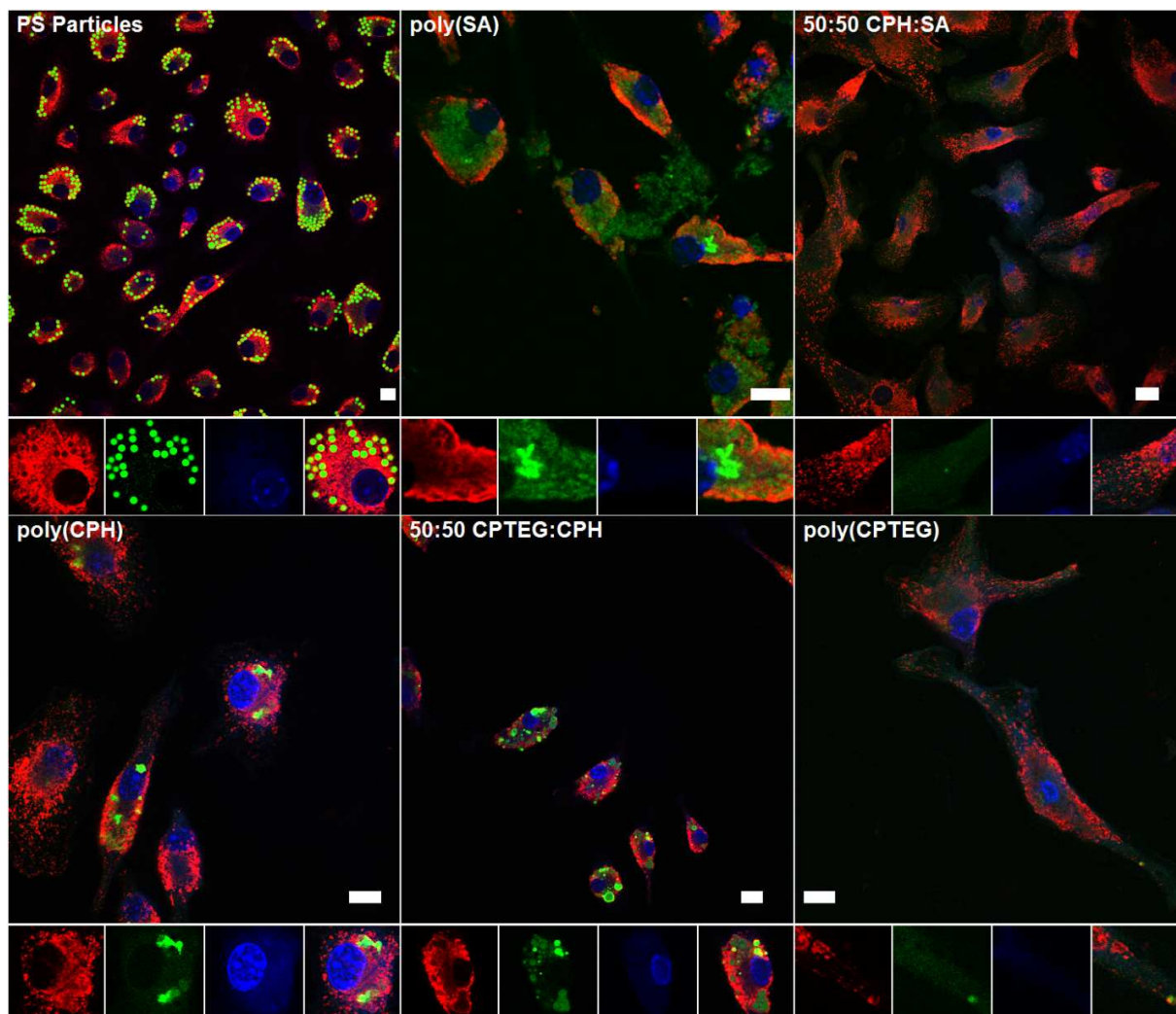


**Figure 5.7.** Confocal photomicrographs of FITC-encapsulated PS particles or polyanhydride nanoparticles (*green*) internalized by BMDC fixed and stained at 48 h. Lysosomes (*red*) were identified using an anti-LAMP-1 (ID-4B) antibody. Significant differences in dendritic cell health and morphology can be seen in representative wide field images shown for each of the particle chemistries examined. In addition chemistry-dependent agglomerate morphology differences were observed. Scale bar = 10  $\mu$ m.

In order to quantify the population of nanoparticle aggregates found intracellularly, epifluorescent microscopy was used to generate images that were processed by ImageJ. All analyzed particles were ordered by size and graphs of agglomerate area (in  $\mu\text{m}^2$ ) v agglomerate count are shown in Fig. 5.8. The PS control had large populations of individual particles corresponding to 0.2  $\mu\text{m}$  at 2.5 h and 2  $\mu\text{m}$  at 48 h post-incubation as expected. There were very few poly(CPH) nanoparticle agglomerates present at either time-point coinciding with the few number of cells present. Both 50:50 CPH:SA and 50:50 CPTEG:CPH showed similar nanoparticle agglomerate count trends at 2 h, but opposing trends at 48 h. There were fewer 50:50 CPH:SA nanoparticle agglomerates at 48 h compared to at 2 h with only slightly increased size distribution. In contrast, 50:50 CPTEG:CPH nanoparticle agglomerates had an almost 10-fold increase in quantity with an expansive size range. Agglomerates of poly(SA) and poly(CPTEG) had very similar trends at both 2 h and 48 h except there were more poly(SA) agglomerates at both time-points. The quantitative data strongly agrees with the qualitative trends and nanoparticle agglomerate behavior observed in Fig. 5.6 and Fig. 5.7.

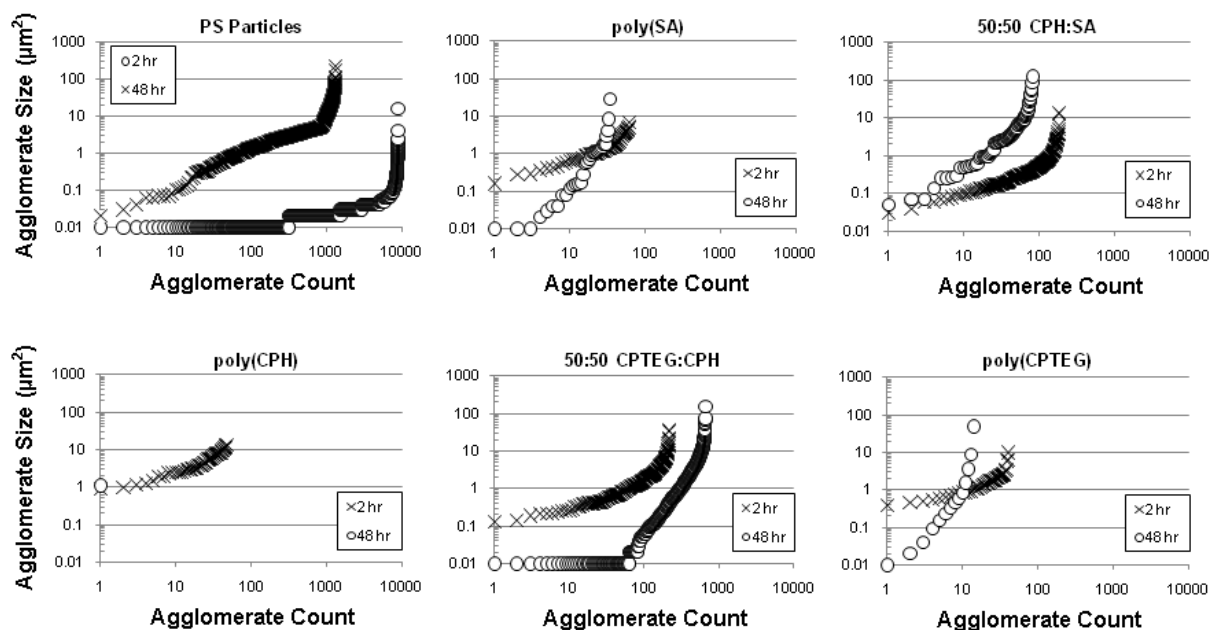


**Figure 5.8.** Chemistry dependent pattern of agglomerates distribution at both 2.5 and 48 h. Morphometric data for individual particles were graphed on scatter plots to reveal striking differences in particle size distributions and total particle counts between 2.5 and 48 hr time points. All agglomerates for each chemistry were ordered by size (smallest to largest). Log scales for both axes were used to allow for easier comparison among times and chemistries.

## 5.5 Discussion

The ability for nanoparticle-based adjuvant and delivery systems to modulate the immune response based solely upon their polymer chemistry would enhance our understanding of how these adjuvants interact with immune cells and lead to rational design of effective nanovaccine platforms. In order to initiate an immune response the capacity for adjuvant chemistry to modulate DC behavior was studied. Our aim in this study was to combine both cell population-based and individual cell-based analyses to observe the effect of polyanhydride chemistry on DCs. While both of these techniques have been used individually in

previous studies focused on particulate adjuvants<sup>22,25,29-38,44</sup>, to our knowledge, this is the first time the analyses have been coupled to enhance our understanding of DC activation exploited by nanoparticles. The knowledge gained from incorporating the results determined by flow cytometry, cytokine analysis, and fluorescent microscopy showed many interesting trends based on polyanhydride chemistry.

Very hydrophobic nanoparticles (poly(CPH)) induced cell death, which was witnessed in all analyses. Poly(CPH) nanoparticle agglomerates drastically reduced the population of viable cells shown by flow cytometry and induced high levels of cytokine secretion. Also, the few cells present in microscopy had very rounded morphologies, which is a characteristic of unhealthy cells. The hydrophobicity of poly(CPH) nanoparticles is more than likely causing strong inflammatory insult to the dendritic cells pushing them towards cell death. This is supported by the very high levels of cytokines (Fig. 5.5), especially TNF- $\alpha$ , secreted from DCs incubated with poly(CPH) nanoparticles. TNF- $\alpha$  is a pro-inflammatory cytokine that can cause cell death and inflammation.<sup>49</sup> While small amounts may be beneficial in the initiation of an immune response, too much can initiate a cytokine storm causing significant tissue damage. DCs incubated with poly(CPH) nanoparticles produced half the amount of TNF- $\alpha$  generated by LPS, an endotoxin, which is known for stimulating a strong inflammatory response *in vivo*.<sup>50</sup> The cytokine production upon stimulation by poly(CPH) nanoparticles was ~15-fold that of cells incubated with 50:50 CPH:SA nanoparticles and ~75-fold

that of cells given no stimulus. This behavior makes poly(CPH) nanoparticles a poor choice as a vaccine adjuvant.

Moderately hydrophobic agglomerates (50:50 CPH:SA and 50:50 CPTEG:CPH) induced moderate cytokine secretion. While they did not induce cytokine production as strongly as poly(CPH) nanoparticle agglomerates, these chemistries were able to induce cytokine secretion greater than no stimulus and less hydrophobic agglomerates (poly(SA) and poly(CPTEG)). In microscopy analysis, these two chemistries displayed similar size v count plots after 2 h (Fig. 5.8) and showed lysosomal-associated agglomerates persisting at 48 h (Fig. 5.7). The rapid internalization and persistence of these particles may be seen as a stress by the DCs, inducing cytokine production.<sup>51</sup> The capacity for nanoparticles of these chemistries to persist even in the strongly degradative environment of the lysosome indicates their long-term delivery potential.

The least hydrophobic agglomerates (poly(SA), 50:50 CPTEG:CPH, and poly(CPTEG)) induced increased cell surface marker expression. CD209 expression was enhanced for all three chemistries whereas MHC I, MHC II, CD40 and CD86 was enhanced for only poly(SA) and 50:50 CPTEG:CPH. The microscopy data shows that these three chemistries were all able to be significantly broken down causing fluorescent payload release by 48 h whereas all other chemistries were not. The inability for poly(CPTEG) nanoparticle agglomerates to initiate any cell surface marker other than CD209 may be due to rapid degradation and a low number of internalized agglomerates. The

mechanism by which CD209 expression could be enhanced by particles is still not well characterized. The behavior of poly(CPTEG) nanoparticle aggregates intracellularly indicates that CD209 activation may occur more quickly or by a different mechanism than the expression of other cell surface markers. Further experiments are necessary to better understand CD209 activation by nanoparticle aggregates. The enhanced cell surface marker expression of MHC I, MHC II, CD40 and CD86 correlates well to the intracellular behavior of poly(SA) and 50:50 CPTEG:CPH nanoparticle agglomerates. DC activation based on successful processing of internalized material would agree with accepted antigen presenting cell activation behavior.<sup>52</sup> The specific nature of enhanced cell surface marker expression also appears to corroborate the intracellular behavior. Nanoparticle agglomerates of poly(SA) appear to be degrading and releasing payload within the cytosol due to the diffusive presence of FITC-dextran similar to previous research.<sup>53</sup> The ability to release payload in the cytosol could cause cross presentation through the endogenous pathway. Fig. 5.4 clearly shows enhanced MHC I expression for DCs exposed to poly(SA) nanoparticles which would correspond to this mode of activation. In contrast, the many dim 50:50 CPTEG:CPH nanoparticle agglomerates appear to release their fluorescent payload, but persist in lysosomal compartments. This behavior corresponds with the lower MHC I expression for DCs incubated with this chemistry. With chemistry-dependent modulation of DC activation, combination vaccines could be used for activation of both the Th1 and Th2 response. This

flexibility allows for the nanovaccine platform to be tailored for a wide range of emerging and re-emerging pathogens.

## **5.6 Conclusions**

Polyanhydride nanoparticles are promising candidates for vaccine delivery applications. This data clearly demonstrates that polymer chemistry affects their interactions with DCs. Nanoparticle hydrophobicity was the strongest correlating property to DC behavior. Incubating DCs with highly hydrophobic nanoparticles induced cell death, but incubation with the least hydrophobic nanoparticles initiated the expression of only CD209. There appears to be a hydrophobicity continuum that is dictated by polymer chemistry and can be tailored to initiate desired DC responses. 50:50 CPTEG:CPH nanoparticles had the unique behavior of releasing some payload while persisting in Lamp-1+ vesicles as large aggregates. This was the only polymer chemistry able to enhance both cell surface marker expression and cytokine secretion. From long-lasting particle persistence to cytosolic delivery, the variance in initiated responses bodes well for the use of these materials as a nanovaccine platform.

## 5.7 References

1. Rosario, M., Fulkerson, J., Soneji, S., Parker, J., Im, E.J., Borthwick, N., Bridgeman, A., Bourne, C., Joseph, J., Sadoff, J.C. & Hanke, T. Safety and immunogenicity of novel recombinant BCG and modified vaccinia virus Ankara vaccines in neonate rhesus macaques. *Journal of Virology*. **84**(15): 7815 – 7821 (2010).
2. Madhan, S., Prabakaran, M. & Kwang, J. Baculovirus as vaccine vectors. *Current Gene Therapy*. **10**(3): 201 – 213 (2010).
3. Torres-Escobar, A., Juarez-Rodriguez, M.D., Gunn, B.M., Branger, C.G., Tinge, S.A. & Curtiss, R. Fine-tuning synthesis of *Yersinia pestis* LcrV from runaway-like replication balanced-lethal plasmid in a *Salmonella enterica* serovar typhimurium vaccine induces protection against a lethal *Y. pestis* challenge in mice. *Infection and Immunity*. **78**(6): 2529 – 2543 (2010).
4. Jechlinger, W., Haller, C., Resch, S., Hofmann, A., Szostak, M.P. & Lubitz, W. Comparative immunogenicity of the hepatitis B virus core 149 antigen displayed on the inner and outer membrane of bacterial ghosts. *Vaccine*. **23**(27): 3609 – 3617 (2005).
5. Wang, D., Xu, J., Feng, Y., Liu, Y., Mchenga, S.S., Shan, F., Sasaki, J. & Lu, C. Liposomal oral DNA vaccine (mycobacterium DNA) elicits immune response. *Vaccine*. **28**(18): 3134 – 3142 (2010).
6. Henriksen-Lacey, M., Christensen, D., Bramwell, V.W., Linderstrom, T., Agger, E.M., Andersen, P. & Perrie, Y. Liposomal cationic charge and antigen adsorption are important properties for the efficient deposition of antigen at the injection site and ability of the vaccine to induce a CMI response. *Journal of Controlled Release*. **145**(2): 102 – 108 (2010).
7. Lee, P.W., Hsu, S.H., Tsai, J.S., Chen, F.R., Huang, P.J., Ke, C.J., Liao, Z.X., Hsiao, C.W., Lin, H.J. & Sung, H.W. Multifunctional core-shell polymeric nanoparticles for transdermal DNA delivery and epidermal Langerhans cells tracking. *Biomaterials*. **31**(8): 2425 – 2434 (2010).
8. Bachelder, E.M., Beaudette, T.T., Broaders, K.E., Frechet, J.M., Albrecht, M.T., Ainslie, K.M., Pesce, J.T. & Keane-Myers, A.M. In vitro analysis of acetalated dextran microparticles as a potent delivery platform for vaccine adjuvants. *Molecular Pharmaceutics*. **7**(3): 826 – 835 (2010).

9. Pawar, D., Goyal, A.K., Mangal, S., Mishra, N., Vaidya, B., Tiwari, S., Jain, A.K. & Vyas, S.P. Evaluation of mucoadhesive PLGA microparticles for nasal immunization. *AAPS Journal*. **12**(2): 130 – 137 (2010).
10. Kipper, M.J., Wilson, J.H., Wannemuehler, M.J. & Narasimhan, B. Single dose vaccine based on biodegradable polyanhydride microspheres can modulate immune response mechanism. *Journal of Biomedical Materials Research Part A*. **76**(4): 798 – 810 (2006).
11. Gaymalov, Z.Z., Yang, Z., Pisarev, V.M., Alakhov, V.Y. & Kabanov, A.V. The effect of the nonionic block copolymer pluronic P85 on gene expression in mouse muscle and antigen-presenting cells. *Biomaterials*. **30**(6): 1232 – 1245 (2009).
12. Coeshott, C.M., Smithson, S.L., Verderber, E., Samaniego, A., Blonder, J.M., Rosenthal, G.J. & Westerink M.A. Pluronic F127-based systemic vaccine delivery systems. *Vaccine*. **22**(19): 2396 – 2405 (2004).
13. Andrianov, A.K., DeCollibus, D.P., Gillis, H.A., Kha, H.H., Marin, A., Prausnitz, M.R., Babiuk, L.A., Townsend, H. & Mutwiri, G. Poly[di(carboxylatophenoxy)phosphazene] in a potent adjuvant for intradermal immunization. *Proceedings of National Academy of Sciences of the United States of America*. **106**(45): 18936 – 18941 (2009).
14. Mutwiri, G., Benjamin, P., Soita, H., Townsend, H., Yost, R., Roberts, B., Andrianov, A.K. & Babiuk, L.A. Poly[di(sodium carboxylatoethylphenoxy)phosphazene] (PCEP) is a potent enhancer of mixed Th1/Th2 immune responses in mice immunized with influenza virus antigens. *Vaccine*. **25**(7): 1204 – 1213 (2007).
15. Torres, M.P., Determan, A.S., Anderson, G.L., Mallapragada, S.K. & Narasimhan, B. Amphiphilic polyanhydrides for protein stabilization and release. *Biomaterials*. **28**(1): 108 – 116 (2007).
16. Determan, A.S., Trewyn, B.G., Lin, V.S., Nilsen-Hamilton, M. & Narasimhan, B. Encapsulation, stabilization, and release of BSA-FITC from polyanhydride microspheres. *Journal of Controlled Release*. **100**(1): 97 – 109 (2004).
17. Kipper, M.J., Shen, E., Determan, A. & Narasimhan, B. Design of an injectable system based on bioerodible polyanhydride microspheres for sustained drug delivery. *Biomaterials*. **23**(22): 4405 – 4412 (2002).

18. Shen, E., Kipper, M.J., Dziadul, B., Lim, M.K. & Narasimhan, B. Mechanistic relationships between polymer microstructure and drug release kinetics in bioerodible polyanhydrides. *Journal of Controlled Release*. **82**(1): 115 – 125 (2002).
19. Determan, A.S., Wilson, J.H., Kipper, M.J., Wannemuehler, M.J. & Narasimhan, B. Protein Stability in the presence of polymer degradation products: consequences for controlled release formulations. *Biomaterials*. **27**(17): 3312 – 3320 (2006).
20. Jain, J.P., Modi, S., Domb, A.J. & Kumar, N. Role of polyanhydrides as localized drug carriers. *Journal of Controlled Release*. **103**(3): 541 – 563 (2005).
21. Determan, A.S., Graham, J.R., Pfeiffer, K.A. & Narasimhan, B. The role of microsphere fabrication methods on the stability and release kinetics of ovalbumin encapsulated in polyanhydride microspheres. *Journal of Microencapsulation*. **23**(8): 832 – 843 (2006).
22. Torres, M.P., Wilson-Welder, J.H., Ramer-Tait, A.E., Bellaire, B.H., Wannemuehler, M.J. & Narasimhan, B. In vitro activation of dendritic cells using polyanhydride microspheres: promising implications for vaccine design. *Biomaterials*, to be submitted.
23. Carrillo-Conde, B., Schiltz, E., Yu, J., Minion, F.C., Phillips, G.J., Wannemuehler, M.J. & Narasimhan, B. Encapsulation into amphiphilic polyanhydride microparticles stabilizes *Yersinia pestis* antigens. *Acta Biomaterialia*. **6**(8): 3110 – 3119 (2010).
24. Ulery, B.D., Phanse, Y., Sinha, A., Wannemuehler, M.J., Narasimhan, B & Bellaire, B.H. Polymer chemistry influences monocytic uptake of polyanhydride nanospheres. *Pharmaceutical Research*. **26**(3): 683 – 690 (2009).
25. Petersen, L.K., Xue, L., Wannemuehler, M.J., Rajan, K. & Narasimhan, B. The simultaneous effect of polymer chemistry and device geometry on the in vitro activation of murine dendritic cells. *Biomaterials*. **30**(28): 5131 – 5142 (2009).
26. Ulery, B.D., Kumar, D., Ramer-Tait, A.E., Metzger, D.W., Wannemuehler, M.J. & Narasimhan, B. Design of a protective single-dose intranasal nanoparticle-based vaccine platform for respiratory infectious diseases. *PLoS One*, submitted for publication.

27. Janeway, C.A., Travers, P., Walport, M. & Schlomchik, M.J. *Immunobiology*. Garland Science, New York, 14 – 15 (2005).
28. den Dunnen, J., Gringhuis, S.I. & Geijtenbeek, T.B.H. Innate signaling by the C-type lectin DC-SIGN dictates immune responses. *Cancer Immunology, Immunotherapy*. **58**(7): 1149 – 1157 (2009).
29. Yoshida, M., Mata, J. & Babensee, J.E. Effect of poly(lactic-co-glycolic acid) contact on maturation of murine bone marrow-derived dendritic cells. *Journal of Biomedical Materials Research Part A*. **80A**(1): 7 – 12 (2007).
30. Yoshida, M. & Babensee, J.E. Differential effects of agarose and poly(lactic-co-glycolic acid) on dendritic cell maturation. *Journal of Biomedical Materials Research Part A*. **79A**(2): 393 – 408 (2006).
31. Yoshida, M. & Babensee, J.E. Poly(lactic-co-glycolic acid) enhances maturation of human monocyte-derived dendritic cells. *Journal of Biomedical Materials Research Part A*. **71A**(1): 45 – 52 (2004).
32. Elamanchili, P., Diwan, M., Cao, M. & Samuel, J. Characterization of poly(D,L-lactic-co-glycolic acid) based nanoparticulate system for enhanced delivery of antigens to dendritic cells. *Vaccine*. **22**(19): 2406 – 2412 (2004).
33. Diwan, M., Elamanchili, P., Lane, H., Gainer, A. & Samuel J. Biodegradable nanoparticle mediated antigen delivery to human cord blood derived dendritic cells for induction of primary T cell responses. *Journal of Drug Targeting*. **11**(8-10): 495 – 507 (2003).
34. Wattendorf, U., Coullerez, G., Voros, J., Textor, M. & Merkle, H.P. Mannose-based molecular patterns on stealth microspheres for receptor-specific targeting of human antigen-presenting cells. *Langmuir*. **24**(20): 11790 – 11802 (2008).
35. Nguyen, D.N., Raghavan, S.S., Tashima, L.M., Lin, E.C., Fredette, S.J., Langer, R.S. & Wang, C. Enhancement of poly(orthoester) microspheres for DNA vaccine delivery by blending with poly(ethylenimine). *Biomaterials*. **29**(18): 2783 – 2793 (2008).

36. Cubillos-Ruiz, J.R., Engle, X., Scarlett, U.K., Martinez, D., Barber, A., Elgueta, R., Wang, L., Nesbeth, Y., Durant, Y., Gerwitz, A.T., Sentman, C.L., Kedl, R. & Conejo-Garcia, J.R. Polyethylenimine-based siRNA nanocomplexes reprogram tumor-associated dendritic cells via TLR5 to elicit therapeutic antitumor immunity. *Journal of Clinical Investigation*. **119**(8): 2231 – 2244 (2009).
37. Gordon, S., Saupe, A., McBurney, W., Rades, T. & Hook, S. Comparison of chitosan nanoparticles and chitosan hydrogels for vaccine delivery. *Journal of Pharmacy and Pharmacology*. **60**(12): 1591 – 1600 (2008).
38. Kong, X., Hellermann, G.R., Zhang, W., Jena, P., Kumar, M., Behera, S., Lockey, R. & Mohapatra, S.S. Chitosan interferon-gamma nanogene therapy for lung disease: modulation of T-cell and dendritic cell immune responses. *Allergy, Asthma, and Clinical Immunology: official journal of the Canadian Society of Allergy and Clinical Immunology*. **4**(3): 95 – 105 (2008).
39. Liu, J., Jiang, Z., Zhang, S. & Saltzman, W.M. Poly(omega-pentadecalactone-co-butylene-co-succinate) nanoparticles as biodegradable carriers for camptothecin delivery. *Biomaterials*. **30**(29): 5707 – 5719 (2009).
40. Nam, H.Y., Kwon, S.M., Chung, H., Lee, S.Y., Kwon, S.H., Jeon, H., Kim, Y., Park, J.H., Kim, J., Her, S., Oh, Y.K., Kwon, I.C., Kim, K. & Jeong, S.Y. Cellular uptake mechanism and intracellular fate of hydrophobically modified glycol chitosan nanoparticles. *Journal of Controlled Release*. **135**(3): 259 – 267 (2009).
41. Ho, Y.P., Chen, H.H., Leong, K.W. & Wang, T.H. Evaluating the intracellular stability and unpacking of DNA nanocomplexes by quantum dots-FRET. *Journal of Controlled Release*. **116**(1): 83 – 89 (2006).
42. Cartiera, M.S., Johnson, K.M., Rajendran, V., Caplan, M.J. & Saltzman, W.M. The uptake and intracellular fate of PLGA nanoparticles in epithelial cells. *Biomaterials*. **30**(14): 2790 – 2798 (2009).
43. Trapani, A., Sitterberg, J., Bakowsky, U. & Kissel, T. The potential of glycol chitosan nanoparticles as carrier for low water soluble drugs. *International Journal of Pharmacy*. **375**(1-2): 97 – 106 (2009).

44. Shen, H., Ackerman, A.L., Cody, V., Giodini, A., Hinson, E.R., Cresswell, P., Edelson, R.L., Saltzman, W.M. & Hanlon, D.J. Enhanced and prolonged cross-presentation following endosomal escape of exogenous antigens encapsulated in biodegradable nanoparticles. *Immunology*. **117**(1): 78 – 88 (2006).
45. Torres, M.P., Vogel, B.M., Narasimhan, B. & Mallapragada, S.K. Synthesis and characterization of novel polyanhydrides with tailored erosion mechanisms. *Journal of Biomedical Materials Research Part A*. **76A**(1): 102 – 110 (2006).
46. ImageJ. Image Processing and Analysis in Java. Retrieved on 29 July 2010 from <http://rsb.info.nih.gov/ij/>.
47. Mathiowitz, E., Chickering, D., Jong, Y.S. & Jacob, J.S. Process for preparing microparticles through phase inversion phenomena. 2003: United State of America Patent No. 6,620,617
48. Gatti, E. & Pierre, P. Understanding the cell biology of antigen presentation: the dendritic cell contribution. *Current Opinion in Cell Biology*. **15**(4): 468 – 473 (2003).
49. Ashkenazi, A. & Dixit, V.M. Death receptors: signaling and modulation. *Science*. **281**(5381): 1305 – 1308 (1998).
50. Krakauer, T., Buckley, M.J. & Fisher, D. Proinflammatory mediators of toxic shock and their correlation to lethality. *Mediators of Inflammation*. [Epub ahead of print]
51. Driscoll, K.E., Carter, J.M., Hassenbein, D.G. & Howard, B. Cytokines and particle-induced inflammatory cell recruitment. *Environmental Health Perspectives*. **105**(Suppl 5): 1159 – 1164 (1997).
52. Watts, C. Antigen processing in the endocytic compartment. *Current Opinion in Immunology*. **13**(1): 26 – 31 (2001).
53. Hu, Y., Litwin, T., Nagaraja, A.R., Kwong, B., Katz, J., Watson, N. & Irvine, D.J. Cytosolic delivery of membrane-impermeable molecules in dendritic cells using pH-responsive core-shell nanoparticles. *Nano Letters*. **7**(10): 3056 – 3064 (2007).

## CHAPTER 6

# Design of a Protective Single-dose Intranasal Nanoparticle-based Vaccine Platform for Respiratory Infectious Diseases

A paper submitted to *PLoS One*, 2010.

Bret D. Ulery<sup>1,\*</sup>, Devender Kumar<sup>2,\*</sup>, Amanda E. Ramer-Tait<sup>3</sup>, Dennis W. Metzger<sup>2</sup>, Michael J. Wannemuehler<sup>3</sup>, and Balaji Narasimhan<sup>1</sup>

\* These authors contributed equally to this work.

<sup>1</sup> Department of Chemical and Biological Engineering, Iowa State University, Ames, Iowa 50011, USA

<sup>2</sup> Center for Immunology and Microbial Disease, Albany Medical College, Albany, NY 12208, USA

<sup>3</sup> Department of Veterinary Microbiology and Preventive Medicine, Iowa State University, Ames, Iowa 50011, USA

## 6.1 Abstract

This chapter focuses on the development and evaluation of degradable polyanhydride nanoparticles as a single dose vaccine-platform. Despite the successes provided by vaccination, many challenges still exist with respect to controlling new and re-emerging infectious diseases. Innovative vaccine platforms composed of adaptable adjuvants able to appropriately modulate immune responses, induce long-lived immunity in a single dose, and deliver immunogens in a safe and stable manner via multiple routes of administration are needed. This work describes the development of a novel biodegradable polyanhydride nanoparticle-based vaccine platform administered as a single intranasal dose that induced long-lived protective immunity against respiratory infectious diseases using *Yersinia pestis*, the causative agent of pneumonic plague, as a model pathogen. The polymer system used was the 50:50 copolymer of poly((1,8-bis(*p*-carboxyphenoxy)-3,6-dioxaoctane)-*co*-(1,6-bis(*p*-carboxyphenoxy)hexane)) (CPTEG:CPH). This formulation was chosen since it possesses stable and extended release kinetics as well as superb APC stimulation properties. F1-V, a fusion protein antigen of *Yersinia pestis*, was delivered solubly and encapsulated within nanoparticles in a single-dose intranasally. Relative to the responses induced by the recombinant protein F1-V alone and MPLA-adjuvanted F1-V, the nanoparticle-based vaccination regimen induced an immune response that was characterized by high titer and high avidity IgG1 antibody specific for F1-V and persisted for at least 23 weeks post-

vaccination. No bacteria were recovered from the lungs, livers, or spleens of mice vaccinated with the nanoparticle-based formulation and histopathological appearance of lung, liver, and splenic tissues from these mice post-vaccination was remarkably similar to uninfected control mice.

## 6.2 Introduction

Natural infections with pathogens stimulate protective and lasting antibody responses because they induce affinity maturation of B cells, a process by which B cells produce antibodies with an increased affinity for antigen during the course of an immune response<sup>1</sup>. Vaccines have been designed to mimic the immune response associated with an active infection yet avoid the undesirable effects of disease. By employing a priming dose followed by two to three booster doses, modern vaccine regimens facilitate the process of affinity maturation, which occurs with repeated or sustained exposure to the same antigen<sup>1</sup>. Vaccines also utilize adjuvants to improve immunogenicity by providing pro-inflammatory signals and prolonging the persistence of vaccine antigens<sup>2</sup>. Unfortunately, current adjuvants approved for human use are not tunable and, as many pathogens have evolved to evade the host immune response, currently available vaccine strategies may not provide adequate induction of long-lived protective immunity. Development of single-dose, tailored nano-adjuvant platforms will not only provide an effective means to induce protective immunity, but will also allow production of cost-effective vaccines that can reduce the need for multiple injections and result in greater patient compliance. Moreover, these novel technologies will obviate the need for hypodermic needles and professionals to administer the vaccine. In this regard, implementation of vaccine delivery systems based on biodegradable polymers offers significant advantages for immunization regimens.

In order to enhance vaccine efficacy and induce long-term, protective immunity, the choice of route (intramuscular<sup>3,4</sup>, subcutaneous<sup>5,6</sup> or intranasal<sup>4,7</sup>), adjuvant (Alhydrogel<sup>5,6</sup>, viral vectors<sup>3</sup>, polyester microparticles<sup>4</sup>, or lipid A mimetics<sup>7</sup>), and vaccination schedule (single-dose<sup>4,5,7</sup> or multiple-doses<sup>3,6</sup>) must all be considered. For respiratory pathogens such as *Yersinia pestis*, intranasal vaccination offers many advantages over parenteral vaccination, including ease of administration and ability to enhance both mucosal and systemic immune responses<sup>8</sup>. While the rapid induction of protection is critical, the ability of vaccine formulations to induce long-lasting protection characterized by high-avidity antibody is equally important<sup>1</sup>. *Y. pestis*, the causative agent of plague, is a Category A agent (<http://www.bt.cdc.gov/agent/agentlist-category.asp>) to which there is no vaccine currently in production. The pursuit of a protective plague vaccine has evolved from the use of killed whole-cell<sup>9</sup> and live-attenuated bacteria<sup>10</sup> to recombinant proteins such as caf1 (i.e., F1) and LcrV (i.e., V)<sup>3,5,7</sup>. In addition, immunization with the fusion protein, F1-V, provides protection in mice<sup>5</sup> and cynomolgus macaques<sup>6</sup>; however, it has been less successful in other non-human primate models such as the African green monkey<sup>11</sup>. To date, only lipid A mimetic adjuvants have been shown to provide long-term, protective immunity against lethal *Y. pestis* challenge<sup>7</sup>.

Multiple biodegradable polymers, including polyesters, have been studied as vaccine delivery vehicles<sup>4,12</sup>. By comparison, the controlled release and adjuvanticity provided by novel polyanhydride carriers, first pioneered by Robert

Langer of MIT in the 1980s, allows for immune system activation, reduction of antigenic dose, prolonged antigen exposure, stability of the encapsulated protein antigen, and immune modulation<sup>13-22</sup>. The results presented herein demonstrate that encapsulation of F1-V into polyanhydride nanoparticles administered as a single intranasal dose successfully induced long-term protection against *Y. pestis* that correlated with a high titer, high avidity F1-V-specific antibody response.

## **6.3 Materials and Methods**

### **6.3.1 Materials**

4-hydroxybenzoic acid (96%), 1-methyl-2-pyrrolidinone anhydrous (99.5%), 1,6-dibromohexane (98.5%), triethylene glycol (99%), N,N-dimethylacetamide (99.8%) and monophosphoryl lipid A (MPLA) were purchased from Sigma-Aldrich (Milwaukee, WI). 4-*p*-fluorbenzonitrile was purchased from Apollo Scientific (Stockport, Cheshire, England). All other chemicals used for synthesis and particle precipitation were purchased from Fisher Scientific (Pittsburgh, PA) and used as received. F1-V was obtained from the NIH Biodefense and Emerging Infection (BEI) Research Resources Repository (Manassas, VA). The following reagent was also obtained through the NIH BEI Research Resources Repository: *Yersinia pestis*, Strain CO92, NR-641.

### **6.3.2 Polymer Synthesis and Characterization**

Synthesis of 1,6-bis(*p*-carboxyphenoxy)hexane (CPH) and 1,8-bis(*p*-carboxyphenoxy)-3,6-dioxaoctane (CPTEG) diacids was accomplished following

previously established methods.<sup>23</sup> Melt polycondensation of 50:50 CPTEG:CPH copolymer was carried out under vacuum (0.3 mm Hg) for 90 minutes at 140 °C. The resulting polymers were dissolved in deuterated chloroform (Cambridge Isotope Laboratories, Andover, MA) to characterize polymer structure by <sup>1</sup>H nuclear magnetic resonance (NMR) on a Varian VXR 300 MHz spectrometer (Varian Inc., Palo Alto, CA). The NMR spectra confirmed the synthesis of the desired copolymer composition. In addition, gel permeation chromatography (Waters HPLC System, Milford, MA using Varian Inc. GPC columns) and differential scanning calorimetry (Auto Q20, TA Instruments, New Castle, DE) were utilized to measure molecular weight and glass transition temperature, respectively. The 50:50 CPTEG:CPH copolymer had a  $M_n$  of 8500 Da, PDI of 1.70, and a  $T_g$  of 13 °C. All data was consistent with previously published work.<sup>23</sup>

### 6.3.3 Nanoparticle Design

Both F1-V encapsulated and blank nanoparticles were fabricated by the polyanhydride anti-solvent nanoencapsulation (PAN) method modified from the protocol reported in Ulery et al.<sup>18</sup> Polymer was dissolved in methylene chloride at 0 °C at a concentration of 20 mg/mL. For encapsulated nanoparticles F1-V was sonicated for 15 s at a concentration of 2% of total batch weight to form a suspension. The polymer/antigen solution was rapidly poured into a bath of pentane held at -20 °C at an anti-solvent to solvent ratio of 80:1. Penetration of anti-solvent into the polymer solution microenvironment caused spontaneous nanoparticle formation; the particles were subsequently filtered by Whatman No.

50 paper filters in a Buchner funnel. This procedure yielded a fine powder with at least 70% recovery and a F1-V encapsulation efficiency greater than 94%.

Nanoparticle morphology was investigated using scanning electron microscopy (SEM, JEOL 840A, JEOL Ltd., Tokyo, Japan). Quasi-elastic light scattering (QELS) was employed to determine nanoparticle size (Zetasizer Nano, Malvern Instruments Ltd., Worcester, UK).

*In vitro* release kinetics of the F1-V antigen were measured by suspending nanoparticles (12.5 mg) in 1 mL of 0.1 M phosphate buffer (pH 7.4) at 37 °C and agitated at 100 rpm. Sodium azide (0.01 % w/w) was added to prevent microbial contamination. At different time points, samples were centrifuged (10,000 rpm for 5 min) and aliquots of 750 µL of supernatant were collected and replaced with fresh buffer. Supernatants were stored at 4 °C until they were studied by micro bicinchoninic acid (micro BCA) assay (Thermo Scientific, Rockford, IL). After 70 days of release, the remaining nanoparticles were analyzed for non-released protein the nanoparticles were suspended in 3 mL of 17 mM sodium hydroxide (Fischer Scientific, Hampton, NH). The solution was withdrawn by syringe and loaded into a dialysis cassette (Slide-A-Lyzers 3,500 MWCO, Pierce Biotechnology Inc., Rockford, IL). The cassette was placed in 800 mL of 17 mM sodium hydroxide solution and incubated at 100 rpm and 37 °C for one week in order to catalyze the degradation of any remaining polymer. After incubation, the protein solution was removed by syringe and quantified by the micro BCA assay. Total protein encapsulated was determined by adding the quantity of protein

released during the experiment to the quantity of protein extracted from remaining nanoparticles<sup>17</sup>. Cumulative release profiles were generated by normalizing the data against the total amount of encapsulated protein and reported as fractional protein release.

#### **6.3.4 Animal Vaccinations**

Adult female mice, strain C57BL/6, at least 8 weeks of age were used for all experiments. Mice were obtained from JAX<sup>®</sup> Breeding and Colony Management Services (Jackson Laboratory, Bar Harbor, ME). The mice were maintained under SPF condition with all bedding, cages, water, and feed sterilized prior to use. Animal procedures were undertaken with approval from either the Iowa State University or the Albany Medical Center Committees on Animal Care and Use.

Mice were first anesthetized by i.p. injection of 100  $\mu\text{L}$  of 80  $\text{mg kg}^{-1}$  ketamine (KetaVed<sup>®</sup>, Vedco Inc. St. Joseph, MO) and 16  $\text{mg kg}^{-1}$  xylazine (Phoenix Scientific, St. Joseph, MO) diluted in sterile phosphate buffered saline (pH 7.4, PBS). After confirming that the mice were completely anesthetized, 40  $\mu\text{L}$  of vaccine (50  $\mu\text{g}$  of F1-V in each dose) was delivered intranasally. Solutions containing nanoparticles (500  $\mu\text{g}$ ) were sonicated prior to use and held at 0  $^{\circ}\text{C}$ . All vaccine solutions were vortexed immediately prior to each administration. Mice were monitored for signs of deep respiration during vaccination and until they were fully awake. Blood samples were drawn from the saphenous vein at 3,

6, 9, 12, 15, 18, and 23 weeks post-vaccination. Sera was isolated and stored at -20 °C until assayed for anti-F1-V specific antibodies.

### **6.3.5 F1-V Specific Enzyme-Linked Immunosorbent Assay (ELISA)**

High protein binding 96-well Costar microtiter plates (Corning Life Sciences, Lowell, MA) were coated overnight with 100 µL PBS containing 0.5 µg/mL F1-V. Plates were blocked for at least 2 h at room temperature with PBS containing 0.05 % Tween 20 (PBS-T) and 2.5 % skim milk as a blocking agent (Nestle, Glendale, CA). PBS-T was used to rinse the plates three times to remove any unbound blocking reagent. Sera samples from individual mice were diluted 1:200, added to the wells and then serially diluted three-fold in PBS-T with 1% goat serum and refrigerated overnight (at least 12 h) at 4 °C. PBS-T was used to wash plates three times followed by the addition of 100 µL of PBS-T with 1% goat serum containing alkaline phosphatase-conjugated goat anti-mouse IgG(H&L) (Jackson Laboratory) at 1 µg/mL. After 2 h of incubation, the microtiter plates were washed with PBS-T three times followed by the addition of 100 µL of sodium carbonate (50 mM) and magnesium chloride (2 mM) buffer (pH 9.3) containing 1 mg/mL phosphatase substrate (Sigma 104, Sigma-Aldrich, St. Louis, MO) and reacted at room temperature for 30 min. Optical density (OD) of each well was measured at 405 nm using a Spectramax 190 Plate Reader (Molecular Devices, Sunnyvale, CA). For this experiment, endpoint titers were defined as the greatest dilution where optical density was still at least twice that of the average optical density of normal mouse serum (1:1800).

Antibody avidity analysis was performed as described previously.<sup>15</sup> Individual serum samples (1:200) were placed into 16 replicate wells of a microtiter plate previously coated with F1-V as described above. Following the wash step to remove unbound serum antibodies, 150  $\mu$ L of 0.1 M sodium phosphate containing sodium thiocyanate (a chaotropic agent) was added to duplicate wells in increasing concentrations from 0 to 5 M. The plates were incubated for 15 min at room temperature and then washed five times with PBS-T followed by the addition of alkaline phosphatase-conjugated goat anti-mouse IgG(H&L) as described above. Avidity index was defined as the concentration of sodium thiocyanate necessary to reduce the OD reading by 50% compared to wells treated with 0.1 M sodium phosphate. This was accomplished by fitting an exponential curve to a plot of OD versus sodium thiocyanate concentration.

### **6.3.6 *Y. pestis* Challenge, Bacterial Burden, and Histopathology**

*Y. pestis* CO92, (NR-641, Biodefense and Emerging Infection Resources, Manassas, VA) and was handled in a Class-II biological safety cabinet in a CDC certified animal biosafety level-3 suite at Albany Medical College. *Y. pestis* CO92 organisms were grown O/N at 37  $^{\circ}$ C in heart-infusion broth supplemented with 0.2 % D-galactose. Vaccinated mice were anesthetized as mentioned earlier, and challenged intranasally with 850 CFU ( $LD_{100}$ ) of *Y. pestis* in 20  $\mu$ L PBS/mouse at 6 or 23 weeks post-vaccination. For vaccine efficacy studies, infected mice were observed for 14 days post-challenge for their survival. For bacterial organ burdens, lungs, livers, and spleens were collected at 6 weeks

post-vaccination and homogenized in one mL of PBS in mini-beadbeater (BioSpec Products Inc., Bartlesville, OK) at 72 h post-infection. Organ homogenates were diluted ten-fold in PBS and 10 or 100  $\mu$ L of homogenates were plated on to Congo red (CR) agar plates. *Y. pestis* colonies were enumerated after 48 h of incubation of CR agar plates at 28 °C. Bacterial burdens were expressed as  $\log_{10}$  means of CFU  $\pm$  standard errors of the means for three mice per group. To determine if vaccines generated immunity is sterilizing, bacterial organ burdens were done on the completion of survival observation period, i.e., 14 days post-infection on 6 weeks and 23 weeks post-vaccination trials. For histopathological studies, vaccinated and infected mice were sacrificed using pentobarbital sodium (100 mg  $\text{kg}^{-1}$ ) and lungs, livers, and spleens were collected at different time points after infection and fixed in 10% buffered formalin for 7 days. The sterility of formalin-fixed organs was confirmed before further tissue processing. Tissues were paraffin-embedded and their 5- $\mu$ M sections cut and mounted on glass slides and later stained with hematoxylin and eosin. Photomicrographs of tissue sections were acquired and analyzed using cellSens™ standard software (version 1.3, Olympus Corporation, Japan) on Olympus BX-41 light microscope equipped with Olympus microscope digital camera DP72. All photomicrographs were resized and converted to CMYK profile in Adobe Photoshop CS2 (Adobe Systems Incorporated, USA). Tissues were analyzed histopathologically for evidence of inflammation, hemorrhage, edema, necrosis, changes in tissue architecture, and bacteria.

### 6.3.7 Statistical Analysis

Analysis of survival was done by Mantel-Cox log rank test and all other statistical analysis was completed utilizing two-tailed t-tests. All statistical analysis was performed using GraphPad Prism 5 software (San Diego, CA).

## 6.4 Results

### 6.4.1 Nanoparticle Characterization

We have previously shown that F1-V encapsulated into amphiphilic polyanhydride particles based on 1,6-bis(*p*-carboxyphenoxy)hexane (CPH) and 1,8-bis(*p*-carboxyphenoxy)-3,6-dioxaoctane (CPTEG) (Fig. 6.1) successfully preserved the antigenicity of F1-V upon release.<sup>24</sup> SEM images of blank (Fig. 6.2a) and 2% F1-V loaded 50:50 CPTEG:CPH nanoparticles (Fig. 6.2b) show similar spherical morphology and size regardless of antigen loading. QELS analysis (Fig. 6.2c) demonstrated that antigen encapsulation did not change nanoparticle size (204 nm vs. 196 nm). It is known that 70-95% of aerosolized nanoparticles (50–200 nm) will deposit deep within the lung.<sup>25</sup> The ability for encapsulated F1-V to be gradually released over time from nanoparticles is shown in Fig. 2d. Antigen release was monitored for 70 days and showed a low initial burst (9%), approximate zero order release through 28 days, and near complete release (93%) by 70 days.

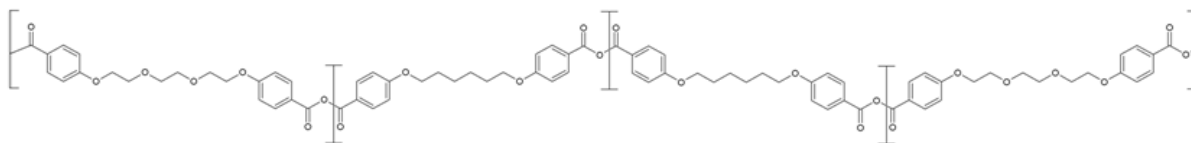


**Figure 6.1.** Chemical structure of a random CPTEG:CPH copolymer.

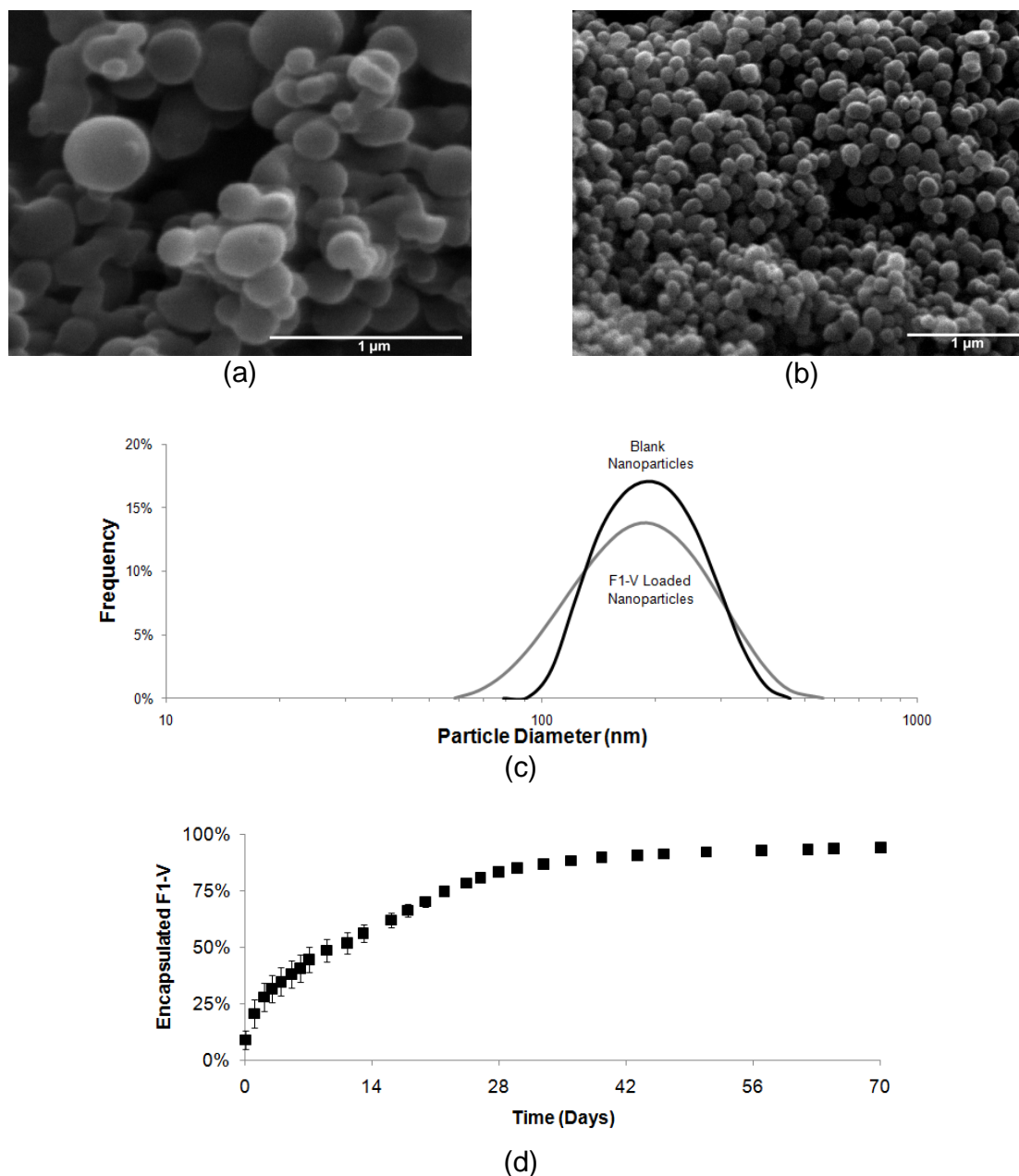


**Figure 6.2.** Material properties of 50:50 CPTEG:CPH nanoparticles. Representative SEM images of (a) blank and (b) 2% F1-V loaded 50:50 CPTEG:CPH nanoparticles (scale bar = 1  $\mu\text{m}$ ). (c) Particle size distribution as determined by QELS for blank ( $204 \pm 62$ ) and 2% F1-V loaded 50:50 CPTEG:CPH nanoparticles ( $196 \pm 77$ ) with  $n = 3$ . (d) In vitro cumulative release of F1-V from 50:50 CPTEG:CPH nanoparticles in pH 7.4 PBS analyzed by micro bicinchoninic acid assay ( $n = 2$ , representative of two separate nanoparticle batches).

### 6.4.2 Protection Against Live *Y. pestis* Challenge

To examine the effectiveness of antigen-encapsulated nanoparticles as intranasal, single-dose vaccines, C57BL/6 mice were vaccinated according to the regimens provided in Table 6.1.

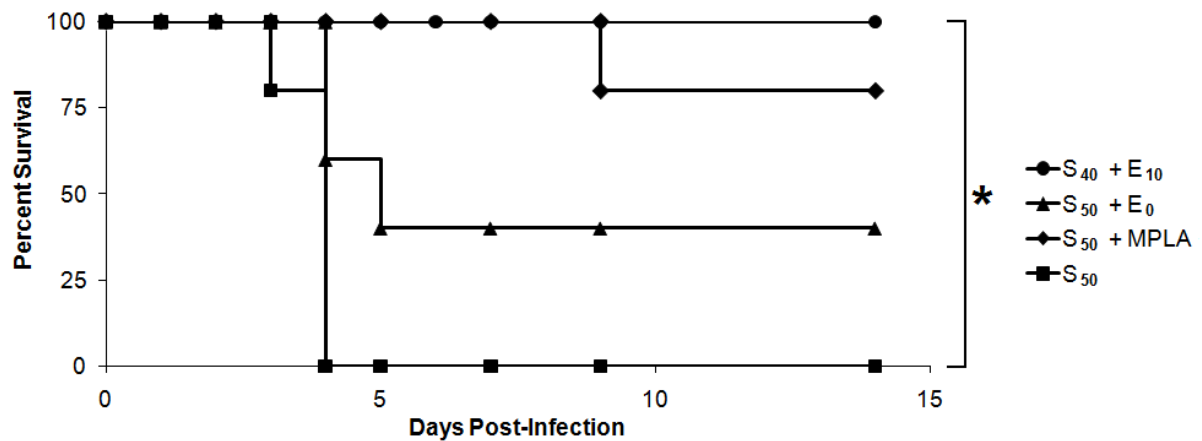
**Table 6.1.** Vaccination regimens employed in this study.

Experimental Group	Soluble F1-V ( $\mu\text{g}$ )	Encapsulated F1-V ( $\mu\text{g}$ )	50:50 CPTEG:CPH Nanoparticles ( $\mu\text{g}$ )	MPLA ( $\mu\text{g}$ )
$S_{50}$	50	-----	-----	-----
$S_{50} + \text{MPLA}$	50	-----	-----	10
$S_{50} + E_0$	50	-----	500	-----
$S_{40} + E_{10}$	40	10	500	-----

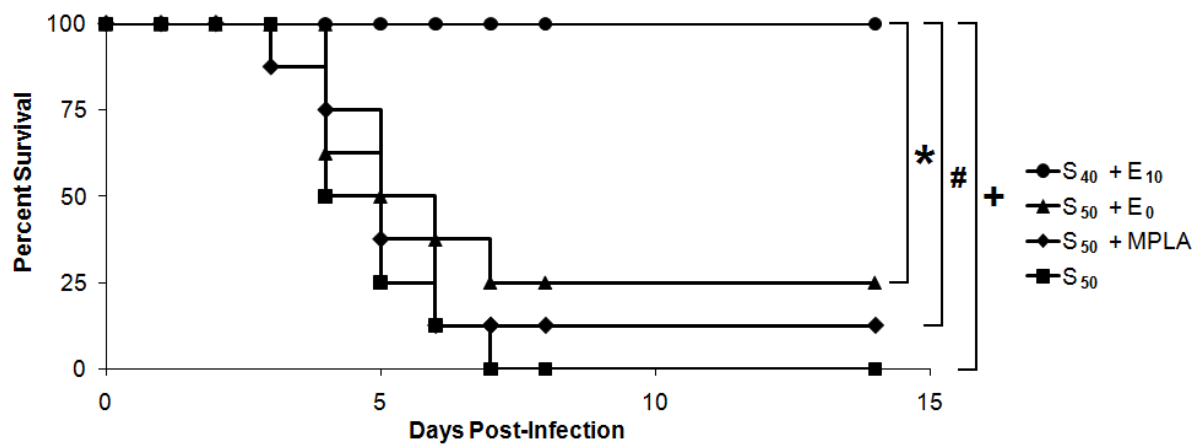
\* Quantities indicate the amounts of immunogen or adjuvant delivered to each mouse in the indicated group. S = soluble protein; E = encapsulated protein. The subscripts indicate the amount of soluble or encapsulated protein (in  $\mu\text{g}$ ) administered per dose.

To study the capacity of the vaccine regimens to provide short-term and long-term protection against pneumonic plague, mice were intranasally challenged at 6 weeks or 23 weeks post-vaccination with 850 CFUs of *Y. pestis* CO92. At 6 weeks post-vaccination (Fig. 6.3a), none of the mice in the  $S_{50}$  treatment group survived the challenge whereas 80% (4/5) of mice treated with  $S_{50} + \text{MPLA}$  and 40% (2/5) of mice treated with  $S_{50} + E_0$ , survived. In contrast, all mice (5/5) treated with  $S_{40} + E_{10}$  survived. When challenged at 23 weeks post-vaccination (Fig. 6.3b), only 12.5% (1/8) of mice treated with  $S_{50} + \text{MPLA}$  and 25% (2/8) of

mice treated with  $S_{50} + E_0$  survived challenge, in comparison to 100% survival of the mice (7/7,  $p < 0.007$ ) vaccinated with  $S_{40} + E_{10}$ .



(a)



(b)

**Figure 6.3.** Impact of vaccination on the survival of C57BL/6 mice challenged with *Y. pestis* CO92. Mice were intranasally challenged with 850 CFU ( $LD_{100}$ ) *Y. pestis* CO92 at (a) 6 weeks post-vaccination ( $n = 5$  per group) or (b) 23 weeks post-vaccination ( $n = 7$  per group). \* =  $p < 0.007$ , # =  $p < 0.001$  and + =  $p < 0.0001$ .

The efficacy of these vaccines for preventing bacterial replication in lungs, livers, and spleens at 72 h post-infection was determined (Fig. 6.4a). Bacterial burdens in lungs, livers, and spleens were consistent with survival of vaccinated mice (Fig. 6.3a) and IgG titers (Fig. 6.7a) and histopathology (Fig. 6.5 and Fig. 6.6). The S<sub>50</sub> + MPLA vaccine regimen was able to reduce the bacterial burdens in lungs, livers, and spleens, but failed to generate effective long-term immunity (Fig. 6.3b).

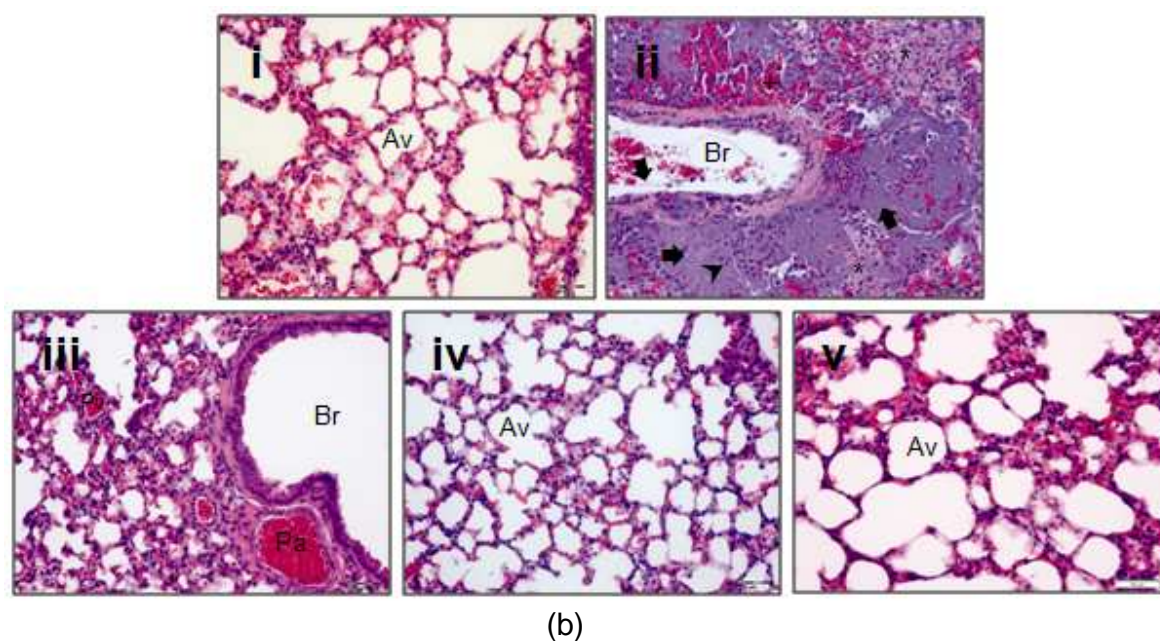
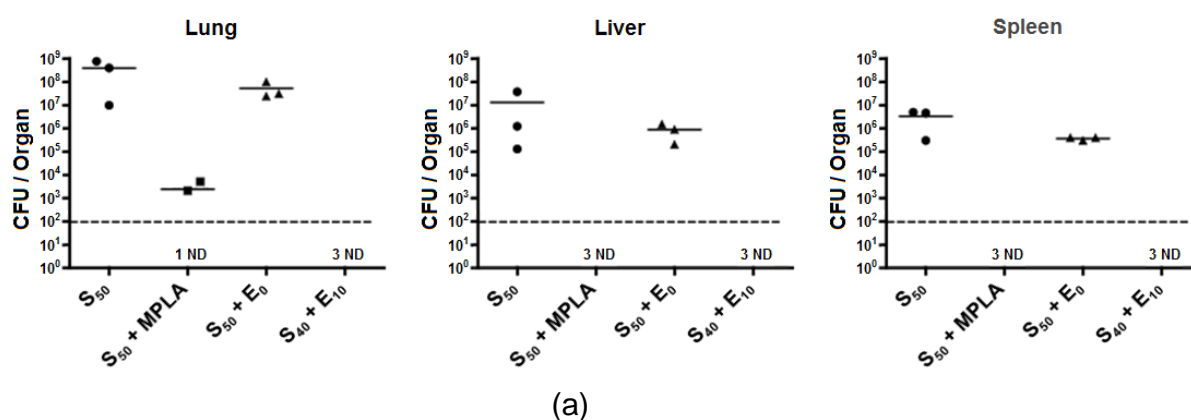


**Figure 6.4.** Bacterial burden and histopathology analysis of vaccinated mice. (a) CFU of *Y. pestis* CO92 at 72 h post-infection in the lungs, livers, and spleens of C57BL/6 mice ( $n = 3$  per group) that were vaccinated 6 weeks prior to challenge. (b) Photomicrographs of lung sections from mice: uninfected and unvaccinated (i) and challenged 6 (ii, iii, and iv) and 23 (v) weeks post-vaccination. S<sub>50</sub> vaccinated mice, 72 h post-challenge (ii) showed severe pathology and loss of tissue architecture due to overwhelming bacterial multiplication in lungs (arrows), neutrophilic infiltration (arrowhead), hemorrhage (+), edema (asterisks), and necrosis. Bronchioles had bacteria clumped with fibrin deposits and neutrophils. Absence of lung pathology was seen in S<sub>40</sub> + E<sub>10</sub> vaccinated mice at 72 h (iii), 14 days (iv), and 21 days post-challenge (v). Av - alveolus, Br - bronchiole, Pa - pulmonary artery, Pv - pulmonary vein. Magnification is 400X. Scale bar = 50 μm.

No bacteria were recovered from the lungs, livers, or spleens of mice treated with  $S_{40} + E_{10}$  (Fig. 6.4a). Regardless of vaccination regimen, no bacteria were detected in lungs, livers, and spleens of mice that survived to day 14 post-infection in both the 6- and 23-week experiments, correlating with vaccination efficacy. Nanoparticle-based vaccines also prevented tissue pathology (Fig. 6.4b, Fig. 6.5 and Fig. 6.6). The mice treated with  $S_{40} + E_{10}$ , when challenged 6 weeks post-vaccination, did not develop pathology in lungs (Fig. 6.4b iii and Fig. 6.5 v), livers (Fig. 6.5 x), and spleens (Fig. 6.5 xv) 72 h post-infection due to their ability to clear bacteria and likely control inflammation. At the end of the survival observation periods in both challenge experiments, histological examination of the lungs from survivors (Fig. 6.6) treated with  $S_{40} + E_{10}$  showed no evidence of lesions and was remarkably similar to uninfected control mice (Fig. 6.2d i and Fig. 6.5 i).

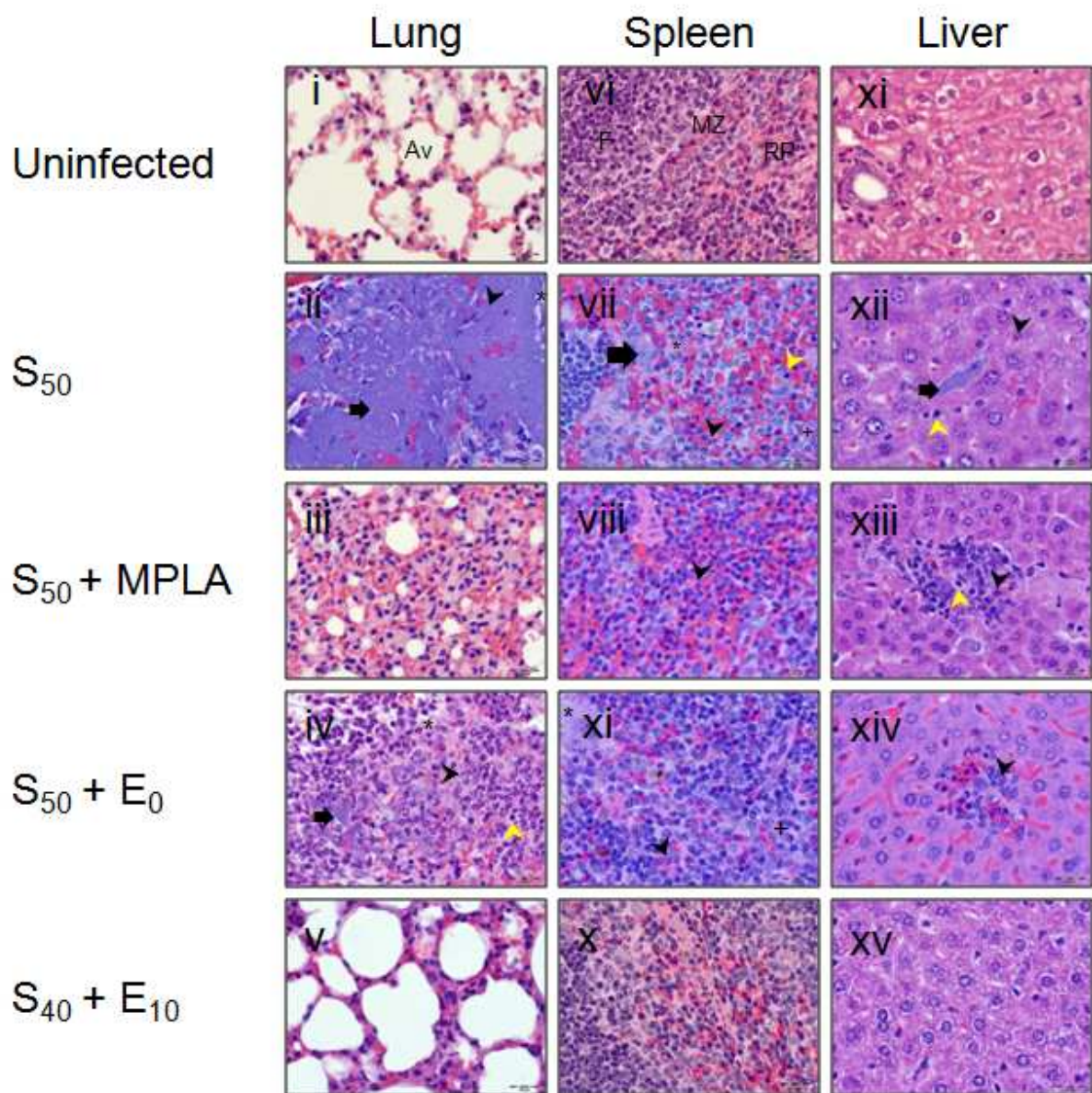


**Figure 6.5.** Histopathological analysis of lungs, spleens, and livers of control and vaccinated mice 6 weeks post-vaccination at 72 h post-challenge.

Lungs: Three out of three S<sub>50</sub> vaccinated mice (ii) lost normal lung architecture due to bacterial multiplication (arrow), neutrophilic infiltrations (black arrowhead) within tissues and bacterial colonies, as well as edema (asterisk), hemorrhages, and necrosis. Similar pathology was also seen in S<sub>50</sub> + E<sub>0</sub> vaccinated mice (iv), although to a lesser extent and with the presence of lymphocytic infiltrations (yellow arrowhead). S<sub>50</sub> + MPLA vaccinated mice (iii) did not show multiplying

bacteria, but had mixed lymphocytic and neutrophilic infiltrations in lung parenchyma. Lungs of  $S_{40} + E_{10}$  vaccinated mice (v) were free of any pathology or bacterial colonies and were remarkably similar to unimmunized and uninfected lungs of control mice (i).

Spleens:  $S_{50}$  vaccinated mice (vii) had bacterial colonies multiplying in spleens (arrow), neutrophilic (black arrowhead) and lymphocytic (yellow arrowhead) infiltrations, edema (asterisk) and necrotic cells (+) in the red pulp and marginal zone. There was also reduction in size of the follicle as well as the marginal zone (data not shown).  $S_{50} + MPLA$  vaccinated mice (viii) had neutrophilic infiltrates in the red pulp.  $S_{50} + E_0$  vaccinated mice (xi) also had edema, necrotic cells, and neutrophilic infiltrates in the red pulp. No bacteria, necrosis or edema were present in  $S_{40} + E_{10}$  (x) vaccinated mice and histology was similar to healthy spleen tissue (vi).

Livers: Bacterial colonies (arrow) are visible in a liver of  $S_{50}$  vaccinated mouse (xii) with neutrophilic (black arrowhead) and lymphocytic (yellow arrowhead) infiltrates in liver parenchyma. Although bacteria were present, neutrophilic infiltration was not as severe as seen in lungs of  $S_{50}$  vaccinated mice. Degenerative changes were also seen in the cytoplasm of the hepatocytes of  $S_{50}$  vaccinated mice.  $S_{50} + MPLA$  vaccinated mice (xiii) also had degenerative changes in the hepatocytes and loosely packed cells were present that mostly included lymphocytes and neutrophils.  $S_{50} + E_0$  vaccinated mice (xiv) had similar hepatic degeneration with loosely packed cells that mostly included neutrophils.  $S_{40} + E_{10}$  vaccinated mice (xv) did not show any pathology like control mice (xi).

The absence of pathology in lungs, spleens and livers of  $S_{40} + E_{10}$  vaccinated mice indicates that nanoparticle-based vaccine can be used to protect mice from *Y. pestis* induced tissue damage.

Av-Alveoli, F - Follicle, Mz - Marginal zone, and RP - Red pulp. Objective lens magnification is 100X. Scale bar = 20  $\mu$ m.

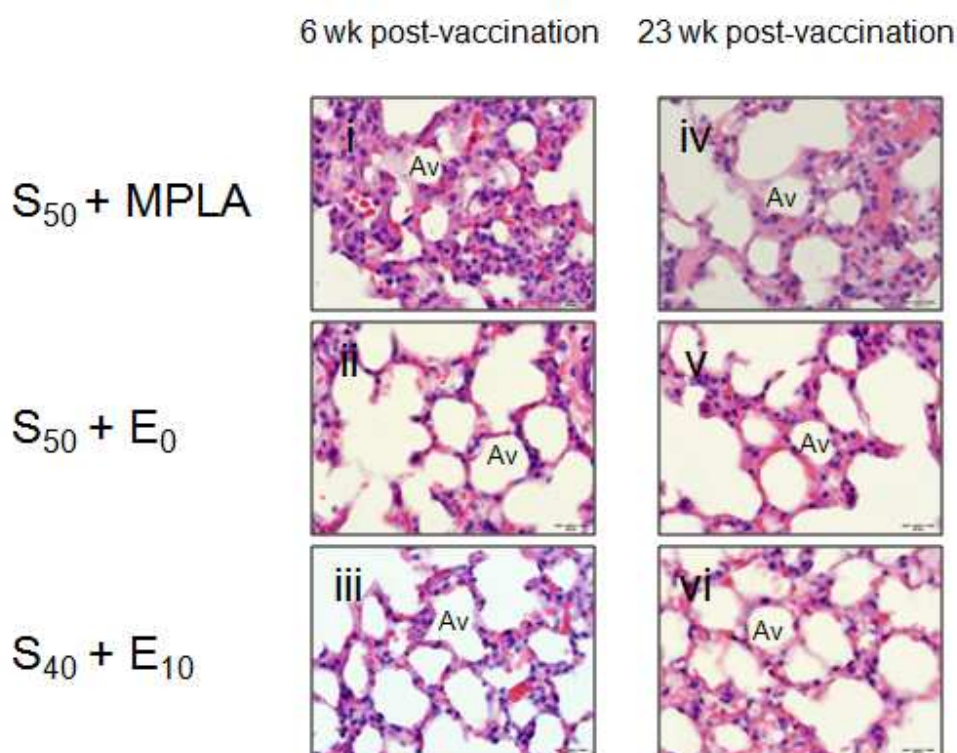


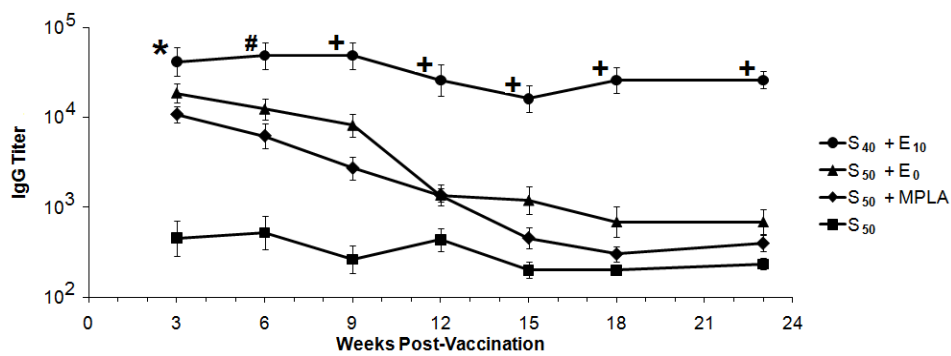
**Figure 6.6.** Histopathological analysis of lungs from mice 23 weeks post-vaccination at 14 days post-challenge. Protected mice had similar lung histology to that of uninfected mice (Supplementary Fig. 1i). Av- Alveoli. Objective lens magnification is 100X, Scale bar = 20  $\mu$ m.

#### 6.4.3 Characterization of Antibody Response

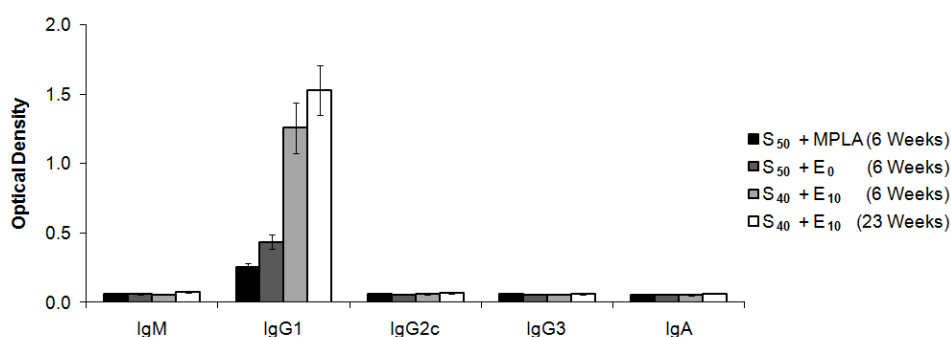
To further characterize the protective immune response, serum samples collected at 3, 6, 9, 12, 15, 18, and 23 weeks post-vaccination were analyzed for anti-F1-V IgG titers (Fig. 6.7a). Prior work has shown that high antibody titers correlate to protection against live *Y. pestis* challenge.<sup>3-8,12</sup> Mice vaccinated with  $S_{50}$  generated low levels of antibody that is in agreement with previous studies evaluating intranasally delivered *Y. pestis* antigens.<sup>7</sup> At 3 weeks post-vaccination, all mice treated with adjuvanted formulations induced demonstrable

titers. Beyond 3 weeks, the anti-F1-V IgG response waned in the mice treated with S<sub>50</sub> + MPLA and S<sub>50</sub> + E<sub>0</sub> while the F1-V- specific IgG response in the S<sub>40</sub> + E<sub>10</sub> vaccinated mice was sustained for at least 23 weeks (Fig. 6.7a). The results also demonstrate that IgG1 was the dominant antibody subtype produced (Fig. 6.7b). In this regard, it has been shown that F1 and V antigen-specific IgG1 facilitates APC phagocytosis and blocks the *Y. pestis* type III secretion system, respectively.<sup>26</sup>

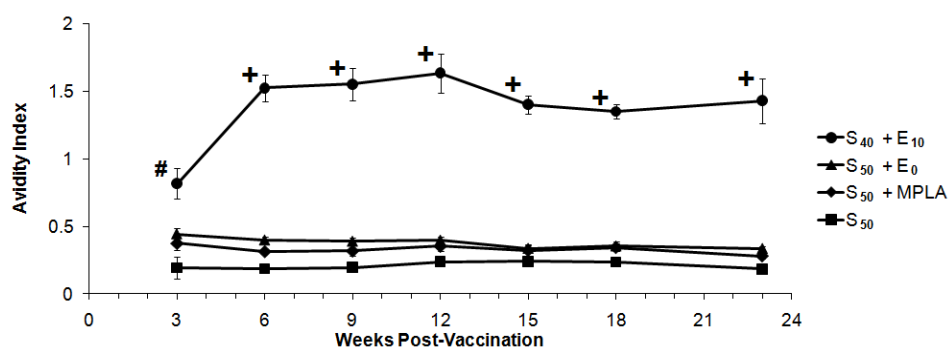
Serum samples were also analyzed for the avidity of the anti-F1-V IgG produced to characterize the affinity maturation of the antibody response (Fig. 6.7c). Others have shown for other bacteria (e.g., *Streptococcus pneumoniae*) that poor antibody avidity correlated to a lack of protection.<sup>27</sup> Average relative avidity of the F1-V-specific IgG was found to be low in the mice treated with S<sub>50</sub>, S<sub>50</sub> + MPLA, and S<sub>50</sub> + E<sub>0</sub> formulations at all time points. In contrast, mice vaccinated with S<sub>40</sub> + E<sub>10</sub> generated higher avidity anti-F1-V specific IgG at 3-weeks post-vaccination, which increased by 6 weeks post-vaccination and was sustained through 23 weeks post-vaccination (Fig. 6.7c).



(a)



(b)



(c)

**Figure 6.7.** Assessment of anti-F1-V antibody response. (a) Kinetics of the IgG antibody titer for each of the treatments over 23 weeks post-vaccination. (b) Antibody isotype induced by various immunization regimen. Optical density was determined by ELISA at a 1:1000 dilution. (c) IgG antibody avidity through 23 weeks post-vaccination. Avidity was analyzed by ELISA at a 1:200 dilution. Data is presented as the mean  $\pm$  SEM ( $n = 7$  per group). \* =  $p < 0.02$ , # =  $p < 0.005$  and + =  $p < 0.0001$  (compared to  $S_{50} + MPLA$ ).

## 6.5 Discussion

These results demonstrate that single-dose intranasal administration of nanovaccines consisting of soluble F1-V together with F1-V encapsulated into polyanhydride nanoparticles ( $S_{40} + E_{10}$ ) was able to induce significant, long-lived antibody titers with high avidity that correlated to long-term protection against a lethal *Y. pestis* challenge. When this result is compared to the immunostimulatory behavior of soluble F1-V administered with blank nanoparticles ( $S_{50} + E_0$ ), it is clear that the presence of antigen-encapsulated nanoparticles is critical to the induction and maintenance of long-lived, high-avidity IgG1 antibody and protection from live challenge. Formulations with both soluble and encapsulated antigen performed the dual functions of enabling the soluble antigen to initiate a primary response<sup>28</sup> and the antigen-encapsulated nanoparticles to provide sustained (or persistent) antigen delivery that maintains antibody titer and dramatically increases the affinity maturation of the antibody response.<sup>29</sup>

While *in vivo* mechanisms that govern nanoparticle-mediated enhancement of immune responses have yet to be elucidated, recent research showed that the activation of complement pathways and antigen presenting cells plays a key role in how some nanoparticles activate an immune response.<sup>30</sup> The capacity for polyanhydride nanoparticle formulations to induce activation<sup>16,18,31</sup> of pulmonary DCs and alveolar macrophages *in vivo* could partially explain their adjuvant capabilities and induction of protective immunity observed in the present work. Activated DCs will traffic to the draining lymph node where they have a

myriad of interactions that facilitate the adaptive immune response.<sup>28</sup> According to studies by Jenkins, activated DCs and soluble antigen work in concert to stimulate the clonal expansion of antigen-specific lymphocytes.<sup>28</sup> The importance of adequate soluble antigen during the initiation of the immune response and the consequent processing and presentation by resident DCs would explain why vaccine regimens employing only antigen-encapsulated nanoparticles were unable to initiate a robust immune response (data not shown). Thus, the nanoparticle-based formulations clearly functioned as adjuvants because they initiated a robust immune response, provided extended antigen delivery, and induced long-term protection against infection.

The potential for extended antigen delivery by 50:50 CPTEG:CPH nanoparticles can be attributed to their presence in the lungs 28 days post-intranasal vaccination using *in vivo* imaging (data not shown). While nanoparticles have been shown to activate and be internalized by APCs *in vitro*<sup>16,18</sup>, the ability for some particles to evade short-term clearance by professional phagocytes would allow for prolonged antigenic exposure because of delayed APC internalization, gradual polymer degradation and release of antigen, or a combination thereof. Prior research shows that vaccines delivered with an adjuvant via multiple doses are able to induce high avidity antibody.<sup>32,33</sup> More mechanistic studies provide evidence that continual presentation of antigen by adjuvants specifically conveys increased avidity.<sup>34</sup> This observation is generally attributed to somatic hypermutation and affinity maturation that occurs

in the germinal centers of lymphoid organs.<sup>35</sup> Clearance avoidance and delayed degradation of nanoparticles would provide a mechanism by which presence of an antigen could be prolonged resulting in the induction of antigen-specific antibody responses with higher titer and avidity.

## 6.6 Conclusions

To our knowledge, the performance of the polyanhydride nanoparticle-based formulations in this work is the first demonstration of the ability of particle-based vaccines to induce long-term protection against lethal challenge after a single vaccination. Using polyanhydride microparticle-based adjuvants, mice vaccinated intramuscularly with a single dose formulation consisting of soluble tetanus toxoid (TT) together with TT-encapsulated particles demonstrated long-lived antibody titer with high avidity, providing yet another example of the capability of the particle-based vaccines to function in a single dose.<sup>15</sup> In addition, the nanovaccine platform technology described here can function as effective adjuvants for a wide range of antigens. For example, in the case of seasonal diseases like influenza, for which immune protection needs to last for six months, particle-based formulations can be designed to encapsulate multiple payloads and provide effective immunity with a single administration. The versatility of the polyanhydride chemistry and the scalability of the particle fabrication process enable the design of combination vaccines with cocktails of microparticles and nanoparticles of different chemistries delivered via one or more routes. The

design and development of customized polyanhydride particle-based vaccines can lead to a highly effective technological platform for vaccine delivery.

### **6.7 Acknowledgements**

The authors acknowledge financial support from the US Department of Defense – Office of Naval Research (ONR Award no. N00014-06-1-1176). B.D.U acknowledges financial support from the Aileen S. Andrew Foundation.

## 6.8 References

1. Lambert, P.H., Liu, M. & Siegrist, C.A. Can successful vaccines teach us how to induce efficient protective immune responses? *Nature Medicine*. **11**(Suppl 4): S54-62 (2005).
2. Zepp, F. Principles of vaccine design-Lessons from nature. *Vaccine*. **28**(Suppl 3):C14-24 (2010).
3. Chiuchiolo, M.J., Boyer, J.L., Krause, A., Senina, S., Hackett, N.R. & Crysal, R.G. Protective immunity against respiratory tract challenge with *Yersinia pestis* in mice immunized with an adenovirus-based vaccine vector expressing V antigen. *The Journal of Infectious Diseases*. **194**(9): 1249 – 1257 (2006).
4. Elvin, S.J., Elyes, J.E., Howard, K.A., Ravichandran, E., Somavarappu, S., Alpar, H.O. & Williamson, E.D. Protection against bubonic and pneumonic plague with a single dose microencapsulated sub-unit vaccine. *Vaccine*. **24**(20): 4433 – 4439 (2006).
5. Anderson, G.W., Heath D.G., Bolt, C.R., Welkos, S.L., Friedlander, A.M. Short- and long-term efficacy of single-dose subunit vaccines against *Yersinia Pestis* in mice. *American Journal of Tropical Medicine and Hygiene*. **58**(6): 793 – 799 (1998).
6. Mett, V., Lyons, J., Musiychuk, K., Chichester, J.A., Brasil, T., Couch, R., Sherwood, R., Palmer, G.A., Streatfield, S.J. & Yusibov, V. A plant-produced plague vaccine candidate confers protection to monkeys. *Vaccine*. **25**(16): 3014 – 3017 (2007).
7. Airhart, C.L. Rohde, H.N., Hovde, C.J., Bohach, G.A., Deobald, C.F., Lee, S.S. & Minnich, S.A. Lipid A mimetics are potent adjuvants for an intranasal pneumonic plague vaccine. *Vaccine*. **26**(44): 5554 – 5561 (2008).
8. Thomas, R.J., Webber, D., Collinge, A., Stagg, A.J., Bailey, S.C., Nunez, A., Gates, A., Jayasekera, P.N., Taylor, R.R., Eley, S. & Titball, R.W. Different pathologies but equal levels of responsiveness to the recombinant F1 and V antigen vaccine and ciprofloxacin in a murine model of plague caused by small- and large-particle aerosols. *Infection and Immunity*. **77**(4): 1315 – 1323 (2009).
9. Haffkine, W.M. Remarks on the plague prophylactic fluid. *British Medical Journal*. **1**(1902): 1461 – 1462 (1897).

10. Girard, G. Immunity in plague. Acquisitions supplied by 30 years of work on the '*Pastuerella pestis* Ev' (Girard and Robic) strain. *Biology and Medicine (Paris)*. **52**: 631 – 731 (1963).
11. Pitt, M.L. Non-human primates as a model for pneumonic plague. Public Workshop on Animal Models and Correlates of Protection for Plague Vaccines. (2004). Retrieved on 9 March 2009 from <http://www.fda.gov/cber/minutes/plague101304t.pdf>.
12. Uppada, J.B., Khan, A.A., Bhat, A.A., Deshmukh, R. & Rao, D.N. Humoral immune responses and protective efficacy of sequential B- and T-cell epitopes of V antigen of *Yersinia pestis* by intranasal immunization in microparticles. *Medical Microbiology and Immunology*. **198**(4): 247 – 256 (2009).
13. Determan, A.S., Trewyn, B.G., Lin, V.S., Nilsen-Hamilton, M. & Narasimhan, B. Encapsulation, stabilization, and release of BSA-FITC from polyanhydride microspheres. *Journal of Controlled Release*. **100**(1): 97 – 109 (2004).
14. Determan, A.S., Wilson, J.H., Kipper, M.J., Wannemuehler, M.J. & Narasimhan, B. Protein stability in the presence of polymer degradation products: consequences for controlled release formulations. *Biomaterials*. **27**(17): 3312 – 3320 (2006).
15. Kipper, M.J., Wilson, J.H., Wannemuehler, M.J. & Narasimhan, B. Single dose vaccine based on biodegradable polyanhydride microspheres can modulate immune response mechanism. *Journal of Biomedical Materials Research Part A*. **76A**(4): 798 – 810 (2006).
16. Petersen, L.K., Xue, L., Wannemuehler, M.J., Rajan, K. & Narasimhan, B. The simultaneous effect of polymer chemistry and device geometry on the in vitro activation of murine dendritic cells. *Biomaterials*. **30**(28): 5131 – 5142 (2009).
17. Torres, M.P., Determan, A.S., Anderson, G.L., Mallapragada, S.K. & Narasimhan, B. Amphiphilic polyanhydrides for protein stabilization and release. *Biomaterials*. **28**(1): 108 – 116 (2007).
18. Ulery, B.D., Phanse, Y., Sinha, A., Wannemuehler, M.J., Narasimhan, B. & Bellaire, B.H. Polymer chemistry influences monocytic uptake of polyanhydride nanospheres. *Pharmaceutical Research*. **26**(3): 683 – 690 (2009).

19. Leong, K.W., D'Amore, P., Marletta, M. & Langer, R. Bioerodible polyanhydrides as drug-carrier matrices. II. Biocompatibility and chemical reactivity. *Journal of Biomedical Materials Research*. **20**(1):51 – 64 (1986).
20. Domb, A.J. & Langer, R. Polyanhydrides I. Preparation of high molecular weight polyanhydrides. *Journal of Polym Science Part A: Polymer Chemistry*. **25**(12): 3373 – 3386 (1987).
21. Tamada, J. & Langer, R. The development of polyanhydrides for drug delivery applications. *Journal of Biomaterials Science, Polymer Edition*. **3**(4):315 – 353 (1992).
22. Tabata, Y., Gutta, S. & Langer, R. Controlled delivery systems for proteins using polyanhydride microspheres. *Pharmaceutical Research*. **10**(4): 487 – 96 (1993).
23. Torres, M.P., Vogel, B.M., Narasimhan, B. & Mallapragada, S.K. Synthesis and characterization of novel polyanhydrides with tailored erosion mechanisms. *Journal of Biomedical Materials Research Part A*. **76A**(1): 102 – 110 (2006).
24. Carrillo-Conde, B., Schiltz, E., Yu, J., Minion, F.C., Phillips, G.J., Wannemuehler, M.J. & Narasimhan, B. Encapsulation into amphiphilic polyanhydride microparticles stabilizes *Yersinia pestis* antigens. *Acta Biomaterialia*. **6**(8): 3110 – 3119 (2010).
25. Dandekar, P., Venkataraman, C. & Mehra, A. Pulmonary targeting of nanoparticle drug matrices. *Journal of Aerosol Medicine and Pulmonary Drug Delivery*. [Epub ahead of print].
26. Cowan, C., Philipovsky, A.V., Wulff-Strobel, C.R., Ye, Z. & Straley, S.C. Anti-LcrV antibody inhibits delivery of Yops by *Yersinia pestis* KIM5 by directly promoting phagocytosis. *Infection and Immunity*. **73**(9): 6127 – 6137 (2005).
27. Lee, L.H., Frasch, C.E., Falk, L.A., Klein, D.L. & Deal, C.D. Correlates of immunity for pneumococcal conjugate vaccines. *Vaccine*. **21**(17-18): 2190 – 2196 (2003).
28. Catron, D.M., Itano, A.A, Paper, K.A., Mueller, D.L. & Jenkins, M.K. Visualizing the first 50 hr of the primary immune response to a soluble antigen. *Immunity*. **21**(3): 341 – 347 (2004).

29. Zinkernagel, R.M. On differences between immunity and immunological memory. *Current Opinion in Immunology*. **14**(4): 523 – 526 (2002).
30. Reddy, S.T., van der Vlies, A.J., Simeoni, E., Angeli, V., Randolph, G.J., O'Neil, C.P., Lee, L.K., Swartz, M.A. & Hubbell, J.A. Exploiting lymphatic transport and complement activation in nanoparticle vaccines. *Nature Biotechnology*. **25**(10): 1159 – 1164 (2007).
31. Ulery, B.D., Pustulka, K., Phanse, Y., Bellaire, B. & Narasimhan, B. Amphiphilic polyanhydride chemistry affects monocytic association of nanospheres. *Proceedings of the 37<sup>th</sup> Annual Biochemical Engineering Symposium*. **37**, 52 – 58 (2008).
32. Siegrist, C.A., Pihlgren, M., Tougne, C., Efler, S.M., Morris, M.L., Al Adhami, M.J., Cameron, D.W., Cooper, C.L., Heathcote, J., Davis, H.L. & Lambert, P.H. Co-administration of CpG oligonucleotides enhances the late affinity maturation process of human anti-hepatitis B vaccine response. *Vaccine*. **23**(5): 615 – 622 (2004).
33. Park, Y.S., Lee, J.H., Hung, C.F., Wu, T.C. & Kim, T.W. Enhancement of antibody responses to bacillus anthracis protective antigen domain IV by use of calreticulin as a chimeric molecular adjuvant. *Infection and Immunity*. **76**(5): 1952 – 1959 (2008).
34. Wang, Y., Huang, G., Wang, J., Molina, H., Chaplin, D.D. & Fu, Y.X. Antigen persistence is required for somatic mutation and affinity maturation of immunoglobulin. *European Journal of Immunology*. **30**(8): 2226 – 2234 (2000).
35. Di Noia, J.M. & Neuberger, M.S. Molecular mechanisms of antibody somatic hypermutation. *Annual Review of Biochemistry*. **76**: 1 – 22 (2007).

# CHAPTER 7

## Conclusions & Future Research

### 7.1 Conclusions

With aluminum salts being the only adjuvant utilized in the U.S. for human vaccines, their limitations (unidirectional immune modulation, delivery route issues, and capacity to induce inflammatory myopathy)<sup>1</sup> necessitate the development of novel vaccine adjuvants. Also, intranasal delivery of vaccines holds promise of reducing vaccine dose and administration time while vaccinating the host mucosally and systemically as evidenced with the intranasal flu vaccine, FluMist<sup>®</sup>.<sup>2</sup> The adjuvant capabilities and deep lung tissue depositing size of polyanhydride nanoparticles make them a promising nanovaccine platform. The ability to reproducibly fabricate CPH:SA nanoparticles and their chemistry-dependent effect on particle and soluble antigen uptake by THP-1 human monocytes was investigated in this thesis (Chapter 4) to better understand the role chemistry plays in immune activation. This analysis was expanded upon in Chapter 5 when both individual cell based (fluorescent microscopy) and cell population based (flow cytometry and multiplex-bead assay) techniques were utilized to determine more complex antigen presenting cell activation effects of both CPH:SA and CPTEG:CPH nanoparticles on murine bone-marrow derived dendritic cells. This research showed a unique, pathogen-

like behavior of 50:50 CPTEG:CPH nanoparticles that correlated to both increased cell surface marker expression and cytokine secretion. To evaluate the adjuvanticity of 50:50 CPTEG:CPH nanoparticles *in vivo*, a F1-V loaded nanoparticle vaccine was delivered intranasally in a single-dose to convey protection against plague (Chapter 6). Results showed that a vaccine formulation of soluble F1-V co-delivered with F1-V loaded nanoparticles was able to maintain high-avidity antibody titers that correlated with complete protection against a lethal *Yersinia pestis* challenge at 6 or 23 weeks post-vaccination. The capacity for polyanhydride nanoparticles to induce near-term and long-lived protection provides a nanovaccine platform in which multiple parameters (polymer chemistry, particle size, antigen loading and delivery route) can be tailored to develop appropriate vaccine strategies against a wide array of infectious diseases.

## 7.2 Future Work

The promising adjuvanticity of polyanhydride nanoparticles in vaccination against plague provide a basis for further research. While F1-V based vaccination conveyed protection, additional study into antigen modification and other protective *Y. pestis* antigens could yield products that lead to dose sparing and immunity against knock-out strains of bacteria designed to function as bioterrorism weapons. In addition, further nanoparticle optimization will lead to vaccine formulations that convey complete protection using the smallest dose possible. While the random copolymers currently being investigated hold great

promise, novel polyanhydride polymer and particle design could yield products with superior material properties and advanced delivery and/or adjuvanticity capacity. Finally, to better understand the intracellular behavior of internalized nanoparticles, new intracellular analytical tools must be developed.

### **7.2.1 *Yersinia pestis* Vaccine Optimization**

In order to enhance the immune response against F1-V,  $\alpha$ -galactose modification of the antigen is being investigated. The  $\alpha$ -galactose modification allows for immune processing of recombinant protein antigens more efficiently. Naturally occurring anti- $\alpha$ -galactose antibodies facilitate antigen processing by attaching to the modified antigen and facilitating uptake and processing by APCs through the Fc $\gamma$  receptor (Fig. 7.1a). The ability for this effect to induce enhanced antibody production against F1-V *in vivo* is shown in Fig. 7.1b.

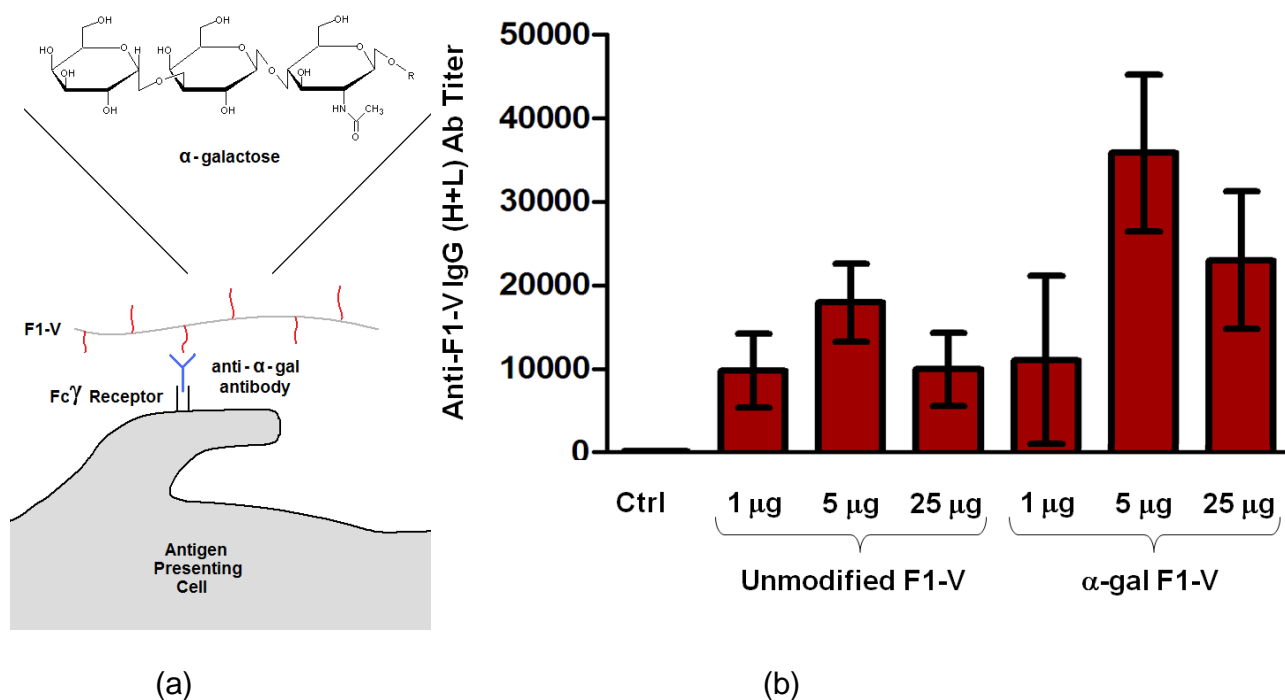


**Figure 7.1.** (a) APC processing and presenting of  $\alpha$ -galactose modified F1-V. (b) Anti-F1-V IgG titers 40 days post-vaccination show that  $\alpha$ -gal modification induced a superior immune response than the antigen alone.

The enhancement of antibody production by  $\alpha$ -gal modification has the capacity to significantly reduce vaccine dose and cost.

Also, identification of novel *Y. pestis* antigens could lead to the development of a multiple antigen vaccine that would convey protection to a heterogenous population of knock-out strains designed to circumvent current vaccine strategies. Three membrane proteins have been identified as possible alternative plague antigen candidates. *Ail* is involved in cell binding and cell invasion, *LamB* is involved in maltose metabolism and *YapM* is an autotransporter. These proteins are currently being purified and evaluated for

their ability to induce protective immune responses. If any of these are effective antigens they will be incorporated into nanoparticle based vaccines either as a single antigen or as a multiple antigen system to improve vaccination against wild-type and knock-out strains of *Y. pestis*.

### 7.2.2 Nanoparticle Vaccine Optimization

While a vaccine formulation of soluble F1-V co-delivered with F1-V loaded 50:50 CPTEG:CPH nanoparticles conveyed long-lived protection against plague, optimization of a number of parameters is necessary. 50:50 CPTEG:CPH nanoparticles induced promising DC activation *in vitro*, but only when compared to the other polymer chemistries (poly(SA), 50:50 CPH:SA, poly(CPH), and poly(CPTEG)) (Chapter 5). Investigation of nanoparticles with finer chemistry differences may provide a better way to determine optimal copolymer chemistry. Approaching this by conventional synthesis and fabrication would be time-consuming, but combinatorial methods allow for high-throughput analysis of a library of copolymer chemistries. Recent research by Petersen et al.<sup>3</sup> shows that 60:40 CPTEG:CPH may enhance cell surface marker expression more than 50:50 CPTEG:CPH nanoparticles (Fig. 7.2).

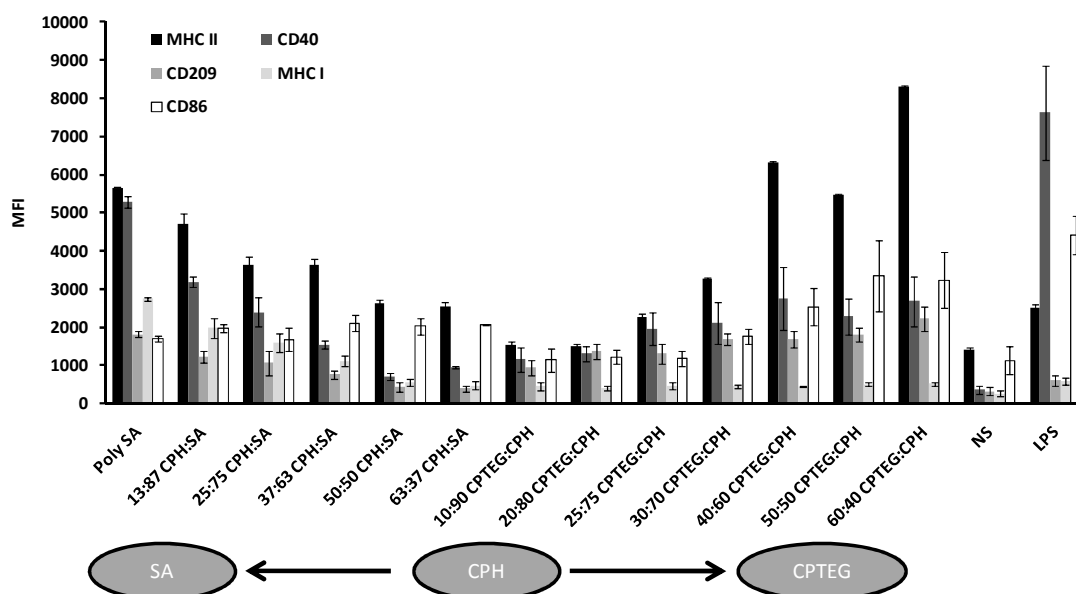


**Figure 7.2.** Cell surface marker expression (mean fluorescence intensity (MFI)) as represented graphically of MHC II, CD209, CD86, CD40 and MHC I upon a 48 h incubation of combinatorially fabricated CPH:SA and CPTEG:CPH nanoparticles with DCs. NS: non-stimulated cells (negative control) and LPS (200ng/mL) (positive control). Error bars represent standard error and minimum n=3.

CPTEG-rich nanoparticles cannot be reproducibly fabricated at this time, but future research could create nanoparticles between 50:50 CPTEG:CPH and poly(CPTEG) that would be stable and optimal for immune activation.

It was determined that encapsulation of 20% of the total F1-V protein within nanoparticles resulted in superior antibody production and protection over 0% and 100% encapsulation, but no other antigen encapsulation percentages were evaluated. Since the results described in this thesis have shown that an antigenic bolus and encapsulated payload are both required to initiate a long-

lasting protective response, there must exist a continuum in which an optimal antigen encapsulation percentage can be determined (Fig. 7.3).

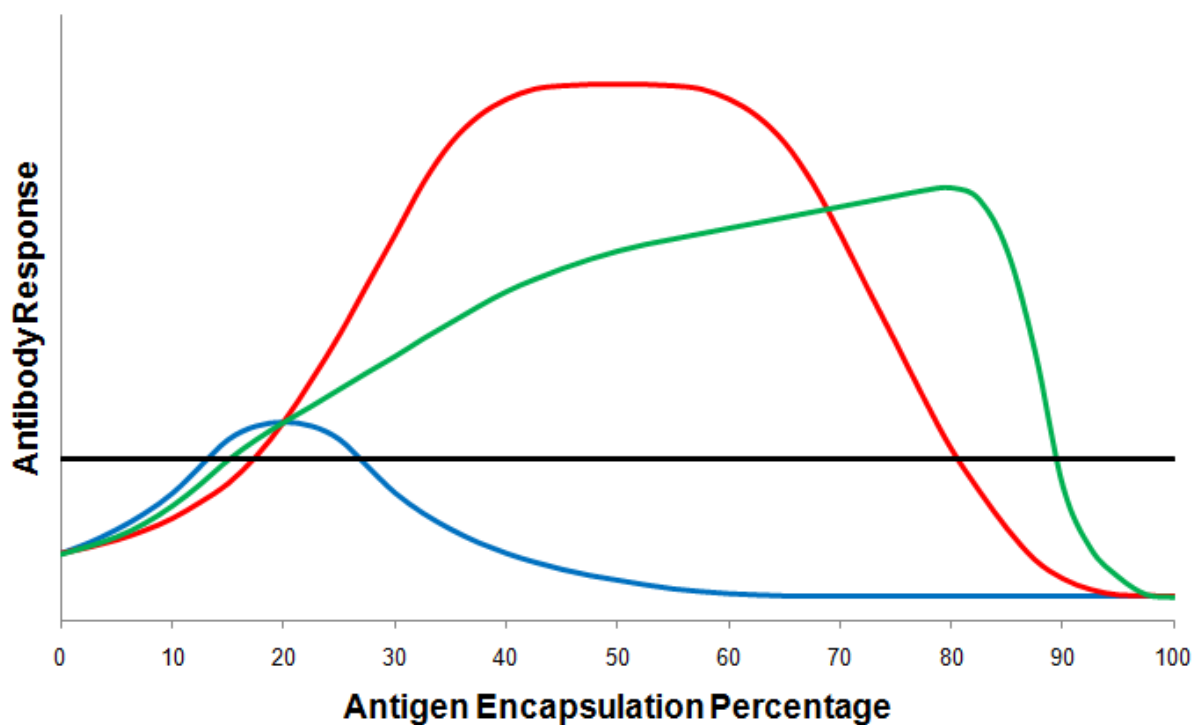


**Figure 7.3.** Potential schematics for antibody response as a function of antigen encapsulation percentage. The blue curve shows high soluble antigen, the green curve shows high encapsulated antigen, and the red curve shows a relatively equal mix of soluble and encapsulated antigen as the best formulation. The black line represents the minimum response necessary for protection.

Currently, it is unknown which profile best fits this continuum. Experiments varying antigen encapsulation percentage and monitoring the antibody response and protection capacity would allow tuning of nanoparticle adjuvanticity. In addition, the ability to reduce total antigen dose is dependent on this profile as shown in Fig. 7.4.

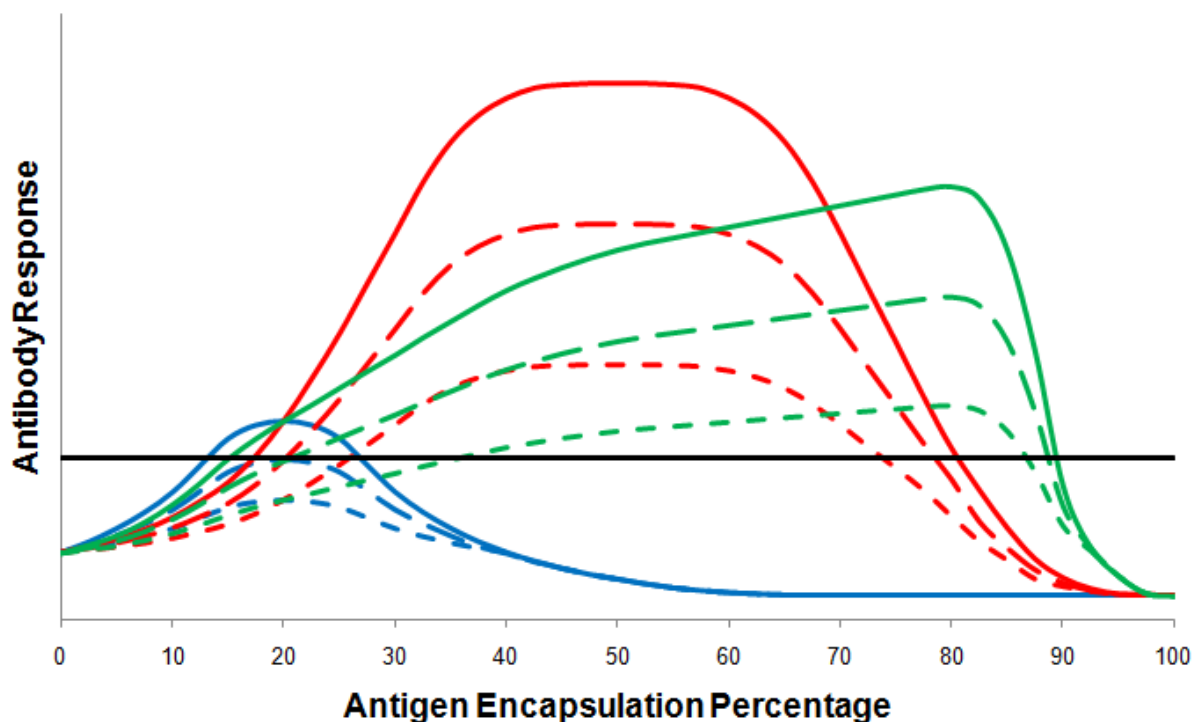


**Figure 7.4.** As total antigen dose is reduced (dashed lines), protective formulation range narrows and is dependent on the antigen encapsulation continuum.

Variation of both antigen encapsulation percentage and total antigenic dose would allow for utilization of the lowest antigenic dose possible reducing vaccine cost.

Current research has analyzed the vaccine adjuvant and delivery capacity of particles composed of a single polymer chemistry of a given size. A logical next step is to investigate the possibility of combination vaccines with nanoparticles of varying chemistry and size. While it has been shown that recombinant proteins encapsulated within CPH:SA particles undergo significant degradation upon release<sup>4</sup>, the capacity for CPH:SA nanoparticles to enhance

monocytic uptake of soluble antigen (Chapter 4) may make blank CPH:SA nanoparticles promising candidates to adjuvant the soluble protein dose. Also, the DC stimulation profile and intracellular trafficking of CPH:SA nanoparticles was different than the 50:50 CPTEG:CPH nanoparticles (Chapter 5). The *in vivo* adjuvanticity mechanism(s) of CPH:SA nanoparticles may be significantly different than CPTEG:CPH nanoparticles. While nanoparticles have shown promise of depositing into deep lung tissue, the ability to create an antigen depot may improve vaccine effectiveness. Intranasally administered antigen loaded 50:50 CPTEG:CPH microparticles would settle in the nasal cavity and may be able to facilitate more gradual antigen delivery. By investigating cocktails of microparticles and nanoparticles of varying chemistries, a vaccine system could be designed with enhanced properties over 50:50 CPTEG:CPH nanoparticles alone.

While intranasal delivery holds many advantages, cocktail vaccines may facilitate the best response by delivery through multiple routes. Microparticle antigen depots may function better in continual delivery if injected subcutaneously rather than residing in the nasal cavity. Heterologous delivery of prime-boost plague vaccination has shown promise over homologous delivery<sup>5</sup>, so replicating this for single-round delivery of particle-based vaccines may increase effectiveness.

### 7.2.3 Novel Polymer & Particle Design

While CPH:SA and CPTEG:CPH random copolymer particles function as promising nanovaccine adjuvants, advancements in polymer development and particle design could lead to materials with superior properties and delivery capabilities. So far research has focused on a copolymer continuum of chemistry going from poly(SA) to poly(CPH) to poly(CPTEG) (Fig. 7.5 top). By investigating terpolymers consisting of a combination of CPH, SA and CPTEG monomers (Fig. 7.5 bottom), novel chemistries with enhanced material properties may be identified.

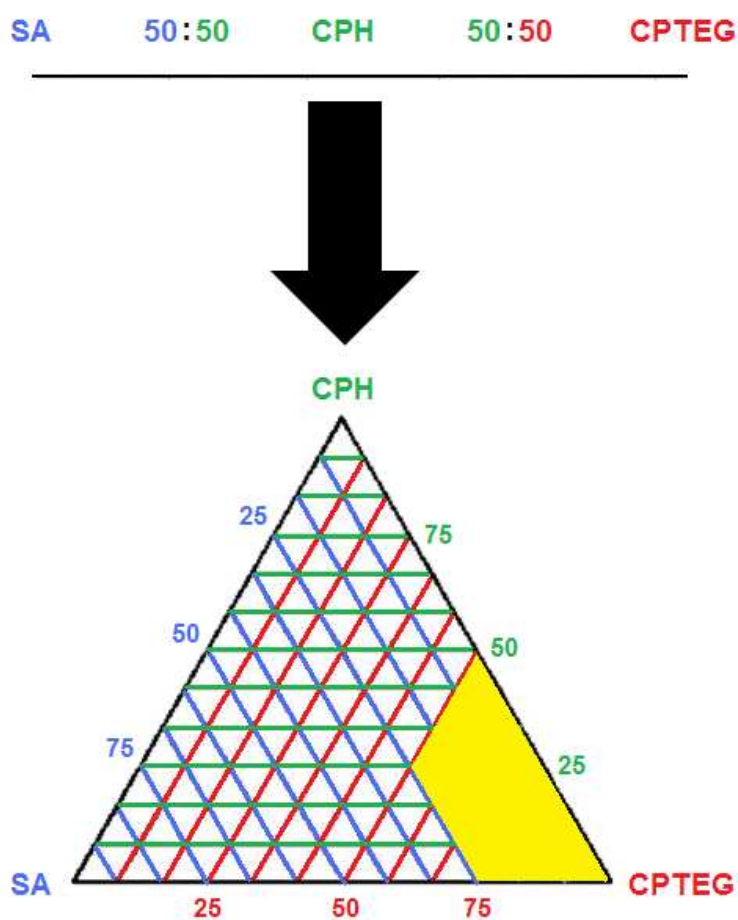
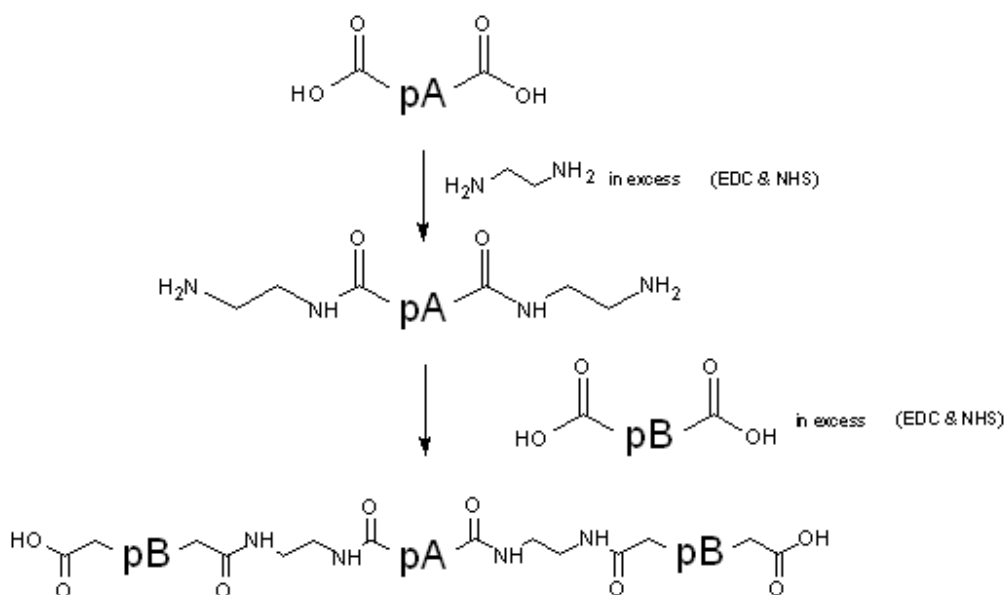


**Figure 7.5.** Current copolymer continuum (top) and terpolymer ternary composition diagram (bottom).

The acidity of SA monomer makes it undesirable in high composition, but its processability makes it an attractive candidate if used in low composition. With current limitations in CPTEG-rich particle fabrication, further research into CPTEG-rich, CPH-poor, SA-poor (yellow area in Fig. 7.5 bottom) terpolymers may yield polyanhydrides with desirable antigen stabilizing capacity that can be reproducibly fabricated into stable nanoparticles. Due to the addition of another

variable, polymer and particle development for terpolymers lends itself to combinatorial evaluation.

While nanoparticles as small as 80 nm have been fabricated by antisolvent nanoprecipitation, smaller particles may have enhanced vaccine delivery effects. Recent research shows 25 nm particles are able to traffic directly through lymphatic vessels to draining lymph nodes<sup>6</sup> and are trafficked intracellularly through a novel, non-degradative pathway.<sup>7</sup> Enhanced design of polyanhydride nanoparticles could be realized by the synthesis of triblock copolymers. A possible schematic for this synthesis is outlined in Scheme 7.1.



**Scheme 7.1.** Synthesis of triblock polyanhydride copolymers with ethylenediamine linkers

By utilizing a reactive linker, high purity triblock polymers consisting of polyanhydrides can be synthesized. While any polymer blocks could be chosen

with this scheme, the protein stabilization capacity of poly(CPTEG) and the ability to maintain structure through gradual surface erosion of poly(CPH) and poly(SA) makes them excellent candidates for internal and external blocks, respectively.

By choosing blocks of significantly different chemistry self assembly or precipitation in the correct solvent would cause the formation of a core-shell particles in which vaccines could be loaded into the core (poly(CPTEG)) and shells (poly(CPH)) would allow for long-term particle structure to be maintained (Fig. 7.6a).

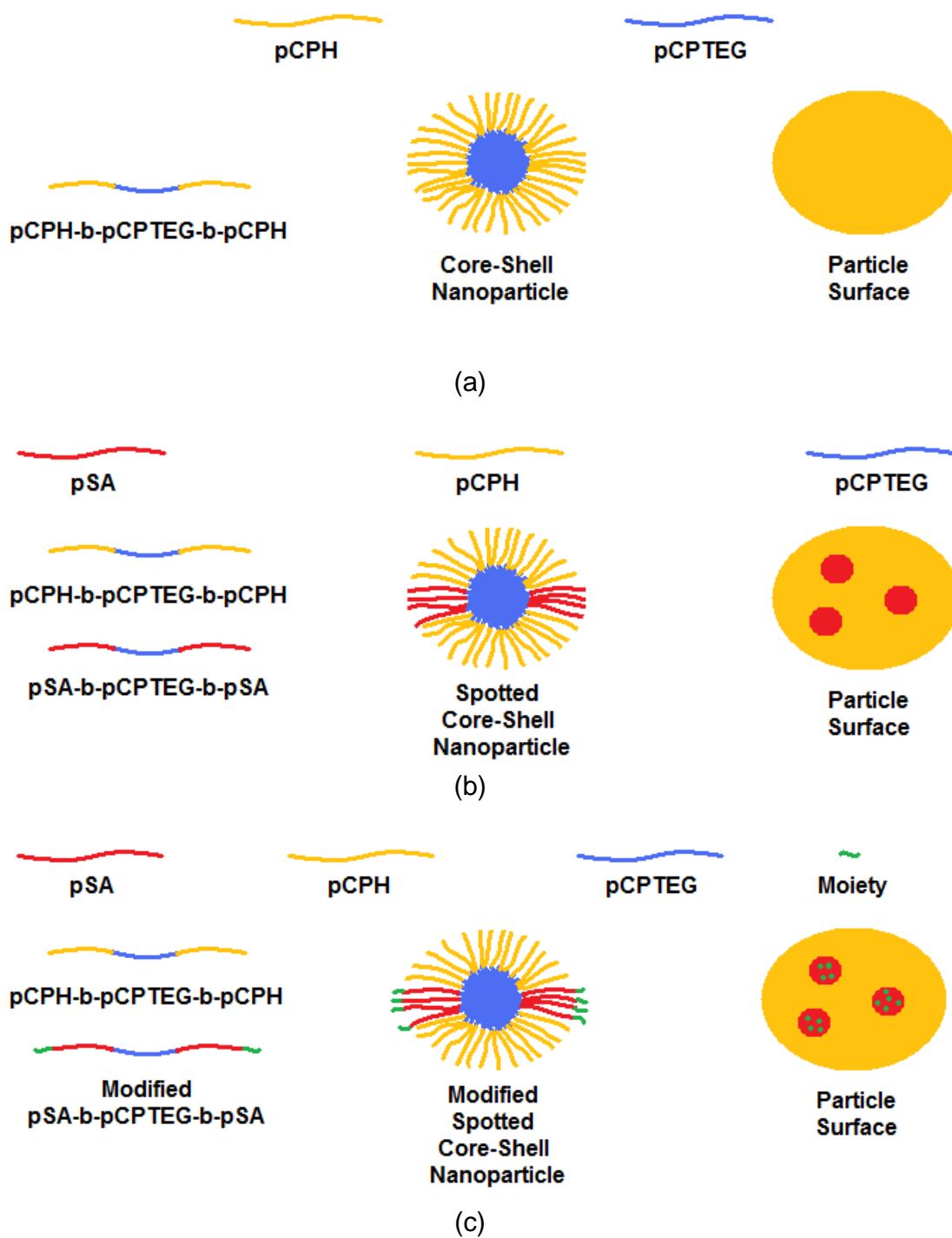


**Figure 7.6.** Triblock fabrication potential for (a) core-shell nanoparticles, (b) spotted core-shell nanoparticles, and (c) modified spotted core-shell nanoparticles.

While the design of single triblock core-shell nanoparticles is novel and holds promise, further engineering could yield the design of nanoparticles with unique functions. Triblocks with poly(CPH-b-CPTEG-b-CPH) and poly(SA-b-CPTEG-b-SA) mixed together could create unique surface architectures (Fig. 7.6b). By having a small amount of poly(SA-b-CPTEG-b-SA) by composition to poly(CPH-b-CPTEG-b-CPH), a segregation effect can occur to create spotted core-shell nanoparticles similar to those developed by Christian et al.<sup>8</sup> Spot size can be tailored by composition and molecular weight to yield a size that could interact with receptors on desired cells like APCs. By first conjugating moieties (e.g., carbohydrates or small peptides) to the ends of poly(SA-b-CPTEG-b-SA) triblocks before particle fabrication (Fig. 7.6c), spotted core-shell nanoparticles could be synthesized with specificity for certain cell receptors in order to facilitate targeted delivery. Carrillo-Conde and co-workers have already shown the capacity for randomly distributed surface carbohydrate-modified nanoparticles to induce enhanced DC activation<sup>9</sup>, so confinement to specific spots on the particle surface has the potential to enhance this effect.

Another route for the design of novel polyanhydride nanoparticles is microemulsion polymerization. This process allows for the synthesis of polymer and formation of nanoparticles to occur in a single step. For this process, anhydride monomers are methacrylated as shown in Fig 7.7.

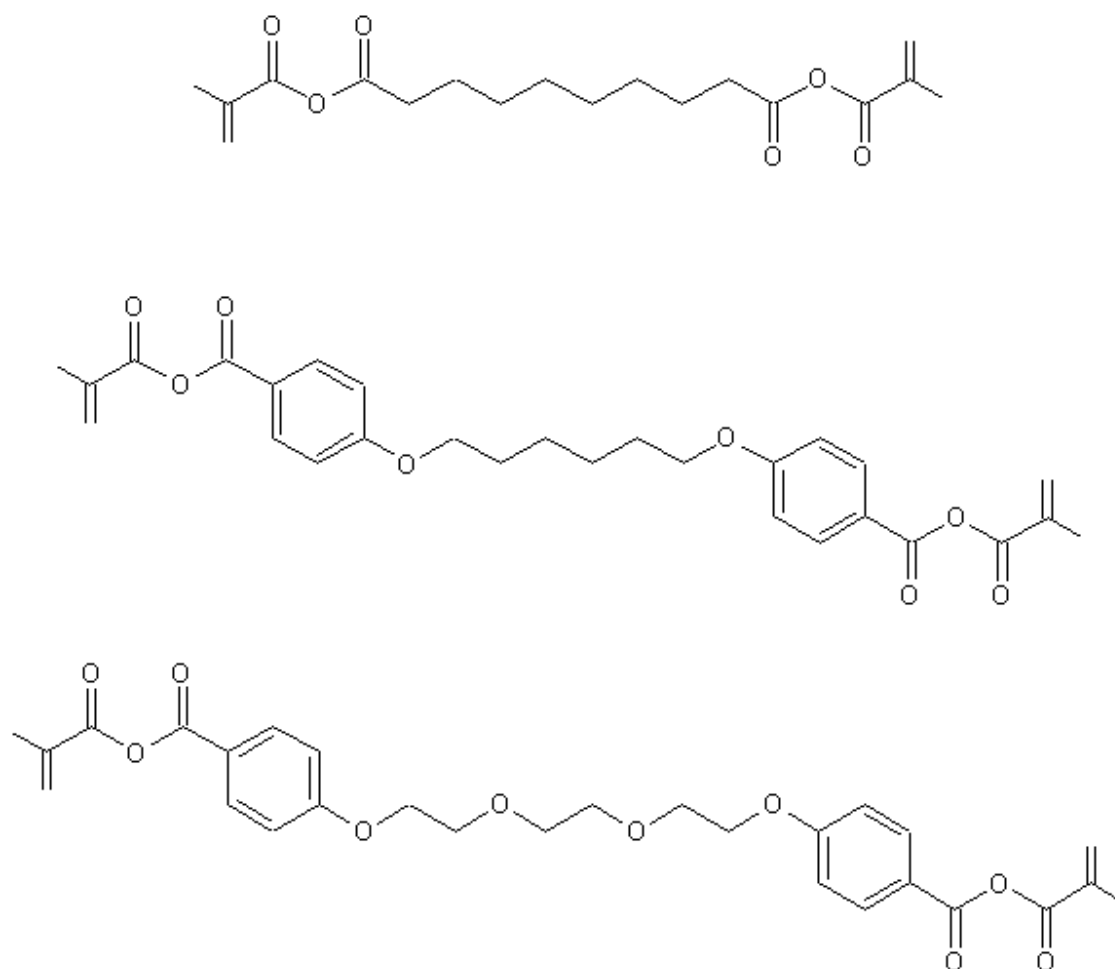


**Figure 7.7.** Chemical structures of (top) methacrylated SA, (middle) methacrylated CPH, and (bottom) methacrylated CPTEG.

Methacrylation allows for the use of reversible addition-fragmentation chain transfer polymerization within microemulsions to synthesize nanoparticles. The microemulsion polymerization process is shown in Fig. 7.8.

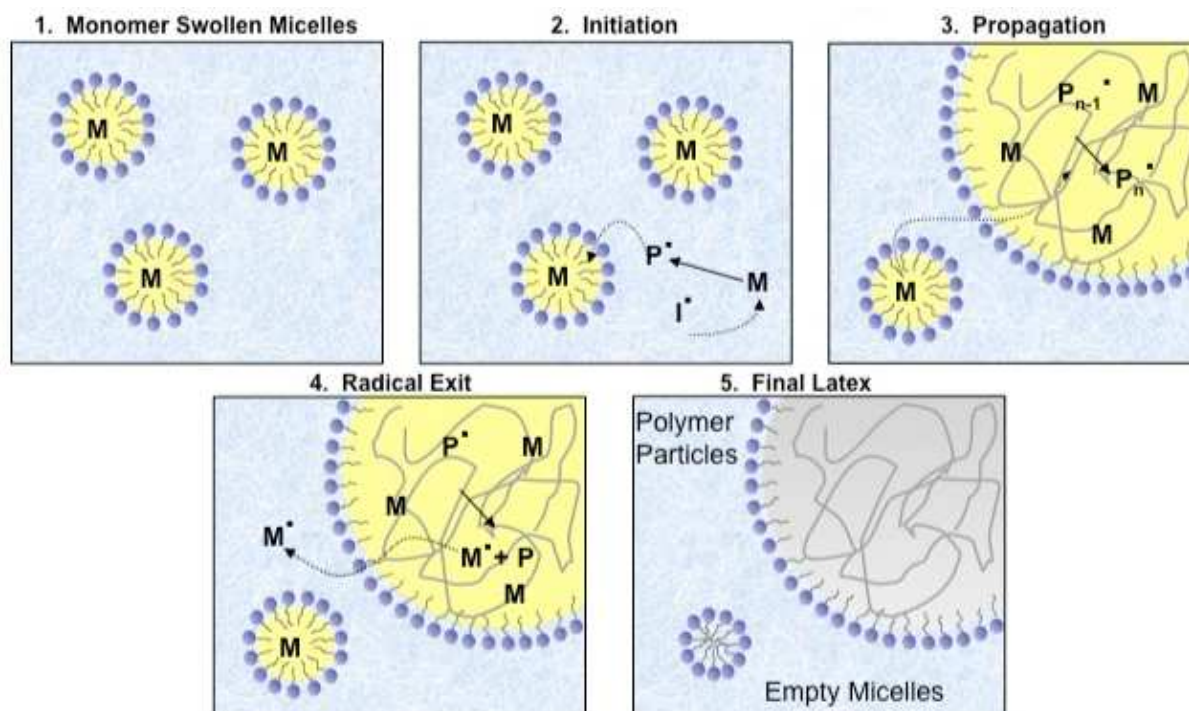


**Figure 7.8.** Fabrication of nanoparticles by microemulsion polymerization where M = monomer, I = initiator, and P = polymer. (Reprinted from O'Donnell & Kaler<sup>10</sup>)

Recent research with RAFT microemulsion polymerization of mSA yielded the fabrication of ultra small nanoparticles (<100 nm) (Fig 7.9).

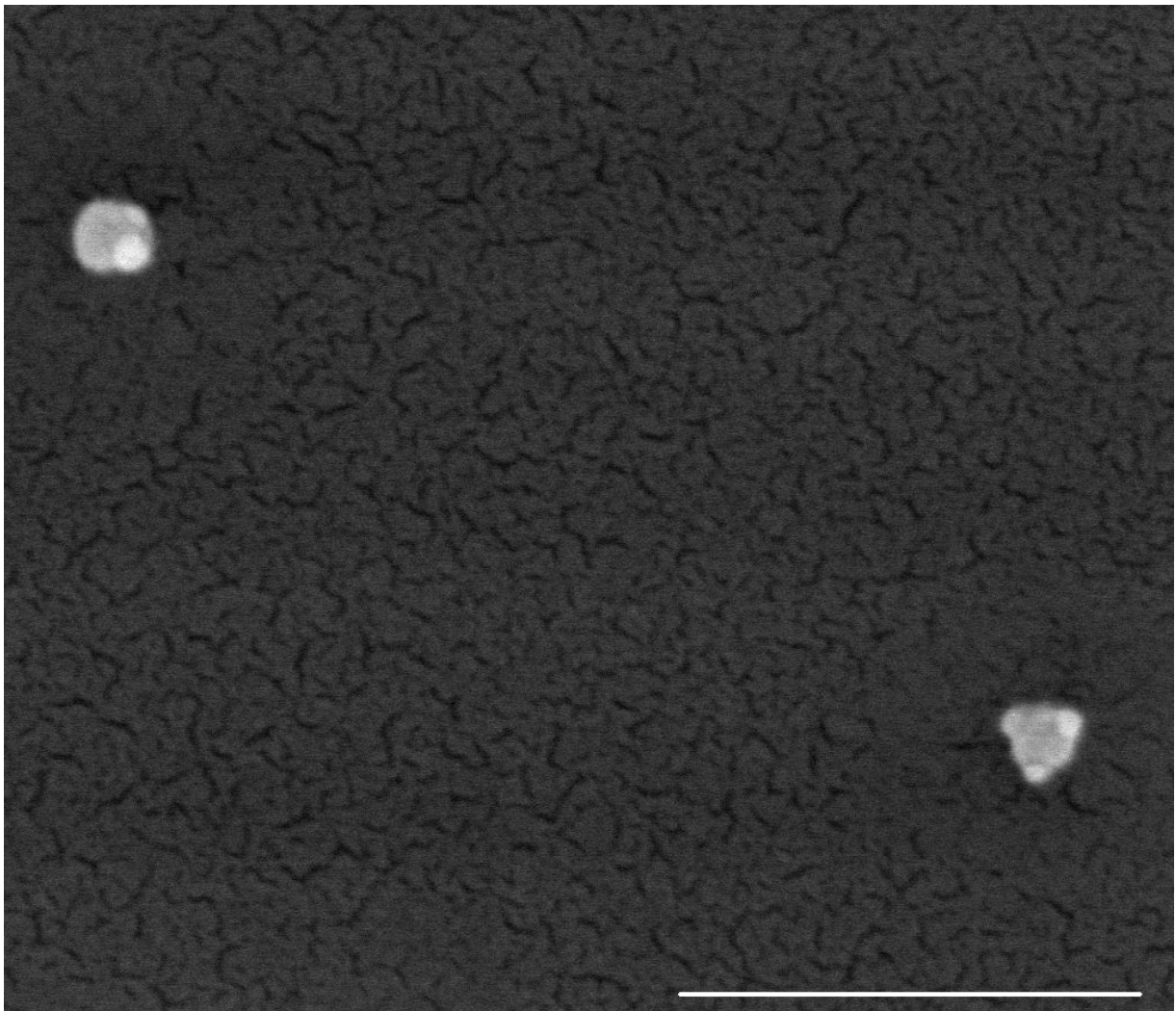


**Figure 7.9.** Scanning transmission electron micrograph of mSA ultra small nanoparticles synthesized by microemulsion polymerization. Scale bar = 1  $\mu\text{m}$ .

The possibility to create nanoparticles with controlled size for vaccine delivery could be realized by this technique.

#### **7.2.4 Novel Intracellular Quantification Tools**

Although we have exceptional capabilities to utilize fluorescent microscopy to monitor intracellular trafficking of polyanhydride nanoparticles, there exist

limitations to current experimental designs and techniques. In our current work, we have used a fluorescently labeled payload that acts as a reporter for nanoparticles. Also, only fluorescent material that is encapsulated can be easily visualized with microscopy. This constraint prevents the ability to accurately link the data generated by fluorescent microscopy to other experiments. By developing novel environmentally-sensitive fluorescent materials these limitations can be overcome. One potential solution is to develop conjugated quantum dots (QDs) that have fluorescence resonance energy transfer (FRET) sensitive to environmental conditions. A reactive QD of interest would be one that can modulate emission within biologically-relevant pH (4 to 8). A proposed system using a pH-responsive polymer linker between a QD and organic fluorescent dye is shown in Fig. 7.10.

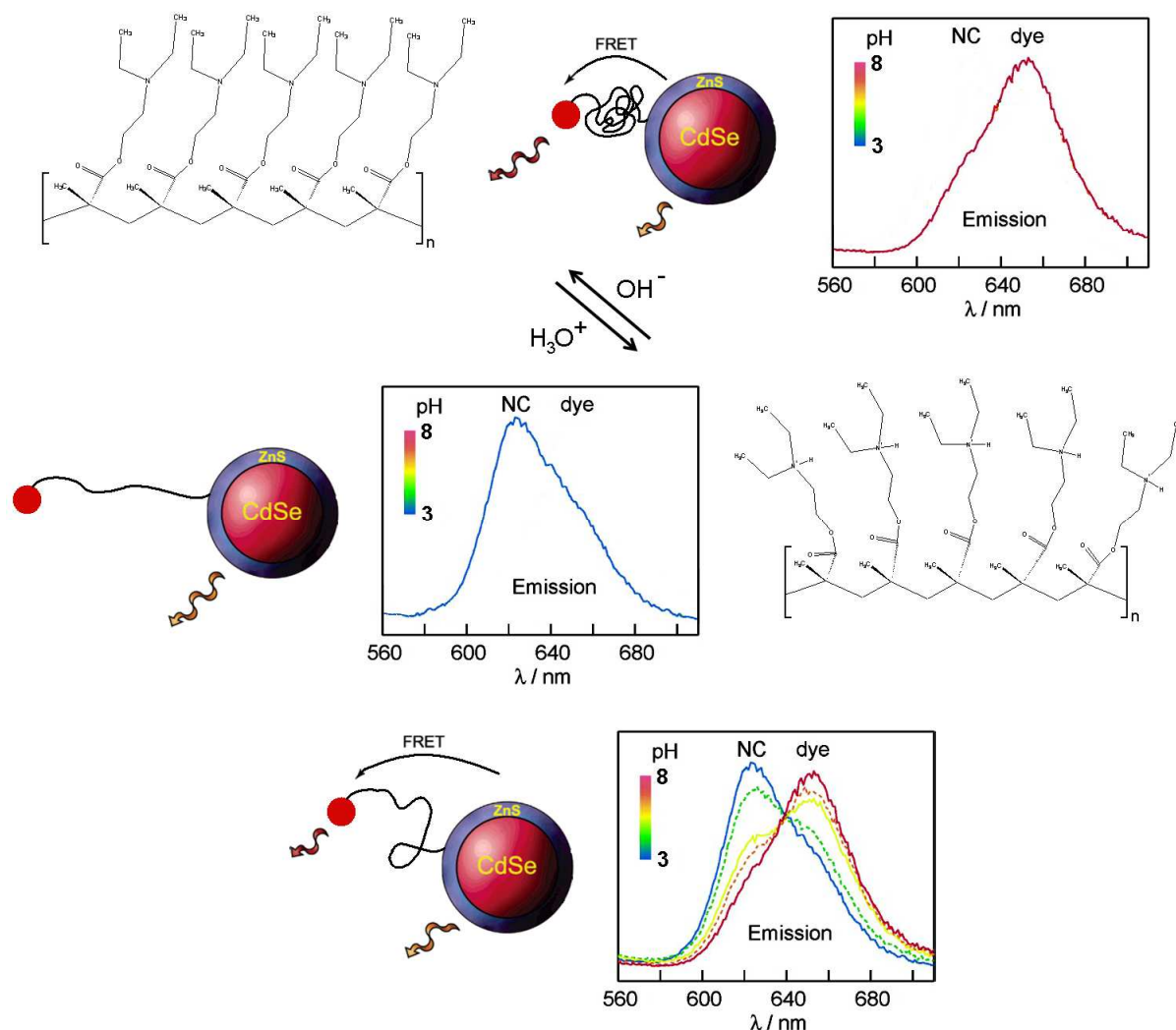


**Figure 7.10.** Cartoon detailing a potential pH-sensitive QD. Poly((diethylamino ethyl) methacrylate) (pDEAEM) has been shown to be a pH-response polymer.<sup>11,12</sup> In high pH, the tertiary amine is non-protonated and the polymer is able to collapse on itself (top left). As pH drops tertiary amines become protonated causing the polymer to expand (middle right). By tethering a QD to a fluorescent dye (red circle) by a pDEAEM chain we will be able to utilize FRET as a reporter for pH. Under high pH conditions, the QD and dye will be close enough physically to allow for FRET (top center) to proceed generating dye-dominant emission (top right). Under low pH conditions, pDEAEM will move the dye away from the QD (middle left) allowing for QD-dominant emission (middle center). In between extreme conditions (bottom), we hope to have variable FRET which we can use to accurately determine local pH levels.

The advantage of this novel system is that the material properties of the linker can be modulated to specific applications whereas current environmentally-sensitive QD-based FRET systems require the modulation of the fluorescent dye (i.e., alcohol protonation<sup>13</sup>) to cause a change in the extinction coefficient of the dye. These materials are normally very narrow in their pH-sensitive range and require extensive research to develop each FRET pair. Some modulations that could be attempted are the use of varying lengths of polymer, non-reactive incorporated subunits (i.e. ethylene glycol methyl methacrylate), multiple cationic polymers, or even multiple fluorescent dyes.

After conjugated QDs are fabricated that have desirable pH-sensitive FRET, they can be encapsulated within polyanhydride nanoparticles. Within nanoparticles, conjugated QDs should have collapsed linkers allowing for significant FRET to occur. As nanoparticles release payload within acidic vesicles of APCs, the pDEAEM linker of conjugated QDs should become protonated and extend. In addition, individual QDs are visible with fluorescent microscopy making them excellent candidates to replace the fluorescent dyes being used currently. This characteristic can be exploited to identify encapsulated versus non-encapsulated QDs giving us additional insight into APC processing of nanoparticles.

#### **7.2.5. Acknowledgments**

The work presented in this chapter is a result of interdisciplinary collaborations and discussions between researchers in chemical engineering,

chemistry, materials science, cell biology, and immunology. Thanks to Yashdeep Phanse for his work on the  $\alpha$ -gal F1-V vaccine and for providing Fig 7.1; Brenda Carrillo for her work on the  $\alpha$ -gal F1-V vaccine and for her assistance in the development of Scheme 7.1; Dr. Chris Minion, Dr. Greg Phillips, and Jing Yu for their work on identifying novel *Y. pestis* antigens; Latrisha Petersen for her work on combinatorial nanoparticle induced DC cell surface marker analysis and for providing Fig. 7.3; Bryce Williams for his work on polyanhydride triblock copolymer synthesis; Dr. Jen O'Donnell and Chelsea Sackett for their work on synthesizing mSA ultra small nanoparticles and for providing Fig. 7.9 and Fig. 7.10; Dr. Aaron Clapp, Dr. Eric Cochran, Dr. Ross Behling, Yanjie Zhang, and Sandeep Kakade for their work on the design of pH sensitive QDs. Special thanks go to Dr. Balaji Narasimhan and Dr. Michael Wannemuehler for their assistance and guidance in all these experiments.

### 7.3 References

1. Gupta, R.K. Aluminum compounds as vaccine adjuvants. *Advanced Drug Delivery Reviews*. **32**(3), 155 – 172 (1998).
2. Rhoner, J., et al. Efficacy of live attenuated influenza vaccine in children: A meta-analysis of nine randomized clinical trials. *Vaccine*. **27**(17), 1101 – 1110 (2009).
3. Petersen, L.K., et al. The role of polymer chemistry in the uptake of polyanhydride nanoparticles and the activation mechanisms of antigen presenting cells. *Biomaterials*, in preparation for publication.
4. Carrillo-Conde B., et al. Encapsulation into amphiphilic polyanhydride microparticles stabilizes *Yersinia pestis* antigens. *Acta Biomaterialia*. **6**(8), 3110 – 3119 (2010).
5. Glynn, A., et al. Protection against aerosolized *Yersinia pestis* challenge following homologous and heterologous prime-boost with recombinant plague antigens. *Infection and Immunity*. **73**(8), 5256 – 5261 (2005).
6. Reddy, S.T., et al. Exploiting lymphatic transport and complement activation in nanoparticle vaccines. *Nature Biotechnology*. **25**(10), 1159 – 1164 (2007).
7. Lai, S.K., Hida, K., Chen, C. & Hanes, J. Characterization of the intracellular dynamics of a non-degradative pathway accessed by polymer nanoparticles. *Journal of Controlled Release*. **125**(2), 107 – 111 (2008).
8. Christian, D.A., et al. Spotted vesicles, striped micelles and Janus assemblies induced by ligand binding. *Nature Materials*. **8**(10), 843 – 849 (2009).
9. Carrillo-Conde, et al. Targeting dendritic cells with functionalized polyanhydride nanoparticles. *Biomaterials*, to be submitted.
10. O'Donnell, J. & Kaler, E.W. Microstructure, kinetics and transport in oil-in-water microemulsion polymerization. *Macromolecular Rapid Communications*. **28**(14), 1445 – 1454 (2007).
11. Anderson, B.C. & Mallapragada, S.K. Synthesis and characterization of injectable, water-soluble copolymers of tertiary amine methacrylates and poly(ethylene glycol) containing methacrylates. *Biomaterials*. **23**(22), 4345 – 4352 (2002).

12. Determan, M.D., Guo, L., Thiyagarajan, P. & Mallapragada, S.K. Supramolecular self-assembly of multiblock copolymers in aqueous solution. *Langmuir*. **22**(4), 1469 – 1473 (2006).
13. Snee, P.T., et al. A ratiometric CdSe/ZnS nanocrystal pH sensor. *Journal of the American Chemical Society*. **128**(41), 13320 – 13321 (2006).